Journal of Double Star Observations

VOLUME 13 NUMBER 2 April 1, 2017

Inside this issue:

Inside this issue:

Visual Observation and Measurements of 33 so far Unconfirmed Tycho Double Stars in Cygnus with 2 Arcseconds Separation

Wilfried R.A. Knapp
Vienna, Austria
wilfried.knapp@gmail.com

Abstract: As already reported (Knapp and Gould 2016), most Tycho Double Star objects in the WDS catalog are unconfirmed. From the huge number of in total nearly 1000 TDS/TDT objects in the Cygnus constellation, all unconfirmed pairs (per beginning of 2016) listed with 2" separation were visually observed and measured based on CCD images.

Introduction

A short holiday trip into the Austrian mountains offered the possibility of using a hotel-owned observatory at an altitude of about 1900 m equipped with a 17 inch Planewave f/6.8 CDK telescope for visual observations for two consecutive nights. Despite the full moon at the date in question I used this opportunity for just another check of Tycho Double Stars as resolution of double star observation is not this sensitive to light polluted skies. But to be on the safe side, I decided to restrict the targets to objects near the zenith with a separation of 2", as resolution with a 17 inch telescope should then be easy even under these imperfect conditions. From a total of about 1000 TDS/TDT objects in Cygnus, there remained 33 pairs with a separation of 2". For counter-checking, I selected 5 already confirmed pairs also in Cygnus with similar 2" separation and magnitude range about 11-12 mag.

Visual Observations

The first session was to some degree spent with getting familiar with the telescope and the GoTo mount with some difficulties with the latter – the number of observed objects was therefore rather small. Things went much smoother in the second session especially after several resynchronizations of the GoTo system. In addition to the GoTo system, very detailed star maps were used to be sure to look at the correct objects. The results are shown in the Table 1.

Measurements based on CCD imaging

Five images with exposure time of 3 seconds were taken per object with remote telescope iT24 (for specifications see Acknowledgements). The images were stacked with VPhot and plate solved with Astrometrica with URAT1 reference stars with Vmags in the range 10.5 to 14.5mag. The RA/Dec coordinates resulting from plate solving were used to calculate Sep and PA using the formula provided by R. Buchheim 2008 (see References). *Err_PA* is the error estimation for PA in degrees calculated as arctan(*Err_Sep*/*Sep*), assuming the worst case that *Err_Sep* points perpendicular to the separation vector. *Mag* is the photometry result based on URAT1 reference stars with Vmags between 10.5 and 14.5mag. *Err_Mag* is calculated as

$$Err\_Mag = \sqrt{dV_{mag}^2 + \left[2.5\log_{10}\left(1+1/SNR\right)\right]^2}$$

with dVmag as the average Vmag error over all used reference stars and SNR as the signal to noise ratio for the given star. Date is the Bessel epoch and N is the number of images used for the reported values. The results are shown in Table 2.

Summary

The comparison of imaging and visual observation results plus the additional check of 2MASS images

(Text continues on page 137)

Table 1: Observation results for all TDS objects in Cyg with 2" separation so far not confirmed plus 5 already confirmed non TDS objects for counter-checking with their WDS data per begin of 2016. Method of observation = V (visual estimate) and aperture = 0.425m

WDS ID	Name	RA	Dec	Sep	M1	M2	PA	Date	Observation notes
21442+3453	HO605	21:44:07.293	+34:52:33.8	2.0	11.34	12.11	340	2016.553	With a magnification of x230 resolution at ~345° with estimated separation ~2"
21545+4052	TDT3230	21:54:30.980	+40:52:16.2	2.0	12.14	12.23	222	2016.553	No resolution
21466+3815	COU1639	21:46:34.778	+38:14:43.4	2.0	11.27	11.56	211	2016.553	With a magnification of x230 resolution at ~210° with estimated separation ~2"
21212+3044	TDT2914	21:21:14.751	+30:44:12.3	2.0	10.86	12.66	17	2016.553	No resolution
21548+4310	TDT3234	21:54:50.817	+43:09:55.0	2.0	11.34	12.42	343	2016.553	No resolution
21279+3439	TDT2980	21:27:56.960	+34:39:10.8	2.0	12.12	12.63	121	2016.553	No resolution
21300+3549	TDT2998	21:30:00.117	+35:49:04.2	2.0	11.53	13.28	209	2016.553	No resolution
21158+3159	TDT2868	21:15:50.729	+31:59:22.6	2.0	11.63	12.58	185	2016.553	No resolution
21245+3632	ES2125	21:24:29.222	+36:31:30.9	2.0	10.41	11.82	36	2016.553	With a magnification of x230 resolution at ~45° with estimated separation ~2"
21195+3745	TDT2904	21:19:32.118	+37:45:29.7	2.0	11.55	13.12	216	2016.553	No resolution
21107+3515	TDS1120	21:10:43.050	+35:15:15.5	2.0	10.18	12.43	244	2016.553	No resolution
21095+3506	TDT2791	21:09:29.133	+35:05:30.9	2.0	11.76	12.61	252	2016.553	No resolution
20592+3231	TDT2675	20:59:14.778	+32:31:29.4	2.0	11.62	12.56	207	2016.553	No resolution
21070+3724	TDT2763	21:07:00.529	+37:24:24.0	2.0	11.35	12.68	215	2016.553	No resolution
21282+4607	TDT2981	21:28:11.977	+46:06:34.7	2.0	11.64	12.07	101	2016.553	No resolution
21068+3834	TDT2758	21:06:49.969	+38:33:32.0	2.0	11.85	12.24	236	2016.553	No resolution
21304+4926	TDT3002	21:30:21.980	+49:26:14.1	2.0	11.30	11.75	295	2016.553	With a magnification of x230 resolution at ~300° with estimated separation 2"
21037+4616	TDT2719	21:03:40.853	+46:16:09.7	2.0	11.87	12.14	220	2016.553	No resolution
20152+3006	TDT2121	20:15:12.978	+30:06:07.6	2.0	11.92	12.18	11	2016.553	No resolution
20107+3015	TDT2051	20:10:43.449	+30:14:40.6	2.0	11.90	12.27	242	2016.553	No resolution
20449+4332	ES1448	20:44:52.852	+43:31:51.6	2.0	10.39	10.80	142	2016.553	With magnification of x230 resolution at about 140° with estimated separation of ~2"
20160+3751	TDT2130	20:15:58.427	+37:50:35.2	2.0	11.28	11.82	236	2016.553	No resolution
20275+4307	TDT2289	20:27:28.320	+43:07:07.3	2.0	11.69	12.24	346	2016.553	No resolution
20330+5922	TDT2359	20:33:00.231	+59:21:55.4	2.0	10.17	12.79	113	2016.553	No resolution
20258+5938	TDT2261	20:25:50.823	+59:37:50.1	2.0	10.08	11.77	134	2016.553	No resolution
19447+3204	TDT1697	19:44:40.740	+32:04:17.0	2.0	12.12	12.45	297	2016.553	No resolution
19466+3243	TDT1729	19:46:34.530	+32:43:16.9	2.0	10.22	12.44	111	2016.553	No resolution
20209+5511	TDT2197	20:20:56.891	+55:10:55.8	2.0	10.81	13.32	241	2016.553	No resolution
19511+3643	ES242	19:51:02.020	+36:42:42.8	2.0	11.00	11.50	30	2016.551	With a magnification of x230 resolution at ~30° with a separation of ~2"
20153+5428	TDT2123	20:15:20.098	+54:27:40.3	2.0	11.27	11.84	328	2016.551	No resolution
20056+5821	TDT1965	20:05:38.448	+58:21:04.6	2.0	11.63	12.41	160	2016.551	No resolution
20071+5431	TDT1991	20:07:05.459	+54:31:00.4	2.0	10.64	12.23	333	2016.551	No resolution
19438+3738	TDT1680	19:43:45.513	+37:38:17.0	2.0	11.86	11.95	273	2016.551	No resolution
19290+3508	POP135	19:28:56.513	+35:06:44.7	2.0	11.11	12.11	35	2016.551	With a magnification of x230 hint of companion at ~40° with a separation of ~2"
19326+4839	TDT1533	19:32:38.038	+48:39:06.2	2.0	11.99	12.01	215	2016.551	No resolution
19209+4710	TDT1391	19:20:56.328	+47:10:09.1	2.0	11.74	12.27	2	2016.551	No resolution
19178+4759	TDT1358	19:17:48.420	+47:59:17.6	2.0	11.40	12.12	234	2016.551	No resolution
19095+4828	TDT1259	19:09:29.552	+48:27:57.0	2.0	11.98	12.00	216	2016.551	With a magnification of x420 resolution at a position angle of ~215° and a separation of ~2"

Table 2. Measurement results for all TDS objects in Cyg with 2" separation so far not confirmed plus 5 already confirmed non TDS objects for counter-checking based on iT24 images (plus one by chance found additional double star). Method of observations = C (CCD or other two-dimensional electronic imaging) and aperture = 0.61m

Name		RA	Dec	dRA	dDec	Sep	Err Sep	PA	Err PA	Mag	Err Mag	SNR	dVmag	Date	N	Notes
HO 605	A	21 44 07.265	34 52 34.08	0.05	0.06	1.864	0.078	340.730	2.399	11.097	0.062	73.94	0.06	2016.587	5	1
	B	21 44 07.215	34 52 35.84							11.326	0.061	80.61				
TDT3230	A	21 54 30.978	40 52 16.06	0.05	0.05	-	0.071	-	-	12.048	0.062	64.21	0.06	2016.587	5	2
	B										-					
COU1639	A	21 46 34.779	38 14 43.75	0.03	0.04	1.754	0.050	204.186	1.633	11.000	0.041	105.02	0.04	2016.587	5	1
	B	21 46 34.718	38 14 42.15							11.290	0.042	91.33				
TDT2914	A	21 21 14.766	30 44 12.24	0.03	0.03	-	0.042	-	-	10.814	0.041	111.80	0.04	2016.587	5	2
	B										-					
TDT3234	A	21 54 50.873	43 09 55.07	0.03	0.04	-	0.050	-	-	11.250	0.071	96.43	0.07	2016.587	5	2
	B										-					
TDT2980	A	21 27 56.985	34 39 10.89	0.03	0.04	-	0.050	-	-	11.917	0.062	69.82	0.06	2016.587	5	2
	B										-					
TDT2998	A	21 30 00.125	35 49 04.03	0.03	0.04	-	0.050	-	-	11.444	0.052	75.82	0.05	2016.587	5	2
	B										-					
TDT2868	A	21 15 50.764	31 59 22.51	0.03	0.04	-	0.050	-	-	11.666	0.062	76.98	0.06	2016.587	5	2
	B										-					
ES 2125	A	21 24 29.230	36 31 31.12	0.04	0.04	2.005	0.057	33.586	1.616	10.360	0.072	66.09	0.07	2016.587	5	1
	B	21 24 29.322	36 31 32.79							11.193	0.071	84.73				
TDT2904	A	21 19 32.121	37 45 29.49	0.03	0.03	-	0.042	-	-	11.709	0.052	82.76	0.05	2016.587	5	2
	B										-					
TDS1120	A	21 10 43.074	35 15 15.38	0.04	0.04	-	0.057	-	-	10.061	0.051	128.41	0.05	2016.587	5	2
	B										-					
TDT2791	A	21 09 29.115	35 05 30.89	0.04	0.04	-	0.057	-	-	11.997	0.062	63.05	0.06	2016.587	5	2
	B										-					
TDT2675	A	20 59 14.781	32 31 29.21	0.03	0.05	-	0.058	-	-	12.186	0.053	58.08	0.05	2016.587	5	2
	B										-					
TDT2763	A	21 07 00.484	37 24 23.36	0.03	0.04	-	0.050	-	-	11.197	0.061	91.60	0.06	2016.587	5	2
	B										-					
TDT2981	A	21 28 11.981	46 06 34.77	0.03	0.04	-	0.050	-	-	11.648	0.061	82.05	0.06	2016.587	5	2
	B										-					
TDT2758	A	21 06 49.966	38 33 32.18	0.03	0.04	-	0.050	-	-	11.851	0.052	77.63	0.05	2016.587	5	2
	B										-					
TDT3002	A	21 30 21.931	49 26 14.27	0.04	0.04	1.664	0.057	311.381	1.947	11.013	0.072	64.96	0.07	2016.587	5	1
	B	21 30 21.803	49 26 15.37							11.608	0.072	65.42				
TDT2719	A	21 03 40.854	46 16 09.61	0.04	0.04	-	0.057	-	-	12.211	0.062	65.15	0.06	2016.587	5	2
	B										-					
TDT2121	A	20 15 12.962	30 06 07.82	0.06	0.07	-	0.092	-	-	12.153	0.111	60.28	0.11	2016.587	5	2
	B										-					
TDT2051	A	20 10 43.433	30 14 40.55	0.06	0.06	-	0.085	-	-	11.050	0.061	105.25	0.06	2016.587	5	2
	B										-					

Table 2 concludes on next page.

Visual Observation and Measurements of 33 so far Unconfirmed Tycho Double Stars in Cygnus ...

Table 2 (conclusion). Measurement results for all TDS objects in Cyg with 2" separation so far not confirmed plus 5 already confirmed non TDS objects for counter-checking based on iT24 images (plus one by chance found additional double star). Method of observations = C (CCD or other two-dimensional electronic imaging) and aperture = 0.61m

Name		RA	Dec	dRA	dDec	Sep	Err Sep	PA	Err PA	Mag	Err Mag	SNR	dVmag	Date	N	Notes
ES 1448	A	20 44 52.839	43 31 51.96	0.05	0.06	1.881	0.078	140.927	2.378	10.239	0.062	74.41	0.06	2016.587	5	1
	B	20 44 52.948	43 31 50.50							10.593	0.061	102.48				
TDT2130	A	20 15 58.445	37 50 35.19	0.06	0.09	-	0.108	-	-	11.587	0.081	73.08	0.08	2016.587	5	2
	B										-					
TDT2289	A	20 27 28.319	43 07 06.90	0.05	0.06	-	0.078	-	-	11.878	0.072	67.63	0.07	2016.587	5	2
	B										-					
TDT2359	A	20 33 00.211	59 21 55.17	0.05	0.07	-	0.086	-	-	10.074	0.051	140.73	0.05	2016.587	5	2
	B										-					
TDT2261	A	20 25 50.823	59 37 50.29	0.07	0.08	-	0.106	-	-	9.921	0.070	132.76	0.07	2016.587	5	2
	B										-					
TDT1697	A	19 44 40.606	32 04 18.18	0.07	0.07	-	0.099	-	-	12.279	0.092	54.42	0.09	2016.587	5	2
	B										-					
TDT1729	A	19 46 34.516	32 43 16.83	0.06	0.07	-	0.092	-	-	10.045	0.080	152.78	0.08	2016.587	5	2
	B										-					
TDT2197	A	20 20 56.897	55 10 55.79	0.06	0.06	-	0.085	-	-	10.677	0.061	118.95	0.06	2016.587	5	2
	B										-					
ES 242	A	19 51 02.024	36 42 42.93	0.06	0.05	1.844	0.078	31.016	2.426	11.088	0.072	68.29	0.07	2016.587	5	1
	B	19 51 02.103	36 42 44.51							11.369	0.073	56.69				
TDT2123	A	20 15 20.106	54 27 40.39	0.05	0.06	-	0.078	-	-	11.459	0.061	81.42	0.06	2016.587	5	2
	B										-					
TDT1965	A	20 05 38.479	58 21 04.77	0.05	0.07	-	0.086	-	-	11.962	0.073	55.29	0.07	2016.587	5	2
	B										-					
TYC3948-01545-1	A	20 05 29.946	58 21 06.72	0.05	0.07	2.651	0.086	78.467	1.859	11.372	0.073	54.85	0.07	2016.587	5	3
	B	20 05 30.276	58 21 07.25							12.963	0.091	18.11				
TDT1991	A	20 07 05.472	54 31 00.36	0.05	0.07	-	0.086	-	-	10.598	0.081	111.35	0.08	2016.587	5	2
	B										-					
TDT1680	A	19 43 45.493	37 38 17.23	0.06	0.06	-	0.085	-	-	11.436	0.061	91.56	0.06	2016.587	5	2
	B										-					
POP 135	A	19 28 56.516	35 06 44.99	0.04	0.05	1.846	0.064	37.220	1.987	11.106	0.062	71.36	0.06	2016.587	5	1
	B	19 28 56.607	35 06 46.46							11.743	0.062	73.08				
TDT1533	A	19 32 38.027	48 39 06.14	0.03	0.03	-	0.042	-	-	11.946	0.053	65.20	0.05	2016.587	5	2
	B										-					
TDT1391	A	19 20 56.331	47 10 09.47	0.03	0.04	2.064	0.050	3.682	1.388	11.821	0.044	55.67	0.04	2016.587	5	1
	B	19 20 56.344	47 10 11.53							12.098	0.045	53.86				
TDT1358	A	19 17 48.423	47 59 17.77	0.03	0.03	-	0.042	-	-	11.456	0.052	78.70	0.05	2016.587	5	2
	B										-					
TDT1259	A	19 09 29.515	48 27 57.21	0.06	0.08	2.275	0.100	204.535	2.516	12.073	0.112	48.54	0.11	2016.587	5	1
	B	19 09 29.420	48 27 55.14							11.957	0.111	60.02				

Table 2 notes:

1. Touching/overlapping star disks
2. Appears as a single star
3. Same image as TDT 1965. Double star confirmed by elongation in 2MASS images, yet no 2MASS catalog entry exists for B nor in any other catalog

Visual Observation and Measurements of 33 so far Unconfirmed Tycho Double Stars in Cygnus ...

(Continued from page 133)

(SDSS images are currently not available for Cyg) should allow for very conclusive assessments per object if bogus or not. The results of this comparison are shown in Table 3.

From 33 so far unconfirmed 2" TDS objects in Cyg only 3 are confirmed as double stars while for the rest we cannot confirm, while from the 5 selected additional 2" double stars in Cygnus all 5 have been fully confirmed.

Potential further research

As the number of so far unconfirmed Tycho Double Stars is huge the field for further research seems also huge. The effort to eliminate all bogus TDS/TDT objects from the WDS catalog is probably much higher than adding them initially especially if we go down in separation far below 2 arcseconds. Counterchecking with SDSS images with much better resolution than 2MASS offers a possibility with reasonable effort down to separations of somewhat less than 1.5" but then things get difficult. It seems out of the question to counter-check the huge number of so far not confirmed TDS objects with visual observation (anyway a rather frustrating task – looking at single stars proposed to be doubles) and taking dedicated images for this purpose especially for separations smaller than 1.5" – the effort would be huge and obviously a waste of time and equipment. The meager ratio of confirmed to bogus from the so far counter-checked TDS objects suggests a crude resolution: All so far not confirmed TDS objects are to be considered suspect with a high probability of at least 85% of being bogus.

Acknowledgements

The following tools and resources have been used for this research:

- Washington Double Star Catalog as data source for the selected objects
- CCD imaging: Images were taken with iTelescope iT24: 610mm CDK with 3962mm focal length. CCD: FLI-PL09000. Resolution 0.62 arcsec/pixel. V-filter. Located in Auberry, California. Elevation 1405m
- Visual observations: 425mm CDK with focal length 2940mm. Located at Gerlitzen, Austria. Elevation 1900m
- Aladin Sky Atlas v9.0 (2MASS and POSS images)
- SIMBAD, VizieR
- 2MASS All Sky Catalog
- AstroPlanner v2.2 for object selection

References

Buchheim, Robert, 2008, "CCD Double-Star Measurements at Altimira Observatory in 2007", *Journal of Double Star Observations*, **4**, 27-31. Formulas for calculating Separation and Position Angle from the RA Dec coordinates given as

$$Sep = \sqrt{\left[\left(RA_2 - RA_1\right)\cos\left(Dec_1\right)\right]^2 + \left(Dec_2 - Dec_1\right)^2}$$

in radians and

$$RA = \arctan\left[\frac{\left(RA_2 - RA_1\right)\cos\left(Dec_1\right)}{Dec_2 - Dec_1}\right]$$

in radians depending on quadrant

Knapp, Wilfried; Gould, Ross, 2016, "Visual Observation and Measurements of some Tycho Double Stars", *Journal of Double Star Observations*, **12**, 427 - 436

Table 3 Overall assessment for all TDS objects in Cyg with 2" separation so far not confirmed plus 5 already confirmed non TDS objects for counter-checking based on iT24 images, visual observation and counter-checking 2MASS and POSS images

Name	Imaging	Visual observation	Aladin images	Overall conclusion
HO 605	Touching/overlapping star disks	With a magnification of x230 resolution at ~345° with estimated separation 2"	2MASS and POSS images suggest elongation	Object as double star confirmed
TDT 3230	Obviously single star	No resolution	2MASS images without hint of elongation	Bogus
COU 1639	Touching/overlapping star disks	With a magnification of x230 resolution at ~210° with estimated separation 2"	2MASS images suggest elongation	Object as double star confirmed
TDT 2914	Obviously single star	No resolution	2MASS images no hint of elongation	Bogus
TDT 3234	Obviously single star	No resolution	2MASS no hint of elongation	Bogus
TDT 2980	Obviously single star	No resolution	2MASS images no hint of elongation	Bogus
TDT 2998	Obviously single star	No resolution	2MASS images no hint of elongation	Bogus
TDT 2868	Obviously single star	No resolution	2MASS images no hint of elongation	Bogus
ES 2125	Touching/overlapping star disks	With a magnification of x230 resolution at ~45° with estimated separation 2"	2MASS and POSS images suggest elongation	Object as double star confirmed
TDT 2904	Obviously single star	No resolution	2MASS images no hint of elongation	Bogus
TDS 1120	Obviously single star	No resolution	**2MASS images slight hint of elongation**	Probably bogus (after rather negative re-checking of 2MASS and POSS images)
TDT 2791	Obviously single star	No resolution	2MASS images no hint of elongation	Bogus
TDT 2675	Obviously single star	No resolution	2MASS J no hint of elongation	Bogus
TDT 2763	Obviously single star	No resolution	2MASS images slight hint of elongation	Bogus
TDT 2981	Obviously single star	No resolution	2MASS images no hint of elongation	Bogus
TDT 2758	Obviously single star	No resolution	2MASS images no hint of elongation	Bogus
TDT 3002	Touching/overlapping star disks	With a magnification of x230 resolution at ~300° with estimated separation 2"	2MASS no hint of elongation but POSS images show hint of elongation	Object as double star confirmed
TDT 2719	Obviously single star	No resolution	2MASS images no hint of elongation	Bogus
TDT 2121	Obviously single star	No resolution	2MASS J no hint of elongation	Bogus
TDT 2051	Obviously single star	No resolution	2MASS J no hint of elongation	Bogus

Table 3 concludes on next page.

Table 3 (conclusion). Overall assessment for all TDS objects in Cyg with 2" separation so far not confirmed plus 5 already confirmed non TDS objects for counter-checking based on iT24 images, visual observation and counter-checking 2MASS and POSS images

Name	Imaging	Visual observation	Aladin images	Overall conclusion
ES 1448	Touching/overlapping star disks	With magnification of x230 resolution at about 140° with estimated separation of 2"	2MASS and POSS images suggest elongation	Object as double star confirmed
TDT 2130	Obviously single star	No resolution	2MASS J no hint of elongation	Bogus
TDT 2289	Obviously single star	No resolution	2MASS J no hint of elongation	Bogus
TDT 2359	Obviously single star	No resolution	2MASS J no hint of elongation	Bogus
TDT 2261	Obviously single star	No resolution	2MASS J no hint of elongation	Bogus
TDT 1697	Obviously single star	No resolution	2MASS J no hint of elongation	Bogus
TDT 1729	Obviously single star	No resolution	2MASS J no hint of elongation	Bogus
TDT 2197	Obviously single star	No resolution	2MASS J no hint of elongation	Bogus
ES 242	Touching/overlapping star disks	With a magnification of x230 resolution at ~30° with a separation of ~2"	2MASS and POSS images suggest elongation	Object as double star confirmed
TDT 2123	Obviously single star	No resolution	2MASS no hint of elongation	Bogus
TDT 1965	Obviously single star	No resolution	2MASS no hint of elongation	Bogus
TDT 1991	Obviously single star	No resolution	2MASS no hint of elongation	Bogus
TDT 1680	Obviously single star	No resolution	2MASS no hint of elongation	Bogus
POP 135	Touching/overlapping star disks	With a magnification of x230 hint of companion at ~40° with a separation of ~2"	2MASS and POSS images suggest elongation	Object as double star confirmed
TDT 1533	Obviously single star	No resolution	2MASS no hint of elongation	Bogus
TDT 1391	Touching/overlapping star disks	**No resolution**	2MASS image suggest hint of elongation	Object as double star confirmed (negative visual observation probably due to observing the wrong object because of initial problems with the GoTo mount)
TDT 1358	Obviously single star	No resolution	2MASS no hint of elongation	Bogus
TDT 1259	Touching/overlapping star disks	With a magnification of x420 resolution at a position angle of ~215° and a separation of ~2"	2MASS images suggest elongation	Object as double star confirmed

CPM Pairs from LSPM so far not WDS Listed

Wilfried R.A. Knapp
Vienna, Austria
wilfried.knapp@gmail.com

John Nanson
Star Splitters Double Star Blog
Manzanita, Oregon
jnanson@nehalemtel.net

Abstract: The LSPM catalog (Lepine and Shara 2005) is a rich source for CPM pairs we thought already exhausted – but as we found during research for our report "A new concept for counter-checking of assumed CPM pairs" (Knapp and Nanson 2016) there are still many potential CPM pairs indicated in LSPM which as of the beginning of 2016 are not listed in the WDS catalog. A first part of about 40 such objects is presented here.

Introduction

CPM pairs seem to us interesting enough to deserve their own catalog, but so far the WDS catalog is the only regularly maintained data base for these objects, so we checked the LSPM catalog for potential CPM pairs currently not WDS listed. The selection from LSPM was done by sorting all LSPM objects by RA and then checking if the next LSPM object is nearer than 30 arcseconds. We then found that in most cases such pairs were identical with LSPM objects with the same object ID, but with E/W/S/N added for differentiation of close objects with large proper motion. Next came a quick first check if such pairs show similar proper motion properties in terms of direction and speed. Assuming that star characteristics are distributed by random according to the general frequency regardless of distance one would expect that only a small part would show the characteristics of common proper motion. But to our surprise most of the pairs checked suggested CPM, which means that if two close stars have large proper motion then speed and direction is mostly very similar – the reason for this "rule" is rather unclear to us.

We then checked as many sources available to us via Aladin for data for these CPM candidates beginning with visual comparison of POSS I and POSS II images. Then if possible we used the Aladin centroid feature to get precise position coordinates in the POSS images allowing the calculation of separation and PA and the PM data based on the comparison between POSS I and POSS II. If the Aladin centroid feature did not work (stars too faint or too close) we then resorted to visual estimations of the centroids. Next came the check of other existing catalog data for the given field of view, especially 2MASS, URAT1, SDSS, WISE, UCAC4, GSC, NOMAD1, APASS etc., for data on both components with 2MASS and URAT1 the most important data source for calculating the PM data by comparison of the positions in 2MASS and URAT1 allowing a CPM rating according to Knapp/Nanson 2016. If URAT1 data was available, then we also checked the VizieR I/330 catalog from Nicholson 2015 (meanwhile, no longer available) based on URAT1 preliminary PM data to show the difference of the estimated PM errors compared to the 2MASS position error based on calculated PM error estimation.

As was to be expected we stumbled over several catalog data quality issues providing some good riddles. SDSS for example provides the currently best available image resolution of ~0.4 arcseconds and delivers with the SDSS DR9 catalog for most objects excellent precise RA/Dec with an unbelievable small position error of 0.001" but suddenly some objects have curious large position errors of ~0.5". Yet it would be of high interest to have SDSS covering the full sky instead of the currently given about a third. SDSS DR9 includes also for many objects PM data based on comparison of different SDSS observations, with a time distance of about 6 years. Despite this rather short time frame, most provided PM data seems with some exceptions rather precise but in nearly all such cases PM data only for the A component was available. Position comparison between 2MASS and SDSS was quite often less satisfying due to the too short time distance but even in cases with 5 or 6 years the calculated PM values were often not very useful.

Another catalog with good RA/Dec precision is WISE even if based on a technical resolution of only ~1.4 arcseconds per pixel. But also this catalog covers so far only a part of the sky and the observation epoch is a bit unclear due to a mix of observation dates. We had here to resort to the NASA/ IPAC Infrared Science Archive to get a precise average observation date. Similar to SDSS we often used WISE position data if available for both components for comparison with 2MASS but the calculated PM values were often not very useful.

Next very annoying errors are PM errors in URAT1 – sometimes you can only wonder what positions Aladin shows in the images for the URAT1 objects, only to realize that Aladin shows as standard epoch J2000 and calculates the URAT1 positions from 2013 back to J2000 with the given PM data. Moving the epoch slider to epoch 2013 shows then the effectively measured URAT1 positions.

We tried also to get the visual magnitudes for each of the components from the various catalogs we used. In the absence of Vmags, where J- and K-band values were available, we used a spreadsheet to estimate Vmags with formulas based on the works of Caldwell et al 1993 and Warner 2007 (http://brucegary.net/dummies/method0.html) provided -0.1 < (J-K)< 1.0.

Spectral class data was scarce in the available catalogs so we had to resort to deriving the spectral class of the objects in question using the B-V color index provided we had these values listed in the same catalog. For this purpose we used a table provided by the Space Telescope Science Institute (http://www.stsci.edu/~inr/intrins.html).

As far as possible (mostly depending on the altitude and availability of each object at the time of our research) we tried then to provide recent precise measurements for position, separation, position angle and visual magnitudes based on images taken with remote telescopes using our usual procedure: stacking with VPhot, plate solving and measuring positions and Vmags with Astrometrica using URAT1 as reference catalog and calculating Sep and PA with the formulas provided by Buchheim 2008. Due to the faintness of some objects we had to use exposure times up to 60 seconds and even then some components were too faint to be resolved.

In total we got in this way an observation history of each object beginning in most cases in the year ~1950 with POSS I and ending 2016 with own new images.

Results of Our Research

In Table 1 we present for the selected objects (plus one Tycho object found by chance as potential CPM during comparing POSS images for another object) as much data as we could find in the images and catalogs available to us including our own measurements of objects in reasonable altitude for imaging with remote telescope iT24. Shown below is a description of the table content per column:.

- LSPM gives the LSPM ID of the selected object in the header line
- RA and Dec give the URAT1 coordinates of the A component in the header line in the traditional HH:MM:SS DD:MM:SS format and in the data lines for the sources referred to in the Notes column in decimal degrees format as these values are directly usable for calculating Sep and PA
- Sep " and PA ° give separation and position angle in the data lines
- M1 and M2 give measured Vmags in the header line for A and B and if available also in the data lines where we had often to resort to estimated values based on calculation from the J- and K-band values if available
- pmRA1 and pmDE1 with e_pm1 give the proper motion data for A and pmRA2, pmDE2 and e_pm2 for B in the header line as well as in the data lines calculated by comparison of positions between catalogs or directly from the catalogs (specified in the Notes column)
- Spc1 and Spc2 give the spectral class for A and B usually based on the B-V color index if available
- Ap indicates in the data lines the used aperture for the observation listed and Me indicates the WDS code for the used observation method
- Date is the Bessel epoch of the (averaged) observation date given in the data lines
- CPM Rat gives the rating of the CPM assessment based on comparison of positions between 2MASS and URAT1 in the header line and the corresponding data line (usually URAT1)
- Source/Notes finally indicates in the header line the overall assessment for the object in question and in the data lines the used source (images and catalogs) and additional explanations if considered necessary.

(Text continues on page 161)

CPM Pairs from LSPM so far not WDS Listed

Table 1: Research results for potential common proper motion pairs found in the LSPM catalog. Headline object position based on URAT1 J2000 coordinates for A (with exception of J1906+1652 – in lack of URAT1 data we had to use the average value of our own measurements)

LSPM	RA	Dec	Sep "	PA °	M1	M2	pmRA1	pmDE1	e_pm1	pmRA2	pmDE2	e_pm2	Spc1	Spc2	Ap	Me	Date	CPM Rat	Source/Notes
J0448+3511	04 48 42.584	+35 11 08.21					221.9	9.2	15.8	212.3	-3.0	20.4						BAB	PM values so far not very precise - but comparison of POSS images strongly suggest CPM
	72.17329167	35.1854444	4.4	335.3											1.2	Pp	1955.857		POSS I.O estimates
	72.17591667	35.1854722	4.5	334.4			193	3		190	5				1.2	Pp	1995.813		POSS II.J estimates. PM values estimated by comparison with POSS I.O
	72.17631700	35.1855580	4.306	332.493	12.4	13.0									1.3	E2	1998.081		2MASS. Vmags estimated from J- and K-mag values
	72.17714600	35.1855890	4.117	333.106			221.9	9.2	15.8	212.3	-3.0	20.4			0.4	Hw	2010.164	BAB	WISE. PM data calculated from position comparison with 2MASS. Large WISE position error results in large PM error
J0709+3217/3218	07 09 38.458	+32 17 50.67					56.56	-127.02	6.26	60.53	-134.20	11.47						ABB	PM data so far not fully convincing, but a potential CPM candidate
	107.40958333	32.2980833	16.7	19.0											1.2	Pp	1987.890		POSS II.J estimates
	107.41008333	32.2975000	17.1	18.2			127	-176		117	-142				1.2	Pp	1999.855		POSS II.N estimates. PM values estimated by comparison with POSS II.J
	107.41022200	32.2974470	16.854	18.605	17.2	17.9									1.3	E2	1998.895		2MASS. M1 and M2 estimated from J- and K-band
	107.41049580	32.2969272	16.760	18.949			56.56	-127.02	6.26	60.53	-134.20	11.47			0.2	Eu	2013.684	ABB	URAT1. PM data calculated from position comparison with 2MASS
J1225+2836	12 25 46.782	+28 36 03.35					-96	-212		-112	-205							?	PM values so far only estimated - but comparison of POSS images strongly suggest CPM
	186.4507917	28.6074722	15.8	55.6											1.2	Pp	1955.290		POSS I.E estimates
	186.4495417	28.6050556	16.1	55.6			-96	-212		-112	-205				1.2	Pp	1996.308		POSS II.N estimates. PM values estimated by comparison with POSS I.E
	186.4451800	28.6015590	16.042	54.889						-80	-260	4.2			2.5	Es	2005.050		SDSS DR9. No PM data for A
J1233+3518	12 33 25.745	+35 18 25.02					-184	48		-197	48							?	PM values so far only estimated - but comparison of POSS images strongly suggest CPM
	188.3604583	35.3064167	2.9	247.8											1.2	Pp	1950.362		POSS I.O estimates
	188.3580833	35.3069167	3.4	250.9			-184	48		-197	48				1.2	Pp	1988.205		POSS II.J estimates - no resolution, but elongation and similar pm obvious
	188.3572010	35.3069200	3.502	266.582			-155	53	2.8						2.5	Es	2004.283		SDSS DR9. No PM data for B

Table 1 continues on the next page.

CPM Pairs from LSPM so far not WDS Listed

Table 1: Research results for potential common proper motion pairs found in the LSPM catalog. Headline object position based on URAT1 J2000 coordinates for A (with exception of J1906+1652 – in lack of URAT1 data we had to use the average value of our own measurements)

LSPM	RA	Dec	Sep "	PA °	M1	M2	pmRA1	pmDE1	e_pm1	pmRA2	pmDE2	e_pm2	Spc1	Spc2	Ap	Me	Date	CPM Rat	Source/Notes
J1234+ 3014	12 34 26.789	+30 14 43.66					-81.20	-154.80	8.70	-90.80	-162.90	10.10						ACB	2MASS error a bit high, ditto vector length difference. Comparison POSS I.E with POSS II.N suggests CPM. Difference in proper motion vector length might be a hint for an orbit
	188.612750	30.247611													1.2	Pp	1950 .272		POSS I.O estimate. Secondary not visible in image.
	188.611542	30.234500	5.522	243.400											1.2	Pp	1997 .414		POSS II.N estimate
	188.611670	30.245541	5.057	240.900	14.400										1.3	E2	1998 .170		2MASS. M1 estimated from J- and K-band, J- and K-band values for M2 not suited for Vmag calculation
	188.611580	30.245399					-88.00	-155.00							0.2	Eu	2000 .000		UCAC4. Secondary not shown in UCAC4.
	188.611522	30.245238	5.261	240.888			-82	-154	2.8	-93.93	-175.57	23.98			2.5	Es	2004 .957		SDSS-DR9. PM data for A from SDSS DR9 catalog and for B calculated from position comparison SDSS DR9 with 2MASS.
	188.611264	30.244873	5.345	239.893	15.450		-81.20	-154.80	8.70	-90.80	-162.90	10.10	K0		02	Eu	2014 .013	ACB	URAT1. Spc1 from V-R values. PM data calculated from position comparison with 2MASS
LSPM	**RA**	**Dec**	**Sep "**	**PA °**	**M1**	**M2**	**pmRA1**	**pmDE1**	**e_pm1**	**pmRA2**	**pmDE2**	**e_pm2**	**Spc1**	**Spc2**	**Ap**	**Me**	**Date**	**CPM Rat**	**Source/Notes**
J1300+ 5027	13 00 04.529	+50 27 15.08					-196.1	-39.3	6.2	-200.6	-37.9	6.2						AAA	Solid CPM candidate
	195.022292	50.454889	2.320	54.381			-196.1	-39.3	6.2	-200.6	-37.9	6.2			1.2	Pp	1953 .289		POSS I.O estimate. Secondary very hard to identify in POSSI image, possible the coordinates for it are off slightly as a result.
	195.091667	50.454333	4.015	68.064			-162	-45		-119	-41				1.2	Pp	1995 .233		POSS II.J estimate. PM data calculated from position comparison with POSSI.
	195.018868	50.454189	4.529	62.904	14.400	16.200									1.3	E2	2000 .026		2MASS. M1 and M2 estimated from J- and K-band
	195.018552	50.454148	4.544	62.849			-184	-34	5.7	-148.59	-28.52	32.43			2.5	Es	2003 .087		SDSS-DR9. PM data for A from SDSS DR9 catalog and for B calculated from position comparison SDSS DR9 with 2MASS.
	195.017706	50.454041	4.481	62.319			-196.1	-39.3	6.2	-200.6	-37.9	6.2			0.2	Eu	2013 .615	AAA	URAT1. PM data calculated from position comparison with 2MASS.
	195.017700	50.454000	4.480	62.300			196.1	-39.3	6	-200.7	-37.9	6.3			0.2	Eu	2013 .615		I/330 MPN 4259 from URAT1.
LSPM	**RA**	**Dec**	**Sep "**	**PA °**	**M1**	**M2**	**pmRA1**	**pmDE1**	**e_pm1**	**pmRA2**	**pmDE2**	**e_pm2**	**Spc1**	**Spc2**	**Ap**	**Me**	**Date**	**CPM Rat**	**Source/Notes**
J1301+ 4057	13 01 13.196	+40 57 11.08					259.94	-576.54	31.38	257.20	-593.96	31.38						AAA	Comparison of POSS images strongly suggests CPM
	195.2999583	40.9618333	4.3	211.5											1.2	Pp	1950 .430		POSS I.O estimate
	195.3040417	40.9552778	4.4	214.7			265	-563		259	-560				1.2	Pp	1992 .380		POSS II.J estimates - no resolution, but elongation and similar pm obvious
	195.3045080	40.9538730	4.741	216.039	13.1										1.3	E2	1998 .290		2MASS. M1 estimated from J- and K-band
	195.3049820	40.9530790	4.819	215.566			259.94	-576.54	31.38	257.20	-593.96	31.38			2.5	Es	2003 .248	AAA	SDSS 9. PM data calculated from position comparison with 2MASS

Table 1 continues on the next page.

CPM Pairs from LSPM so far not WDS Listed

Table 1 (continued). Research results for potential common proper motion pairs found in the LSPM catalog. Headline object position based on URAT1 J2000 coordinates for A (with exception of J1906+1652 – in lack of URAT1 data we had to use the average value of our own measurements)

LSPM	RA	Dec	Sep "	PA °	M1	M2	pmRA1	pmDE1	e_pm1	pmRA2	pmDE2	e_pm2	Spc1	Spc2	Ap	Me	Date	CPM Rat	Source/Notes
J1331+3821	13 31 37.727	+38 21 41.35					132.44	-98.65	5.52	127.98	-100.31	5.48						AAA	Solid CPM candidate
	202.9051250	38.3629167	10.9	185.6											1.2	Pp	1950.461		POSS I.E estimates
	202.9066250	38.3618333	10.5	183.8			93	-85		100	-79				1.2	Pp	1996.219		POSS II.J estimates. PM values estimated by comparison with POSS I.E
	202.9071160	38.3615340	10.415	186.239	14.3	16.7									1.3	E2	1998.295		2MASS. M1 and M2 estimated from J- and K -band
	202.9073520	38.3614110	10.450	186.514			132.67	-88.18	16.90	121.99	-93.92	16.90			2.5	Es	2003.316		SDSS DR9. PM data calculated from position comparison with 2MASS
	202.9078000	38.3611000	10.46	186.5			132.5	-98.6	5.3	128	-100.3	5.3			0.2	Eu	2013.725		I/330 MPN4526 from URAT1
	202.9078377	38.3611125	10.457	186.526			132.44	-98.65	5.52	127.98	-100.31	5.48			0.2	Eu	2013.725	AAA	URAT1. PM data calculated from position comparison with 2MASS
LSPM	**RA**	**Dec**	**Sep "**	**PA °**	**M1**	**M2**	**pmRA1**	**pmDE1**	**e_pm1**	**pmRA2**	**pmDE2**	**e_pm2**	**Spc1**	**Spc2**	**Ap**	**Me**	**Date**	**CPM Rat**	**Source/Notes**
J1347+0746	13 47 18.815	+07 46 12.03					-157.1	27.2	13.9	-152.7	31.3	6.4						AAB	Solid CPM candidate based on URAT1-2MASS comparison; PM from POSSII.J estimate below not dependable -- see note under POSSI.O estimate.
	206.830417	7.769639	14.916	170.247											1.2	Pp	1950.297		POSS I.O estimate. Primary and secondary too faint to register for Aladin PHOT tool; secondary very hard to distinguish in POSSI image.
	206.828667	7.770194	11.563	170.381			-142	45		-155	120				1.2	Pp	1994.042		POSS II.J estimate. PM data calculated from position comparison with POSSI. See note on POSSI.
	206.828813	7.769966	11.240	172.300	18.820										1.2	Pp	1993.316		GSC2.3. M1 is GSC Vmag.
	206.828387	7.770011	11.495	171.883	16.200	16.800									1.3	E2	2000.231		2MASS. M1 and M2 estimated from J- and K -band
	206.828280	7.770051	11.446	171.560			-160	24	4.2	-163	13	5.7			2.5	Es	2003.319		SDSS-DR9. PM data from SDSS DR9 catalog
	206.827969	7.770100	11.245	171.463			-148.1	31.8	13.0	-143.5	57.6	13.5			0.4	Hw	2010.298		WISE. PM data calculated from position comparison with 2MASS. Large WISE position error results in large PM error
	206.827800	7.770100	11.440	171.600			-157.1	27.2	6.2	-152.7	31.3	6.4			0.2	Eu	2013.515		I/330 MPN 4663 from URAT1.
	206.827804	7.770111	11.442	171.644			-157.1	27.2	13.9	-152.7	31.3	6.4			0.2	Eu	2013.525	AAB	URAT1. PM data calculated from position comparison with 2MASS
LSPM	**RA**	**Dec**	**Sep "**	**PA °**	**M1**	**M2**	**pmRA1**	**pmDE1**	**e_pm1**	**pmRA2**	**pmDE2**	**e_pm2**	**Spc1**	**Spc2**	**Ap**	**Me**	**Date**	**CPM Rat**	**Source/Notes**
J1351+4337	13 51 24.343	+43 37 10.24					-173.00	23.56	13.29	-168.11	24.20	14.24						AAB	Despite the rather large 2MASS position error a solid CPM candidate
	207.8548750	43.6188611	6.8	43.0											1.2	Pp	1955.279		POSS I.E estimates
	207.8512500	43.6195833	6.6	48.0			-224	62		-219	48				1.2	Pp	1997.368		POSS II.N estimates. PM values estimated by comparison with POSS I.E
	207.8514100	43.6195140	6.337	45.219	15.11	16.95									1.3	E2	2000.313		2MASS. M1 and M2 estimated from J- and K -band
	207.8512680	43.6195730	6.405	45.407			-184	10	4.2	-105.36	83.87	65.81			2.5	Es	2003.232		SDSS 9. PM data for A from SDSS DR9 catalog and for B calculated from position comparison with 2MASS
	207.8508500	43.6196440	6.728	48.516			-143.7	46.1	33.8	-90.4	45.4	10.9			0.4	Hw	2010.466		WISE. PM data calculated from position comparison with 2MASS. Large WISE RA position error makes pm values suspect
	207.8505206	43.6196017	6.380	45.467	15.987		-173.00	23.56	13.29	-168.11	24.20	14.24	M0		0.2	Eu	2013.757	AAB	URAT1. PM data calculated from position comparison with 2MASS. Spectral class A based on B-V color index
	207.8505000	43.6196000	6.38	45.5			-173.0	23.6	6.0	-168.1	24.2	6.2			0.2	Eu	2013.757		I/330 MPN4696 from URAT1
	207.8503458	43.6196167			15.939										0.61	C	2016.519		iT24 1x60s. No resolution of B

Table 1 continues on the next page.

CPM Pairs from LSPM so far not WDS Listed

Table 1 (continued). Research results for potential common proper motion pairs found in the LSPM catalog. Headline object position based on URAT1 J2000 coordinates for A (with exception of J1906+1652 – in lack of URAT1 data we had to use the average value of our own measurements)

LSPM	RA	Dec	Sep "	PA °	M1	M2	pmRA1	pmDE1	e_pm1	pmRA2	pmDE2	e_pm2	Spc1	Spc2	Ap	Me	Date	CPM Rat	Source/Notes
J1414+5920	14 14 17.570	+59 20 20.98					19.9	-167.3	5.8	10.3	-173.9	6.1						BAA	Solid CPM candidate even if PM direction seems slightly different
	213.572333	59.341556	9.640	50.900											1.2	Pp	1953.202		POSS I.O estimate. Secondary almost impossible to see in image, tagged manually.
	213.572917	59.339361	9.478	52.270			24	-179		-16	-297				1.2	Pp	1997.530		POSS II.N estimate. PM data calculated from position comparison with POSSI. Secondary tagged manually, results checked twice to confirm PM results.
	213.573205	59.339105	10.160	48.600	11.740								M0		1.2	Pp	1998.765		GSC 2.3. M1 is Vmag. Epoch shown is mean epoch (Epoch of primary is 2000.000; Epoch of secondary is 1997.529).
	213.573199	59.339203	9.508	51.726	11.700	17.200									1.3	E2	1999.123		2MASS. M1 and M2 estimated from J - and K-band
	213.573357	59.338526	9.406	51.089			19.9	-167.3	5.8	10.3	-173.9	6.1			0.2	Eu	2013.369	BAA	URAT1. PM data calculated from position comparison with 2MASS.
	213.573400	59.338500	9.510	51.100			19.9	-167.3	5.5	10.3	-173.9	6.3			0.2	Eu	2013.369		I/330 MPN 4915 from URAT1.
LSPM	**RA**	**Dec**	**Sep "**	**PA °**	**M1**	**M2**	**pmRA1**	**pmDE1**	**e_pm1**	**pmRA2**	**pmDE2**	**e_pm2**	**Spc1**	**Spc2**	**Ap**	**Me**	**Date**	**CPM Rat**	**Source/Notes**
J1417+7031	14 17 58.064	+70 31 47.52			14.12	15.51	-141	136		-141	134							?	PM values so far only estimated - but comparison of POSS images strongly suggests CPM
	214.4975417	70.5281667	4.8	340.4											1.2	Pp	1955.386		POSS I.O estimates
	214.4926250	70.5297500	4.7	340.0			-141	136		-141	134				1.2	Pp	1997.289		POSS II.N estimates. PM values estimated by comparison with POSS I.O
	214.4899917	70.5303056	3.414	344.540	14.122	15.509									.61	C	2016.505		iT24 stack 5x10s. Err_Sep=0.022", Err_PA=0.375°, Err_M1=0.036, Err_M2=0.053
LSPM	**RA**	**Dec**	**Sep "**	**PA °**	**M1**	**M2**	**pmRA1**	**pmDE1**	**e_pm1**	**pmRA2**	**pmDE2**	**e_pm2**	**Spc1**	**Spc2**	**Ap**	**Me**	**Date**	**CPM Rat**	**Source/Notes**
J1418+3219	14 18 29.115	+32 19 26.95			10.37	16.40	112.22	-150.90	11.30	108.48	-151.18	10.99						AAB	Despite the rather large 2MASS position error a solid CPM candidate
	214.6185000	32.3266111	6.9	129.6											1.2	Pp	1950.278		POSS I.E estimates
	214.6208333	32.3244167	6.4	132.5			158	-176		144	-174				1.2	Pp	1995.146		POSS II.N estimates. PM values estimated by comparison with POSS I.E
	214.6212500	32.3242230	6.203	134.794	10.4	15.0									1.3	E2	1998.341		2MASS. M1 and M2 estimated from J - and K-band
	214.6215040	32.3240410	6.316	137.524											2.5	Es	2004.291		SDSS DR9
	214.6218203	32.3235750	6.244	135.319	10.323		112.22	-150.90	11.30	108.48	-151.18	10.99	G0		0.2	Eu	2014.016	AAB	URAT1. PM data calculated from position comparison with 2MASS. Spectral class A from B-V color index
	214.6218000	32.3236000	6.24	135.3			112.2	-150.8	5.3	108.5	-151.2	5.1			0.2	Eu	2014.016		I/330 MPN4963 from URAT1
	214.6219625	32.3233806	5.628	134.437	10.368	16.395									0.61	C	2016.519		iT24 1x60s. Overlapping star disks. SNR B <20. Err_Sep=0.028", Err_PA=0.288°, Err_M1=0.030, Err_M2=0.076

Table 1 continues on the next page.

CPM Pairs from LSPM so far not WDS Listed

Table 1 (continued). Research results for potential common proper motion pairs found in the LSPM catalog. Headline object position based on URAT1 J2000 coordinates for A (with exception of J1906+1652 – in lack of URAT1 data we had to use the average value of our own measurements)

LSPM	RA	Dec	Sep "	PA °	M1	M2	pmRA1	pmDE1	e_pm1	pmRA2	pmDE2	e_pm2	Spc1	Spc2	Ap	Me	Date	CPM Rat	Source/Notes
J1418+3634	14 18 55.328	+36 34 29.50					-202.19	45.13	9.76	-198.50	45.76	9.85						AAA	Solid CPM candidate
	214.7349583	36.5738333	12.0	189.8											1.2	Pp	1950.362		POSS I.E estimates
	214.7318750	36.5744722	12.0	189.8			-212	55		-212	55				1.2	Pp	1992.380		POSS II.N estimates. PM values estimated by comparison with POSS I.E
	214.7316100	36.5746690	11.928	189.797	15.8	17.1									1.3	E2	1998.301		2MASS. M1 and M2 estimated from J - and K-band
	214.7312520	36.5746900	11.912	189.542			-206.35	15.07	29.91	-195.40	16.51	29.91			2.5	Es	2003.316		SDSS 9. PM data calculated from position comparison with 2MASS
	214.7305350	36.5748617	11.911	189.391			-202.19	45.13	9.76	-198.50	45.76	9.85			0.2	Eu	2013.598	AAA	URAT1. PM data calculated from position comparison with 2MASS
	214.7303167	36.5749083			18.063										0.61	C	2016.519		iT24 1x60s. SNR A <20. No resolution of B
	214.7302917	36.5748611			18.371										0.61	C	2016.521		iT24 1x60s. SNR A <20. No resolution of B
LSPM	**RA**	**Dec**	**Sep "**	**PA °**	**M1**	**M2**	**pmRA1**	**pmDE1**	**e_pm1**	**pmRA2**	**pmDE2**	**e_pm2**	**Spc1**	**Spc2**	**Ap**	**Me**	**Date**	**CPM Rat**	**Source/Notes**
J1422+5111	14 22 18.413	+51 11 56.53			16.58	17.19	-164.1	69.8	5.9	-161.5	65.8	6						AAA	Solid CPM candidate
	215.580333	51.198306	4.856	194.573											1.2	Pp	1953.278		POSS I.O estimate. Both stars tagged manually; Aladin centroid located midway between the pair.
	215.576750	51.198972	5.071	189.603			-183	54		-175	48				1.2	Pp	1996.536		POSS II.N estimate. PM data calculated from position comparison with POSSI. Both stars tagged manually; Aladin centroid located midway between the pair.
	215.577164	51.198918	4.907	190.100	15.390										1.2	Pp	1994.442		GSC2.3. M1 is Vmag.
	215.576766	51.199024	5.145	190.740	14.600	15.200									1.3	E2	1999.390		2MASS. M1 and M2 estimated from J - and K-band
	215.576536	51.199086	5.186	190.350			-175.3	75.4	28.7	-166.1	59.6	28.7			2.5	Es	2002.350		SDSS-DR9. PM data calculated from position comparison with 2MASS. Time frame too short to allow for reliable PM results
	215.575940	51.199279	5.125	189.757			-168.2	82.9	13.3	-160.1	83.2	17.7			0.4	Hw	2010.465		WISE. PM data calculated from position comparison with 2MASS
	215.575722	51.199302	5.198	190.029			-164.1	69.8	5.9	-161.5	65.8	6			0.2	Eu	2013.691	AAA	URAT1. PM data calculated from position comparison with 2MASS
	215.575700	51.199300	5.200	190.000			-164.1	69.8	5.6	-161.6	65.8	5.7			0.2	Eu	2013.691		I/330 MPN 4993 from URAT1.
							-161.2	68.3	2.6	-160.3	67.4	2.8			0.2	Eu	2013.691		PM data calculated from position comparison SDSS DR9 to URAT1
	215.575533	51.199350	5.331	191.699	16.580	17.190									0.61	C	2016.519		iT24 1x60s. Err Sep = 0.014, Err PA = 0.152, Err M1 = 0.039, Err M2 = 0.050.

Table 1 continues on the next page.

CPM Pairs from LSPM so far not WDS Listed

Table 1 (continued). Research results for potential common proper motion pairs found in the LSPM catalog. Headline object position based on URAT1 J2000 coordinates for A (with exception of J1906+1652 – in lack of URAT1 data we had to use the average value of our own measurements)

LSPM	RA	Dec	Sep "	PA °	M1	M2	pmRA1	pmDE1	e_pm1	pmRA2	pmDE2	e_pm2	Spc1	Spc2	Ap	Me	Date	CPM Rat	Source/Notes
J1511+0912	15 11 33.050	+09 12 23.70					-107	27		-111	23							?	Comparison of POSS images suggests CPM. PM data estimated
	227.889083	9.206194	3.023	136.703											1.2	Pp	1951.518		POSS I.E estimate. Both stars tagged manually
	227.887750	9.206528	3.077	141.269			-107	27		-111	23				1.2	Pp	1995.624		POSS II.N estimate. Both stars tagged manually
	227.887696	9.206590			15.680										1.3	E2	2000.272		2MASS. M1 and M2 estimated from J - and K-band, secondary not identified in 2MASS.
	227.887582	9.206693	3.427	140.000											2.5	Es	2003.245		SDSS-DR9. No secondary in 2MASS for PM comparison
	227.887153	9.206882					-144.2	78.5							0.2	Eu	2013.655		URAT1. Secondary not identified in URAT1.
LSPM	**RA**	**Dec**	**Sep "**	**PA °**	**M1**	**M2**	**pmRA1**	**pmDE1**	**e_pm1**	**pmRA2**	**pmDE2**	**e_pm2**	**Spc1**	**Spc2**	**Ap**	**Me**	**Date**	**CPM Rat**	**Source/Notes**
J1524+3146	15 24 34.482	+31 46 48.79			14.35	19.02	-206.4	43.2	6.0	-214.2	39.1	5.9						AAA	Solid CPM candidate
	231.148167	31.780306	4.823	258.033											1.2	Pp	1954.482		POSS I.O estimate. Both centroids tagged manually.
	231.145458	31.780750	5.808	255.032			-198	38		-219	26				1.2	Pp	1996.309		POSS II.N estimate. Both centroids tagged manually.
	231.145380	31.780588	5.695	253.890	14.300	17.200									1.3	E2	1998.246		2MASS. M1 and M2 estimated from J - and K-band
	231.145027	31.780644	5.880	253.679			-193	43	4.2	-247.0	25.6	18.2			2.5	Es	2003.314		SDSS-DR9. PM data for A from SDSS DR9 catalog and for B calculated from position comparison with 2MASS.
	231.144336	31.780774	5.851	253.720			-206.4	43.2	6.0	-214.2	39.1	5.9			0.2	Eu	2013.779	AAA	URAT1. PM data calculated from position comparison with 2MASS. Attention: Aladin shows URAT1 J2000 positions in image wrong due to wrong URAT1 PM data
	231.144192	31.780825			14.323										0.61	C	2016.505		iT24 stack 5x10s. No resolution of B. Err M1 = 0.100.
	231.144204	31.780817	4.861	250.784	14.351	19.016									0.61	C	2016.516		iT24 1x60s. SNR B <10. Err Sep = 0.089, Err PA = 1.054, Err M1 = 0.061, Err M2 = 0.236.
LSPM	**RA**	**Dec**	**Sep "**	**PA °**	**M1**	**M2**	**pmRA1**	**pmDE1**	**e_pm1**	**pmRA2**	**pmDE2**	**e_pm2**	**Spc1**	**Spc2**	**Ap**	**Me**	**Date**	**CPM Rat**	**Source/Notes**
J1524+3942	15 24 17.987	+39 42 22.16			15.72	18.12	-41.18	178.93	5.92	-44.28	176.05	5.95						AAA	Solid CPM candidate
	231.0755417	39.7042222	6.7	140.1											1.2	Pp	1955.244		POSS I.O estimates
	231.0748333	39.7061389	6.8	138.6			-47	164		-41	164				1.2	Pp	1997.412		POSS II.N estimates. PM values estimated by comparison with POSS I.O
	231.0749560	39.7061270	6.630	137.832	13.913	15.735									1.3	E2	1999.393		2MASS. M1 and M2 estimated from J - and K-band
	231.074778	39.7066740	6.363	136.965			-44.7	178.5	21.3	-54.5	202.3	9.5			0.4	Hw	2010.423		WISE. PM data calculated from position comparison with 2MASS. Large WISE position error results in large PM error
	231.0747000	39.7068000	6.64	138.4			-41.1	179.0	5.7	-44.2	176.1	5.7			0.2	Eu	2013.693		I/330 MPN5488 from URAT1
	231.0747428	39.7068397	6.644	138.413			-41.18	178.93	5.92	-44.28	176.05	5.95			0.2	Eu	2013.693	AAA	URAT1. PM data calculated from position comparison with 2MASS
	231.0747042	39.7069750	6.485	138.141	15.715	18.116									0.61	C	2016.519		iT24 1x60s. SNR B <20. Err_Sep=0.014", Err_PA=0.125°, Err_M1=0.043, Err_M2=0.088

Table 1 continues on the next page.

CPM Pairs from LSPM so far not WDS Listed

Table 1 (continued). Research results for potential common proper motion pairs found in the LSPM catalog. Headline object position based on URAT1 J2000 coordinates for A (with exception of J1906+1652 – in lack of URAT1 data we had to use the average value of our own measurements)

LSPM	RA	Dec	Sep "	PA °	M1	M2	pmRA1	pmDE1	e_pm1	pmRA2	pmDE2	e_pm2	Spc1	Spc2	Ap	Me	Date	CPM Rat	Source/Notes
J1532+1733	15 32 33.356	+17 33 18.20			16.67	18.17	-294.50	81.00	7.50	-300.20	77.30	7.30						ABA	Solid CPM candidate. Difference of PM vector length might be a hint for an orbit
	233.144042	17.553861	2.417	24.468											1.2	Pp	1950 .291		POSS I.O estimate. Center of secondary difficult to locate because image is blurred with primary.
	233.140708	17.555250	2.738	18.265			-259.00	113.00		-263.00	122.00				1.2	Pp	1994 .450		POSS II.N estimate. PM data calculated from position comparison with POSSI.
	233.140220	17.554731	4.274	26.879	15.000	16.000									1.3	E2	1999 .133		2MASS. M1 and M2 estimated from J - and K-band
	233.139269	17.555085	4.573	32.102			-291.0	113.6	15.1	-246.7	119.1	6.9			0.4	Hw	2010 .349		WISE. PM data calculated from position comparison with 2MASS
	233.138983	17.555055	4.171	24.909			-294.50	81.00	7.50	-300.20	77.30	7.30			0.2	Eu	2013 .704	ABA	URAT1. PM data calculated from position comparison with 2MASS
	233.138733	17.555067			16.670										.61	C	2016 .510		iT24 stack 5x10s. No resolution of B. SNR A <20. Err M1 = 0.084.
	233.138754	17.555097	4.399	29.190	16.673	18.168									.61	C	2016 .516		iT24 1x60s. SNR B <20. Err Sep = 0.042, Err PA = 0.553, Err M1 = 0.056, Err M2 = 0.092.
																			NOTE: No UCAC4 data for this pair.
LSPM	**RA**	**Dec**	**Sep "**	**PA °**	**M1**	**M2**	**pmRA1**	**pmDE1**	**e_pm1**	**pmRA2**	**pmDE2**	**e_pm2**	**Spc1**	**Spc2**	**Ap**	**Me**	**Date**	**CPM Rat**	**Source/Notes**
J1604+4620	16 04 12.236	+46 20 15.94			9.98	15.14	-160.7	-76.3	11.2	-165.8	-75.7	11.3						AAB	Solid CPM candidate despite the rather large 2MASS position error
	241.051027	46.337776	6.481	58.448	9.200	11.700									1.3	E2	1999 .349		2MASS. M1 and M2 estimated from J - and K-band
	241.050973	46.337744	6.152	57.226											2.5	Es	2001 .375		SDSS-DR9. Time frame too short to allow for reliable calculated PM results with 2MASS and SDSS DR9 position error in this case far too large to make a useful PM calculation SDSS DR9 to URAT1
	241.050343	46.337500	6.225	57.579			-154.4	-90.2	8.3	-178.7	-95.1	26.8			0.4	Hw	2010 .362		WISE. PM data calculated from position comparison with 2MASS. Large WISE position error results in large PM error
	241.050100	46.337500	6.450	58.100			-160.7	-76.3	5.7	-165.8	-75.7	5.8			0.2	Eu	2013 .630		I/330 MPN 5773 from URAT1.
	241.050099	46.337472	6.448	58.064			-160.7	-76.3	11.2	-165.8	-75.7	11.3			0.2	Eu	2013 .630	AAB	URAT1. PM data calculated from position comparison with 2MASS
	241.050033	46.337383	6.517	55.085	9.928	15.292									.61	C	2016 .519		iT24 1x60s. Overlapping star disks. Err Sep = 0.028, Err PA = 0.249, Err M1 = 0.050, Err M2 = 0.059.
	241.049967	46.337289	6.420	53.600	9.975	15.135									.61	C	2016 .521		iT24 1x60s. Overlapping star disks. Err Sep = 0.061, Err PA = 0.543, Err M1 = 0.050, Err M2 = 0.069.
																			Note: Primary and secondary in POSS images merged in glare of primary, not possible to separate the two for measurements.

Table 1 continues on the next page.

CPM Pairs from LSPM so far not WDS Listed

Table 1 (continued). Research results for potential common proper motion pairs found in the LSPM catalog. Headline object position based on URAT1 J2000 coordinates for A (with exception of J1906+1652 – in lack of URAT1 data we had to use the average value of our own measurements)

LSPM	RA	Dec	Sep "	PA °	M1	M2	pmRA1	pmDE1	e_pm1	pmRA2	pmDE2	e_pm2	Spc1	Spc2	Ap	Me	Date	CPM Rat	Source/Notes
J1638+1658	16 38 33.088	+16 58 12.27			16.40	19.38	40.02	-162.37	5.30	39.71	-158.60	5.32						AAA	Solid CPM candidate
	249.6371667	16.9725278	4.5	113.4											1.2	Pp	1950.204		POSS I.O estimates
	249.6377083	16.9706667	4.6	111.6			44	-159		48	-157				1.2	Pp	1992.317		POSS II.N estimates. PM values estimated by comparison with POSS I.O
	249.6378370	16.9701860	5.253	112.826	15.0	16.5									1.3	E2	1997.561		2MASS. M1 and M2 estimated from J - and K-band
	249.6379070	16.9698960	5.272	112.269			35.83	-155.18	12.61	41.46	-149.29	12.61			2.5	Es	2004.289		SDSS 9. PM data calculated from position comparison with 2MASS (catalog PM data for A seems suspect)
	249.6380000	16.9695000	5.22	112.1			40.0	-162.3	5.1	39.8	-158.6	5.2			0.2	Eu	2013.539		I/330 MPN6001 from URAT1
	249.6380231	16.9694639	5.219	112.144	16.231		40.02	-162.37	5.30	39.71	-158.60	5.32	M0		0.2	Eu	2013.539	AAA	URAT1. PM data calculated from position comparison with 2MASS. Spectral class A based on B-V color index
	249.6380750	16.9693222	5.400	113.576	16.401	19.378									.61	C	2016.519		iT24 1x60s. SNR B <10. Err_Sep=0.014", Err_PA=0.150°, Err_M1=0.046, Err_M2=0.192
LSPM	**RA**	**Dec**	**Sep "**	**PA °**	**M1**	**M2**	**pmRA1**	**pmDE1**	**e_pm1**	**pmRA2**	**pmDE2**	**e_pm2**	**Spc1**	**Spc2**	**Ap**	**Me**	**Date**	**CPM Rat**	**Source/Notes**
J1644+4153	16 44 28.918	+41 53 02.18			12.54	16.33	34.15	-225.45	5.60	32.49	-227.83	5.60						AAA	Solid CPM candidate
	251.1195417	41.8879722	7.1	40.3											1.2	Pp	1953.379		POSS I.O estimate
	251.1203018	41.8847909	6.592	39.357	12.52		36.9	-222.4		214.1	-8.2		M0		0.2	Eu	1988.835		UCAC4 mean epoch. PM values obviously wrong, probably typo. Spectral class A from B-V color index
	251.1202300	41.8853390	6.916	36.008											1.2	Pp	1990.610		GSC2.2 mean epoch
	251.1199583	41.8852222	7.0	40.8											1.2	Pp	1993.379		POSS II.F estimates
	251.1203750	41.8850556	7.3	37.6			52	-243		49	-234				1.2	Pp	1996.618		POSS II.N estimates
	251.1202970	41.8848950	7.285	38.528	12.2	14.1									1.3	E2	1998.429		2MASS. M1 and M2 estimated from J - and K-band
	251.1203790	41.8847430	7.177	38.693											2.5	Es	2001.290		SDSS DR7
	251.1204917	41.8839381	7.263	38.362	12.52		34.15	-225.45	5.60	32.49	-227.83	5.60	M0		0.2	Eu	2013.638	AAA	URAT1. PM data calculated from position comparison with 2MASS. Spectral class A from B-V color index
	251.1205208	41.8838444	6.985	38.456	12.592	16.407									.61	C	2016.499		iT24 stack 5x5s. SNR B<20. Err_Sep=0.085", Err_PA=0.701°, Err_M1=0.041, Err_M2=0.095
	251.1204917	41.8838639	7.151	39.348	12.542	16.328									.61	C	2016.510		iT24 stack 5x10s. SNR B<20. Err_Sep=0.085", Err_PA=0.685°, Err_M1=0.051, Err_M2=0.092

Table 1 continues on the next page.

CPM Pairs from LSPM so far not WDS Listed

Table 1 (continued). Research results for potential common proper motion pairs found in the LSPM catalog. Headline object position based on URAT1 J2000 coordinates for A (with exception of J1906+1652 – in lack of URAT1 data we had to use the average value of our own measurements)

LSPM	RA	Dec	Sep "	PA °	M1	M2	pmRA1	pmDE1	e_pm1	pmRA2	pmDE2	e_pm2	Spc1	Spc2	Ap	Me	Date	CPM Rat	Source/Notes
J1647+1501	16 47 10.643	+15 01 15.33					-155.1	-26.6	6.9	-157.8	-23.4	7.4						AAA	Solid CPM candidate
	251.796250	15.021667	12.214	357.281											1.2	Pp	1950 .376		POSS I.O estimate. Secondary tagged manually.
	251.794542	15.021139	12.621	356.710			-135	-43		-138	-34				1.2	Pp	1992 .317		POSS II.N estimate. PM data calculated from position comparison with POSSI. Secondary tagged manually.
	251.794804	15.021013	12.820	355.600	14.670										1.2	Pp	1989 .256		GSC2.3. M1 is Vmag.
	251.794330	15.020923	12.532	355.863	14.500	17.900									1.3	E2	2000 .321		2MASS. M1 and M2 estimated from J - and K-band
	251.794135	15.020893	12.756	355.814			-150	-29	2.8	-173.2	-16.22	24.78			2.5	Es	2004 .316		SDSS-DR9. PM data for A from SDSS DR9 catalog and for B calculated from position comparison with 2MASS.
	251.793736	15.020825	12.575	355.652			-155.1	-26.6	6.9	-157.8	-23.4	7.4			0.2	Eu	2013 .685	AAA	URAT1. PM data calculated from position comparison with 2MASS
	251.793700	15.020800	12.580	355.700			-155.2	-26.5	6.1	-157.8	-23.4	6.4			0.2	Eu	2013 .685		I/330 MPN 6063 from URAT1.
	251.793688	15.020742			14.933										.61	C	2016 .506		iT27 stack 5x10s. SNR A <20, no resolution of B. Err M1 = 0.111
	251.793813	15.020897			14.935										.61	C	2016 .522		iT27 stack 5x10s. SNR A <20, no resolution of B. Err M1 = 0.118
LSPM	**RA**	**Dec**	**Sep "**	**PA °**	**M1**	**M2**	**pmRA1**	**pmDE1**	**e_pm1**	**pmRA2**	**pmDE2**	**e_pm2**	**Spc1**	**Spc2**	**Ap**	**Me**	**Date**	**CPM Rat**	**Source/Notes**
J1708+3558	17 08 48.075	+35 58 04.19			16.10	16.73	11.17	147.21	6.45	11.04	149.21	6.48						AAA	Solid CPM candidate
	257.1997917	35.9660556	5.2	237.4											1.2	Pp	1954 .507		POSS I.O estimates
	257.2001667	35.9675278	5.2	237.4			28	136		28	136				1.2	Pp	1993 .489		POSS II.N estimates. PM values estimated by comparison with POSS I.O
	257.2003060	35.9677620	5.738	236.917	14.2	14.6									1.3	E2	1998 .355		2MASS. M1 and M2 estimated from J - and K-band
	257.200312	35.9678610	5.756	236.906											2.5	Es	2001 .225		SDSS 9. No catalog PM data available. Time distance to 2MASS too short to make reasonable PM data calculations
	257.200407	35.9682860	5.587	236.612			24.9	159.8	13.8	37.0	164.7	11.7			0.4	Hw	2010 .162		WISE. PM data calculated from position comparison with 2MASS. Large WISE position error results in large PM error
	257.2004000	35.9684000	5.73	237.1			11.2	147.2	5.3	11.1	149.2	5.3			0.2	Eu	2013 .678		I/330 MPN6235 from URAT1
	257.2003649	35.9683900	5.729	237.101			11.17	147.21	6.45	11.04	149.21	6.48			0.2	Eu	2013 .678	AAA	URAT1. PM data calculated from position comparison with 2MASS
	257.2003708	35.9685167	5.742	237.149	16.101	16.730									.61	C	2016 .519		iT24 1x60s. Err_Sep=0.022", Err_PA=0.223°, Err_M1=0.035, Err_M2=0.041

Table 1 continues on the next page.

CPM Pairs from LSPM so far not WDS Listed

Table 1 (continued). Research results for potential common proper motion pairs found in the LSPM catalog. Headline object position based on URAT1 J2000 coordinates for A (with exception of J1906+1652 – in lack of URAT1 data we had to use the average value of our own measurements)

LSPM	RA	Dec	Sep "	PA °	M1	M2	pmRA1	pmDE1	e_pm1	pmRA2	pmDE2	e_pm2	Spc1	Spc2	Ap	Me	Date	CPM Rat	Source/Notes
J1714+0517	17 14 45.267	+05 17 43.19			18.19	19.37	-18.70	-145.60	15.20	-31.40	-144.40	15.90						BAC	Relatively large 2MASS errors make it hard to come to a conclusion, but visual comparison of POSS images strongly suggests CPM
	258.689333	5.297389	5.420	157.305											1.2	Pp	1950.523		POSS I.O estimate. Aladin picks central point between the two stars as centroid, so ineffective in this case; estimates done manually here, also for POSSII image.
	258.688625	5.295555	4.514	152.401			-54	-141		-54	-120				1.2	Pp	1997.281		POSS II.F estimate. PM data calculated from position comparison with POSSI.
	258.688746	5.295443	4.418	154.100											1.2	Pp	1997.281		GSC2.3 (same epoch for both stars)
	258.688611	5.295315	4.415	154.616	17.61	18.51									1.3	E2	2000.403		2MASS. M1 and M2 estimated from J- and K-band
	258.688611	5.295315	4.324	156.453			-18.70	-145.60	15.20	-31.40	-144.40	15.90			0.2	Eu	2013.527	BAC	URAT1. No Vmag for either component. PM data calculated from position comparison with 2MASS
	258.688533	5.294658	4.037	167.393	18.185	19.368									.61	C	2016.516		iT24 1x60s. SNR A <20 and B <10. Err Sep = 0.071, Err PA = 1.003, Err M1 = 0.087, Err M2 = 0.197.
LSPM	**RA**	**Dec**	**Sep "**	**PA °**	**M1**	**M2**	**pmRA1**	**pmDE1**	**e_pm1**	**pmRA2**	**pmDE2**	**e_pm2**	**Spc1**	**Spc2**	**Ap**	**Me**	**Date**	**CPM Rat**	**Source/Notes**
J1723+0425	17 23 51.722	+04 25 31.81					-115	-103		-112	-103							?	PM values so far only estimated - but comparison of POSS images strongly suggest CPM
	260.9671667	4.4269722	5.0	302.8											1.2	Pp	1950.524		POSS I.O estimates
	260.9656667	4.4256389	4.9	303.8			-115	-103		-112	-103				1.2	Pp	1997.281		POSS II.F estimates - no resolution, but elongation and similar pm obvious
	260.9654920	4.4254900	4.560	302.628	10.4										1.3	E2	2000.441		2MASS. Vmag estimated from J- and K-mag values
	260.9649625	4.4250556			10.341										.61	C	2016.505		iT24 stack 5x10s. No resolution of B
LSPM	**RA**	**Dec**	**Sep "**	**PA °**	**M1**	**M2**	**pmRA1**	**pmDE1**	**e_pm1**	**pmRA2**	**pmDE2**	**e_pm2**	**Spc1**	**Spc2**	**Ap**	**Me**	**Date**	**CPM Rat**	**Source/Notes**
J1756+0931	17 56 58.420	+09 31 52.84					-86	-222		-93	-234							?	PM data only estimates but POSSI/POSSII comparison suggests strongly CPM
	269.244417	9.534639	2.835	170.994											1.2	Pp	1950.376		POSS I.O estimate. Secondary tagged manually.
	269.243375	9.531972	3.303	177.433			-86	-222		-93	-234				1.2	Pp	1993.527		POSS II.F estimate. Secondary tagged manually.
	269.243409	9.531318			13.154										1.3	E2	2000.411		2MASS. M1 and M2 estimated from J- and K-band. Secondary not shown in 2MASS.
	269.243143	9.530490			13.521		-71.2	-224.1					M0		0.2	Eu	2013.703		URAT1. PM data from URAT1 data, M1 is URAT1 Vmag, Spc1 is from URAT1 B-V data. Potential secondary shown in URAT1 is located too far away at 10.43” and has an f.mag of 17.11, no PM data shown for it.
	269.243083	9.530311			13.542										.61	C	2016.505		iT24 stack 5x10s. No resolution of B. Err M1 = 0.042.
	269.243046	9.530294			13.617										.61	C	2016.516		iT24 1x60s. No resolution of B. Err M1 = 0.110.
																			Notes: Secondary not identified in SDSS-DR9, primary identified appears to be wrong star also based on magnitude; secondary not identified in WISE.

Table 1 continues on the next page.

CPM Pairs from LSPM so far not WDS Listed

Table 1 (continued). Research results for potential common proper motion pairs found in the LSPM catalog. Headline object position based on URAT1 J2000 coordinates for A (with exception of J1906+1652 – in lack of URAT1 data we had to use the average value of our own measurements)

LSPM	RA	Dec	Sep "	PA °	M1	M2	pmRA1	pmDE1	e_pm1	pmRA2	pmDE2	e_pm2	Spc1	Spc2	Ap	Me	Date	CPM Rat	Source/Notes
J1801+1754	18 01 55.661	+17 54 22.33					-30.4	-204.5	6.8	-25.2	-202.9	6.8						AAA	Solid CPM candidate
	270.482333	17.909306	4.655	101.147											1.2	Pp	1952.539		POSS I.O estimate. Both POSSI and POSSII tagged manually; Aladin phot tool places centroid midway between the two stars.
	270.482208	17.906806	3.570	88.395			-10	-204		-32	-181				1.2	Pp	1993.699		POSS II.F estimate. PM data calculated from position comparison with POSSI. Obvious sign of tandem motion for this pair from POSSI to POSSII images. Differences in PA and PM are result of secondary's shift in position of one full pixel between images.
	270.481918	17.906191	4.923	92.179	14.300	14.900									1.3	E2	2000.193		2MASS. M1 and M2 estimated from J - and K-band
	270.481875	17.905689	5.050	91.184			-14.7	-180.2	14.8	-1.7	-172.0	20.1			0.4	Hw	2010.220		WISE. PM data calculated from position comparison with 2MASS. Large WISE RA position error makes pm values suspect
	270.481800	17.905400	4.990	92.100			-30.4	-204.5	6.1	-25.2	-202.8	6			0.2	Eu	2013.725		I/330 MPN 6605 from URAT1.
	270.481798	17.905424	4.991	92.075			-30.4	-204.5	6.8	-25.2	-202.9	6.8			0.2	Eu	2013.725	AAA	URAT1. PM data calculated from position comparison with 2MASS
LSPM	**RA**	**Dec**	**Sep "**	**PA °**	**M1**	**M2**	**pmRA1**	**pmDE1**	**e_pm1**	**pmRA2**	**pmDE2**	**e_pm2**	**Spc1**	**Spc2**	**Ap**	**Me**	**Date**	**CPM Rat**	**Source/Notes**
J1820+3122	18 20 14.124	+31 22 42.11			11.81	17.96	-10.55	186.16	5.49	-14.56	185.11	5.60						AAA	Solid CPM candidate
	275.0587917	31.3759722	14.4	353.4											1.2	Pp	1951.520		POSS I.O estimates
	275.0586667	31.3782778	14.3	352.3			-9	188		-14	186				1.2	Pp	1995.695		POSS II.N estimates. PM values estimated by comparison with POSS I.O
	275.0588580	31.3782770	14.091	351.584	11.581	15.765									1.3	E2	1998.295		2MASS. M1 and M2 estimated from J - and K-band
	275.0588000	31.3791000	14.03	351.3			-10.5	186.2	5.3	-14.5	185.1	5.4			0.2	Eu	2013.595		I/330 MPN6710 from URAT1
	275.0588050	31.3790758	14.029	351.308	11.787		-10.55	186.16	5.49	-14.56	185.11	5.60	K6		0.2	Eu	2013.595	AAA	URAT1. PM data calculated from position comparison with 2MASS. Spectral class A from B-V color index
	275.0587875	31.3792222	14.131	351.348	11.806	17.964									.61	C	2016.519		iT24 1x60s. SNR B <20. Err_Sep=0.092", Err_PA=0.374°, Err_M1=0.030, Err_M2=0.070

Table 1 continues on the next page.

CPM Pairs from LSPM so far not WDS Listed

Table 1 (continued). Research results for potential common proper motion pairs found in the LSPM catalog. Headline object position based on URAT1 J2000 coordinates for A (with exception of J1906+1652 – in lack of URAT1 data we had to use the average value of our own measurements)

LSPM	RA	Dec	Sep "	PA °	M1	M2	pmRA1	pmDE1	e_pm1	pmRA2	pmDE2	e_pm2	Spc1	Spc2	Ap	Me	Date	CPM Rat	Source/Notes
J1827+5016	18 27 40.643	+50 16 13.06			10.63	13.87	199.40	86.70	10.22	184.01	83.21	6.47						ABA	Solid CPM candidate despite some PM vector length difference (hint for orbit?)
	276.9137917	50.2691667	4.6	223.8											1.2	Pp	1950.382		POSS I.O estimates
	276.9178333	50.2703056	4.8	229.6			211	93		200	98				1.2	Pp	1994.464		POSS II.N estimates. PM values estimated by comparison with POSS I.O
	276.9180260	50.2699280	4.651	235.863	10.3	10.8									1.3	E2	1998.487		2MASS. M1 and M2 estimated from J - and K-band
	276.9193444	50.2702944	4.860	236.865	10.567		199.40	86.70	10.22	184.01	83.21	6.47	M0		0.2	Eu	2013.739	ABA	URAT1. PM data calculated from position comparison with 2MASS. Spectral class A based on B-V color index
	276.9195792	50.2703639	4.750	237.102	10.631	13.867									.61	C	2016.510		iT24 stack 5x10s. Err_Sep=0.014", Err_PA=0.171°, Err_M1=0.020, Err_M2=0.027
LSPM	**RA**	**Dec**	**Sep "**	**PA °**	**M1**	**M2**	**pmRA1**	**pmDE1**	**e_pm1**	**pmRA2**	**pmDE2**	**e_pm2**	**Spc1**	**Spc2**	**Ap**	**Me**	**Date**	**CPM Rat**	**Source/Notes**
J1852+3058	18 52 58.852	+30 58 10.31					-61.6	-191.9	5.6	-64.5	-191.2	5.6						AAA	Solid CPM candidate
	283.245833	30.972306	10.301	359.285											1.2	Pp	1951.507		POSS I.O estimate. Secondary tagged manually.
	283.245167	30.969861	10.607	357.915			-47	-200		-52	-193				1.2	Pp	1995.550		POSS II.N estimate. Secondary tagged manually.
	283.245153	30.969385	13.670	0.400		13.960									1.2	Pp	1992.446		GSC2.3. M2 is Vmag. Epoch shown is mean epoch (Epoch of primary is 1995.554; Epoch of secondary is 1989.338).
	283.245251	30.969620	10.446	356.714	11.000	13.300									1.3	E2	1998.306		2MASS. M1 and M2 estimated from J - and K-band
	283.245214	30.969539	9.911	355.900	11.351		-63.1	-195.1		-58	-198		M0		0.2	Eu	2000.167		UCAC4. M1 is Vmag, Spc1 is from UCAC4 B-V data. Epoch shown is mean epoch of RA of Primary (2000.38), Dec of primary (1999.67), and RA and Dec of secondary (2000.000)
	283.245031	30.968980	10.489	357.166			-56.7	-192.5	7.8	-50.0	-188.6	17.8			0.4	Hw	2010.274		WISE. PM data calculated from position comparison with 2MASS
	283.245000	30.968800	10.450	356.500			-61.6	-191.9	5.5	-64.4	-191.2	5.4			0.2	Eu	2013.384		I/330 MPN 7003 from URAT1.
	283.244950	30.968817	10.452	356.468			-61.6	-191.9	5.6	-64.5	-191.2	5.6			0.2	Eu	2013.384	AAA	URAT1. PM data calculated from position comparison with 2MASS

Table 1 continues on the next page.

CPM Pairs from LSPM so far not WDS Listed

Table 1 (continued). Research results for potential common proper motion pairs found in the LSPM catalog. Headline object position based on URAT1 J2000 coordinates for A (with exception of J1906+1652 – in lack of URAT1 data we had to use the average value of our own measurements)

LSPM	RA	Dec	Sep "	PA °	M1	M2	pmRA1	pmDE1	e_pm1	pmRA2	pmDE2	e_pm2	Spc1	Spc2	Ap	Me	Date	CPM Rat	Source/Notes
J1859+3054	18 59 50.054	+30 54 36.89			15.65	20.40	-42.57	-211.50	5.56	-43.94	-206.76	5.59						AAA	Solid CPM candidate
	284.9592917	30.9139167	6.0	58.9											1.2	Pp	1950.458		POSS I.O estimates
	284.9587917	30.9112500	6.0	62.0			-34	-213		-31	-220				1.2	Pp	1995.550		POSS II.N estimates. PM values estimated by comparison with POSS I.O
	284.9587690	30.9111440	6.199	62.543	14.5	16.4									1.3	E2	1998.309		2MASS. M1 and M2 estimated from J - and K-band
	284.9585586	30.9102472	6.227	61.723			-42.57	-211.50	5.56	-43.94	-206.76	5.59			0.2	Eu	2013.527	AAA	URAT1. PM data calculated from position comparison with 2MASS
	284.9585417	30.9100528			15.781										.61	C	2016.499		iT24 stack 2x5s. SNR A<20. No resolution of B. Err_M1=0.078
	284.9585292	30.9100750	5.360	62.678	15.654	20.400									.61	C	2016.508		iT24 1x60s. SNR B<10. Err_Sep=0.092", Err_PA=0.985°, Err_M1=0.043, Err_M2=0.497
	284.9585125	30.9100556			15.737										.61	C	2016.510		iT24 stack 5x10s. No resolution of B. Err_M1=0.073
LSPM	**RA**	**Dec**	**Sep "**	**PA °**	**M1**	**M2**	**pmRA1**	**pmDE1**	**e_pm1**	**pmRA2**	**pmDE2**	**e_pm2**	**Spc1**	**Spc2**	**Ap**	**Me**	**Date**	**CPM Rat**	**Source/Notes**
J1901+3132	19 01 15.072	+31 32 17.67			12.98	17.91	-200.30	23.90	5.60	-201.00	26.10	5.60						AAA	Solid CPM candidate
	285.316917	31.537833	8.468	112.936											1.2	Pp	1950.458		POSS I.O estimate.
	285.314562	31.538058	9.201	113.400	12.620										1.2	Pp	1987.472		GSC2.3. M1 is Vmag.
	285.313833	31.538083	9.216	111.650			-215.00	20.00		-197.00	18.00				1.2	Pp	1994.499		POSS II.N estimate. PM data calculated from position comparison with POSSI.
	285.313788	31.538141	9.113	114.531	12.500	15.500									1.3	E2	1998.309		2MASS. M1 and M2 estimated from J - and K-band
	285.313662	31.538156	8.690	115.400	12.409	16.501									0.2	Eu	2001.905		UCAC4. M1 and M2 are UCAC4 f.mags. Epoch shown is mean for A, epoch for secondary is 2000.
	285.313003	31.538192	8.878	112.255			-201.2	15.3	7.9	-207.3	50.5	25.2			0.4	Hw	2010.282		WISE. PM data calculated from position comparison with 2MASS. Large WISE position error results in large PM error
	285.312799	31.538242	9.096	114.355	12.963		-200.30	23.90	5.60	-201.00	26.10	5.60			0.2	Eu	2013.442	AAA	URAT1. M1 is Vmag. PM data calculated from position comparison with 2MASS
	285.312604	31.538258	8.875	114.639	12.942	18.123									.61	C	2016.510		iT24 stack 5x10s. SNR B <10. Err Sep = 0.099, Err PA = 0.639, Err M1 = 0.061, Err M2 = 0.147.
	285.312596	31.538258	9.131	113.903	12.975	17.906									.61	C	2016.516		iT24 1x60s. Err Sep = 0.092, Err PA = 0.578, Err M1 = 0.040, Err M2 = 0.071.
LSPM	**RA**	**Dec**	**Sep "**	**PA °**	**M1**	**M2**	**pmRA1**	**pmDE1**	**e_pm1**	**pmRA2**	**pmDE2**	**e_pm2**	**Spc1**	**Spc2**	**Ap**	**Me**	**Date**	**CPM Rat**	**Source/Notes**
J1905+3237	19 05 07.578	+32 37 52.60			12.51	15.05	-156.11	-180.37	5.55	-154.97	-181.34	5.58						AAA	Solid CPM candidate
	286.2852917	32.6345833	4.4	233.7											1.2	Pp	1951.518		POSS I.O estimates
	286.2828750	32.6323056	4.8	235.4			-166	-186		-175	-188				1.2	Pp	1995.624		POSS II.N estimates. PM values estimated by comparison with POSS I.O
	286.2828460	32.6318860	4.562	242.355	12.2	13.6									1.3	E2	1998.312		2MASS. M1 and M2 estimated from J - and K-band
	286.2827418	32.6318084	5.103	239.251											0.2	Eu	2000.580		UCAC4 with averaged observation epoch
	286.2820594	32.6311206	4.537	242.170			-156.11	-180.37	5.55	-154.97	-181.34	5.58			0.2	Eu	2013.552	AAA	URAT1. PM data calculated from position comparison with 2MASS
	286.2819167	32.6309694	4.503	242.778	12.512	15.052									.61	C	2016.510		iT24 stack 5x10s. Err_Sep=0.071", Err_PA=0.900°, Err_M1=0.081, Err_M2=0.101

Table 1 continues on the next page.

CPM Pairs from LSPM so far not WDS Listed

Table 1 (continued). Research results for potential common proper motion pairs found in the LSPM catalog. Headline object position based on URAT1 J2000 coordinates for A (with exception of J1906+1652 – in lack of URAT1 data we had to use the average value of our own measurements)

LSPM	RA	Dec	Sep "	PA °	M1	M2	pmRA1	pmDE1	e_pm1	pmRA2	pmDE2	e_pm2	Spc1	Spc2	Ap	Me	Date	CPM Rat	Source/Notes
J1906 +1652	19 06 52.110	+16 52 07.20			15.40	17.10	21	132		35	169							?	No final CPM conclusion due to lack of data but comparison POSS images suggests CPM
	286.716375	16.866279	2.438	10.173											1.2	Pp	1953.623		POSS I.O estimate. Both stars tagged manually.
	286.716625	16.867778	4.027	14.448			21	132		35	169				1.2	Pp	1994.439		POSS II.N estimate. Both stars tagged manually.
	286.716928	16.867865	3.750	13.700	13.771	14.799									1.3	E2	1997.531		2MASS. M1 and M2 estimated from J- and K-band
	286.717088	16.868706			15.515										.61	C	2016.502		iT24 stack 5x10s. SNR A<20. No resolution of B - has to be fainter than 16.5mag. Err M1 = 0.087.
	286.717138	16.868650	3.566	15.885	15.399	17.055									.61	C	2016.505		iT24 stack 5x10s. SNR B<20. Err Sep = 0.036, Err PA = 0.579, Err M1 = 0.068, Err M2 = 0.110.
	286.717142	16.868653	3.645	15.064	15.343	17.037									.61	C	2016.505		iT24 1x60s. Err Sep = 0.028, Err PA = 0.445, Err M1 = 0.071, Err M2 = 0.082.
	286.717129	16.868661	3.604	13.825	15.395	17.102									.61	C	2016.508		iT24 1x60s. Err Sep = 0.028, Err PA = 0.450, Err M1 = 0.062, Err M2 = 0.075.
																			Notes: Neither of the pair is identified in SDSS-DR9; secondary is identified in WISE, but not primary. Neither star identified in GSC 2.3 or UCAC4; only one star identified in URAT1, which appears to be the secondary.
LSPM	**RA**	**Dec**	**Sep "**	**PA °**	**M1**	**M2**	**pmRA1**	**pmDE1**	**e_pm1**	**pmRA2**	**pmDE2**	**e_pm2**	**Spc1**	**Spc2**	**Ap**	**Me**	**Date**	**CPM Rat**	**Source/Notes**
J1909 +5659	19 09 00.342	+56 59 48.77			14.36	19.25	-200	-21		-202	-16							?	Visually comparison of POSS images suggests CPM but hard facts are missing
	287.255833	56.997472	4.576	91.252											1.2	Pp	1952.569		POSS I.E estimate. Hint of pointed elongation manually tagged
	287.251958	56.997250	4.495	88.725			-200	-21		-202	-16				1.2	Pp	1990.505		POSS II.N estimate. Hint of pointed elongation manually tagged. PM data calculated from position comparison with POSSI
	287.251399	56.996876			13.445										1.3	E2	2000.327		2MASS. M1 estimated from J- and K-band. Secondary not identified in 2MASS.
	287.250400	56.996650			14.379		-149.4	-62							0.2	Eu	2013.432		URAT1. M1 is Vmag. B component not identified in URAT1.
	287.250063	56.996564			14.343										.61	C	2016.502		iT24 stack 5x10s. No resolution of B - has to be fainter than 16.5mag. Err M1 = 0.045.
	287.250167	59.996600	4.019	93.424	14.360	19.248									.61	C	2016.508		iT24 1x60s. SNR B <5. Err Sep = 0.022, Err PA = 0.319, Err M1 = 0.042, Err M2 = 0.433.
																			Notes: Secondary not shown in GSC 2.3, USNO B1, and UCAC4; neither of the two stars is identified by SDSS-DR9; secondary not identified in WISE.

Table 1 continues on the next page.

CPM Pairs from LSPM so far not WDS Listed

Table 1 (continued). Research results for potential common proper motion pairs found in the LSPM catalog. Headline object position based on URAT1 J2000 coordinates for A (with exception of J1906+1652 – in lack of URAT1 data we had to use the average value of our own measurements)

LSPM	RA	Dec	Sep "	PA °	M1	M2	pmRA1	pmDE1	e_pm1	pmRA2	pmDE2	e_pm2	Spc1	Spc2	Ap	Me	Date	CPM Rat	Source/Notes
J1910+0937	19 10 17.367	+09 37 18.58																??	No final CPM conclusion due to lack of data. Own imaging suggests that the assumed secondary does not exist
	287.572348	9.621815	3.365	210.800	13.40	13.52									1.3	E2	1999.590		2MASS. M1 and M2 estimated from J- and K-band. VizieR data includes a note that the photometry for both components is unreliable, probably because of overlapping star disks.
	287.572863	9.622258					128.8	112.5							0.2	Eu	2013.781		URAT1. Secondary not identified in URAT1.
	287.573000	9.622386			14.266										.61	C	2016.502		iT24 stack 5x10s. No resolution of B. Err M1 = 0.065.
	287.572979	9.622336			14.215										.61	C	2016.508		iT24 1x60s. No resolution of B. Err M1 = 0.061. The faintest stars resolved in this image are around 19mag and it seems rather implausibly that there is not even a hint of an elongation for a secondary of similar brightness with the given separation. Companion has to be extremely faint, might be even bogus
																			Notes: Comparison of POSS I.O and POSS II.N images shows proper motion of the primary but no trace of the secondary. Neither of the pair is identified in SDSS-DR9; secondary not identified in WISE, URAT1, GSC2.3 and UCAC4.
LSPM	**RA**	**Dec**	**Sep "**	**PA °**	**M1**	**M2**	**pmRA1**	**pmDE1**	**e_pm1**	**pmRA2**	**pmDE2**	**e_pm2**	**Spc1**	**Spc2**	**Ap**	**Me**	**Date**	**CPM Rat**	**Source/Notes**
J1916+3753	19 16 20.514	+37 53 24.85					66.25	172.92	6.08	65.22	169.29	6.10						AAA	Solid CPM candidate
	289.0839583	37.8881111	11.4	71.0											1.2	Pp	1955.378		POSS I.O estimates
	289.0853750	37.8901944	10.7	74.3			108	202		96	180				1.2	Pp	1992.552		POSS II.N estimates. PM values estimated by comparison with POSS I.O
	289.0854400	37.8901600	10.943	74.135	13.86	14.23									1.3	E2	1998.399		2MASS. M1 and M2 estimated from J- and K-band
	289.0856030	37.8904930	10.932	74.451			66.2	172.9	6.1	65.2	169.3	6.1			2.5	Es	2005.435		SDSS 9. PM data calculated from position comparison with 2MASS
	289.0857400	37.8907390	10.862	74.270			71.6	175.1	9.9	65.6	171.2	9.1			0.4	Hw	2010.302		WISE. PM data calculated from position comparison with 2MASS
	289.0858000	37.8909000	10.91	74.4			66.3	172.9	5.4	65.3	169.3	5.4			0.2	Eu	2013.529		I/330 MPN7467 from URAT1
	289.0857933	37.8908878	10.908	74.424			66.25	172.92	6.08	65.22	169.29	6.10			0.2	Eu	2013.529	AAA	URAT1. PM data calculated from position comparison with 2MASS

Table 1 continues on the next page.

CPM Pairs from LSPM so far not WDS Listed

Table 1 (continued). Research results for potential common proper motion pairs found in the LSPM catalog. Headline object position based on URAT1 J2000 coordinates for A (with exception of J1906+1652 – in lack of URAT1 data we had to use the average value of our own measurements)

LSPM	RA	Dec	Sep "	PA °	M1	M2	pmRA1	pmDE1	e_pm1	pmRA2	pmDE2	e_pm2	Spc1	Spc2	Ap	Me	Date	CPM Rat	Source/Notes
J1926+ 4421	19 26 03.485	+44 21 36.55			10.30	15.33	67.97	209.89	5.59	62.59	207.41	5.71						ABA	Solid CPM candidate despite some PM vector length difference which might be a hint for an orbit
	291.5120417	44.3560833	6.0	28.7											1.2	Pp	1951 .518		POSS I.O estimates
	291.5132917	44.3586111	6.1	28.2			73	206		73	209				1.2	Pp	1995 .624		POSS II.J estimates - no resolution, but elongation and similar pm obvious
	291.5134020	44.3587720	6.032	30.885	10.4	14.3									1.3	E2	1998 .435		2MASS. Vmags estimated from J- and K-mag values
	291.5134280	44.3588598	6.821	30.794											0.2	Eu	2000 .580		UCAC4. Epoch averaged
	291.5138031	44.3596575	5.892	30.552	10.32		67.97	209.89	5.59	62.59	207.41	5.71	G0		0.2	Eu	2013 .466	ABA	URAT1. PM data calculated from position comparison with 2MASS. Spectral class A based on B-V color index
	291.5138833	44.3598528	5.849	29.312	10.301	15.331	68.57	215.36	4.70	55.68	211.10	4.70			.61	C	2016 .502		iT24 stack 4x10s. SNR B<10. PM values calculated by comparison with 2MASS positions
LSPM	RA	Dec	Sep "	PA °	M1	M2	pmRA1	pmDE1	e_pm1	pmRA2	pmDE2	e_pm2	Spc1	Spc2	Ap	Me	Date	CPM Rat	Source/Notes
J1937+ 4445	19 37 52.430	+44 45 14.53			16.38	18.88	-8.00	171.80	5.60	-8.00	172.20	5.70						AAA	Solid CPM candidate. This object is meanwhile included in the WDS catalog as DEA 288
	294.468208	44.751861	11.908	203.739											1.2	Pp	1951 .518		POSS I.O estimate.
	294.468292	44.753944	11.633	203.330			5.00	188.00		5.00	195.00				1.2	Pp	1995 .624		POSS II.J estimate. PM data calculated from position comparison with POSSI.
	294.468533	44.753600	11.780	204.900											1.2	Pp	1991 .453		GSC2.3
	294.468462	44.753963	11.725	204.653	15.300	17.000									1.3	E2	1998 .448		2MASS. M1 and M2 estimated from J - and K-band
	294.468458	44.754204					-9.00	172.00							0.2	Eu	2000 .000		UCAC4. Secondary not shown in UCAC4.
	294.468415	44.754681	11.737	204.622			-8.00	171.80	5.60	-8.00	172.20	5.70			0.2	Eu	2013 .444	AAA	URAT1. PM data calculated from position comparison with 2MASS
	294.468488	44.754850			16.517										.61	C	2016 .510		iT24 stack 5x10s. Err M1 = 0.061.
	294.468417	44.754822	11.426	208.087	16.377	18.876									.61	C	2016 .516		iT24 1x60s. SNR B <10. Err Sep = 0.022, Err PA = 0.112, Err M1 = 0.036, Err M2 = 0.121.
LSPM	RA	Dec	Sep "	PA °	M1	M2	pmRA1	pmDE1	e_pm1	pmRA2	pmDE2	e_pm2	Spc1	Spc2	Ap	Me	Date	CPM Rat	Source/Notes
J1959+ 3432	19 59 46.938	+34 32 24.20					-51.4	-123.3	5.6	-47	-121.1	5.7						AAA	Solid CPM candidate
	299.946208	34.542028	4.635	166.120											1.2	Pp	1950 .603		POSS I.O estimate. Both stars tagged manually.
	299.945452	34.540333	4.030	172.956			-53	-138		-67	-127				1.2	Pp	1994 .513		POSS II.N estimate. Both stars tagged manually.
	299.945585	34.540258	4.391	167.600											1.2	Pp	1991 .593		GSC2.3.
	299.945603	34.540112	4.624	167.104	15.500	16.600									1.3	E2	1998 .358		2MASS. M1 and M2 estimated from J - and K-band
	299.945300	34.539600	4.580	166.000			-51.4	-123.3	5.5	-47	-121.1	5.5			0.2	Eu	2013 .460		I/330 MPN 7967 from URAT1.
	299.945339	34.539590	4.579	165.952			-51.4	-123.3	5.6	-47	-121.1	5.7			0.2	Eu	2013 .460	AAA	URAT1. PM data calculated from position comparison with 2MASS

Table 1 continues on the next page.

CPM Pairs from LSPM so far not WDS Listed

Table 1 (continued). Research results for potential common proper motion pairs found in the LSPM catalog. Headline object position based on URAT1 J2000 coordinates for A (with exception of J1906+1652 – in lack of URAT1 data we had to use the average value of our own measurements)

LSPM	RA	Dec	Sep "	PA °	M1	M2	pmRA1	pmDE1	e_pm1	pmRA2	pmDE2	e_pm2	Spc1	Spc2	Ap	Me	Date	CPM Rat	Source/Notes
J2021+1622	20 21 54.918	16 22 29.86					164.90	-41.38	6.78	172.51	-43.67	6.70						ABA	Solid CPM candidate despite some PM vector length difference - hint for an orbit?
	305.4762500	16.3756111	4.5	15.0											1.2	Pp	1951.513		POSS I.O estimates
	305.4782917	16.3750278	4.4	13.2			181	-54		177	-54				1.2	Pp	1990.472		POSS II.J estimates. PM values estimated by comparison with POSS I.O
	305.4788160	16.3749620	4.559	12.158	17.0	17.0									1.3	E2	1999.822		2MASS. M1 and M2 estimated from J - and K-band
	305.4795000	16.3748000	4.55	13.9			164.9	-41.4	6.20	172.5	-43.7	6.10			0.2	Eu	2013.505		I/330 MPN8123 from URAT1
	305.4794656	16.3748056	4.551	13.857			164.90	-41.38	6.78	172.51	-43.67	6.70			0.2	Eu	2013.505	ABA	URAT1. PM data calculated from position comparison with 2MASS
LSPM	**RA**	**Dec**	**Sep "**	**PA °**	**M1**	**M2**	**pmRA1**	**pmDE1**	**e_pm1**	**pmRA2**	**pmDE2**	**e_pm2**	**Spc1**	**Spc2**	**Ap**	**Me**	**Date**	**CPM Rat**	**Source/Notes**
J2035+0711	20 35 50.843	+07 11 24.28			14.39	15.37	131.00	-66.20	6.60	120.20	-66.00	6.80						ACA	Visual comparison of POSS images suggests CPM. Significant difference in pm vector length might be a hint for an orbit
	308.959833	7.191000	3.737	293.664											1.2	Pp	1951.602		POSS I.O estimate.
	308.961667	7.190306	4.716	293.761			148.00	-57.00		128.00	-48.00				1.2	Pp	1991.695		POSS II.F estimate. PM data calculated from position comparison with POSSI.
	308.961849	7.190067	4.134	296.100	13.990		138.00	-65.00		84.70	-39.40		M0		0.2	Eu	2000.000		UCAC4. Epoch shown is for primary. Secondary has a mean epoch of 1999.095 (RA = 1998.97, Dec = 1999.22).
	308.961862	7.190070	4.145	297.124	13.100	13.800									1.3	E2	2000.444		2MASS. M1 and M2 estimated from J - and K-band
	308.962150	7.189922	4.349	293.568			104.0	-53.9	13.3	74.0	-69.1	25.8			0.4	Hw	2010.337		WISE. PM data calculated from position comparison with 2MASS. Large WISE position error results in large PM error
	308.962333	7.189834	4.330	296.338	14.040		131.00	-66.20	6.60	120.20	-66.00	6.80			0.2	Eu	2013.052	ACA	URAT1. M1 is URAT1 Vmag. PM data calculated from position comparison with 2MASS.
	308.962458	7.189772	4.226	296.565	14.389	15.367									.61	C	2016.511		iT24 stack 5x10s. Err Sep = 0.028, Err PA = 0.383, Err M1 = 0.028, Err M2 = 0.039.
LSPM	**RA**	**Dec**	**Sep "**	**PA °**	**M1**	**M2**	**pmRA1**	**pmDE1**	**e_pm1**	**pmRA2**	**pmDE2**	**e_pm2**	**Spc1**	**Spc2**	**Ap**	**Me**	**Date**	**CPM Rat**	**Source/Notes**
J2044+5042	20 44 07.570	+50 42 33.08			17.17	18.29	-102.76	121.69	6.01	-95.51	121.00	5.96						AAA	Solid CPM candidate
	311.0331667	50.7078333	4.1	170.6											1.2	Pp	1954.486		POSS I.O estimates
	311.0320000	50.7093333	4.3	175.0			-66	134		-73	127				1.2	Pp	1994.655		POSS II.N estimates. PM values estimated by comparison with POSS I.O
	311.0315670	50.7091710	4.606	173.063	15.3	15.6									1.3	E2	1999.467		2MASS. M1 and M2 estimated from J - and K-band
	311.0310960	50.7096150	4.590	170.596			-98.0	145.9	19.6	-80.3	149.9	22.7			0.4	Hw	2010.421		WISE. PM data calculated from position comparison with 2MASS. Large WISE position error results in large PM error
	311.0309308	50.7096481	4.614	171.928			-102.76	121.69	6.01	-95.51	121.00	5.96			0.2	Eu	2013.638	AAA	URAT1. PM data calculated from position comparison with 2MASS
	311.0308292	50.7098083			17.198										.61	C	2016.510		iT24 stack 5x10s. SNR A<20. Err_M1=0.166
	311.0308083	50.7097278	4.441	172.255	17.170	18.289									.61	C	2016.516		iT24 1x60s. SNR B <20

Table 1 continues on the next page.

CPM Pairs from LSPM so far not WDS Listed

Table 1 (continued). Research results for potential common proper motion pairs found in the LSPM catalog. Headline object position based on URAT1 J2000 coordinates for A (with exception of J1906+1652 – in lack of URAT1 data we had to use the average value of our own measurements)

LSPM	RA	Dec	Sep "	PA °	M1	M2	pmRA1	pmDE1	e_pm1	pmRA2	pmDE2	e_pm2	Spc1	Spc2	Ap	Me	Date	CPM Rat	Source/Notes
J2110+1038	21 10 43.446	+10 38 28.05			16.82	17.47	-20	-222		-23	-231							?	PM data so far only estimated, as WISE PM data seems s bit suspect - but certainly a potential CPM candidate
	317.68100000	10.6443056	4.5	13.2											1.2	Pp	1951.575		POSS I.O estimates
	317.68075000	10.6415833	4.1	12.5			-20	-222		-23	-231				1.2	Pp	1995.712		POSS II.N estimates. PM values estimated by comparison with POSS I.O
	317.68102400	10.6410970	4.586	11.571	14.9	15.3									1.3	E2	2000.502		2MASS. M1 and M2 estimated from J - and K-band
	317.68101800	10.6410920	4.574	11.512											2.5	Es	2000.740		SDSS DR9. Observation epoch difference with 2MASS far too small to calculate reliable PM values
	317.68103300	10.6405570	4.535	10.427			3.2	-197.0	9.0	-6.8	-200.3	12.3			0.4	Hw	2010.369		WISE. PM data calculated from position comparison with 2MASS
	317.68095417	10.6401639	4.658	11.132	16.819	17.473									.61	C	2016.508		iT24 1x60s. Err_Sep=0.014, Err_PA=0.174°, Err_M1=0.049, Err_M2=0.067
LSPM	**RA**	**Dec**	**Sep "**	**PA °**	**M1**	**M2**	**pmRA1**	**pmDE1**	**e_pm1**	**pmRA2**	**pmDE2**	**e_pm2**	**Spc1**	**Spc2**	**Ap**	**Me**	**Date**	**CPM Rat**	**Source/Notes**
J2124+1323	21 24 05.343	+13 23 59.11			15.59	16.31	80.6	159.5	6.2	72.1	154.7	6.2						AAA	Solid CPM candidate
	321.020250	13.396972	4.296	37.686											1.2	Pp	1951.576		POSS I.O estimate. Both centroids tagged manually.
	321.021125	13.398778	4.652	41.202			69	147		79	150				1.2	Pp	1995.698		POSS II.N estimate. Both centroids tagged manually.
	321.021577	13.398770	4.431	34.500	14.31	15.01									1.3	E2	1998.880		2MASS. M1 and M2 estimated from J - and K-band
	321.021640	13.398866	4.409	34.300		15.12	73	139						M0	0.2	Eu	2000.720		UCAC4. M2 is Vmag, Spc2 is from UCAC4 B-V data. Epoch shown is mean epoch (Epoch of primary is 2000.000, Epoch of secondary is 2001.44).
	321.021816	13.399184	4.331	33.521			85.0	151.3	9.4	72.9	147.3	9.4			2.5	Es	2008.372		SDSS-DR9. PM data calculated from position comparison with 2MASS
	321.021835	13.399311	4.436	35.520			78.6	169.4	13.6	84.3	165.9	22.9			0.4	Hw	2010.381		WISE. PM data calculated from position comparison with 2MASS
	321.021890	13.399373	4.338	33.691			80.6	159.5	6.2	72.1	154.7	6.2			0.2	Eu	2013.438	AAA	URAT1. PM data calculated from position comparison with 2MASS. Attention: Aladin shows URAT1 J2000 positions in image wrong due to wrong URAT1 PM data. All URAT1 mag data besides fmag ident for both components and thus obviously wrong for at least one component
	321.021958	13.399494	3.943	33.715	15.526	16.463									.61	C	2016.502		iT24 stack 10x10s. SNR B<20. Err Sep = 0.071, Err PA = 1.027, Err M1 = 0.062, Err M2 = 0.099
	321.021967	13.399492	4.248	33.808	15.592	16.310									.61	C	2016.505		iT24 stack 5x10s. Err Sep = 0.028, Err PA = 0.381, Err M1 = 0.053, Err M2 = 0.066.

Table 1 concludes on the next page.

Table 1 (conclusion). Research results for potential common proper motion pairs found in the LSPM catalog. Headline object position based on URAT1 J2000 coordinates for A (with exception of J1906+1652 – in lack of URAT1 data we had to use the average value of our own measurements)

LSPM	RA	Dec	Sep "	PA °	M1	M2	pmRA1	pmDE1	e_pm1	pmRA2	pmDE2	e_pm2	Spc1	Spc2	Ap	Me	Date	CPM Rat	Source/Notes
TYC-4030-00975-1	01 14 58.386	+60 41 35.55					22.32	-21.1	5.87	21.46	-21.49	5.90						AAC	Despite the in relation to the PM vector length rather large pm error a solid CPM candidate
	18.74258333	60.6935278	12.6	126.5											1.2	Pp	1952.706		POSS I.O estimates
	18.74325000	60.6935556	12.7	126.1			29	2		32	2				1.2	Pp	1993.683		POSS II.N estimates. PM values estimated by comparison with POSS I.O
	18.74331200	60.6931750	12.394	126.837											1.2	Pp	1990.275		GSC 2.2 mean epoch
	18.74326200	60.6932140	12.578	126.577	10.5	13.9									1.3	E2	1999.020		2MASS. M1 and M2 estimated from J - and K-band
	18.74330450	60.6931784	12.557	126.641	10.706		20.9	-13.3		26.5	-15		G0		0.2	Eu	2000.203		UCAC4 mean epoch
	18.74335000	60.6931640	12.399	127.359			14.0	-16.3	29.0	-8.1	-18.9	8.6			0.4	Hw	2010.087		WISE. PM data calculated from position comparison with 2MASS with a somewhat suspect result
	18.74344500	60.6931294	12.570	126.631	10.665		22.32	-21.1	5.87	21.46	-21.49	5.90	G0		0.2	Eu	2013.441	AAC	URAT1. PM data calculated from position comparison with 2MASS

CPM Pairs from LSPM so far not WDS Listed

(Continued from page 141)

Summary

Of the 47 objects checked for CPM

- 22 got a triple A rating based on position comparison between 2MASS and URAT1 (according to the method presented in Knapp/Nanson 2016), which means solid CPM
- 15 got a rating between AAB to BAC, which means probably CPM with caveats but all of them with CPM confirmation by comparison of POSS images
- 9 remained without rating due to missing URAT1 positions for the secondary
- 1 remained as suspect due to missing evidence for the secondary.

One object (J1937+4445) was during the research for this report added to the WDS catalog as CPM pair DEA 288 but we kept this object in the report to provide the additional observations we found in the diverse catalogs or made ourselves.

Acknowledgements

The following tools and resources have been used for this research:

- Washington Double Star catalog
- 2MASS All Sky catalog
- iTelescope: Images were taken with iT24: 610mm CDK with 3962mm focal length. CCD: FLI-PL09000. Resolution 0.62 arcsec/pixel. V-filter. Located in Auberry. California. Elevation 1405m
- AAVSO APASS
- UCAC4 catalog
- URAT1 catalog
- WISE catalog
- SDSS catalog
- IGSL catalog
- LSPM catalog
- VizieR I/330 catalog
- Aladin Sky Atlas v9.0
- SIMBAD, VizieR
- AstroPlanner V2.2
- NASA/ IPAC Infrared Science Archive

Special thanks to Brian Mason at the USNO for his useful advice while working on this report.

References

Buchheim, R., 2008, "CCD Double-Star Measurements at Altimira Observatory in 2007", *Journal of Double Star Observations*, **4**, 27 - 31. Formulas for calculating Separation and Position Angle from the RA Dec coordinates given as

$$Sep = \sqrt{\left[\left(RA_2 - RA_1\right)\cos\left(Dec_1\right)\right]^2 + \left(Dec_2 - Dec_1\right)^2}$$

in radians and

$$RA = \arctan\left[\frac{\left(RA_2 - RA_1\right)\cos\left(Dec_1\right)}{Dec_2 - Dec_1}\right]$$

in radians depending on quadrant

Knapp W. and Nanson J., 2016, "A New Concept for Counter-Checking of Assumed CPM Pairs, *JDSO*, **13**, 31 - 51.

Student Observation of HR 2282 (Furud)

Reed Estrada[1], Chris Estrada[1], Payton Anker[2], Destiny Barrientos[2], Charlie Colbert[2], Edward Dondelinger[2], Lindsey Gillette[2], Jeremy Goodrow[2], Tara Izadi[3], Colin Mayo[2], Jordan Milton [2], Sarah Stuart[2], Nick Varela[2]

1. High Desert Research Initiative
2. Vanguard Preparatory, Apple Valley, California
3. Academy For Academic Excellence, Apple Valley, California

Abstract: A selected team of 8th graders measured the separation and the position angle of double star HR 2282 also known as Furud. They used a 22- inch Newtonian Alt/Az telescope to determine the scale constant, separation, and the position angle. The separation angle was 169.6 arc seconds and the position angle was 339.7 degrees. The results were compared to the 1999 Washington Double Star Catalog and were found to be extremely close.

Introduction

A three-day Double Star Workshop was hosted from March 11 through March 13, 2016 at Vanguard Preparatory School. Astronomers chose thirty-three eighth grade students attending Vanguard to participate in the workshop. The students were then split up into three teams and matched with an instructor. The astronomers who led the students were Chris and Reed Estrada (Green Team, see Figure 1), Mark Brewer (Red Team), and Sean Gillette (Purple Team).

Figure 1: Team that participated in the study of HR2282 (Green Team). Top Row (left to right): Astronomers Reed and Chris Estrada, Nick Varela, Charlie Colbert, Colin Mayo, Edward Dondelinger, and Jeremy Goodrow. Bottom Row (left to right): Tara Izadi, Peyton Anker, Destiny Barrientos, Lindsey Gillette, Sarah Stuart, and Jordan Milton.

Equipment and Procedures

The Green Team used a 22-inch Newtonian Alt/Az telescope with a Celestron Micro Guide Eyepiece attached to a Bell and Howell High Definition Video Camera. The usage of the video camera counterbalanced the necessity for the drive motors and negated the field rotation in Alt/Az telescope.

The calibration star, Bellatrix (Gamma Orionis), was used to determine the scale constant on the date of B2016.186. The eyepiece was rotated so that the sky would drift parallel to the linear scale. Bellatrix was then positioned on the eastern edge of the linear scale; the star moved across the linear scale. The team of students determined the amount of time it took for the star to drift to the western edge of the linear scale using a stopwatch that read to the nearest 0.01 seconds. Ten drift times were used to determine the scale constant using the equation

$$Z = \frac{15.0411 t \cos(dec)}{D}$$

where Z was the scale constant in arc seconds per division; 15.0411 is the Earth's rotational rate in arcseconds per second; t was the average drift time in seconds (50.09); D was the number of division marks on the

Student Observation of HR 2282 (Furud)

Figure 2: Nick Varela looking through telescope at Double Star HR 2282 (Furud).

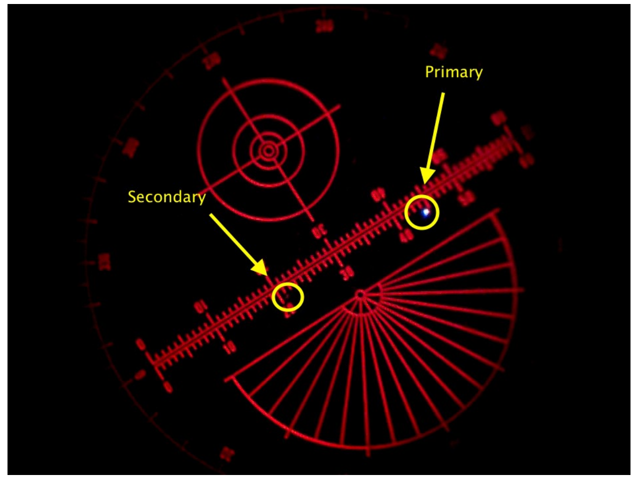

Figure 3: Primary and secondary star being measured.

linear scale (60). These determined that the scale constant for the 22-inch telescope was 7.02 arc seconds per division.

The telescope was pointed at HR 2282 on the date of B2016.186. A Bell and Howell DNV16HDZ Video Camera was used to capture images through the Celestron astrometric eyepiece to determine the position angle and separation of the double star. The videos were downloaded to a computer. Selected still images were taken of the separation and position angle of the star (see Figures 3 and 4.). The student team evaluated the gathered digital data. The average position value was multiplied by the scale constant to find the final separation. Ten measurements were then made to find the average position angle. Each student looked at a different picture of the double star along the astrometric eyepiece scale to allow for a statistical average of the separation measurement. The stars dithered or moved along the scale in real time as observed through the eyepiece of the telescope. To simulate this movement, and to get an average position, ten samples and ten pictures were taken. Each was observed by an individual student.

Results of the measurements are given in Table 1.

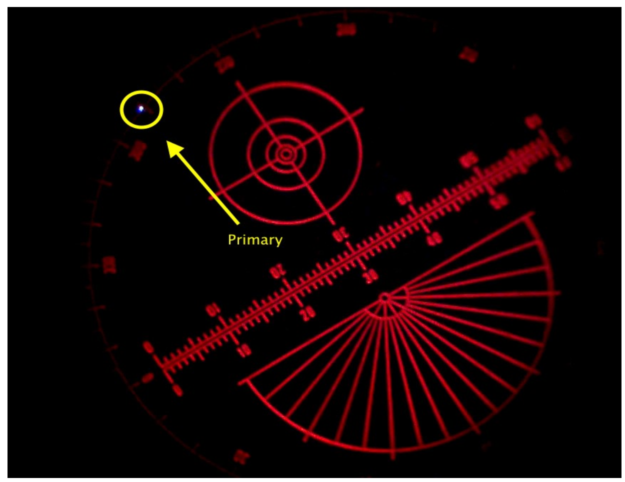

Figure 4: Position angle being measured

Conclusion

The students in the Vanguard Preparatory Double Star Workshop 2016 successfully measured the separation and position angle of the double star HR 2282. Their measurements compared well with the WDS catalogue with a difference of 1.7 arcseconds on the separation and a 2.6 difference of the position angle.

Acknowledgements

This research used the Washington Double Star Catalog maintained at the U.S. Naval Observatory. The team would like to thank Antelope Valley Astronomy Club, High Desert Shuttle, and CalRTA (California Retired Teachers Association) for generous financial contributions. They also thank Starbucks for providing food and drinks, and the High Desert Astronomical Society for training. The students thank Vanguard Preparatory School in Apple Valley, California for use of their facilities. The group thanks Vanguard Preparatory staff members Monica Arcilla, Pam Gillette, Sean Gillette, Brian Goodrow, Wendy Thielen, and all volunteering parents for supporting the workshop. They also thank astronomers Chris and Reed Estrada for leading and assisting their group.

Student Observation of HR 2282 (Furud)

Table 1: Measurements of HR 2282 (Furud). Measurements were made on B2016.186.

Parameters	# of Obv.	Average Values	Mean	SD	Standard Error of Mean	WDS Value (1999)	Difference	% Difference
Separation (a.s.)	10	169.6	29.3	1.5	0.4	173	3.4	1%
Position Angle(deg)	10	339.7	249.7	2.2	6.3	338	1.7	1%

References

Mason, Brian. 2012. *Washington Double Star Catalog.* Astronomy Department, U.S. Naval Observatory. Conner, Donald. "The Star Furud."

The Star Furud. (2013). Astronomy. Retrieved from http://all-abouta-stronomy.blogspot.com/2013/11/the-star-furud.html

Student Measurements of Double Star STF 747AB

Grace Bateman[1], Benjamin Funk[1], Travis Gillette[1], Breauna Rhoades[1], Mark Rhoades[2], Ruth Schlosser[1], Scott Sharpe[1], and Leone Thompson[1]

1. Apple Valley High School, Apple Valley, California
2. Vanguard Preparatory Parent

Abstract: Data gathered from a 22-Inch Newtonian Alt/Az telescope and a Celestron Micro Guide eyepiece were used to measure the double star STF 747AB. Students from Apple Valley High School determined the separation to be 39.97 arc sec and the position angle to be 227.91 degrees. The students also used data from the digitized sky survey and determined a separation of 39.99 arc sec and a position angle of 225 degrees. The research was semi-independent from the Vanguard Double Star Workshop 2016 in Apple Valley, California.

Introduction

Vanguard Preparatory School hosted a three day double star workshop from March 11 through March 13. A number of high school students participated in measuring scale constant, plate scale, separation, and position angle of the double star system STF 747AB. These students had participated in previous double star workshops hosted by Vanguard Preparatory and worked semi-independently using images that were gathered by Chris and Reed Estrada on March 10 with a 22-inch Newtonian Alt/Az telescope and a Celestron Micro Guide eyepiece fitted with a Bell and Howell High Definition Video Camera as well as images gathered from the Digitized Sky Survey.

The double star system STF 747AB is located in the Orion constellation. STF 747AB has a blue primary star with a magnitude of 4.7 and a blue secondary star with a magnitude of 5.5. The right ascension and declination are listed in the Washington Double Star Catalog as 053502.68-060007.2. The double star was first measured in 1825 and a total of 49 measurements have been documented in the WDS. The latest measurement of STF 747AB was in 2014 with a separation of 35.9 arc sec and a position angle of 224 degrees. This star was selected for its magnitude, position angle, and separation.

Figure 1: The authors from left to right in the back row: Scott Sharpe, Travis Gillette, Benjamin Funk, and Ruth Schlosser. The authors from left to right in the front row: Grace Bateman, Breauna Rhoades, and Leone Thompson. Picture was taken by Mark Rhoades.

Equipment and Procedures

The team, pictured in Figure 1, in this study used a 22-inch Newtonian Alt/Az telescope (Figure 2) with a Celestron Micro Guide eyepiece fitted with a Bell and Howell high definition video camera. The use of the video camera offsets the need for a drive motor and negates the field rotation common with telescopes that use Alt/Az.

The star Bellatrix was used to calibrate the telescope to the Celestron Micro Guide eyepiece for separation measurements. To calibrate the telescope, the

Figure 2: This is a picture of the telescope used to collect digital data of the double star. Picture taken by Chris Estrada.

eyepiece was rotated so that the star would drift parallel to the linear scale. The star was placed on the eastern-most part of the linear scale and allowed to drift along the linear scale. A video was taken of the drift. The process was repeated seven times. The videos were then viewed 15 times to determine the average scale constant using the equation

$$Z = \frac{15.0411\, t \cos(dec)}{D}$$

where Z is the scale constant in arc sec per division; 15.0411 is the rotation of the earth in arc sec per second; t is the average drift time in seconds; dec is the declination of the calibration star (20.982); and D is the number of tick marks on the linear scale. The result for the 22-inch Newtonian Alt/Az with a Celestron Micro Guide eyepiece was 7.95 arc sec per tick mark.

The authors also used data from the digitized sky survey in order to measure separation and position angle of STF 747AB. The students aligned an image of the double star system on a coordinate plane and used the formula:

$$\frac{206264.806 \text{ arc sec(pixel size)}}{\text{(focal length)}}$$

in order to determine the plate scale. The pixel size was 15 microns and the focal length was 3073.4 millimeters. The plate scale was determined to be 1.01 arc sec per pixel. In order to determine the separation, the authors then used the formula

$$d = \sqrt{(x_2 - x_1)^2 + (y_2 - y_1)^2}$$

where d is the distance between the primary and secondary star, (x_1,y_1) are the coordinates of the primary star, and (x_2,y_2) are the coordinates of the secondary star. The distance between the primary and secondary star was determined to be 39.59 pixels. This measurement was multiplied by the plate scale constant of 1.01 arc sec/pixel to be converted into arc seconds. The measured separation was 39.99 arc seconds. The authors then used the formula

$$\theta = \arctan\frac{\Delta y}{\Delta x}$$

where θ is the position angle, Δy is the difference between the y coordinates of the primary and secondary stars, and Δx is the difference between the x coordinates of the primary and secondary stars. From this formula the authors found a position angle of 45 degrees, and when adjusted by 180 degrees, the measured position angle is 225 degrees.

Observation and Analysis

Our video data was recorded on B2016.191904 (March 10, 2016) in Antelope Valley, California and our measurement results are presented in Table 1. The Digitized Sky Survey Data was imaged on B1990.983571 at Palomar Observatory and reduced on B2016.194642. Results of the reduction are given in Table 2.

Conclusion

The students' results measured from video data were slightly different from values published in the Washington Double Star Catalog in 2014 with a separation and position angle difference of 4.17 arc sec and 3.91 degrees. The authors have concluded that the large separation difference may have been due to random and systematic errors such as the Micro Guide eyepiece ± 0.5 arc sec, the stopwatch ± 0.5 sec, the author' difference in vision, and reaction time. The authors also found the difference from the digitized sky survey to be 4.1 arc sec and 1.0 degrees. The authors have concluded that the large separation difference may have been due to random and systematic errors. The pixel size ± 0.5 microns and the focal length ± 2.0 mm, and star's centroid values ± 0.5 were determined from DS9.

Student Measurements of Double Star STF 747AB

Table 1: Measurements of Double Star System STF 747AB From our Video Data. Taken on B2016.191904

Parameters	# Obs	Mean	SD	Standard Error of Mean	WDS Value	Difference	% Difference
Scale Constant arc sec / division	15	7.94	0.88	0.226	NA	NA	NA
Separation (arc sec)	12	39.97	0.68	0.197	35.9	4.17	11%
Position Angle (degrees)	12	227.91	1.24	0.357	224	3.91	1.7%

Table 2: Double Star System STF 747AB with Digitized Sky Survey Data. Data gathered on B1990.983571.

	Student Measured Value	WDS Published Value	Difference	Percent Difference
Plate Scale (arc sec/pixel)	1.01 arc sec/pixels	N/A	N/A	N/A
Separation (arc sec)	39.99 arc sec	35.9 arc sec	4.09 arc sec	10.78%
Position Angle (degrees)	225 degrees	224 degrees	1 degree	0.45%

Acknowledgements

This research has made use of the Washington Double Star Catalog maintained at the U.S. Naval Observatory. Some of the data presented in this paper were obtained from the Mikulski Archive for Space Telescopes (MAST). STScI is operated by the Association of Universities for Research in Astronomy, Inc., under NASA contract NAS5-26555. Support for MAST for non-HST data is provided by the NASA Office of Space Science via grant NNX09AF08G and by other grants and contracts.

The authors would like to thank Vanguard Preparatory for the use of their facility. The authors would also like to thank Dr. Sean Gillette, Pam Gillette, Debbie Wolf, Wendy Thielen, and all volunteering parents.

The authors would like to thank the astronomers Mark Brewer, Reed Estrada, and Chris Estrada.

The authors would like to thank the sponsors from Antelope Valley Astronomy Club for their generous donation, Starbucks for donating food/drinks, High Desert Shuttle for a second generous donation, and High Desert Astronomical Society for providing training.

References

Mason, Brian. (2012). Washington Double Star Catalog. Astronomy Department, U.S. Naval Observatory. Retrieved from www.ad.usno.navy.mil/wds/wds.html

Digitized Sky Survey. (1994). Association of Universities for Research in Astronomy. Retrieved from https://archive.stsci.edu/cgi-bin/dss_search?v=poss2ukstu_red&r=+05+35+02.68&d= -06+00+07.2&e=J2000&h=15.0&w=15.0&f=gif&c=none&fov=NONE&v3=

Student Measurements of STFA 10AB (Theta Tauri)

Sean Gillette[1,3,4], Chris Estrada[3], Reed Estrada[3], Sophia Aguilera[1], Valerie Chavez[1], Jalynn Givens[1], Sarah Lindorfer[1], Kaylie Michels[1], Makenzie Mobley[1], Gabriel Reder[1], Kayla Renteria[1], Jenna Shattles[1], Aiden Wilkin[1], Maisy Woodbury[1], Breauna Rhoades[2], and Mark Rhoades[4]

1. Vanguard Preparatory School, Apple Valley, California
2. Apple Valley High School
3. High Desert Research Initiative
4. Vanguard Preparatory School Parent

Abstract: Eighth grade students at Vanguard Preparatory School measured the double star STFA 10AB using a 22-inch Newtonian Alt/Az telescope and a Celestron Micro Guide eyepiece. Bellatrix was used as the calibration star. The calculated means of multiple observations of STFA 10AB resulted in a separation of 45.18," a scale constant of 7.88 arcseconds per division, and position angle of 257.9°. These measurements were compared to the most recent values in the Washington Double Star Catalog.

Introduction

On March 11-13, 2016, eleven eighth grade students (Figure 1) observed the double star, q Tauri, at Vanguard Preparatory Double Star Workshop. The calibration star (Bellatrix) had a right ascension of 0.5 hours 25 minutes 7.86 seconds, and a declination of 6.3497. The Observations were made at 34° 29' 19.84" North latitude and 117° 09' 47.48" West longitude. Students were planning to measure the double star Theta Taurus on March 4-6, but the sky was cloudy and the weather was windy. The students used video recordings of Theta Taurus that had been recorded on Thursday, March 10 (B2016.191904), to determine the scale constant, separation, and position angle.

Figure 1: The authors from left to right in the back row: Sarah Lindorfer, Jenna Shattles, Gabriel Reder, Kaylie Michels, Jalynn Givens, and Sean Gillette. The authors from left to right in the front row: Aiden Wilkin, Maisy Woodbury, Makenzie Mobley, Kayla Renteria, Sophia Aguilera, and Valerie Chavez.

Equipment

The team used a 22-inch Newtonian Alt/Az telescope with a Celestron Micro Guide eyepiece attached to a Bell and Howell High Definition Video Camera shown in Figure 2.

Procedures

The star Bellatrix in the constellation Orion was used to calibrate the linear scale of the eyepiece. The students positioned Bellatrix on the edge of the linear scale, then the sidereal motor was disengaged to allow the star to drift parallel to the linear scale. Using a stop-

Student Measurements of STFA 10AB (Theta Taurus)

Figure 2: Telescope used to record measurements used on March 10th, 2016.

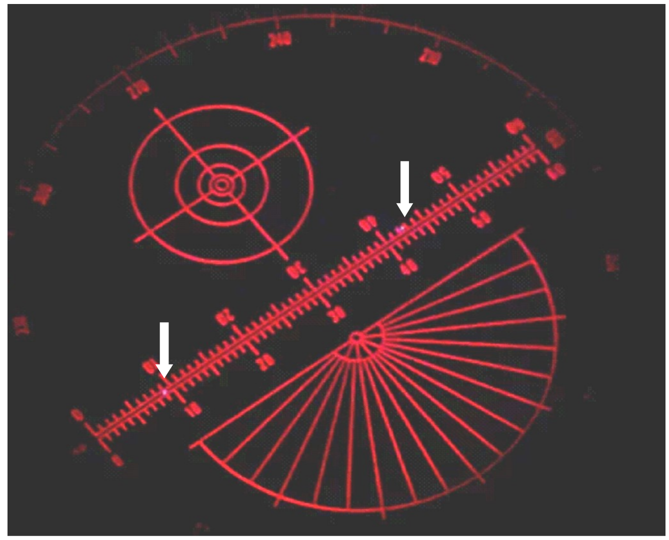

Figure 3: Separation of Theta Taurus in view of the 22-inch Newtonian Alt/Az telescope using a Celestron Micro Guide eyepiece. Arrows indicate the stars.

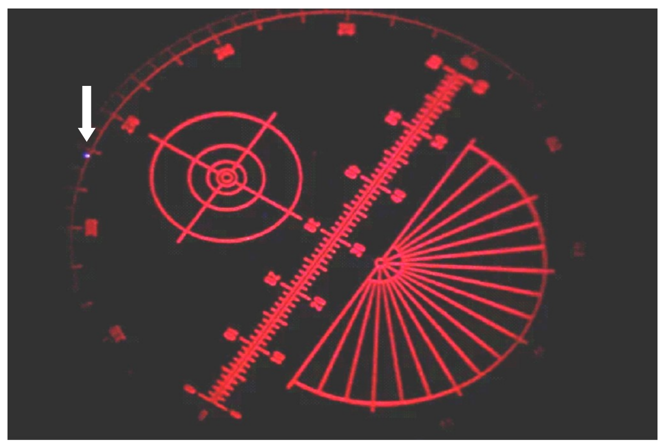

Figure 4: Position angle of Theta Taurus in view of the 22-inch Newtonian Alt/Az telescope using a Celestron Micro Guide eyepiece. Arrow indicates B component.

watch that reads to the nearest hundredth of a second, the students determined the amount of time it took the star to drift. A total of fifteen drifts was recorded to determine the scale constant using the equation

$$Z = \frac{15.0411\, t \cos(dec)}{D}$$

Z is the scale constant in arcseconds per division; 15.0411 is the Earth's rotational rate in arcseconds per second; t is the average drift time in seconds (63.24); cos(dec) is the declination of the calibration star in degrees; and D is the number of division marks on the linear scale (60).

Observation and Analysis

The results the students got from the 22-inch Newtonian telescope and the eyepiece was a scale constant of 7.88 arcseconds per division. Theta Tauri (STFA 10AB) has an apparent magnitude of +3.14, a right ascension of 04h 28m 34.49603sec, and a declination of +15° 57' 43.8494". The stars are separated by 337 arcseconds and their position angle was 346° as listed in the WDS. Figures 3 and 4 show the appearance of q Tauri in our eyerpiece. The stars are spectroscopic binaries and have closer companions.

15 observations were gathered to determine an average time of drift of 31.61, standard deviation of 0.44, and standard error of mean 0.11. Five separate measurements were gathered to determine an average of 45.18 arcseconds, a standard deviation of .46, standard error of mean 0.2, with a published value of 337 difference of 18.82 and difference of 5.43%. Ten position angle measurements were gathered to determine an average of 257.9 standard deviation of 4.84, standard error of mean 1.53 with a published value of 346 and difference of 1.9 and 0.55%. The measurements are summarized in Table 1.

Conclusion

The students produced a small difference from the observations recorded in 2011 of one standard deviation. The students compared it to a published value of 337 difference of 18.82 and percentage of difference of 5.43%. The measured separation differs from the WDS

Student Measurements of STFA 10AB (Theta Taurus)

value

Table 1: Measurements of STFA 10AB. Performed on 2016.175

Parameters	# Obs	Mean	SD	Standard Error of Mean	WDS Value	Difference	% Difference
Scale Constant a.s./division	15	7.88	44	0.11	NA	NA	NA
Separation (a.s.)	5	45.18	.46	.21	337	18.82	5.43%
Position Angle (degrees)	10	257.90	4.84	1.53	346	1.9	0.55%

by 4.2 standard deviations. An error may have occurred due to the students' level of experience.

Acknowledgements

The students would like to thank Mark Brewer, Reed Estrada, and Chris Estrada for providing astronomical leadership and equipment. The students would also like to thank Pam Gillette, Debbie Wolf, Monica Arcilla, and Wendy Thielen for helping run the event. The following businesses gave generous donations for the event: Lucerne Valley, CA; Starbucks, Apple Valley CA; High Desert Shuttle; CalRTA; High Desert Astronomical Society; Antelope Valley Astronomy Club; and Vanguard Preparatory.

References

Mason, Brian.(2012). Washington Double Star Catalog. Astronomy Department, U.S. Naval Observatory. Retrieved from www.ad.usno.navy.mil/wds/wds.html

Digitized Sky Survey. (1994). Association of Universities for Research in Astronomy. Retrieved from https://archive.stsci.edu/cgi-bin/dss_search?v=poss2ukstu_red&r=+05+35+02.68&d= -

Data and Analysis of the Double Stars STFA 10AB and STFA 1744AB

Marisa Arcilla[1], Sam Bowden[1], Jacqueline DeBlase[1], Anthony Hall[1],Corielyn Hall[1], Alyssa Hernandez[1], Danielle Renna[1], Fatima Rodriguez[1],Cassandra Salazar[1], Andres Sanchez[1], Dayton Teeter[1], Mark Brewer[2], Benjamin Funk[3], Travis Gillette[3], and Scott Sharpe[3]

1. Vanguard Preparatory, Apple Valley, California
2. High Desert Research Initiative
3. Apple Valley High School

Abstract: Eighth grade students at Vanguard Preparatory School measured the double stars STFA 10AB and STFA 1744AB. A 22-inch Newtonian Alt/Az telescope and a 14-inch Celestron Schmidt Cassegrain telescope were used. The star Bellatrix was used as the calibration star to determine the scale constant of the 22-inch telescope to be 7.8 "/tick marks. The double star STFA 1744AB was used as the calibration star to determine the scale constant of the 14-inch telescope to be 5.1 "/tick marks. The separation and position angle of STFA 10AB was determined by the 22-inch telescope to be 347.9" and 339.3°. The separation and position angle of STFA 1744AB was determined by the 14-inch telescope to be 3.6" and 158.1°. The measurements that were calculated were compared to the most recent measurements listed in the Washington Double Star Catalog.

Introduction

Vanguard Preparatory School held a double star workshop from March 11 through March 13, 2016. Thirty-three students were separated into three different groups to collect three sets of data from double stars. This team pictured in Figure 1 measured the scale constant, the position angle, and separation of STFA 10 AB and STFA 1744 AB. The measurements and calculations were done at Vanguard Preparatory School. The double star STFA 10AB is located in the constellation Taurus. The Washington Double Star Catalog lists the right ascension and declination as 04h 28m 39.74s and +15d 52m 15.2s. The WDS lists the magnitudes of primary and secondary stars as 3.41 and 3.94. The double star STFA 1744 AB is located in the constellation Ursa Major. The Washington Double Star Catalog lists the right ascension and declination of STFA 1744 AB as 13h 24m 18.4s and +54d 52m 33s. The magnitudes of the primary and secondary stars are listed as 2.23 and 3.88.

Figure 1: Team members for the present study. Top Row (left to right): Dayton Teeter, Andres Sanchez, Sam Bowden, Corielyn Hall, Cassandra Salazar, Danielle Rena, and Mark Brewer. Bottom Row (left to right): Fatima Rodriguez, Marisa Arcilla, Anthony Hall, Jacqueline DeBlase, and Alyssa Hernandez.

Data and Analysis of the Double Stars STFA 10AB and STFA 1744AB

Figure 2: An image of the 22-inch Newtonian Alt/ Az telescope with a Celestron 12.5 mm Micro Guide eyepiece.

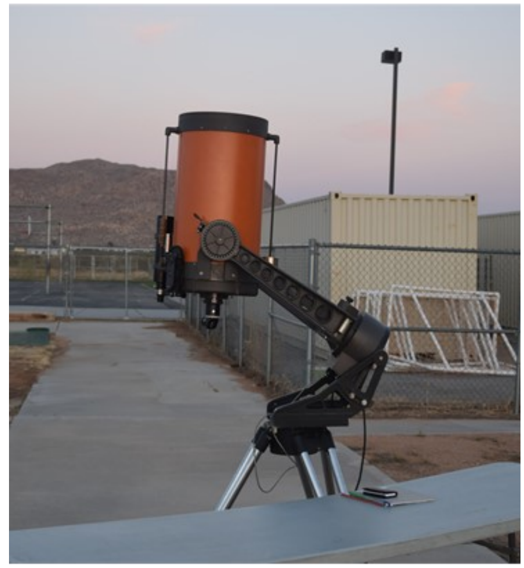

Figure 3: An image of the Celestron 14-inch Schmidt Cassegrain telescope.

A 22-inch Newtonian Alt/Az telescope, shown in Figure 2, was used to measure the scale constant, separation, and position angle of STFA 10AB. A 14-inch Celestron Schmidt Cassegrain telescope, shown in Figure 3, was used to measure the scale constant, separation, and position angle of STFA 1744AB.

Equipment and Procedures

Data was gathered from a 22-inch Newtonian Alt/Az telescope equipped with a Celestron 12.5 mm Micro Guide Eyepiece fitted with a Bell and Howell High Definition Video Camera. The use of the video camera eliminates the need for the drive motor and negates the field rotation common in Alt/Az telescopes. The 14-inch Celestron Schmidt-Cassegrain telescope equipped with a Celestron 12.5mm Micro Guide astrometric eyepiece was used.

The drift time was determined by timing the star's movement along the linear scale. The star was positioned on the outer edge of the eyepiece. The drive motor was turned off so the observers could watch the star drift. The star drift was timed with a stopwatch that reads to the nearest hundredth of a second. The stopwatch was started as soon as the star's centroid crossed the first tick mark on the linear scale, and the stopwatch was stopped as soon as the star's centroid crossed the last tick mark on the linear scale. A total of 15 drift times were recorded to determine an average, a standard deviation, and standard mean of the error.

The scale constant was determined by the following equation

$$Z = \frac{15.0411\, t \cos(dec)}{D}$$

where Z equals the scale constant in units of "/tick marks, 15.0411 equals the earth's sidereal rotation rate in units of "/seconds, t equals the average drift time in units of seconds, cos(dec) equals the cosine of the star's declination in degrees, and D equals the total displacement of the linear scale (60) in units of tick marks.

The separation was determined by aligning both stars on the linear scale. The eyepiece was adjusted so both stars aligned precisely. The tick marks between the star's centroids were recorded. A total of 10 measurements were recorded to determine an average, a standard deviation, and standard mean of the error for the separation. The scale constant was multiplied to the average separation for units to be determine in arc seconds.

The position angle was determined by aligning both stars on the linear scale. The eyepiece was adjusted so the stars were aligned precisely. The primary star was positioned on the 30 tick mark. The drive motor was turned off to allow the stars to drift to the outer protractor scale. The drive motor was turned on once the primary star reached the protractor, and the position angle was recorded. A total of 10 measurements were recorded to determine an average, a standard deviation, and a standard mean of the error for the position angle.

Data and Analysis of the Double Stars STFA 10AB and STFA 1744AB

Table 1: STFA 10AB. Measurements made on B2016.191904

Parameters	# Obs	Mean	SD	Standard Error of Mean	WDS Value	Difference	% Difference
Scale Constant a.s. / division	15	7.8	NA	NA	NA	NA	NA
Separation (a.s.)	15	347.9	0.62	0.18	341.2	6.7	1.93
Position Angle (degrees)	10	339.3	4.22	1.33	347	-7.7	2.27

Table 2: STFA 1744AB. Measurements made on B2016.194642

Parameters	# Obs	Mean	SD	Standard Error of Mean	WDS Value	Difference	% Difference
Scale Constant a.s. / div	5	5.14	NA	NA	NA	NA	NA
Separation (a.s.)	15	16.9	0.42	0.19	14.4	2.5	16.0
Position Angle (degrees)	10	158.0	0.64	0.19	153	5.0	3.21

Observation and Analysis (STFA 10 AB)

On March 11, 2016 (B2016.191904) observations were gathered of the double star STFA 10 AB with a 22 -inch Newtonian Alt/Az telescope. The scale constant was determined to be 7.8 "/tick marks. The average separation was 32.75 divisions. The average position angle was 249.3°. A separation and position angle difference of 6.7 and 7.7° was determined compared to the Washington Double Star Catalog. The results are summarized in Table 1.

Observation and Analysis (STFA 1744AB)

On March 12, 2016 (B2016.194642) the double star STFA 1744AB was measured with a 14 inch Celestron Cassegrain telescope and a Celestron astrometric eyepiece. The scale constant was determined to be 5.4 arc seconds/divisions. The average separation was determined to be 3.3". The average position angle was determined to be to 158.1°. The standard error of means for position is 0.19 and separation is 0.19. A difference of -2.5 arc seconds and -5.1 degrees was determined for the data gathered compared to the Washington Double Star Catalog.

Conclusion

The separation and position angle differences of STFA 10AB were compared to the Washington Double Star Catalog and determined to be 6.7" and -7.7°. The large differences were determined to be related to harsh weather conditions. The disturbances were greater as a storm front was moving in. The separation and position angle differences of STFA 1744AB were compared to the WDS and determined to be 2.5" and 5.0°. The large differences were determined to be related to the experience of the authors.

Acknowledgements

This research used the Washington Double Star Catalog maintained at the U.S. Naval Observatory. A thank you goes out to Vanguard Preparatory School for allowing the use of their facilities. Thank you to Chris Estrada, Reed Estrada, Sean Gillette, Pam Gillette, Debbie Wolf, Monica Arcilla, and Wendy Thielen. A thank you goes out to Apple Valley Starbucks for donating snacks/drinks. A thank you goes out to High Desert Astronomical Society for training the students. A thank you goes out to Antelope Valley Astronomy Club, High Desert Shuttle, and CalRTA (California Retired Teachers Association) for their generous financial donations.

References

Mason, Brian.(2012). Washington Double Star Catalog. Astronomy Department, U.S. Naval Observatory. Retrieved from www.ad.usno.navy.mil/wds/wds.html.

STT Doubles with Large ΔM – Part VIII: Tau Per Ori Cam Mon Cnc Peg

Wilfried R.A. Knapp
Vienna, Austria
wilfried.knapp@gmail.com

John Nanson
Star Splitters Double Star Blog
Manzanita, Oregon
jnanson@nehalemtel.net

Abstract: The results of visual double star observing sessions suggested a pattern for STT doubles with large delta_M of being harder to resolve than would be expected based on the WDS catalog data. It was felt this might be a problem with expectations on one hand, and on the other might be an indication of a need for new precise measurements, so we decided to take a closer look at a selected sample of STT doubles and do some research. Again like for the other STT objects covered so far several of the components show parameters quite different from the current WDS data.

1. Introduction

As follow up to our reports so far we finish this STT series with objects in the constellations Tau, Per, Ori, Cam, Mon, Cnc and Peg (see Table1). All values based on WDS data as of beginning of 2016.

Table 1. WDS catalog data per begin of 2016 for the selected STT objects

WDS ID	Name		RA	Dec	Sep	M1	M2	PA	Δ_M	Con
05417+1614	STT114	AB	05:41:40.770	+16:14:02.4	3.0	8.40	10.60	278	2.20	Tau
03334+2322	STT57	CD	03:33:26.530	+23:23:03.5	9.9	7.67	12.00	320	4.33	Tau
05272+1758	STT107	AB	05:27:10.090	+17:57:44.0	10.0	5.39	10.10	306	4.71	Tau
05272+1758	STT107	AC	05:27:10.090	+17:57:44.0	10.0	5.39	11.80	347	6.41	Tau
05459+2555	STT116	AC	05:45:55.390	+25:54:49.3	17.9	7.27	12.90	65	5.63	Tau
04162+3452	STT76	AB	04:16:10.609	+34:52:07.7	3.8	7.7	12.40	210	4.70	Per
02533+4834	STT48	AB	02:53:21.070	+48:34:11.9	6.6	6.5	10.60	318	4.10	Per
03483+5044	STT63	AB	03:48:18.080	+50:44:12.4	6.8	6.2	11.20	270	5.00	Per
05379+0715	STT518	AB	05:37:55.590	+07:14:55.5	2.1	8.8	12.80	240	4.00	Ori
05135+0158	STT517	AB,C	05:13:31.550	+01:58:03.7	6.5	6.13	13.00	138	6.87	Ori
06282+7032	STT136	AB	06:28:14.490	+70:32:07.0	5 5.0	6.04	11.00	82	5.00	Cam
07012+1146	STT163	AB,C	07:01:09.851	+11:46:28.7	14.5	6.41	12.00	165	5.59	Mon
09162+2324	STT198	AB	09:16:11.281	+23:24:10.4	14.6	7.74	12.00	121	4.50	Cnc
23074+2035	STT488	AB	23:07:25.502	+20:34:53.802	14.6	6.7	10.40	335	3.70	Peg
22148+2231	STT467	AB	22:14:48.567	+22:31:24.299	23.9	6.7	10.70	274	4.00	Peg

STT Doubles with Large ΔM – Part VIII: Tau Per Ori Cam Mon Cnc Peg

2. Further Research

Following the procedure for the earlier parts of our report we concluded again that the best approach would be to check historical data on all objects, observe them visually with the target of comparing with the existing data and obtain as many images as possible suitable for photometry.

2.1 Historical Research and Catalog Comparisons

Quite a few of the stars in this survey have notable historical aspects which merit some comment. Three main research sources were used for this section of this paper, the first of which was W.J. Hussey's *Micrometrical Observations of the Double Stars Discovered at Pulkowa*, published in 1901, which provided preliminary historical information on each of the stars. Hussey's book includes his observations and measures of all the stars originally listed in Otto Wilhelm Struve's 1845 Pulkovo Catalog, as well as data beginning with the date of first measure and continuing through the following years up to 1900. That data, plus inclusion of the background for the Pulkovo Catalog, makes Hussey's book a valuable source of reference. Another source consulted were the two volumes (*Part I and Part II*) which make up S.W. Burnham's *A General Catalogue of Double Stars Within 121° of the North Pole.* The third source consulted was Otto Struve's 1845 *Catalogue de 514 Étoiles Doubles et Multiples*. In addition, Bill Hartkopf of the USNO graciously provided the text files for STT 57, STT 116, STT 467, and STT 518.

Several of the stars mentioned below were dropped from the second edition of Otto Struve's Pulkovo Catalogue (published in 1850) because the separations exceeded 16", which was the maximum catalog separation established for stars with companions fainter than ninth magnitude (Hussey, 1901, p. 16). Fortunately, Hussey included all of the rejected stars in his 1901 book.

STT 198 (Cnc): Otto Struve's 1845 catalog shows an estimated separation of ten seconds for this pair, but no exact measure. Apparently he decided the separation of this pair exceeded 16" since it was dropped from his 1850 catalog. Dembowski reported he was unable to see the secondary in 1865 and 1866. Interestingly, according to S.W. Burnham, the only measures of STT 198 as of the time of Hussey's writing are those of Hussey and Burnham.

STT 163 (Mon): The C component was added by S.W. Burnham in 1879, with measures of 14.18" and 155.5 degrees, later supplemented with another measure by him in 1905 of 14.33" and 160.4 degrees.

STT 517 (Ori): The C component was added in 1878 by Asaph Hall, using the 26 inch USNO Clark refractor, with measures of 6.74" and 134.7 degrees, later supplemented with an 1888 measure of 6.90" and 138.3 degrees. Burnham refers to it as Hl 2 on p. 51 of his 1906 Catalog, Part I.

STT 518 (Ori): Hussey states that because of the faintness of the B component (WDS magnitude is 12.8), neither Otto Struve nor Dembowski attempted measurements of it. The first known measure of the AB pair was made by Hussey in 1898 while using the Lick 36 inch refractor, with a separation of 1.49" and a position angle of 281.7 degrees. The C component was first measured by Burnham in 1905 at 40.21" and 238.4 degrees, but the WDS text file for STT 518 also shows an 1898 measure of 40.405" and 238.6 degrees which was made from a photographic plate, and is the one listed as Obs1 in the WSD catalog.

STT 467 (Peg): This is another pair which was rejected by Otto Struve in his 1850 catalog because the distance exceeded the 16" limit. His 1845 catalog shows an estimated separation of 16", and a look at the WDS text file for STT 467 shows Mädler provided measures in 1843 of 22.95" and 272.5 degrees. The first recorded observation of this pair was made in 1827 by Nanson Herschel, who estimated a separation of 20" and a position angle of 270 degrees, which also comes from the STT 467 WDS text file.

STT 488 (Peg): According to Hussey, Otto Struve rejected this pair because the companion was considered too faint to measure. Struve's 1845 catalog shows an estimated distance of 12 seconds, with magnitudes of 7 and 11. Hussey shows Mädler also looked at this pair in 1845 and estimated a distance of 14". The first actual measure of STT 488 appears to have been made in 1865 by Dembowski, who recorded a separation of 13.46" and a position angle of 335.0 degrees. Both Burnham and Hussey refer to this pair as HO 486, attributing it to G.W. Hough, who measured the two stars in 1892 at 14.0" and 334.0 degrees.

STT 57 (Tau): What is now the CD pair was originally the AB pair, first measured by Otto Struve in 1854 at 10.0" and 319 degrees. See Figure 1. What is now the AC pair was first measured F.G.W. Struve in 1823 at 71.64" and 34.6 degrees. That pair is identified by both Hussey and Burnham as σ 95, and was also assigned by Otto Struve to the appendix of his 1845 catalog as number 35. The WDS text file for STT 57 shows what is now the AB pair was added to this system in 1907 by S.W. Burnham with measures of 34.95" and 169.6 degrees

STT 107 (Tau): See Figure 2. Hussey notes the C component was first seen in 1850 by Otto Struve, but

(Text continues on page 177)

STT Doubles with Large ΔM – Part VIII: Tau Per Ori Cam Mon Cnc Peg

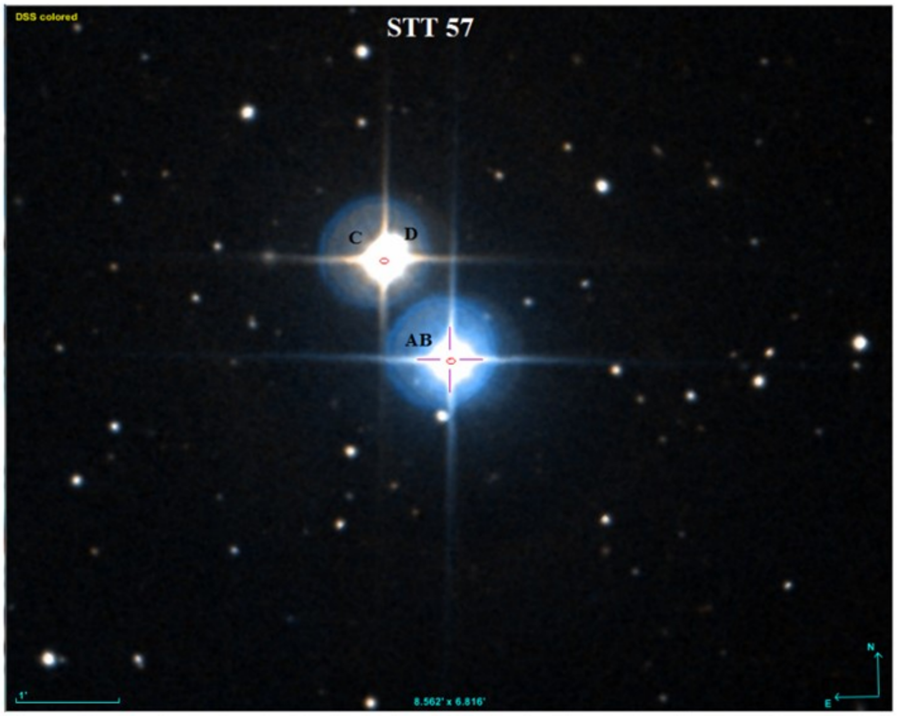

V	WDS	Disc	Comp	Obs1	Obs2	pa1	pa2	sep1	sep2	mag1	mag2	DM	No...	n	RAJ2000	DEJ2000
VizieR	03334+2322	STT 57	AB	1907	2000	170	170	35.0	33.50	7.17	12.80	+22 504	N		03 33 23.73	+23 22 05.6
VizieR	03334+2322	STT 57	AC	1854	2013	35	34	71.4	69.00	7.17	7.67		N D		03 33 23.73	+23 22 05.6
VizieR	03334+2322	STT 57	CD	1854	2014	319	320	10.0	9.90	7.67	12.00	+22 505	N		03 33 26.53	+23 23 03.5

Figure 1. Aladin image with component labels of STT 57 added.

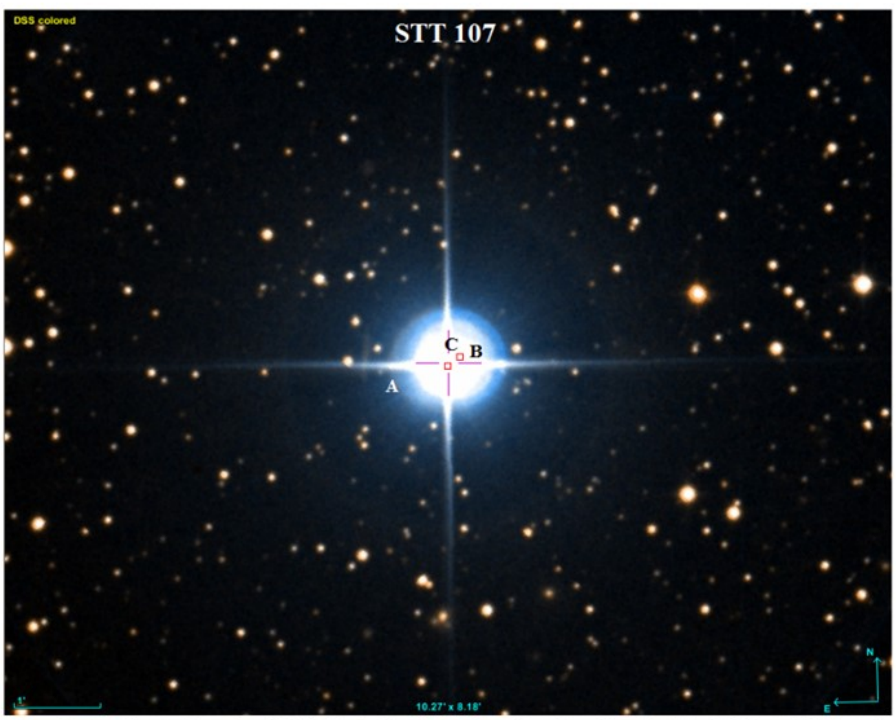

V	WDS	Disc	Comp	Obs1	Obs2	pa1	pa2	sep1	sep2	mag1	mag2	DM	No...	n	RAJ2000	DEJ2000
VizieR	05272+1758	MCA 19	Aa,Ab	1979	2015	80	163	0.1	0.00	5.80	6.80		NO		05 27 10.09	+17 57 44.0
VizieR	05272+1758	STT 107	AB	1843	2015	317	306	10.7	10.00	5.39	10.10	+17 928	N		05 27 10.09	+17 57 44.0
VizieR	05272+1758	STT 107	AC	1899	2015	341	347	10.0	10.00	5.39	11.80		N		05 27 10.09	+17 57 44.0
VizieR	05272+1758	STT 107	BC	1899	2015	58	57	5.8	7.00	10.10	11.80		N		05 27 09.51	+17 57 49.9

Figure 2. Aladin image with component lables of STT 107 added.

STT Doubles with Large ΔM – Part VIII: Tau Per Ori Cam Mon Cnc Peg

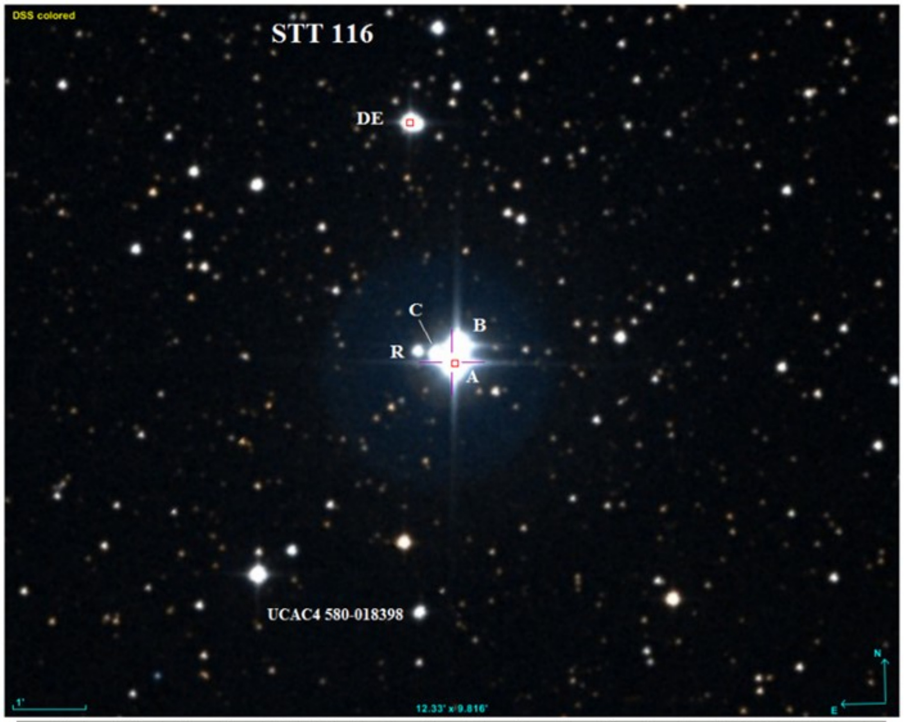

V	WDS	Disc	Comp	Obs1	Obs2	pa1	pa2	sep1	sep2	mag1	mag2	DM	No...	n	RAJ2000	DEJ2000
VizieR	05459+2555	STF 785	AB	1830	2011	349	348	13.8	14.70	7.27	8.32	+25 963	N D		05 45 55.39	+25 54 49.3
VizieR	05459+2555	STT 116	AC	1846	2011	66	65	18.3	17.90	7.27	12.90		N		05 45 55.39	+25 54 49.3
VizieR	05459+2555	STT 116	AD	1898	2010	10	11	201.2	201.50	7.27	10.22		N		05 45 55.39	+25 54 49.3
VizieR	05459+2555	STT 116	AR	1908	2011	72	73	31.3	31.90	7.27	13.25		N		05 45 55.39	+25 54 49.3
VizieR	05459+2555	STT 116	DE	1890	2009	250	253	6.9	5.90	10.23	11.90	+25 964	N		05 45 58.11	+25 58 07.6

Figure 3. Aladin image with components of STT 116 labeled.

(Continued from page 175)

not measured, although Struve noted it was closer to B than to A. He left a sketch showing a position angle of about 335 degrees. Hussey provided the first measures for the AC pair, measuring it once at the end of 1898 and twice at the beginning of 1899, resulting in an averaged separation of 10.0" and averaged position angle of 341.1 degrees.

STT 116 (Tau): See Figure 3. The AB pair, STF 785, was first measured by F.G.W. Struve in 1830 at 13.81” and 348.6 degrees. The AC, AD, AR, and DE components are all labeled as STT 116 in the WDS, but the AC pair is the only one that was discovered by Otto Struve, who measured it at 18.26" and 66 degrees in 1846. AD was first measured by S. W. Burnham in 1911 at 201.40” and 9.8 degrees. The WDS text file shows the 1898 Obs1 measure for AD was made on a photographic plate of that date. Two other measures are also listed in the text file which were made from 1908 and 1909 plates. The AR pair received its first measure of 31.93" and 72.1 degrees in 1908, by Erich Przybyllok, who was associated with the Heidelberg Observatory, while using a 12.5 inch refractor. The WDS Obs1 measure for the AR pair, which is also from 1908, was made from a photographic plate. And the last pair, DE, was first measured in 1890 by Kenneth J. Tarrant at 6.89" and 250.4 degrees according to the WDS text file.

2.2 Visual Observations

Both John Nanson and Wilfried Knapp made visual observations of the stars included in this report. Nanson used a 127mm f/9.3 refractor, a 152mm f/10 refractor, and a 235mm SCT, while Knapp utilized 140mm and 185mm refractors as well as a masking device to evaluate what could be seen at lesser apertures.

STT 136 (Cam): Nanson made one observation of this pair with the 152mm refractor and may have had a glimpse of B, but it was far from definitive. The best result was at 152x, which seemed to show a faint speck of a light on the edge of the primary at the correct PA. An attempt was made to resolve B at 607x, but it would not come to focus because of poor seeing. Thus, no conclusion was reached on the magnitude of B. Knapp made one observation with the 185mm refractor and was able to resolve B with the aperture reduced to 140mm, suggesting a magnitude much fainter than the WDS value of 11.0.

STT 198 (Cnc): Knapp was unable to resolve this pair with both the 140mm and 185mm refractors, suggesting the magnitude of B is much fainter than the

WDS value of 12.0, a conclusion reinforced by being able to easily see a 12.36 magnitude star in the 140mm refractor. Nanson found B very tough to see in the 152mm refractor, able to detect it only with averted vision, which also indicates a magnitude fainter than the WDS value, especially when the 14.6" separation of the pair is taken into consideration.

STT 163 (Mon): Using the 152mm refractor, Nanson observed C with averted vision, which was made more difficult than normal because the first quarter moon was slightly less than 10 degrees to the north with haze in the sky. UCAC4 509-033885 was of similar difficulty (Vmag 11.890), suggesting the WDS magnitude of 12.0 for C is close. Knapp used the 185mm refractor to observe C and found it was still visible with the aperture reduced to 140mm, which also indicates the WDS value for C is close.

STT 517 (Ori): Knapp detected C as a spot of light at 360x in the 185mm refractor in difficult seeing, indicating C might be a bit brighter than the WDS value of 13.0. Nanson caught the C component at 152x, 203x, and 253x with the 152mm refractor. Averted vision was needed at 152x, but C was seen with direct vision several times at 203x and 253x. The first quarter moon was about 35 degrees to the northeast with some haze in the air, which would make it very unlikely the star is as faint as 13.0. No obvious comparison stars seen.

STT 518 (Ori): Nanson needed magnifications of 487x and 607x to detect the B component of STT 518 in the 152mm refractor. Based on that, the WDS listed separation of 2.1" is probably about right, but given the interference from the moon, it's possible B is about half a magnitude brighter than the WDS value of 12.8. C was rather difficult to see at 203x and 253x, and not visible at 152x. It seemed to be just slightly brighter (slightly easier to see) than STT 517 C above, suggesting the magnitudes for one of the two stars is wrong (the WDS value for STT 518 C is 12.25). Knapp was unable to resolve B definitively in the 185mm refractor under difficult seeing conditions, but was able to detect the much wider separated C (39.5") with the aperture reduced to 100mm.

STT 467 (Peg): Using the 235mm SCT, Nanson Found B to be about half a magnitude brighter than a 12.8 magnitude comparison star, indicating B may be in the 12.2 to 12.3 range. At a minimum, B certainly seemed fainter than the WDS 10.7 magnitude.

STT 488 (Peg): Nanson found B appeared slightly brighter in the 235mm SCT than a 12.6 magnitude comparison star, and noted it appeared distinctly fainter than the WDS value of 10.4.

STT 48 (Per): Magnifications of 152x, 253x, and 380x may have resulted in a glimpse of the secondary, but it was far from conclusive. This observation, as well as the next one, were made by Nanson with the 152mm refractor under difficult seeing conditions.

STT 63 (Per): A clear elongation of the secondary was seen by at 253x, followed by a brief glimpse of the secondary, which wasn't seen again with the further observation.

STT 76 (Per): No observations made for this pair be either observer.

STT 57 (Tau): Knapp was unable to definitively resolve the B component with the 185mm refractor, suggesting it's fainter than the 12.8 magnitude listed for it in the WDS. D could be seen with the aperture reduced to 140mm, which seems to confirm the WDS value of 12.0 for it. Nanson was able to detect B with averted vision while using the 152mm refractor at 253x, which suggested the 12.8 magnitude is probably close. The much tighter D was seen at 152x with averted vision, again suggesting the WDS listed magnitude of 12.0 is about right.

STT 107 (Tau): Nanson detected the B component with averted vision in the 152mm refractor at 152x, 190x, and 253x, but found it was very tough and somewhat indistinct, which would seem to indicate a fainter magnitude for it than the 10.10 magnitude listed in the WDS. On the same night, C (WDS magnitude of 11.8) was impossible to detect in the glare caused by the primary. However, in a prior observation of STT 107 on 1-15-2015 during better seeing conditions, Nanson detected both the B and C components with a 127mm refractor at 295x, which would indicate the WDS values for both stars are about right. Using the 185mm refractor, Knapp observed B with the aperture reduced to 150mm, but was unable to detect C, leading to the conclusion both stars are fainter than the WDS listed values.

STT 114 (Tau): Knapp was able to resolve B with the aperture of the 185mm refractor reduced to 110mm, leading to the conclusion the WDS magnitude of 10.6 is about right. Nanson had a glimpse of the secondary in the 152mm refractor at 152x and consistently detected an elongation of the primary, which seems consistent with the 3.0" separation and the 2.6 magnitudes of difference between the primary and the secondary.

STT 116 (Tau): Nanson found C was easily seen in the 152mm refractor at 152x and appeared similar in magnitude to a comparison star of 12.3 magnitude, suggesting it may be about half a magnitude brighter than the WDS value of 12.90. The DE pair appeared distinctly elongated at 152x and was easily split at 253x, though in the poor seeing it was blurred more often than not. Knapp resolved C and E with the aperture of

STT Doubles with Large ΔM – Part VIII: Tau Per Ori Cam Mon Cnc Peg

the 185mm refractor reduced to 110mm, and also resolved R at 250x with the aperture reduced to 150mm, all of which led to the conclusion that each of the three stars seems to be a bit brighter than the WDS values.

2.3 Photometry and Astrometry Results

Several hundred images taken with iTelescope remote telescopes were, in a first step, plate solved and stacked with AAVSO VPhot. The stacked images were then plate solved with Astrometrica with URAT1 reference stars with Vmags in the range 10.5 to 14.5mag. The RA/Dec coordinates resulting from plate solving with URAT1 reference stars in the 10.5 to 14.5mag range were used to calculate Sep and PA using the formula provided by R. Buchheim (2008). *Err_PA* is the error estimation for PA in degrees calculated as

$$Err\_PA = \arctan\left(\frac{Err\_Sep}{Sep}\right)$$

assuming the worst case that *Err_Sep* points perpendicular to the separation vector. Mag is the photometry result based on UCAC4 reference stars with Vmags between 10.5 and 14.5mag. *Err_Mag* is calculated as

$$Err\_Mag = \sqrt{dV_{mag}{}^2 + \left[2.5\log_{10}\left(1+\frac{1}{SNR}\right)\right]^2}$$

with *dVmag* as the average *Vmag* error over all used reference stars and *SNR* is the signal to noise ratio for the given star. The results are shown in Table 2.

3. Summary

Tables 3 and 4 below compare the final results of our research with the WDS data that was current at the time we began working on our current group of stars.

In Table 3 the results of our photometry have been averaged for each star. Because we're aware that both the NOMAD-1 and the UCAC4 catalogs are frequently consulted when making WDS evaluations of magnitudes changes, the data from those catalogs has also been included for each of the stars.

Red type has been used in Tables 3 and 4 to call attention to significant differences from the WDS data. With regard to Table 3 those magnitudes that differ by two tenths of a magnitude or more from the WDS values have been highlighted. In Table 4 differences in separation in excess of two-tenths of an arc second are highlighted as are all position angles which differ by more than a degree.

Subsequent to our measures, as a quality check for our astrometry results we turned to the URAT1 catalog for the most recent precise professional measurements available. We used its coordinates to calculate the Sep and PA for all objects in this report for which URAT1 data was available and compared these values with our results, which are shown in Table 5.

Global Summary

As this report is our last in this sequence of wide STT doubles we take this opportunity for a summary over all eight reports:

1) In total we checked about 100 objects and suggested WDS catalog visual magnitude changes for most of them based on own measurements from images specifically taken for this project.
2) We soon found that for many objects also the astrometry data given in the WDS catalog needed an update so we extended our reports to include RA/Dec coordinates, separation and position angle with the corresponding error estimations. Some objects also show significant different proper motion for the components demonstrating the need of frequent measurements to keep the catalog values up to date.
3) We also made visual observations for all objects to counter-check visual impression with measurement results and got a mixed bag of often different impressions by different observers and in several cases the visual impressions regarding magnitudes did not match at all the measurement results.

Follow Up

The images we took for this series of reports include besides so far not measured components of the covered STT objects other double stars as well – in these cases we do not suspect any issues with the current WDS catalog data but any double star visited is worth just another recent measurement. We intend to use the available material for another report covering the mentioned additional objects.

Acknowledgements:

The following tools and resources have been used for this research:

- Washington Double Star Catalog as data source for the selected objects
- iTelescope: Images were taken with
  - iT24: 610mm CDK with 3962mm focal length. CCD: FLI-PL09000. Resolution 0.62 arcsec/pixel. V-filter. Located in Auberry. California. Elevation 1405m
  - iT11: 510mm CDK with 2280mm focal length. CCD: FLI ProLine PL11002M. Resolution 0.81 arcsec/pixel. B- and V-Filter. Located in Mayhill. New Mexico.

(Text continues on page 188)

STT Doubles with Large ΔM – Part VIII: Tau Per Ori Cam Mon Cnc Peg

Table 2. Photometry and astrometry results for the selected STT objects. Date is the Bessel epoch and N is the number of images used for the reported values. iT in the Notes column indicates the telescope used with number of images and exposure time given (Specifications of the used telescopes: See Acknowledgements). The average results over all used images are given in the line below the individual stacks in bold. The error estimation over all used images is calculated as root mean square over the individual Err values. The N column in the summary line gives the total number of images used and Date the average Bessel epoch.

STT 114	RA	Dec	dRA	dDec	Sep	Err Sep	PA	Err PA	Mag	Err Mag	SNR	dVmag	Date	N	Notes
A	05 41 40.778	16 14 02.37	0.07	0.05	2.997	0.086	281.355	1.644	7.877	0.090	136.87	0.09	2016.093	4	iT18 stack 4x3s. Overlapping star disks
B	05 41 40.574	16 14 02.96							9.338	0.092	56.54				
A	05 41 40.777	16 14 02.47	0.08	0.08	2.807	0.113	277.987	2.308	7.862	0.081	106.77	0.08	2016.085	5	iT18 stack 5x3s. Overlapping star disks. SNR B<20
B	05 41 40.584	16 14 02.86							9.679	0.102	16.52				
A	**05 41 40.777**	**16 14 02.42**	**0.075**	**0.067**	**2.900**	**0.100**	**279.726**	**1.984**	**7.870**	**0.086**			**2016.089**	**9**	**Overlapping star disks. Both stars too bright for reliable photometry**
B	**05 41 40.579**	**16 14 02.91**							**9.509**	**0.097**					

STT 57	RA	Dec	dRA	dDec	Sep	Err Sep	PA	Err PA	Mag	Err Mag	SNR	dVmag	Date	N	Notes
C	03 33 26.531	23 23 03.09	0.07	0.07	9.932	0.099	319.657	0.571	7.510	0.080	230.47	0.08	2016.090	3	iT18 stack 3x3s. C too bright for reliable photometry
D	03 33 26.064	23 23 10.66							11.532	0.085	36.08				
C	03 33 26.533	23 23 03.12	0.10	0.05	10.003	0.112	319.796	0.640	7.511	0.080	221.06	0.08	2016.085	4	iT18 stack 4x3s. C too bright for reliable photometry
D	03 33 26.064	23 23 10.76							11.545	0.086	33.48				
C	03 33 26.522	23 23 03.23	0.04	0.09	9.983	0.098	320.112	0.565	7.513	0.070	175.07	0.07	2016.093	5	iT18 stack 5x3s. C too bright for reliable photometry
D	03 33 26.057	23 23 10.89							11.516	0.081	26.70				
C	03 33 26.475	23 23 03.32	0.15	0.10	9.727	0.180	321.479	1.062	7.414	0.071	75.45	0.07	2016.023	5	iT27 stack 5x3s. C too bright for reliable photometry. Component B resolved with 14.566Vmag (compared with 12.8mag in WDS)
D	03 33 26.035	23 23 10.93							11.482	0.077	34.65				
C	03 33 26.529	23 23 03.03	0.16	0.07	10.033	0.175	319.422	0.997	7.488	0.060	165.74	0.06	2016.026	5	iT27 stack 5x3s. C too bright for reliable photometry. Component B resolved with 14.659Vmag (compared with 12.8mag in WDS)
D	03 33 26.055	23 23 10.65							11.552	0.061	85.67				
C	**03 33 26.518**	**23 23 03.16**	**0.114**	**0.078**	**9.935**	**0.138**	**320.086**	**0.795**	**7.487**	**0.073**			**2016.064**	**22**	**C too bright for reliable photometry**
D	**03 33 26.055**	**23 23 10.78**							**11.525**	**0.078**					

Table 2 continues on the next page.

STT Doubles with Large ΔM – Part VIII: Tau Per Ori Cam Mon Cnc Peg

Table 2 (continued). Photometry and astrometry results for the selected STT objects. Date is the Bessel epoch and N is the number of images used for the reported values. iT in the Notes column indicates the telescope used with number of images and exposure time given (Specifications of the used telescopes: See Acknowledgements). The average results over all used images are given in the line below the individual stacks in bold. The error estimation over all used images is calculated as root mean square over the individual Err values. The N column in the summary line gives the total number of images used and Date the average Bessel epoch.

STT 107	RA	Dec	dRA	dDec	Sep	Err Sep	PA	Err PA	Mag	Err Mag	SNR	dVmag	Date	N	Notes
A	05 27 10.104	17 57 43.70	0.07	0.08	10.176	0.106	305.854	0.599	5.336	0.060	511.81	0.06	2016.090	4	iT18 stack 4x3s. A too bright for reliable photometry
B	05 27 09.526	17 57 49.66							11.066	0.066	40.18				
A	05 27 10.105	17 57 43.72	0.07	0.09	10.152	0.114	305.809	0.643	5.362	0.090	435.83	0.09	2016.093	5	iT18 stack 5x3s. A too bright for reliable photometry
B	05 27 09.528	17 57 49.66							11.164	0.099	26.60				
A	05 27 10.109	17 57 43.70	0.06	0.07	10.193	0.092	305.852	0.518	5.340	0.080	502.15	0.08	2016.085	5	iT18 stack 5x3s. A too bright for reliable photometry
B	05 27 09.530	17 57 49.67							11.098	0.086	34.59				
A	05 27 10.089	17 57 44.26	0.11	0.12	9.837	0.163	303.784	0.948	6.059	0.092	53.70	0.09	2016.023	4	iT27 stack 4x3s. A too bright for reliable photometry
B	05 27 09.516	17 57 49.73							11.099	0.094	39.73				
A	05 27 10.088	17 57 44.05	0.11	0.12	10.053	0.163	305.444	0.928	6.380	0.061	111.35	0.06	2016.026	4	iT27 stack 4x3s. A too bright for reliable photometry
B	05 27 09.514	17 57 49.88							11.100	0.062	65.33				
A	**05 27 10.099**	**17 57 43.89**	**0.087**	**0.098**	**10.081**	**0.131**	**305.359**	**0.744**	**5.695**	**0.078**			**2016.064**	**22**	**A too bright for reliable photometry**
B	**05 27 09.523**	**17 57 49.72**							**11.105**	**0.083**					
STT 107	**RA**	**Dec**	**dRA**	**dDec**	**Sep**	**Err Sep**	**PA**	**Err PA**	**Mag**	**Err Mag**	**SNR**	**dVmag**	**Date**	**N**	**Notes**
A	05 27 10.104	17 57 43.70	0.07	0.08	9.939	0.106	346.889	0.613	5.336	0.060	511.81	0.06	2016.090	4	iT18 stack 4x3s. A too bright for reliable photometry. SNR C<20
C	05 27 09.946	17 57 53.38							12.604	0.102	12.63				
A	05 27 10.105	17 57 43.72	0.07	0.09	10.092	0.114	346.675	0.647	5.362	0.090	435.83	0.09	2016.093	5	iT18 stack 5x3s. A too bright for reliable photometry. SNR C<10
C	05 27 09.942	17 57 53.54							12.845	0.138	9.95				
A	05 27 10.109	17 57 43.70	0.06	0.07	10.030	0.092	346.927	0.527	5.340	0.080	502.15	0.08	2016.085	5	iT18 stack 5x3s. A too bright for reliable photometry. SNR C<10
C	05 27 09.950	17 57 53.47							12.765	0.143	8.68				
A	05 27 10.089	17 57 44.26	0.11	0.12	9.442	0.163	346.721	0.988	6.059	0.092	53.70	0.09	2016.023	4	iT27 stack 4x3s. A too bright for reliable photometry. SNR C<20
C	05 27 09.937	17 57 53.45							12.738	0.128	11.39				
A	05 27 10.088	17 57 44.05	0.11	0.12	9.570	0.163	346.110	0.975	6.380	0.061	111.35	0.06	2016.026	4	iT27 stack 4x3s. A too bright for reliable photometry. SNR C<20
C	05 27 09.927	17 57 53.34							13.077	0.118	10.20				
A	**05 27 10.099**	**17 57 43.89**	**0.087**	**0.098**	**9.814**	**0.131**	**346.669**	**0.765**	**5.695**	**0.078**			**2016.064**	**22**	**A too bright for reliable photometry. SNR C<20**
C	**05 27 09.940**	**17 57 53.44**							**12.806**	**0.127**					

Table 2 continues on the next page.

STT Doubles with Large ΔM – Part VIII: Tau Per Ori Cam Mon Cnc Peg

Table 2 (continued). Photometry and astrometry results for the selected STT objects. Date is the Bessel epoch and N is the number of images used for the reported values. iT in the Notes column indicates the telescope used with number of images and exposure time given (Specifications of the used telescopes: See Acknowledgements). The average results over all used images are given in the line below the individual stacks in bold. The error estimation over all used images is calculated as root mean square over the individual Err values. The N column in the summary line gives the total number of images used and Date the average Bessel epoch.

STT 116	RA	Dec	dRA	dDec	Sep	Err Sep	PA	Err PA	Mag	Err Mag	SNR	dVmag	Date	N	Notes
A	05 45 55.397	25 54 49.25	0.08	0.07	17.783	0.106	64.735	0.342	7.237	0.090	269.89	0.09	2016.090	4	iT18 stack 4x3s: A too bright for reliable photometry. Component R measured with 12.814Vmag with SNR 20.47
C	05 45 56.589	25 54 56.84							11.675	0.095	36.33				
A	05 45 55.400	25 54 49.24	0.06	0.06	17.787	0.085	64.812	0.273	7.244	0.070	281.94	0.07	2016.085	5	iT18 stack 5x3s: A too bright for reliable photometry. Component R measured with 12.948Vmag with SNR 19.65
C	05 45 56.593	25 54 56.81							11.679	0.076	37.07				
A	05 45 55.399	25 54 49.26	0.08	0.08	17.772	0.113	64.504	0.365	7.249	0.080	172.94	0.08	2016.093	5	iT18 stack 5x3s: A too bright for reliable photometry. Component R measured with 13.089Vmag with SNR 8.68
C	05 45 56.588	25 54 56.91							11.661	0.095	20.52				
A	**05 45 55.399**	**25 54 49.25**	**0.074**	**0.070**	**17.781**	**0.102**	**64.684**	**0.329**	**7.2433333**	**0.081**			**2016.089**	**14**	**A too bright for reliable photometry. Component R measured with averaged 12.950Vmag**
C	**05 45 56.590**	**25 54 56.85**							**11.671667**	**0.089**					
STT 76	**RA**	**Dec**	**dRA**	**dDec**	**Sep**	**Err Sep**	**PA**	**Err PA**	**Mag**	**Err Mag**	**SNR**	**dVmag**	**Date**	**N**	**Notes**
A	04 16 10.639	34 52 07.29	0.03	0.03	3.550	0.042	211.099	0.685	7.501	0.030	354.56	0.03	2016.236	5	iT24 stack 5x3s. A too bright for reliable photometry. Overlapping star disks. SNR B<20
B	04 16 10.490	34 52 04.25							12.489	0.079	14.34				
A	**04 16 10.639**	**34 52 07.29**	**0.030**	**0.030**	**3.550**	**0.042**	**211.099**	**0.685**	**7.501**	**0.030**			**2016.236**	**5**	**A too bright for reliable photometry. Overlapping star disks. SNR B<20**
B	**04 16 10.490**	**34 52 04.25**							**12.489**	**0.079**					
STT 48	**RA**	**Dec**	**dRA**	**dDec**	**Sep**	**Err Sep**	**PA**	**Err PA**	**Mag**	**Err Mag**	**SNR**	**dVmag**	**Date**	**N**	**Notes**
A	02 53 21.068	48 34 11.82	0.16	0.12	6.526	0.200	316.327	1.755	6.167	0.100	194.65	0.10	2016.172	5	iT18 stack 5x3s. A too bright for reliable photometry. Overlapping star disks. SNR B <20
B	02 53 20.614	48 34 16.54							11.498	0.118	16.73				
A	02 53 21.070	48 34 11.73	0.10	0.10	6.609	0.141	317.597	1.226	6.165	0.080	395.94	0.08	2016.258	5	iT24 stack 5x3s. A too bright for reliable photometry. Overlapping star disks
B	02 53 20.621	48 34 16.61							11.357	0.094	21.93				
A	**02 53 21.069**	**48 34 11.78**	**0.133**	**0.110**	**6.567**	**0.173**	**316.966**	**1.511**	**6.166**	**0.091**			**2016.215**	**10**	**A too bright for reliable photometry. Overlapping star disks**
B	**02 53 20.618**	**48 34 16.58**							**11.428**	**0.107**					

Table 2 continues on the next page.

STT Doubles with Large ΔM – Part VIII: Tau Per Ori Cam Mon Cnc Peg

Table 2 (continued). Photometry and astrometry results for the selected STT objects. Date is the Bessel epoch and N is the number of images used for the reported values. iT in the Notes column indicates the telescope used with number of images and exposure time given (Specifications of the used telescopes: See Acknowledgements). The average results over all used images are given in the line below the individual stacks in bold. The error estimation over all used images is calculated as root mean square over the individual Err values. The N column in the summary line gives the total number of images used and Date the average Bessel epoch.

STT 63	RA	Dec	dRA	dDec	Sep	Err Sep	PA	Err PA	Mag	Err Mag	SNR	dVmag	Date	N	Notes
A	03 48 18.072	50 44 12.50	0.11	0.10	6.324	0.149	271.359	1.347	6.100	0.070	349.80	0.07	2016.172	4	iT18 stack 4x3s. A too bright for reliable photometry. Overlapping star disks. SNR B <10
B	03 48 17.406	50 44 12.65							11.573	0.137	8.69				
A	03 48 18.067	50 44 12.35	0.12	0.11	6.894	0.163	268.753	1.353	6.225	0.100	303.25	0.10	2016.255	1	iT24 1x3s. A too bright for reliable photometry. Overlapping star disks. SNR B <20
B	03 48 17.341	50 44 12.20							11.438	0.116	18.24				
A	03 48 18.068	50 44 12.18	0.09	0.08	6.959	0.120	270.494	0.991	6.212	0.090	348.90	0.09	2016.258	5	iT24 stack 5x1s. A too bright for reliable photometry. Overlapping star disks
B	03 48 17.335	50 44 12.24							11.190	0.093	42.48				
A	03 48 18.025	50 44 12.61	0.04	0.04	6.644	0.057	267.153	0.488	7.021	0.050	187.41	0.05	2016.236	5	iT24 stack 5x3s. A too bright for reliable photometry. Overlapping star disks
B	03 48 17.326	50 44 12.28							11.314	0.053	59.40				
A	**03 48 18.058**	**50 44 12.41**	**0.095**	**0.087**	**6.703**	**0.129**	**269.423**	**1.100**	**6.390**	**0.080**			**2016.230**	**15**	**A too bright for reliable photometry. Overlapping star disks**
B	**03 48 17.352**	**50 44 12.34**							**11.379**	**0.105**					
STT 518	**RA**	**Dec**	**dRA**	**dDec**	**Sep**	**Err Sep**	**PA**	**Err PA**	**Mag**	**Err Mag**	**SNR**	**dVmag**	**Date**	**N**	**Notes**
A															**No resolution of B in any of the images taken**
B															
STT 517	**RA**	**Dec**	**dRA**	**dDec**	**Sep**	**Err Sep**	**PA**	**Err PA**	**Mag**	**Err Mag**	**SNR**	**dVmag**	**Date**	**N**	**Notes**
AB	05 13 31.509	01 58 03.43	0.12	0.11	7.110	0.163	132.795	1.312	6.388	0.100	153.04	0.10	2016.026	5	iT27 stack 5x3s. A too bright for reliable photometry. Overlapping star disks. SNR B <20
C	05 13 31.857	01 57 58.60							11.522	0.115	18.87				
AB	05 13 31.527	01 58 03.67	0.12	0.12	7.362	0.170	135.044	1.320	6.483	0.080	162.27	0.08	2016.032	5	iT27 stack 5x3s. A too bright for reliable photometry. Overlapping star disks
C	05 13 31.874	01 57 58.46							11.457	0.091	24.16				
AB	05 13 31.545	01 58 03.73	0.12	0.12	7.017	0.170	137.702	1.385	6.313	0.081	111.63	0.08	2016.035	5	iT27 stack 5x3s. A too bright for reliable photometry. Overlapping star disks. SNR B <20
C	05 13 31.860	01 57 58.54							11.448	0.105	15.55				
AB	05 13 31.550	01 58 03.51	0.10	0.08	6.727	0.128	135.770	1.091	6.143	0.090	161.50	0.09	2016.031	4	iT24 stack 4x3s. A too bright for reliable photometry. Overlapping star disks. SNR B <20
C	05 13 31.863	01 57 58.69							11.519	0.117	13.91				
AB	**05 13 31.533**	**01 58 03.59**	**0.115**	**0.109**	**7.051**	**0.159**	**135.311**	**1.288**	**6.332**	**0.088**			**2016.031**	**19**	**A too bright for reliable photometry. Overlapping star disks. SNR B <20**
C	**05 13 31.863**	**01 57 58.57**							**11.487**	**0.108**					

Table 2 continues on the next page.

STT Doubles with Large ΔM – Part VIII: Tau Per Ori Cam Mon Cnc Peg

Table 2 (continued). Photometry and astrometry results for the selected STT objects. Date is the Bessel epoch and N is the number of images used for the reported values. iT in the Notes column indicates the telescope used with number of images and exposure time given (Specifications of the used telescopes: See Acknowledgements). The average results over all used images are given in the line below the individual stacks in bold. The error estimation over all used images is calculated as root mean square over the individual Err values. The N column in the summary line gives the total number of images used and Date the average Bessel epoch.

STT 136	RA	Dec	dRA	dDec	Sep	Err Sep	PA	Err PA	Mag	Err Mag	SNR	dVmag	Date	N	Notes
A	06 28 14.458	70 32 07.41	0.12	0.14	5.373	0.184	80.789	1.966	5.811	0.130	218.05	0.13	2016.194	2	iT18 stack 2x3s. SNR B<20. A too bright for reliable photometry
B	06 28 15.519	70 32 08.27							10.806	0.152	13.26				
A	06 28 14.545	70 32 07.41	0.08	0.08	5.334	0.113	83.865	1.215	6.016	0.080	402.55	0.08	2016.258	4	iT24 stack 4x1s. SNR B<20. A too bright for reliable photometry. Overlapping star disks
B	06 28 15.606	70 32 07.98							10.616	0.097	19.30				
A	06 28 14.490	70 32 07.25	0.06	0.07	5.466	0.092	81.689	0.966	5.970	0.070	517.69	0.07	2016.236	5	iT24 stack 5x3s. A too bright for reliable photometry. Overlapping star disks
B	06 28 15.572	70 32 08.04							10.757	0.087	20.78				
A	06 28 14.452	70 32 07.28	0.10	0.08	5.593	0.128	83.120	1.312	5.828	0.080	168.06	0.08	2016.247	5	iT24 stack 5x3s. A too bright for reliable photometry. Overlapping star disks
B	06 28 15.563	70 32 07.95							10.315	0.085	37.58				
A	06 28 14.475	70 32 07.50	0.14	0.11	5.504	0.178	85.624	1.853	5.899	0.080	183.76	0.08	2016.247	5	iT24 stack 5x3s. A too bright for reliable photometry. Overlapping star disks
B	06 28 15.573	70 32 07.92							10.334	0.084	39.76				
A	**06 28 14.484**	**70 32 07.37**	**0.104**	**0.099**	**5.452**	**0.144**	**83.025**	**1.511**	**5.905**	**0.091**			**2016.237**		**A too bright for reliable photometry. Overlapping star disks**
B	**06 28 15.567**	**70 32 08.03**							**10.566**	**0.104**					
STT 163	**RA**	**Dec**	**dRA**	**dDec**	**Sep**	**Err Sep**	**PA**	**Err PA**	**Mag**	**Err Mag**	**SNR**	**dVmag**	**Date**	**N**	**Notes**
AB	07 01 09.858	11 46 28.35	0.09	0.06	14.235	0.108	165.970	0.435	6.707	0.080	334.27	0.08	2016.194	4	iT18 stack 4x3s. AB too bright for reliable photometry
C	07 01 10.093	11 46 14.54							11.767	0.086	33.50				
AB	07 01 09.824	11 46 28.40	0.04	0.04	14.436	0.057	164.483	0.225	7.020	0.040	318.94	0.04	2016.236	5	iT24 stack 5x3s. AB too bright for reliable photometry
C	07 01 10.087	11 46 14.49							11.778	0.041	111.68				
AB	07 01 09.855	11 46 28.11	0.11	0.11	13.885	0.156	165.296	0.642	6.718	0.061	133.17	0.06	2016.247	5	iT24 stack 5x3s. AB too bright for reliable photometry
C	07 01 10.095	11 46 14.68							11.721	0.061	91.17				
AB	07 01 09.829	11 46 28.25	0.11	0.11	14.268	0.156	164.357	0.625	6.721	0.050	153.43	0.05	2016.247	5	iT24 stack 5x3s. AB too bright for reliable photometry
C	07 01 10.091	11 46 14.51							11.733	0.052	78.84				
AB	07 01 09.848	11 46 28.36	0.09	0.10	14.216	0.135	165.769	0.542	6.793	0.060	307.52	0.06	2016.258	5	iT24 stack 5x3s. AB too bright for reliable photometry
C	07 01 10.086	11 46 14.58							11.788	0.061	90.92				
AB	**07 01 09.843**	**11 46 28.29**	**0.092**	**0.089**	**14.207**	**0.128**	**165.172**	**0.515**	**6.792**	**0.060**			**2016.237**		**AB too bright for reliable photometry**
C	**07 01 10.090**	**11 46 14.56**							**11.757**	**0.062**					

Table 2 continues on the next page.

STT Doubles with Large ΔM – Part VIII: Tau Per Ori Cam Mon Cnc Peg

Table 2 (continued). Photometry and astrometry results for the selected STT objects. Date is the Bessel epoch and N is the number of images used for the reported values. iT in the Notes column indicates the telescope used with number of images and exposure time given (Specifications of the used telescopes: See Acknowledgements). The average results over all used images are given in the line below the individual stacks in bold. The error estimation over all used images is calculated as root mean square over the individual Err values. The N column in the summary line gives the total number of images used and Date the average Bessel epoch.

STT 198	RA	Dec	dRA	dDec	Sep	Err Sep	PA	Err PA	Mag	Err Mag	SNR	dVmag	Date	N	Notes
A	09 16 11.137	23 24 08.77	0.04	0.06	14.994	0.072	115.141	0.276	7.632	0.080	241.96	0.08	2016.194	5	iT18 stack 5x3s. A too bright for reliable photometry
B	09 16 12.123	23 24 02.40							12.864	0.095	20.71				
A	09 16 11.143	23 24 08.97	0.08	0.09	15.019	0.120	115.348	0.459	7.623	0.041	147.39	0.04	2016.247	5	iT24 stack 5x3s. A too bright for reliable photometry
B	09 16 12.129	23 24 02.54							12.980	0.045	51.04				
A	09 16 11.146	23 24 08.76	0.05	0.05	14.944	0.071	115.104	0.271	7.664	0.060	168.26	0.06	2016.258	4	iT24 stack 4x3s. A too bright for reliable photometry
B	09 16 12.129	23 24 02.42							13.019	0.063	52.52				
A	09 16 11.137	23 24 08.83	0.03	0.03	15.077	0.042	115.202	0.161	7.666	0.040	452.98	0.04	2016.236	5	iT24 stack 5x3s. A too bright for reliable photometry
B	09 16 12.128	23 24 02.41							12.977	0.043	71.78				
A	**09 16 11.141**	**23 24 08.83**	**0.053**	**0.061**	**15.008**	**0.081**	**115.199**	**0.311**	**7.646**	**0.058**			**2016.234**	**19**	**A too bright for reliable photometry**
B	**09 16 12.127**	**23 24 02.44**							**12.960**	**0.065**					
STT 488	**RA**	**Dec**	**dRA**	**dDec**	**Sep**	**Err Sep**	**PA**	**Err PA**	**Mag**	**Err Mag**	**SNR**	**dVmag**	**Date**	**N**	**Notes**
A	23 07 25.489	20 34 53.50	0.13	0.13	14.888	0.184	334.704	0.708	6.706	0.110	498.01	0.11	2015.637	4	iT11 stack 4x3s. A too bright for reliable photometry
B	23 07 25.036	20 35 06.96							11.976	0.112	48.39				
A	23 07 25.482	20 34 53.35	0.04	0.06	14.897	0.072	334.900	0.277	6.649	0.060	363.13	0.06	2015.639	5	iT18 stack 5x3s. A too bright for reliable photometry
B	23 07 25.032	20 35 06.84							11.958	0.068	34.23				
A	23 07 25.482	20 34 53.15	0.07	0.08	14.954	0.106	334.884	0.407	6.406	0.110	506.90	0.11	2015.700	5	iT21 stack 5x3s. A too bright for reliable photometry
B	23 07 25.030	20 35 06.69							11.898	0.112	47.27				
A	23 07 25.482	20 34 53.32	0.02	0.04	14.909	0.045	334.802	0.172	6.695	0.050	412.76	0.05	2015.615	5	iT24 stack 5x3s. A too bright for reliable photometry
B	23 07 25.030	20 35 06.81							11.964	0.052	78.81				
A	23 07 25.484	20 34 53.42	0.03	0.05	14.782	0.058	334.571	0.226	6.684	0.060	388.37	0.06	2015.620	5	iT24 stack 5x3s. A too bright for reliable photometry
B	23 07 25.032	20 35 06.77							11.950	0.062	76.69				
A	23 07 25.480	20 34 53.33	0.06	0.04	14.858	0.072	334.949	0.278	6.627	0.090	401.71	0.09	2015.632	5	iT24 stack 5x3s. A too bright for reliable photometry
B	23 07 25.032	20 35 06.79							11.903	0.091	74.40				
A	**23 07 25.483**	**20 34 53.345**	**0.069**	**0.074**	**14.881**	**0.101**	**334.802**	**0.388**	**6.628**	**0.084**			**2015.640**	**29**	**A too bright for reliable photometry**
B	**23 07 25.032**	**20 35 06.810**							**11.942**	**0.086**					

Table 2 concludes on the next page.

STT Doubles with Large ΔM – Part VIII: Tau Per Ori Cam Mon Cnc Peg

Table 2. (conclusion). Photometry and astrometry results for the selected STT objects. Date is the Bessel epoch and N is the number of images used for the reported values. iT in the Notes column indicates the telescope used with number of images and exposure time given (Specifications of the used telescopes: See Acknowledgements). The average results over all used images are given in the line below the individual stacks in bold. The error estimation over all used images is calculated as root mean square over the individual Err values. The N column in the summary line gives the total number of images used and Date the average Bessel epoch.

STT 467	RA	Dec	dRA	dDec	Sep	Err Sep	PA	Err PA	Mag	Err Mag	SNR	dVmag	Date	N	Notes
A	22 14 48.588	22 31 24.42	0.13	0.16	23.011	0.206	273.289	0.513	6.654	0.090	492.60	0.09	2015.637	5	iT11 stack 5x3s. A too bright for reliable photometry
B	22 14 46.930	22 31 25.74							11.083	0.091	79.18				
A	22 14 48.580	22 31 24.19	0.19	0.07	23.051	0.202	273.233	0.503	6.626	0.070	328.88	0.07	2015.639	5	iT18 stack 5x3s. A too bright for reliable photometry
B	22 14 46.919	22 31 25.49							11.012	0.073	55.25				
A	22 14 48.576	22 31 24.01	0.08	0.12	22.986	0.144	273.417	0.359	6.394	0.110	509.10	0.11	2015.700	5	iT21 stack 5x3s. A too bright for reliable photometry
B	22 14 46.920	22 31 25.38							10.901	0.111	84.98				
A	22 14 48.579	22 31 24.14	0.03	0.03	23.025	0.042	273.311	0.106	6.708	0.040	441.06	0.04	2015.615	5	iT24 stack 5x3s. A too bright for reliable photometry
B	22 14 46.920	22 31 25.47							11.038	0.041	120.59				
A	22 14 48.579	22 31 24.43	0.02	0.02	23.039	0.028	272.662	0.070	6.852	0.030	509.59	0.03	2015.620	5	iT24 stack 5x3s. A too bright for reliable photometry
B	22 14 46.918	22 31 25.50							11.036	0.031	134.65				
A	22 14 48.578	22 31 24.17	0.03	0.02	23.025	0.036	273.287	0.090	6.747	0.040	444.94	0.04	2015.632	5	iT24 stack 5x3s. A too bright for reliable photometry
B	22 14 46.919	22 31 25.49							11.024	0.041	123.19				
A	**22 14 48.580**	**22 31 24.227**	**0.101**	**0.088**	**23.023**	**0.134**	**273.200**	**0.334**	**6.664**	**0.070**			**2015.640**	**30**	**A too bright for reliable photometry**
B	**22 14 46.921**	**22 31 25.512**							**11.016**	**0.071**					

Table 3. Photometry and Visual Results Compared to WDS

	WDS Mag	NOMAD-1 VMag	UCAC4 VMag	UCAC4 f. mag	Average of Photometry Measures	Results of Visual Observations
STT 114 B	10.6	-	-	-	9.509	Two observations suggesting the WDS value of 10.6 for B is about right.
STT 57 D	12.0	-	-	-	11.525	Two observations suggesting the WDS value of 12.0 for D is about right.
STT 107 B	10.1	-	-	-	11.105	Three observations of B suggesting it's fainter than the WDS value of 10.1.
STT 107 C	11.8	-	-	-	12.806	One observation suggesting C is fainter than the WDS value of 11.8, one suggesting it's close to the WDS value.
STT 116 C	12.9	-	-	11.684	11.672	Two observations suggesting C is about half a magnitude brighter than the WDS value of 12.9.
STT 76 B	12.4	-	-	-	12.489	No observations made of this pair.
STT 48 B	10.6	-	10.548	-	11.428	One inconclusive observation.
STT 63 B	11.2	-	-	-	11.379	One inconclusive observation.
STT 518 B	12.8	-	-	-	Not Resolved	One observation suggesting the magnitude of B lies somewhere between the WDS value of 12.8 and a bit brighter than that value.
STT 517 C	13.0	-	-	-	11.487	Two observations suggesting C is brighter than the WDS value of 13.0.
STT 136 B	11.0	-	10.506	-	10.566	One inconclusive observation and one suggesting C is much fainter than the WDS value of 11.0.
STT 163 C	12.0	-	-	11.366	11.757	Two observations suggesting the WDS value of 12.0 for C is reasonably close.
STT 198 B	12.0	-	-	12.872	12.960	Two observations suggesting B is notably fainter than the WDS value of 12.0.
STT 488 B	10.4	-	-	12.022	11.942	One observation suggesting B is distinctly fainter than the WDS value of 10.4.
STT 467 B	10.7	11.5	-	10.969	11.016	One observation suggesting a value for B in the 12.2 to 12.3 range.

STT Doubles with Large ΔM – Part VIII: Tau Per Ori Cam Mon Cnc Peg

Table 4. Astrometry Results Compared to WDS

	WDS Coordinates	WDS Sep	WDS PA	Astrometry Coordinates	Astrometry Sep	Astrometry PA
STT 114 AB	05:41:40.770 +16:14:02.4	3.0	278	05 41 40.777 +16 14 02.42	2.9	279.726
STT 57 CD	03:33:26.530 +23:23:03.5	9.9	320	03 33 26.518 +23 23 03.16	9.935	320.086
STT 107 AB	05:27:10.090 +17:57:44.0	10.0	306	05 27 10.099 +17 57 43.89	10.081	305.359
STT 107 AC	05:27:10.090 +17:57:44.0	10.0	347	05 27 10.099 +17 57 43.89	9.814	346.669
STT 116 AC	05:45:55.390 +25:54:49.3	17.9	65	05 45 55.399 +25 54 49.25	17.781	64.684
STT 76 AB	04:16:10.609 +34:52:07.7	3.8	210	04 16 10.639 +34 52 07.29	**3.550**	**211.099**
STT 48 AB	02:53:21.070 +48:34:11.9	6.6	318	02 53 21.069 +48 34 11.78	6.567	**316.966**
STT 63 AB	03:48:18.080 +50:44:12.4	6.8	270	03 48 18.058 +50 44 12.41	6.703	269.423
STT 517 AB,C	05:13:31.550 +01:58:03.7	6.5	138	05 13 31.533 +01 58 03.59	**7.051**	**135.311**
STT 136 AB	06:28:14.490 +70:32:07.0	5.0	82	06 28 14.484 +70 32 07.37	**5.452**	**83.025**
STT 163 AB,C	07:01:09.851 +11:46:28.7	14.5	165	07 01 09.843 +11 46 28.29	**14.207**	165.172
STT 198 AB	09:16:11.281 +23:24:10.4	14.6	121	09 16 11.141 +23 24 08.83	**15.008**	**115.199**
STT 488 AB	23:07:25.502 +20:34:53.802	14.6	335	23 07 25.483 +20 34 53.345	**14.881**	334.802
STT 467 AB	22:14:48.567 +22:31:24.299	23.9	274	22 14 48.580 +22 31 24.227	**23.023**	273.200

Table 5 Astrometry Results Compared with URAT1 Coordinates

Object	URAT1 Sep	iTelescope Sep	Err Sep	Within Error Range?	URAT1 PA	iTelescope PA	Err PA	Within Error Range?
STT 57CD	9.929	9.935	0.138	Yes	319.955	320.086	0.795	Yes
STT 107AB	10.211	10.081	0.131	Yes	305.795	305.359	0.744	Yes
STT 107AC	10.114	9.814	0.131	No (1)	346.461	346.669	0.765	Yes
STT 116AC	17.770	17.781	0.102	Yes	64.783	64.684	0.329	Yes
STT 63AB	7.090	6.703	0.129	No (2)	270.137	269.423	1.100	Yes
STT 163AB,C	14.221	14.207	0.128	Yes	165.748	165.172	0.515	No (3)
STT 198AB	14.909	15.008	0.081	No (3)	115.630	115.199	0.311	No (3)
STT 488AB	14.944	14.881	0.101	Yes	334.847	334.802	0.388	Yes
STT 467AB	22.992	23.023	0.134	Yes	273.384	273.200	0.334	Yes

Notes: All astrometry results in this report are to some degree influenced by the difficulty of centroid detection due to the brightness of the primaries, so the calculated error range is probably a bit on the optimistic side.

(1) Two measurements based on iT27 images regarding separation are obviously outliers, without them the averaged separation would be 10.020" and thus within the error range

(2) One iT18 image delivered an outlier result here, but even without this outlier the comparison with URAT1 stays outside the error range. Given the brightness of the primary the reason for this might be a less than perfect URAT1 centroid detection as our result here corresponds very well with the current WDS catalog value

(3) Result only slightly outside the given error range.

STT Doubles with Large ΔM – Part VIII: Tau Per Ori Cam Mon Cnc Peg

(Continued from page 179)

Elevation 2225m

- iT18: 318mm CDK with 2541mm focal length. CCD: SBIG-STXL-6303E. Resolution 0.73 arcsec/pixel. V-filter. Located in Nerpio. Spain. Elevation 1650m
- iT21: 431mm CDK with 1940mm focal length. CCD: FLI-PL6303E. Resolution 0.96 arcsec/pixel. V-filter. Located in Mayhill. New Mexico. Elevation 2225m

- AAVSO VPhot for initial plate solving
- AAVSO APASS providing Vmags for faint reference stars (indirect via UCAC4)
- UCAC4 catalog (online via the University of Heidelberg website and Vizier and locally from USNO DVD) for counterchecks
- URAT1 catalog for high precision plate solving
- Aladin Sky Atlas v8.0 for counterchecks
- SIMBAD. VizieR for counterchecks
- 2MASS All Sky Catalog for counterchecks
- URAT1 Survey (preliminary) for counterchecks
- AstroPlanner v2.2 for object selection. session planning and for catalog based counterchecks
- MaxIm DL6 v6.08 for plate solving on base of the UCAC4 catalog
- Astrometrica v4.9.1.420 for astrometry and photometry measurements

References

Buchheim, Robert, 2008, "CCD Double-Star Measurements at Altimira Observatory in 2007", *Journal of Double Star Observations*, **4**, 27-31. Formulas for calculating Separation and Position Angle from the RA Dec coordinates given as

$$Sep = \sqrt{\left[\left(RA_2 - RA_1\right)\cos\left(Dec_1\right)\right]^2 + \left(Dec_2 - Dec_1\right)^2}$$

in radians and

$$RA = \arctan\left[\frac{\left(RA_2 - RA_1\right)\cos\left(Dec_1\right)}{Dec_2 - Dec_1}\right]$$

in radians depending on quadrant

Burnham, S.W., 1906, *A General Catalogue of Double Stars Within 120° of the North Pole. Part I*, University of Chicago Press, Chicago.

Burnham, S.W., 1906, *A General Catalogue of Double Stars Within 120° of the North Pole. Part II*, University of Chicago Press, Chicago.

Greaney, Michael, 2012. "Some Useful Formulae" in *Observing and Measuring Visual Double Stars. 2nd Edition*, R.W. Argyle, ed., pg 359, Springer, New York.

Hussey, W.J., 1901, *Micrometrical Observations of the Double Stars Discovered at Pulkowa Made with the Thirty-Six-Inch and Twelve-Inch Refractors of Lick Observatory*, pp. 14-16, A.J. Johnston, Sacramento.

Knapp, Wilfried; Nanson, John; Smith, Steven, 2015, "STT Doubles with Large Δ M – Part I: Gem", *Journal of Double Star Observations*, **11**, 390-401.

Knapp, Wilfried; Nanson, John; Smith, Steven, 2016, "STT Doubles with Large Δ M – Part II: Leo and UMa", *Journal of Double Star Observations*, **12**, 111-127.

Knapp, Wilfried; Nanson, John, 2016, "STT Doubles with Large Δ M – Part III: Vir. Ser. CrB. Com and Boo", *Journal of Double Star Observations*, **12**, 128-142.

Knapp, Wilfried; Nanson, John, 2016, "STT Doubles with Large Δ M – Part IV: Ophiuchus and Hercules", *Journal of Double Star Observations,* **12**, 361-373.

Knapp, Wilfried; Nanson, John, 2016. "STT Doubles with Large Δ M – Part V: Aquila, Delphinus, Cygnus and Aqarius", *Journal of Double Star Observations*, **12**, 474-487.

Knapp, Wilfried; Nanson, John, 2016. "STT Doubles with Large Δ M – Part VI", Cygnus Multiples", *Journal of Double Star Observations*, **12**, 519-534.

Knapp, Wilfried; Nanson, John, 2017, "STT Doubles with Large Δ M – Part VII: Andromeda, Pisces, Auriga", *Journal of Double Star Observations*, **13**, 75-86.

Struve, Otto Wilhelm, 1845, *Catalogue de 514 Étoiles Doubles et Multiples Découvertes Sur L'Hémisphère Céleste Boréal par La Grand Lunette de L'Observatoire Central de Poulkova*. L'Académie Impériale des Sciences, St. Pétersbourg.

Zacharias, Norbert et al., 2015, "The First U.S. Naval Observatory Robotic Astrometric Telescope Catalog (URAT1)", *The Astronomical Journal*, **150**, 1-12.

Determining Binary Star Orbits Using Kepler's Equation

Cory Boulé, Kaitlyn Andrews, Andrew Penfield, Ian Puckette,
Keith A. Goodale and Steven A. Harfenist

Keene State College, Keene NH

Abstract: Students calculated ephemerides and generated orbits of four well-known binary systems. Using an iterative technique in Microsoft® Excel® to solve Kepler's equation, separation and position angle values were generated as well as plots of the apparent orbits. Current position angle and separation values were measured in the field and compared well to the calculated values for the stars: STF1196AB,C, STF296AB, STF296AB and STF60AB.

Introduction

During the spring of 2015 students from Keene State College calculated tables of ephemerides and measured the separation and position angles of four binary stars. The ephemerides included separation ρ, position angle θ, and year at which they occur. Values generated in the table were plotted in Microsoft Excel for an entire orbit and the orbital positions generated were compared to the measured results for the dates the images were taken. The stars studied included: ζ Cancri (Tegmine - WDS 08122+1739 STF1196AB,C), θ Persei (WDS 02442+4914A STF296AB), δ Geminorum (Wasat - WDS 07201+2159 STF1066) and η Cassiopeiae (Achird - WDS 00491+5749 STF60AB) . These particular stars were chosen because they could be split and measured with our equipment, they were visible at the time of observation and the orbital elements were available from the Washington Double Star (WDS) catalog (Mason & Hartkopf, 2013).

Image acquisition was made at Otter Brook Dam in Roxbury NH, near the Keene State College campus, preferred for its darker sky. Images of the four binary pairs were captured using the software BackyardEOS on a laptop computer interfaced with a digital single lens reflex Canon 60Da camera mounted on a Celestron 9.25" Schmidt-Cassegrain telescope on an Orion Atlas mount. The binary systems were located by entering their right ascensions and declinations into the hand controller of the telescope and manually centered. Short exposures at ISO 800 were taken with the telescope tracking and were saved to the computer. Forty five second exposures were taken with the telescope drive turned off also at ISO 800. The long exposure produced a star trail as the pair drifted across the field, indicating West. The images were later analyzed indoors using Adobe Photoshop to measure separation and position angle. A more detailed description of this process is described elsewhere (Walsh et al., 2015).

Brief History of Star Systems

Zeta Cancri (ζ Can., Figure 1) This system actually contains two binary pairs approximately 83 light years (ly) from Earth that orbit around their common center of mass every 1115 years. Also known as Tegmine, "the shell of the crab", it was first resolved as a double star in 1756 by Johann Tobias Meyer. William Herschel discovered its triple-nature in 1781. John Herschel around 1831 noticed deviations in the orbit of the assumed single, leading Otto Wilhelm von Struve to postulate a fourth component orbiting closely to it (Argyle, 2004). The main components of the system ζ^1 and ζ^2 are separated by 6.1" (Mason and Hartkopf, 2013). The components of ζ^1, denoted ζ^A and ζ^B, are both yellow white dwarf stars of class F separated by approximately one arc second and orbiting approximately once every 60 years. They have estimated masses slightly greater than one solar mass. The components of ζ^2, denoted ζ^C

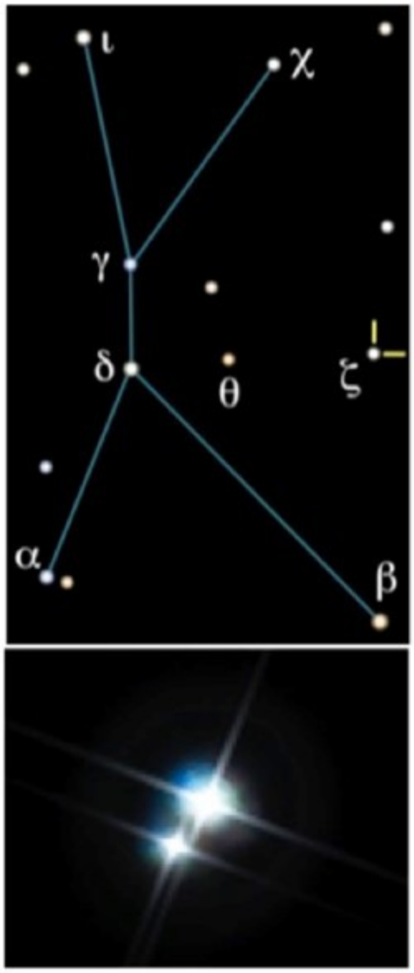

Figure 1. The system ζ-Cancri WDS 08122+1739, STF1196AB,C located in the constellation Cancer. Telescope image captured by KSC students in 2015. Image modified from Stellarium software version 0.12.2.

and ζ^D, comprise a G-type and red dwarf star pair, though it is thought that ζ^D may actually be a close pair of two red dwarfs. Components C and D are separated by approximately 0.3" orbiting once every 17 years (Kaler, 2009).

Theta Persei (θ Per., Figure 2) This binary star system in the constellation Perseus is approximately 36 ly away from Earth. The primary is a main sequence yellowish dwarf star of type F7V (Kaler, 2010; Mason & Hartkopf, 2013) under investigation for the potential of harboring earthlike planets as it is very similar to our sun. The secondary is of spectral type M1V, a red dwarf that orbits the primary every 2720 years (Mason & Hartkopf, 2013).

Eta Cassiopeiae (η Cas., Figure 3). This binary star system was discovered in 1799 by William Herschel (Carro, 2011). The primary is a G-type star quite similar to our sun that orbits a cooler and dimmer K-type star every 480 years (Carro, 2011; Mason & Hartkopf, 2013). It is approximately 19.4 ly from Earth (Kaler, 2005). The WDS catalog lists the apparent magnitudes of the primary and secondary components as 3.52 and 7.36 (Mason & Hartkopf, 2013).

Delta Geminorum (δ Gem., Figure 4) This star system is also known as Wasat, meaning "middle" in Arabic, and is actually a triple star system (Kaler, 2004). The main component is a class F sub giant approximately 59 ly from Earth. It forms a tight spectroscopic binary with a period of just over six years. The inner components are orbited by a third class K star every 1200 years (Wenger et. al., 2000).

Solving Kepler's Equation

Before beginning work on the four target stars, the students researched other binary pairs in the WDS catalog to become familiar with its data format. Preliminary work consisted of introducing students to Excel

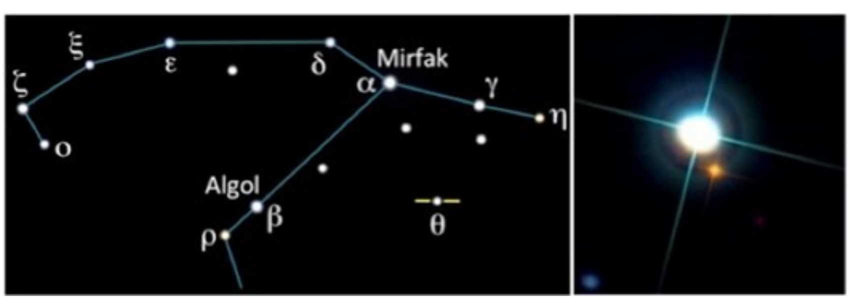

Figure 2. The system θ-Persei WDS 02442+4914A STF296AB as located in the constellation Perseus. Telescope image captured by students in 2015. Image modified from Stellarium software version 0.12.2

Determining Binary Star Orbits Using Kepler's Equation

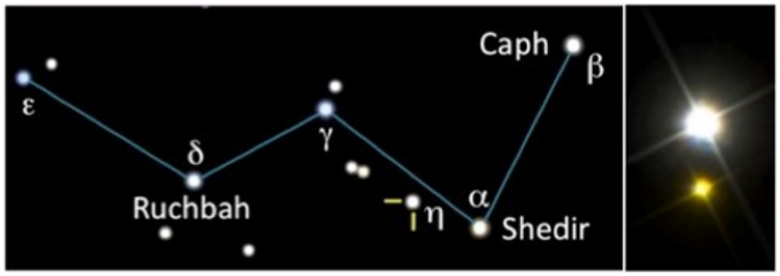

Figure 3. The system η-Cassiopeiai WDS 00491+5749 STF60AB as located in the constellation Cassiopia. Telescope image captured by KSC students in 2015. Image modified from Stellarium software version 0.12.2.

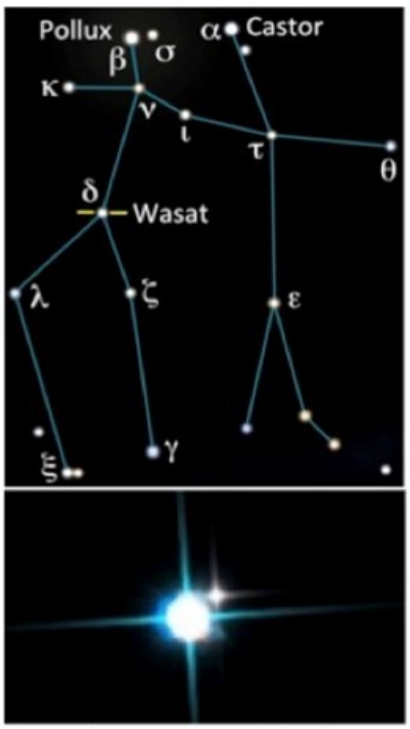

Figure 4. The system δ-Geminorum WDS 07201+2159 STF1066WDS 02442+4914A STF296AB as located in the constellation Perseus. Telescope image captured by KSC students in 2015. Image modified from Stellarium software version 0.12.2.

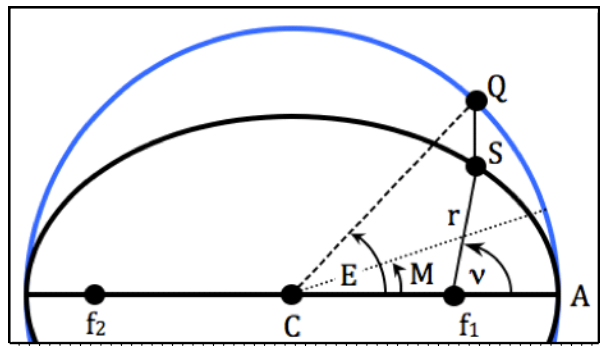

*Figure 5. Parameters used to calculate ephemerides of binary star orbits. The primary is located at f_1. and the secondary is at S. An auxiliary circular orbit (blue) with radius equal to the semi major axis of the elliptical orbit is circumscribed. True anomaly (**ν**), mean anomaly (**M**), and eccentric anomaly (**E**) are measured relative to periastron passage A. Point Q is the projection of point S on the auxiliary circular orbit.*

through the calculation of Gamma Virginis' orbit as outlined in the text Astronomical Algorithms (Meuss, 2009). We determine the Keplerian orbit of the secondary with respect to the primary through seven orbital elements obtained from the Sixth Catalog of Orbits of Visual Binary Stars (Mason and Hartkopf, 2016).

Two of these elements describe the shape of the orbit; the eccentricity e and the semi major axis a (see Figure 5 where a = CA). Three parameters describe the orientation of the true orbit to its apparent orbit as seen from Earth's line of sight (see Figure 6, the plane of apparent orbit, Alzener, 2004). The orientation of the apparent orbit to the true orbit is defined by the inclination angle i, the position angle of the ascending node Ω and the longitude of the periastron ω (Figure 6). The last two orbital elements are the period P in years and the time of periastron T. Table 1 lists the orbital elements used for our four stars (Mason and Hartkopf, 2016).

The calculations begin by first determining the mean anomaly. The mean anomaly M is the angle from periastron A that a fictitious body moving at constant angular speed would make on the auxiliary, circular orbit (blue), with the same period as the secondary. The auxiliary orbit has radius equal to the elliptical orbit's semi major axis, a = CA. (Marion, 1970; Coswell, 1993). The mean anomaly should not be confused with the true anomaly ν, the true angular position within the

$$r(\nu) = \frac{a\left(1-e^2\right)}{1+e\cos(\nu)}$$

Determining Binary Star Orbits Using Kepler's Equation

orbit described in polar coordinates by

The mean anomaly is calculated beginning with first determining the mean annual motion **n** of the secondary in degrees per year,

$$n = \frac{360^o}{P}$$

and the mean anomaly M for each time t is,

$$M = n(t - T) \quad (1)$$

The mean anomaly and other parameters used herein are defined in the orbit diagram shown in Figure 5. The primary is located at the focus f_1 of the elliptical orbit and the secondary located at S.

Kepler's equation comes from his geometrical solution to this problem, which stated algebraically is given by,

$$E = M + e \sin E \quad (2)$$

and must be solved for the eccentric anomaly E, as defined in Figure 5. Kepler's equation is transcendental in E and must be solved numerically. We chose an iterative method as outlined by Meuss (Meuss, 2009). This method was used because Excel could be employed, and for eccentricities less than 0.95 it is an easy and quick method for students to master, converging to an appropriate number of significant figures for most examples in a reasonable number of iterations, details of which are show in the Appendices (Sinnott, 1985). To begin the iterative process, the first term simply approximates the eccentric anomaly as the mean anomaly,

$$E_0 = M \quad (3)$$

Successive iterations yield better approximations of E,

$$\begin{aligned} E_1 &= M + e_0 \sin E_0 \\ E_2 &= M + e_0 \sin E_1 \\ E_3 &= M + e_0 \sin E_2 \end{aligned} \quad (4)$$

To report our angle E in degrees, the eccentricity e must be converted into degrees e_0 by multiplying it by 180°/π. The number of iterations at which the eccentric anomaly converged to eight decimal points accuracy in the radian measure of E depended on the binary system investigated. Eccentric anomaly values converged within 6 to 13 iterations with an average of 11 for Zeta Cancri, within 4 to 8 iterations and an average of 10 for Theta Persei, within 3 to 7 iterations with an average of 9 for Delta Gemini and within 7 to 26 iterations and an

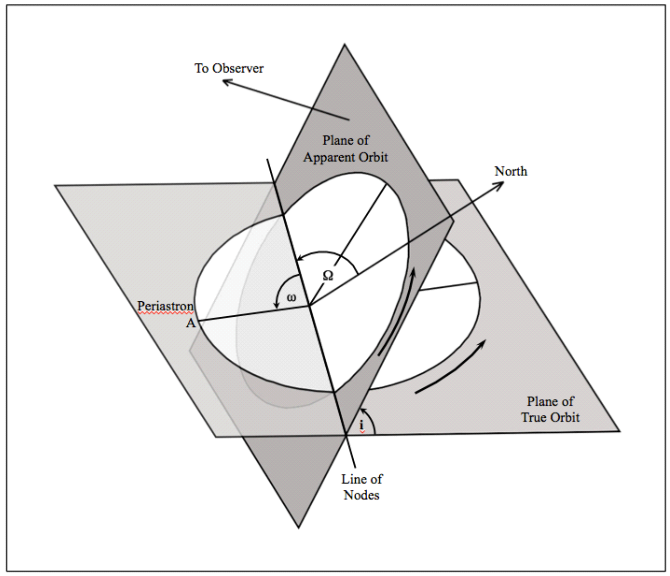

*Figure 6. Geometric relationship between apparent and true orbit. The three parameters that relate the two orbits are given by; **i** - the inclination angle, **ω** - the longitude of the periastron and **Ω** - the position angle of the ascending node. The direction of orbital motion is indicated by arrows in the orbital planes shown. Adapted from Alzener (2004), page 57.*

average of 17 for Eta Cassiopiea. The average number of iterations for convergence seemed to be proportional to the eccentricity of the orbits, but further investigation is needed to fully understand this trend (see Appendices 1-4).

Once the eccentric anomaly of the orbit at time t is found, the radial distance r is determined via,

$$r = a(1 - e\cos E) \quad (5)$$

where the polar representation of the elliptical orbit is now written in terms of the eccentric anomaly E rather than the true anomaly ν. The radius vector is in the same units as the semi major axis, arc seconds. The true anomaly is then

$$\nu = 2\tan^{-1}\left[\sqrt{\frac{1+e}{1-e}}\tan\left(\frac{E}{2}\right)\right]$$

which should also be reduced to within the interval 0° < ν < 360° (Marion, 1970). The (apparent) position angle can now be found by computing

$$\theta = \tan^{-1}\left[\frac{\sin(\nu+\omega)\cos(i)}{\cos(\nu+\omega)}\right] + \Omega \quad (6)$$

Determining Binary Star Orbits Using Kepler's Equation

*Table 1. Orbital Elements of our four star systems. Elements include: the eccentricity **e**, semi major axis length a in arc seconds, orbital inclination i, position angle of ascending node Ω, longitude of the periastron ω, orbital period P and time of periastron passage T, see Figure 6 for details of elements.*

	e	a(")	i(°)	Ω(°)	ω(°)	P(yr)	T(yr)
ζ Can.	0.24	7.7	146	74.2	345.5	1115	1970
θ Per.	0.13	22.289	75.44	128	100.64	2720	1613
δ Gem.	0.11	6.9753	63.28	18.38	57.19	1200	1437
η Cas.	0.497	11.9939	34.76	98.42	88.59	480	1889.6

And last, the apparent separation is given by (Cowell, 1993),

$$\rho = r\sqrt{\sin^2(\nu+\omega)\cos^2(i)+\cos^2(\nu+\omega)}$$

To plot the apparent orbit, the x and y coordinates in arc seconds were simply found through

$$x = \rho\cos\theta$$
$$y = \rho\sin\theta$$

In Table 2 we present calculated and measured separation and position angles for our four star pairs as well as the most recent measurements from the WDS catalog. The calculated apparent orbits of our chosen binary stars are shown in Figures 7 and 8. The Excel-generated ephemerides are plotted from the position angle and separations for different times (representative years shown on plots) within a full orbit, with (ρ, θ) values converted to (x, y) coordinates. Values measured from telescope images captured by the students are shown in red text. Included in appendices 1 through 4 are examples of the generated data for each star pair.

Conclusion

All four stars' measured separations compared well to the calculated values. The largest difference in separation was 0.6" for the star Eta Casssiopeiae and the smallest difference was for Zeta Cancri at just 0.1". The largest difference for position angle θ was 4.4° for the star δ Geminorum, the smallest difference 0.3° for both η Casseipeia and θ Persei.

The project was successful from an educational standpoint. The goal of introducing students to Excel for solving computational problems was met. Students were introduced to basic numerical methods for solving Kepler's equation and the results were then successfully used to calculate the apparent orbits of the four binary star systems. Students also learned, or gained further experience in, working with telescopes to capture and analyze double star data as well as basic techniques of

Table 2. Calculated, measured and WDS-provided separation ρ and position angle θ values for our four binary star pairs. Last dates measured for the WDS are in parenthesis and our measurement dates are shown on our generated orbits (Figures 7 and 8).

	Calculated		Measured		WDS	
	ρ (")	θ (°)	ρ (")	θ (°)	ρ (")	θ (°)
ζ Can.	5.9	66.2	6	64	6.1	68
θ Per.	20.3	304.7	19.9	305	20.7	305
δ Gem.	5.5	228.2	5.3	232.6	5.6	230
η Cas.	13.4	323.7	12.8	324	12.8	324

Determining Binary Star Orbits Using Kepler's Equation

processing of raw image files. Students learned about the information available in the WDS and how to use and reference the database. In addition, each student was tasked with reading and familiarizing themselves with a paper from the Journal of Double Star Observations (JDSO) and presented a short talk to the research group summarizing the paper.

Difficulties encountered during the project included the time of setup, polar alignment and breakdown of the telescope. The complexity of polar alignment with a German equatorial mount also presented problems for the students. Guidance from the instructors was required during most stages of the setup. As expected, the complexity of setting up the spreadsheet for the computations and troubleshooting erroneous results proved challenging and time consuming. This was dealt with by breaking the process down into manageable steps presented in concise lectures followed by examples that students could emulate in their own spreadsheets. Even when students obtained unreasonable and incorrect values in their computations, the experience gained in pinpointing and correcting the problem turned out to be valuable lessons learned. After approximately six, hour long working sessions all of the students had their spreadsheets working and orbits plotted. Even with the many difficulties encountered during the project, student response was positive.

Future work at Keene State College will include continued measuring of separation and position angle of double star pairs as well as refining our techniques of measuring even closer separations, higher magnitude systems, measuring neglected doubles and photometry

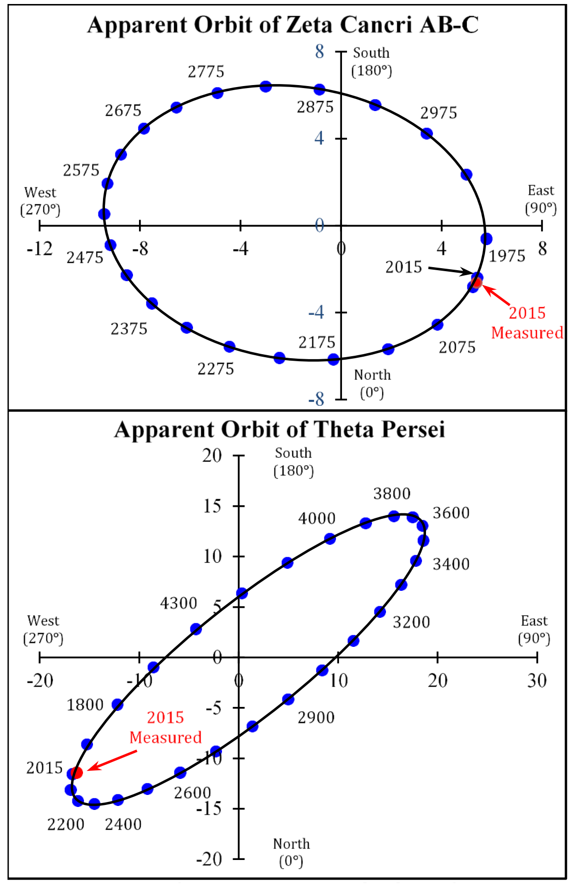

Figure 7. Microsoft® Excel® generated orbits of Zeta Cancri and Theta Persei as viewed from Earth. The primary is located at the origin. Representative location dates are shown as well as measured data points with dates shown in red text.

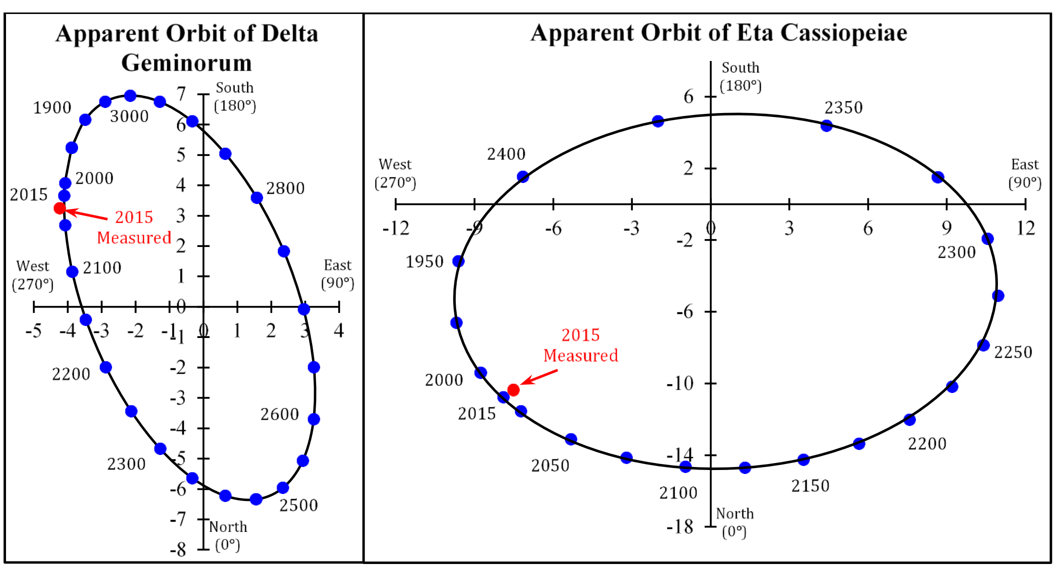

Figure 8. Microsoft Excel generated apparent orbits of Delta Geminorum and Eta Cassiopeiae as viewed from Earth. The primary is located at the origin. Representative location dates are shown as well as measured data points with dates shown in red text.

of double star components. Comparing observer measurements obtained from the WDS over longer time intervals would also prove useful in validating our computational methods as well as observer measurements.

References

Alzener, Andreas, 2004, *Observing and Measuring Visual Double Stars*, *Ch. 7: The Orbital Elements of a Visual Binary Star*, 2nd ed, Bob Argyle editor, Springer, New York, 53-59

Argyle, Robert, *Observing and Measuring Visual Double Stars*, London, Springer, 2004

Carro, Joseph M., 2011, *Astrometric Measurements of Five Double Stars*, Journal of Double Star Observations, **7**, P. 240 – 245.

Cowell, Peter, 1993, *Solving Kepler's Equation Over Three Centruries*, Willmann-Bell, Inc, Virginia, 1-4.

Kaler, Jim, 2009 (http://stars.astro.illinois.edu/sow/tegmine.html)

Kaler, Jim, 2010 (http://stars.astro.illinois.edu/sow/thetaper.html)

Kaler, Jim, 2005 (http://stars.astro.illinois.edu/sow/achird.html)

Kaler, Jim, 2004 (http://stars.astro.illinois.edu/sow/wasat.html)

Marion, Jerry B., 1970, *Classical Dynamics of Particles and Systems*, Academic Press Inc., 254-263

Mason, Brian and Hartkopf, William, July 2013, *The Washington Double Star Catalog,* Astronomy Department, U.S. Naval Observatory.

Mason, Brian and Hartkopf, William, April 2016, *The Sixth Catalog of Orbits of Visual Binary Stars*, Astronomy Department, U.S. Naval Observatory.

Meuss, Jean, 2009, *Astronomical Algorithms*, 2nd ed., Willmann-Bell, Inc, Virginia, 193-196, 397-399

Sinnott, Roger W., August 1985, *Astronomical Computing: A Computer Assault on Kepler's Equation*, Sky and Telescope, **70**, 2, 158.

Walsh, Ryan M. et. Al., 2015, *Determining the Separation and Position Angles of Orbiting Binary Stars: Comparison of Three Methods*, Journal of Double Star Observations, **11**, 158-163.

Wenger, M. et. al., 2000, The SIMBAD Astronomical Database.

Determining Binary Star Orbits Using Kepler's Equation

Appendix 1 - Ephemermides of Zeta Cancri

The mean anomaly M is first calculated from equation 1 for a given date t. Kepler's equation (equation 2) is then used to determine the eccentric anomaly E iteratively following equations 3 and 4 in radian measure. The apparent separation ρ and position angle θ are found using equations 5 and 6, respectively and the x,y coordinates used to plot the orbits are determined from equations 7. The number of iterations n necessary for the eccentric anomaly values to converge to the eighth decimal with value E_n are shown in the last columns of the second table.

t(year)	M (°)	ρ(")	θ(°)	X(")	Y(")
1975	1.61434978	5.81495607	354.01507603	5.78326087	-0.60630671
2015	14.52914798	5.92660286	336.18379309	5.42192585	-2.39318647
2025	17.75784753	5.93912859	331.80753485	5.23454357	-2.80585140
2075	33.90134529	5.94359997	310.02406812	3.82238468	-4.55145647
2125	50.04484305	5.96940709	288.24848308	1.86925216	-5.66919019
2175	66.18834081	6.15888466	267.17606954	-0.30342935	-6.15140560
2225	82.33183857	6.55589362	248.00015523	-2.45586451	-6.07852537
2275	98.47533632	7.10836264	231.42487695	-4.43234996	-5.55725591
2325	114.61883408	7.72574379	217.39181655	-6.13811397	-4.69155347
2375	130.76233184	8.32333369	205.42629428	-7.51712186	-3.57362040
2425	146.90582960	8.83687504	194.97543363	-8.53674569	-2.28349152
2475	163.04932735	9.22154285	185.54789631	-9.17834664	-0.89151865
2525	179.19282511	9.44722651	176.73246065	-9.43186786	0.53847691
2575	195.33632287	9.49462306	168.17241241	-9.29304093	1.94608770
2625	211.47982063	9.35318507	519.52740922	-8.76243429	3.27136304
2675	227.62331839	9.02114338	510.42894026	-7.84608812	4.45195789
2725	243.76681614	8.50804645	500.42514346	-6.55794174	5.42035557
2775	259.91031390	7.84091186	488.90913882	-4.92477623	6.10135050
2825	276.05381166	7.07572062	475.04211022	-2.99504109	6.41058119
2875	292.19730942	6.31433062	457.76890916	-0.85355818	6.25637352
2925	308.34080717	5.71363680	436.26692101	1.35641177	5.55029663
2975	324.48430493	5.43722229	411.18762386	3.40789944	4.23669774
3025	340.62780269	5.51172323	385.25477646	4.98491042	2.35154441

t(year)	E0	E1	E2	E3	E4	E6	E7	·	En	n
1975	0.02817572	0.03493700	0.03655889	0.03694790	0.03704120	0.03706357	0.03706894		0.03707063	12
2015	0.25358147	0.31379087	0.32766146	0.33082062	0.33153809	0.33170093	0.33173788		0.33174872	12
2025	0.30993291	0.38313165	0.39965136	0.40331624	0.40412586	0.40430455	0.40434398		0.40435514	12
2075	0.59169010	0.72555360	0.75094203	0.75544875	0.75623780	0.75637560	0.75639966		0.75640474	11
2125	0.87344728	1.05741863	1.08250903	1.08540031	1.08572495	1.08576129	1.08576535		1.08576586	9
2175	1.15520447	1.37477508	1.39060830	1.39131888	1.39134938	1.39135069	1.39135074		1.39135075	8
2225	1.43696166	1.67481546	1.67566443	1.67564319	1.67564373	1.67564371				6
2275	1.71871885	1.95609791	1.94112328	1.94244903	1.94233367	1.94234373	1.94234285		1.94234292	8
2325	2.00047604	2.21865985	2.19184603	2.19566038	2.19512628	2.19520124	2.19519072		2.19519201	11
2375	2.28223323	2.46401510	2.43269104	2.43847332	2.43741731	2.43761056	2.43757521		2.43758067	13
2425	2.56399042	2.69503443	2.66763774	2.67352853	2.67226869	2.67253844	2.67248070		2.67249088	13
2475	2.84574761	2.91571920	2.89949746	2.90328454	2.90240174	2.90260760	2.90255960		2.90256868	12
2525	3.12750479	3.13088577	3.13007440	3.13026911	3.13022239	3.13023360	3.13023091		3.13023143	11
2575	3.40926198	3.34578571	3.36059549	3.35712045	3.35793485	3.35774394	3.35778869		3.35778019	13
2625	3.69101917	3.56569159	3.59225924	3.58648341	3.58773295	3.58746233	3.58752092		3.58751049	14
2675	3.97277636	3.79548123	3.82678977	3.82089820	3.82199567	3.82179084	3.82182905		3.82182304	12
2725	4.25453355	4.03925295	4.06688466	4.06282240	4.06341050	4.06332517	4.06333754		4.06333598	11
2775	4.53629074	4.30000240	4.31641068	4.31486202	4.31500564	4.31499230	4.31499354		4.31499344	9
2825	4.81804793	4.57938634	4.58016756	4.58014277	4.58014356	4.58014353				6
2875	5.09980511	4.87759192	4.86307271	4.86252463	4.86250492	4.86250422	4.86250419			7
2925	5.38156230	5.19332196	5.16878701	5.16612732	5.16584676	5.16581725	5.16581415		5.16581379	9
2975	5.66331949	5.52389727	5.49810224	5.49366735	5.49291615	5.49278925	5.49276782		5.49276346	12
3025	5.94507668	5.86546787	5.84771463	5.84383575	5.84299247	5.84280934	5.84276958		5.84275855	13

Appendix 2. Calculated ephemerides of Theta Persei.

See appendix 1 caption for details.

t(year)	M (°)	ρ(")	θ(°)	X(")	Y(")
1900	37.98529412	17.49932933	569.43439189	-15.24049819	-8.59963613
2000	51.22058824	20.04235230	574.05873572	-16.60436516	-11.22456873
2015	53.20588235	20.31989665	574.66225318	-16.71349919	-11.55669263
2100	64.45588235	21.36944320	577.84790247	-16.87421653	-13.11159484
2200	77.69117647	21.49401836	221.38413750	-16.12683574	-14.20978516
2300	90.92647059	20.51971434	225.07012617	-14.49185948	-14.52737709
2400	104.16176471	18.60776636	229.33192518	-12.12623234	-14.11394552
2500	117.39705882	15.96091103	234.81758588	-9.19638137	-13.04520030
2600	130.63235294	12.83200767	242.78968550	-5.86753860	-11.41194162
2700	143.86764706	9.59232928	256.13704263	-2.29832602	-9.31291998
2800	157.10294118	6.98465832	281.23872731	1.36129142	-6.85071803
2900	170.33823529	6.46196771	320.27647586	4.97013994	-4.12973797
3000	183.57352941	8.48842578	351.49397324	8.39505573	-1.25555227
3100	196.80882353	11.62964713	368.23090498	11.50985192	1.66493275
3200	210.04411765	14.89767702	377.67387200	14.19450707	4.52291384
3300	223.27941176	17.85423257	383.80732505	16.33498144	7.20708000
3400	236.51470588	20.24654166	388.31504091	17.82410103	9.60332607
3500	249.75000000	21.88777719	391.98924578	18.56406449	11.59527058
3600	262.98529412	22.62555397	395.27489517	18.47129201	13.06625671
3700	276.22058824	22.33880048	398.49199152	17.48447103	13.90378652
3800	289.45588235	20.94856052	401.96417679	15.57657540	14.00758676
3900	302.69117647	18.44053685	406.16778174	12.77097389	13.30246688
4000	315.92647059	14.90351765	412.07589439	9.15995726	11.75627583
4100	329.16176471	10.61086379	422.37100433	4.92072926	9.40089644
4200	342.39705882	6.35823434	447.11559888	0.31995293	6.35017906
4300	355.63235294	5.13678419	506.90471205	-4.30341095	2.80485401
4400	368.86764706	8.63532063	546.41461795	-8.58125876	-0.96475935
4500	382.10294118	13.03676407	560.93661641	-12.17602868	-4.65849150

t (year)	E0	E1	E2	E3	E4	E6	E7		En	n
1900	0.66296845	0.742978146	0.750911394	0.751668143	0.751740038	0.751746866	0.751747514		0.75174758	8
2000	0.89396791	0.995311109	1.003028592	1.003571362	1.003609289	1.003611938	1.003612123		1.00361214	8
2015	0.928617828	1.032720901	1.040248385	1.04074672	1.040779487	1.040781641	1.040781782		1.04078179	8
2100	1.124967369	1.242260327	1.248014414	1.248253734	1.248263599	1.248264006	1.248264022			7
2200	1.355966829	1.482978487	1.485465873	1.485493833	1.485494142	1.485494146				6
2300	1.586966289	1.716949294	1.715580314	1.715606111	1.715605627	1.715605637				6
2400	1.817965749	1.944014897	1.939016371	1.939251787	1.939240768	1.939241284	1.93924126			7
2500	2.048965209	2.16438428	2.156727297	2.157280902	2.157241089	2.157243953	2.157243747		2.15724376	8
2600	2.279964668	2.378622152	2.369803967	2.37062904	2.37055214	2.37055931	2.370558641		2.37055870	8
2700	2.510964128	2.587618954	2.579353328	2.580264807	2.580164526	2.580175562	2.580174348		2.58017447	9
2800	2.741963588	2.792543554	2.78642416	2.787170873	2.787079846	2.787090944	2.787089591		2.78708974	9
2900	2.972963048	2.99478115	2.991980057	2.992340207	2.992293909	2.992299861	2.992299096		2.99229918	9
3000	3.203962508	3.195859682	3.196911256	3.196774757	3.196792475	3.196790175	3.196790473		3.19679044	9
3100	3.434961968	3.397368669	3.402072455	3.401481222	3.401555495	3.401546164	3.401547336		3.40154721	9
3200	3.665961427	3.600874758	3.608331814	3.607464467	3.607565183	3.607553486	3.607554844		3.60755470	10
3300	3.896960887	3.807838504	3.816615813	3.815721886	3.815812643	3.815803426	3.815804362		3.81580428	9
3400	4.127960347	4.019536777	4.027934792	4.027240994	4.027298043	4.027293351	4.027293737		4.02729371	9
3500	4.358959807	4.236994933	4.24337519	4.242997922	4.243020099	4.243018795			4.24301887	7
3600	4.589959267	4.460932338	4.464047635	4.463947479	4.46395068	4.463950577				6
3700	4.820958727	4.691724155	4.690986483	4.6909885	4.690988494					4
3800	5.051958186	4.929381415	4.925006768	4.924885544	4.92488222	4.924882129				6
3900	5.282957646	5.17355043	5.166537931	5.166135134	5.166112172	5.166110863	5.166110789		5.16611078	8
4000	5.513957106	5.423531583	5.415466949	5.414785867	5.414728642	5.414723836	5.414723433		5.41472340	8
4100	5.744956566	5.678316491	5.671031523	5.670254474	5.670171824	5.670163035	5.670162101		5.67016199	9
4200	5.975956026	5.936641579	5.931801651	5.931210383	5.931138223	5.931129417	5.931128343		5.93112819	10
4300	6.206955485	6.197055204	6.195772411	6.195606275	6.19558476	6.195581974	6.195581613		6.19558156	9
4400	6.437954945	6.45799477	6.460564611	6.460893524	6.460935611	6.460940996	6.460941685		6.46094179	100
4500	6.668954405	6.717869742	6.723700552	6.72438713	6.724467851	6.72447734	6.724478455		6.72447860	9

Appendix 3 - Ephemermides of Delta Geminorum

See Appendix 1 caption for details.

t(year)	M (°)	ρ(")	θ(°)	X(")	Y(")
1950.0	153.90000000	6.534057908	126.4820132	-3.884957443	5.253667139
2000.0	168.90000000	5.765875819	135.0986561	-4.084104075	4.07006362
2015.3	173.49000000	5.50164909	138.2440158	-4.10416323	3.663875939
2050.0	183.90000000	4.881105045	146.6695106	-4.078236902	2.682008618
2100.0	198.90000000	4.038600047	163.3094004	-3.868452327	1.159899536
2150.0	213.90000000	3.488314255	186.9262739	-3.46285705	-0.42066304
2200.0	228.90000000	3.491802777	214.5203462	-2.876983607	-1.978800635
2250.0	243.90000000	4.038715957	238.0915046	-2.134720701	-3.428439019
2300.0	258.90000000	4.848351334	254.8187933	-1.269650532	-4.679155712
2350.0	273.90000000	5.648093446	266.6857402	-0.326530365	-5.638646779
2400.0	288.90000000	6.25055473	275.8551423	0.637642451	-6.217945523
2450.0	303.90000000	6.528257367	283.7710349	1.554002599	-6.340600931
2500.0	318.90000000	6.401409806	291.4904236	2.345129029	-5.956376192
2550.0	333.90000000	5.84674056	300.1070115	2.932822154	-5.057957037
2600.0	348.90000000	4.921759477	311.3347443	3.250611066	-3.69557087
2650.0	363.90000000	3.813426459	328.697279	3.258321823	-1.981302668
2700.0	378.90000000	2.953928475	358.5175292	2.952939756	-0.076421408
2750.0	393.90000000	2.998510963	397.7754342	2.370076217	1.836792509
2800.0	408.90000000	3.918295635	426.2987654	1.575027528	3.587802805
2850.0	423.90000000	5.083793843	442.6760305	0.648079763	5.04231618
2900.0	438.90000000	6.121345566	453.0858037	-0.329520614	6.112469853
2950.0	453.90000000	6.876011876	460.7709413	-1.285010444	6.754871389
3000.0	468.90000000	7.289216272	467.2247798	-2.158491255	6.962297707
3050.0	483.90000000	7.351799955	113.2637003	-2.903692953	6.754075052
3100.0	498.90000000	7.085238396	119.4806056	-3.486850724	6.167858231

t (year)	E0	E1	E2	E3	E4	E6	E7		En	n
1950.0	2.68606172	2.73445503	2.72961980	2.73010769	2.73005850	2.73006346	2.73006296		2.73006301	8
2000.0	2.94786111	2.96903852	2.96674801	2.96699617	2.96696929	2.96697220	2.96697189		2.96697192	8
2015.3	3.02797172	3.04044315	3.03907920	3.03922846	3.03921213	3.03921391	3.03921372		3.03921374	8
2050.0	3.20966049	3.20217881	3.20300009	3.20290992	3.20291982	3.20291873	3.20291885		3.20291884	8
2100.0	3.47145988	3.43582897	3.43955888	3.43916645	3.43920772	3.43920338	3.43920383		3.43920379	8
2150.0	3.73325927	3.67190731	3.67762074	3.67707950	3.67713069	3.67712585	3.67712631		3.67712627	9
2200.0	3.99505866	3.91216668	3.91843846	3.91794497	3.91798369	3.91798065	3.91798089		3.91798087	8
2250.0	4.25685805	4.15807501	4.16332925	4.16302633	4.16304372	4.16304272	4.16304278			7
2300.0	4.51865743	4.41071524	4.41362498	4.41353032	4.41353339	4.41353329				6
2350.0	4.78045682	4.67071155	4.67055234	4.67055307						3
2400.0	5.04225621	4.93818682	4.93504847	4.93497171	4.93496985	4.93496980				6
2450.0	5.30405560	5.21275425	5.20754078	5.20726697	5.20725266	5.20725192	5.20725188			7
2500.0	5.56585498	5.49354371	5.48774388	5.48729599	5.48726151	5.48725886	5.48725866		5.48725864	8
2550.0	5.82765437	5.77926106	5.77453915	5.77408490	5.77404126	5.77403707	5.77403667		5.77403662	9
2600.0	6.08945376	6.06827634	6.06599533	6.06575025	6.06572392	6.06572110	6.06572079		6.06572076	8
2650.0	6.35125315	6.35873483	6.35955569	6.35964573	6.35965560	6.35965668	6.35965680		6.35965682	8
2700.0	6.61305254	6.64868345	6.65236814	6.65274641	6.65278522	6.65278920	6.65278961		6.65278965	8
2750.0	6.87485192	6.93620389	6.94168646	6.94216445	6.94220603	6.94220965	6.94220996		6.94220999	8
2800.0	7.13665131	7.21954328	7.22524583	7.22561619	7.22564015	7.22564170	7.22564180			8
2850.0	7.39845070	7.49723373	7.50152482	7.50168872	7.50169494	7.50169518	7.50169519			7
2900.0	7.66025009	7.76819228	7.76984555	7.76986098	7.76986112					4
2950.0	7.92204947	8.03179475	8.03031509	8.03034376	8.03034321	8.03034322				6
3000.0	8.18384886	8.28791825	8.28365380	8.28385012	8.28384112	8.28384154	8.28384152			7
3050.0	8.44564825	8.53694960	8.53097559	8.53138878	8.53136030	8.53136227	8.53136213		8.53136214	8
3100.0	8.70744764	8.77975892	8.77358114	8.77412290	8.77407549	8.77407964	8.77407928		8.77407931	8

Appendix 4 - Ephemermides of Eta Casseiopiea

See Appendix 1 caption for details.

t(year)	M (°)	ρ(")	θ(°)	X(")	Y(")
1950	-314.70000000	10.12608090	288.22790152	-9.61795254	-3.16741272
1975	-295.95000000	11.72848105	304.27683511	-9.69154956	-6.60538680
2000	-277.20000000	12.84586963	316.97065450	-8.76567269	-9.39038597
2015	-265.95000000	13.34669772	323.69063860	-7.90317831	-10.75519003
2025	-258.45000000	13.62430057	327.91836593	-7.23623403	-11.54376381
2050	-239.70000000	14.15666586	337.86273268	-5.33461155	-13.11308918
2075	-220.95000000	14.50107906	347.21149132	-3.20985613	-14.14136194
2100	-202.20000000	14.69357101	356.22180312	-0.96822105	-14.66163623
2125	-183.45000000	14.75508650	365.07860235	1.30615434	-14.69716089
2150	-164.70000000	14.69499338	373.93496055	3.53885281	-14.26251560
2175	-145.95000000	14.51234633	382.93872459	5.65613567	-13.36474187
2200	-127.20000000	14.19534132	392.25724339	7.57635786	-12.00443738
2225	-108.45000000	13.71875419	402.11042183	9.19926934	-10.17731104
2250	-89.70000000	13.03840804	412.82938497	10.38952364	-7.87768258
2275	-70.95000000	12.08061833	424.98444505	10.94737200	-5.10846216
2300	-52.20000000	10.72399286	439.72332633	10.55195589	-1.91317791
2325	-33.45000000	8.78572401	99.89572701	8.65501129	1.50987616
2350	-14.70000000	6.23023716	134.77009850	4.42308444	4.38773052
2375	4.05000000	5.05953409	203.39208558	-2.00874187	4.64368833
2400	22.80000000	7.33064774	257.71823462	-7.16287357	1.55937118

t (year)	E0	E1	E2	E3	E4	E6	E7		En	n
1950	-5.49255116	-5.13928382	-5.04015401	-5.02200935	-5.01918385	-5.01875786	-5.01869396		-5.01868274	10
1975	-5.16530192	-4.71841132	-4.66831093	-4.66878465	-4.66877433	-4.66877455	-4.66877455			7
2000	-4.83805269	-4.34497168	-4.37422337	-4.36920037	-4.37003449	-4.36989516	-4.36991841		-4.36991507	10
2015	-4.64170315	-4.14594426	-4.22232749	-4.20319810	-4.20775296	-4.20665394	-4.20691829		-4.20686696	12
2025	-4.51080345	-4.02386753	-4.12702685	-4.09654796	-4.10510835	-4.10266565	-4.10335963		-4.10320590	14
2050	-4.18355422	-3.75444663	-3.89767764	-3.84257324	-3.86300543	-3.85531248	-3.85819305		-3.85740694	17
2075	-3.85630498	-3.53057110	-3.66782103	-3.60667403	-3.63340270	-3.62161056	-3.62679284		-3.62520828	20
2100	-3.52905575	-3.34126888	-3.43047480	-3.38746995	-3.40808230	-3.39817247	-3.40293016		-3.40138603	21
2125	-3.20180651	-3.17189831	-3.18674691	-3.17937247	-3.18303441	-3.18121586	-3.18211893		-3.18181929	21
2150	-2.87455728	-3.00570218	-2.94188717	-2.97315247	-2.95787675	-2.96535132	-2.96169647		-2.96289708	26
2175	-2.54730804	-2.82558638	-2.70176226	-2.75892369	-2.73288671	-2.74482687	-2.73936743		-2.74108248	24
2200	-2.22005881	-2.61593418	-2.46944481	-2.52952485	-2.50561568	-2.51525880	-2.51138950		-2.51249947	22
2225	-1.89280957	-2.36426387	-2.24139439	-2.28218429	-2.26926542	-2.27342586	-2.27209291		-2.27241680	19
2250	-1.56556034	-2.06255353	-2.00366808	-2.01671947	-2.01396015	-2.01454991	-2.01442415		-2.01444626	13
2275	-1.23831110	-1.70809245	-1.73063418	-1.72897590	-1.72910639	-1.72909617	-1.72909697		-1.72909692	9
2300	-0.91106187	-1.30376891	-1.39044795	-1.40000116	-1.40083048	-1.40090037	-1.40090624		-1.40090678	9
2325	-0.58381263	-0.85776354	-0.95973425	-0.99087508	-0.99955602	-1.00190445	-1.00253436		-1.00276446	19
2350	-0.25656340	-0.38268110	-0.44214766	-0.46922055	-0.48130243	-0.48664161	-0.48899043		-0.49082707	22
2375	0.07068583	0.10578745	0.12316419	0.13174379	0.13597326	0.13805650	0.13908216		0.14007632	24
2400	0.39793507	0.59053032	0.67466547	0.70837922	0.72128515	0.72612917	0.72793323		0.72899803	20

Binaries not in the WDS

T. V. Bryant III

Little Tycho Observatory
703 McNeill Road, Silver Spring, Md 20910
rkk_529@hotmail.com

Abstract: Using the UCAC4 astrometric catalog, a search for binaries not yet listed in the WDS was done. Seven of the unlisted binaries found were observed from the Little Tycho observatory and then manually checked using Aladin's DSS images.

A program was written to extract entries from the UCAC4 astrometric catalog[1]. The criteria for a star to be extracted were:

- The star needed to be brighter than 13.0 mv. This is the visual magnitude limit of my telescope.
- The star needed to be fainter than 8.0mv. Anything brighter has probably already found its way into the WDS.
- The star needed to have a proper motion greater than 2 mas/year. To be considered as a binary, a pair needs to show a good degree of common proper motion (CPM).
- The star needed to be north of the celestial equator. The Little Tycho observatory has a poor southern horizon, further compounded by severe light pollution in the south. Northern declinations are preferred.

A list of possible pairs was generated. These pairs were then manually checked using the images from Aladin/DSS[2] and proper motions from the UCAC4. Those pairs that had similar proper motions and were within 1.5mv of each other were then checked for prior WDS[3] membership. If they were absent from the WDS, they were chosen for observation.

The sky has been pretty well mined for CPM pairs, so those found are rather faint, in the 11 - 13 mv range.

In the Figures 1 through 7 below, the UCAC4 data from the primary star are listed in the tables to the left of the image. The images are from Aladin/DSS; all other data are from the UCAC4.

The magnitude sources are from APASS data or the UCAC4 fit model magnitude (F) data.

ρ refers to the separation of the pair in arc seconds. θ refers to the position angle in degrees. Both measures for each star were determined from the Aladin/DSS images using their "dist" tool.

"PM" refers to proper motion in milliarcseconds (mas) per year.

References

1) The Fourth US Naval Observatory CCD Astrographic Catalog (UCAC4). Zacharias, et al, 2012. http://www.usno.navy.mil/USNO/astrometry/optical-IR-prod/ucac

2) Aladin web site, http://aladin.u-strasbrg.fr

3) The Washington Double Star Catalog Brian D. Mason, Gary L. Wycoff, William I. Hartkopf, Geoffrey G. Douglass, and Charles E. Worley, 2001. http://ad.usno.navy.mil/wds/

Binaries not in the WDS

Primary RA, Dec: J2000	18:44:37.25 27:26:55.33
mv primary	11.7 APASS
mv secondary	12.9 APASS
ρ	10.7"
θ	334°
Primary PM in RA	1.4
Primary PM in Dec	-12.2
Secondary PM in RA	2.8
Secondary PM in Dec	-5.2
Primary UCAC4 Number	588-088331
Secondary UCAC4 Number	588-068327

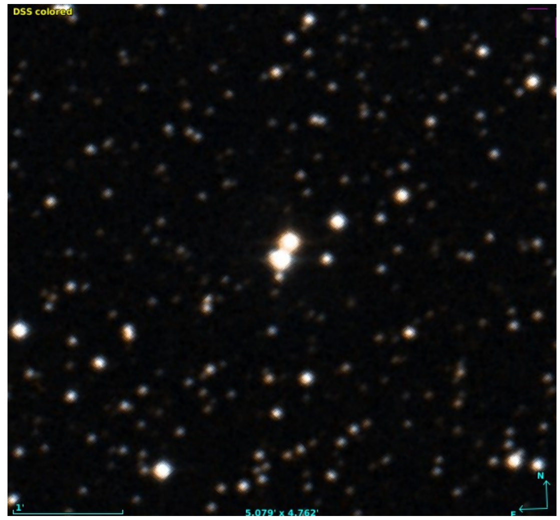

Figure 1. Primary UCAC4 number 588-088331.

Primary RA, Dec: J2000	19:41:48.67 18:29:50.03
mv primary	11.1 APASS
mv secondary	11.7 F
ρ	16.3"
θ	55°
Primary PM in RA	10.7
Primary PM in Dec	-4.3
Secondary PM in RA	11.3
Secondary PM in Dec	-5.2
Primary UCAC4 Number	543-103360
Secondary UCAC4 Number	543-103370

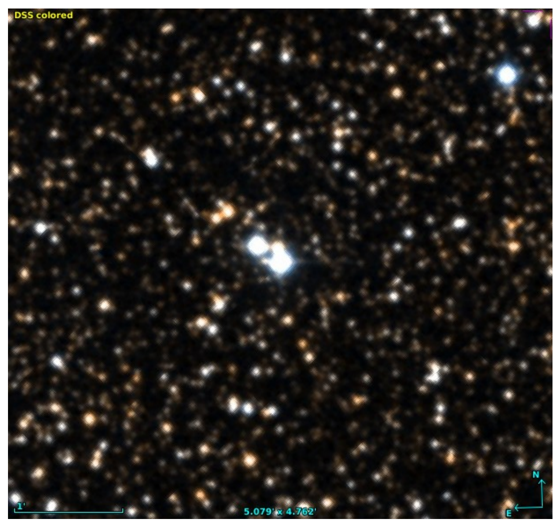

Figure 2. Primary UCAC4 number 543-103360.

Primary RA, Dec: J2000	20:5:53.18 22:54:12.83
mv primary	11.9 APASS
mv secondary	12.7 F
ρ	21.1"
θ	156°
Primary PM in RA	3.6
Primary PM in Dec	-11.9
Secondary PM in RA	7.4
Secondary PM in Dec	-9.7
Primary UCAC4 Number	565-103726
Secondary UCAC4 Number	565-103733

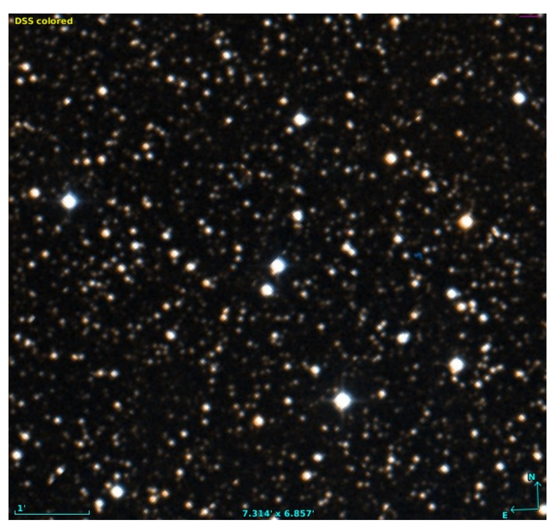

Figure 3. Primary UCAC4 number 565-103726.

Binaries not in the WDS

Primary RA, Dec: J2000	20:26:24.22 25:37:23.81
mv primary	11.9 APASS
mv secondary	12.5 F
ρ	16.1"
θ	357°
Primary PM in RA	19.7
Primary PM in Dec	5.8
Secondary PM in RA	22.2
Secondary PM in Dec	3.2
Primary UCAC4 Number	579-100187
Secondary UCAC4 Number	579-100186

Figure 4. Primary UCAC4 number 579-100187.

Primary RA, Dec: J2000	21:24:41.42 27:07:36.97
mv primary	11.1 APASS
mv secondary	12.7 APASS
ρ	21.6"
θ	268°
Primary PM in RA	15.1
Primary PM in Dec	8.0
Secondary PM in RA	16.1
Secondary PM in Dec	9.7
Primary UCAC4 Number	586-119848
Secondary UCAC4 Number	586-119837

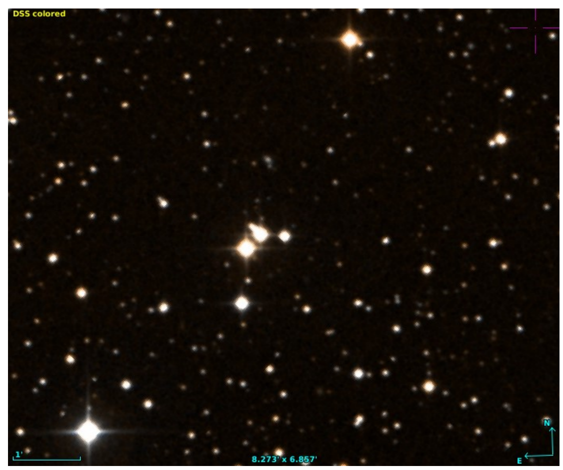

Figure 5. Primary UCAC4 number 586-119848. The 10.3mv (APASS) star at ρ = 17.5", θ = 135° from the primary is not a part of this system.

Primary RA, Dec: J2000	21:42:46.68 57:1:59.16
mv primary	11.4 APASS
mv secondary	12.0 F
ρ	11.8"
θ	358°
Primary PM in RA	8.3
Primary PM in Dec	4.2
Secondary PM in RA	5.2
Secondary PM in Dec	5.8
Primary UCAC4 Number	736-079756
Secondary UCAC4 Number	736-079755

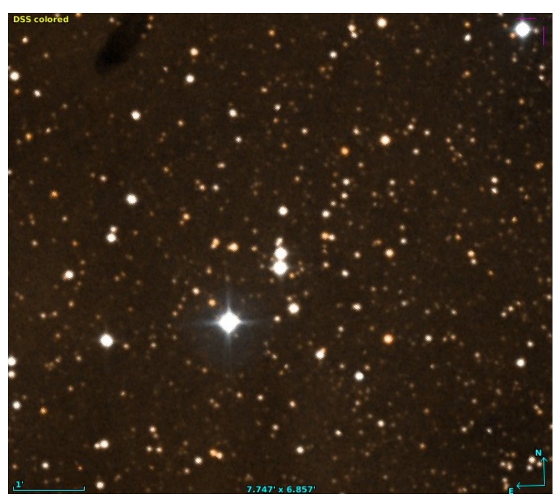

Figure 6. Primary UCAC4 number 736-079755.

Binaries not in the WDS

Primary RA, Dec: J2000	21:56:24.1 48:28:44.31
mv primary	12.4 APASS
mv secondary	12.8 F
ρ	13.3"
θ	128°
Primary PM in RA	9.9
Primary PM in Dec	-5.7
Secondary PM in RA	10.2
Secondary PM in Dec	-3.4
Primary UCAC4 Number	693-105883
Secondary UCAC4 Number	693-105890

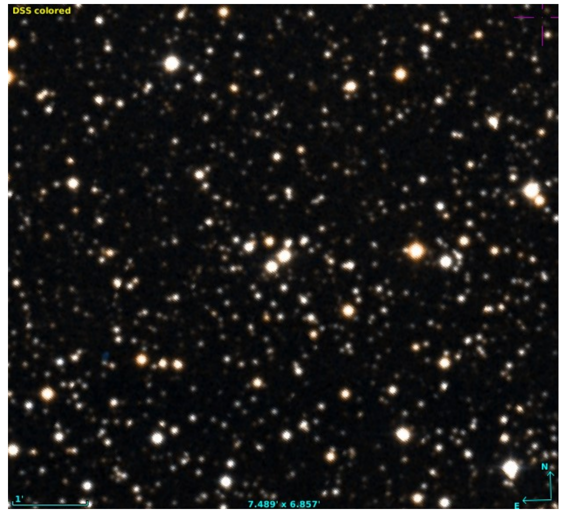

Figure 7. Primary UCAC4 number 693-105883.

Speckle Interferometry Observation of Binary Star WDS 05491+6248

Frances Eunice Alviola Lim[1], Kyle Andrei De Matias[1], Kelly Richardson[1], Eddy Bañuelos[1],Will Crooks[1], Spencer Raines[1], Jesse Wilson[1], and Russell Genet[1, 2]

1. Cuesta College, San Luis Obispo, California
2. California Polytechnic State University, San Luis Obispo, California

Abstract: We report a new observation of binary WDS 05491+6248 from the night of October 20, 2013, with the 2.1-meter telescope at Kitt Peak National Observatory. A new position angle of θ = 336.39° and separation of ρ = 0.802″ was determined.

Introduction

Using Kitt Peak National Observatory's 2.1-meter telescope, the binary star WDS 05491+6248 was observed on October 20, 2013. Observations of this binary were made with a portable speckle interferometry camera by students from various schools in a research seminar (Genet et al. 2013). The observations were analyzed by a Cuesta College student team in an astronomy research seminar (Figure 1).

WDS 05491+6248 was chosen for our project due to its unique orbit derived from speckle interferometry data falling closely along the curve. Would the new observation conform to the current orbit, or would it deviate?

Figure 1. Participants in Cuesta College's Astronomy Research Seminar, left to right: Eddy Bañuelos, Will Crooks, Jesse Wilson, Kelly Richardson, Frances Eunice Alviola Lim, Kyle Andrei De Matias, and Spencer Raines.

Methods

The Kitt Peak National Observatory is home to one of the largest arrays of astronomical telescopes in the world, including the 2.1-meter telescope used to observe our binary star. Originally built in the 1960's, this telescope has been used in many pioneering astronomical observations. It was initially equipped with a film imaging camera and spectrographs, but was later upgraded to include other instruments, including a CCD (Charge Coupled Device) imager.

Speckle interferometry is a technique devised by Antoine Labeyrie in 1970. It was known that, when viewing an astronomical object, there was a loss of resolution due to the poor seeing induced by the atmosphere. A Fourier transform of many short exposure images overcomes the seeing limitations (Labeyrie, 1970). Originally, the speckle interferometry techniques required high speed Tri-X film to make the observations, but with the introduction of CCD cameras, the process has been digitized and can efficiently gather larger amounts of data (Harshaw, 2015).

Before our data was reduced, the speckle interferometry camera was calibrated. A series of observations of binaries with known orbits was used to establish the camera angle with respect to celestial north and the camera's pixel scale. These values were -11.0492° and 0.01166"/px as reported by Wallace (2015).

To reduce our data, we used the speckle interferometry reduction program PlateSolve 3 (PS3) developed by David Rowe. The squares of each Fourier transform were computed and then averaged. The data was then processed, resulting in an autocorrellelogram. This autocorrellelogram shows the primary star in the center, and the secondary star on both sides (Rowe & Genet, 2015).

Results

The resulting binary position angle, θ, was 336.39°, while the separation, ρ, was 0.802″. An image of the autocorrellelogram of WDS 05491+6248 can be seen in Figure 2.

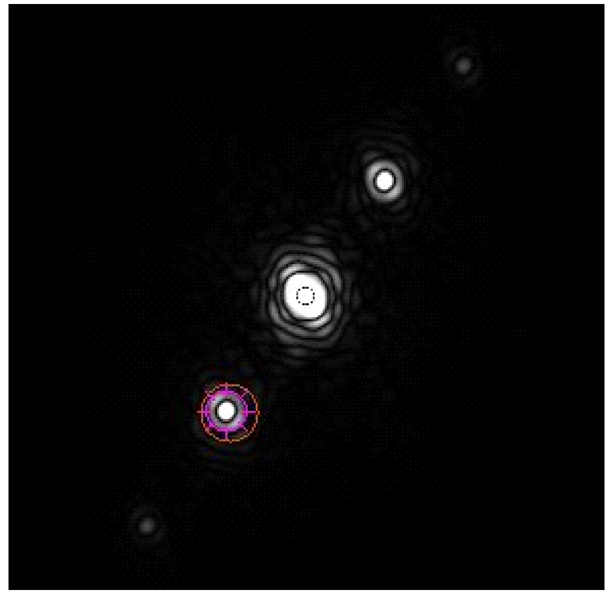

Figure 2. The autocorrellelogram of WDS 05491+6248

Discussion

Brian Mason from the U.S Naval Observatory provided data from previous observations. The first observation, made in 1831, was a visual observation made by Friedrich Georg von Struve with a filar micrometer.

Observations using speckle interferometry tend to be more accurate than visual observations. Our observation, a speckle interferometry observation, remains very close to the predicted orbit of the binary system.

Using CAD software, we plotted the position of our calculated observation. A cross was drawn with each leg having a length of 1/2 unit. The width and height of the cross had a total length of one unit. Then the bottom leg was deleted and redrawn to the separation length of 0.802″ or 0.802 units. Next, the bottom leg was rotated exactly 336.39 degrees counter clockwise. Once the exact location of the calculated observation had been laid out using this program, we overlaid the template

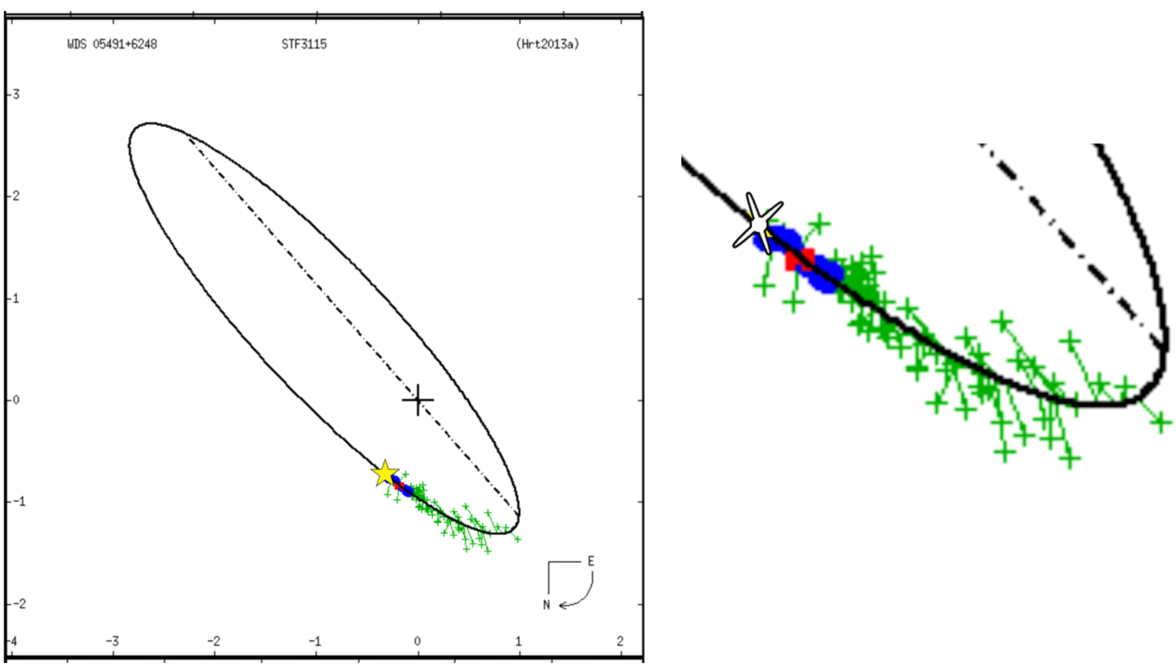

Figure 2. *Orbital plot of all observations (left) and a close up view of our point (right).*

onto the current image of the binary's previous observations and estimated orbit. Scaling the template was accomplished by using the width of the plus sign to match the scale provided at the bottom of the orbit image. Once the scale had been accurately calibrated, the template was then moved so the cross in the template covered the cross in the orbit image. The resulting location of the tip of the rotated leg was the position of the calculated observation.

The location of our calculated observation placed it right on the predicted orbit. The new location was on track with the previous observations (Figure 2).

Conclusion

Our team successfully calculated a new position angle and separation for the binary star WDS 05491+6248. Our data point was graphed along with past observations. The new θ and ρ values corresponded with the trend present in past observations, adding more validity to the calculated orbit of the binary, as well as further supporting that it is indeed a gravitationally bound system.

Acknowledgments

We thank Kitt Peak National Observatory for the use of their 2.1-meter telescope which aided the collection of images from a speckle interferometry camera. We also thank Brian Mason from the US Naval Observatory for supplying past observations made by other astronomers for WDS 05491+6248. We also thank Jolyon Johnson for his advice, and Richard Harshaw and Vera Wallen for their external reviews.

References

Genet, R., Johnson, J., Buchheim, R., & Harshaw, R. 2016. *Small Telescope Astronomical Research Handbook.* Santa Margarita, CA: Collins Foundation Press.

Harshaw, W. 2015. Calibrating a CCD camera for speckle interferometry. *Journal of Double Star Observations,* 11, 314.

Labeyrie, A. 1970. Attainment of diffraction limited resolution in large telescopes by Fourier analyzing speckle patterns in star images. Astronomy and Astrophysics 6, 85.

Rowe, D., & Genet, R. 2015. User's guide to PSE speckle interferometry reduction program. *Journal of Double Star Observations,* 11, 266.

Wallace, D., 2016. An Investigation of Six Poorly Described Close Visual Double Stars Using Speckle Interferometry. Master's thesis, University of North Dakota.

Data Mining for Double Stars on VLT Survey Telescope Image Archive

Lucian Curelaru

Brasov Astronomy Club
Brasov, Romania
astroclubul.brasov@gmail.com

Abstract: The article presents a set of methods and tools used to identify and measure double stars on already existing images produced by the ESO VLT Survey Telescope in Paranal Chile. A precision analysis and a first set of measurements are included.

Introduction

Recently the idea of using existing telescope images to extract other data than what the telescope was targeting is having more and more success. This approach can be quite laborious sometimes, but also is encouraged by the fact that telescope time on big instruments has a big cost. I was involved in the last several years in different data-mining projects connected with asteroids, being part of the EURONEAR team [1] which has a lot of projects based on data mining. Starting from their ideas and having some previous experience in double star astronomy, I decided to apply this approach to the double star field as well. Using some already build scripts which I've adapted, I managed to start my first data mining project for neglected double stars. I think the idea can be a very succesful one on double star field maybe even much more than in asteroid field for many reasons. One, for measuring a double star even single isolated pictures are useful, but for asteroids you need in general three successive pictures from same sky region and same period of time. The second reason is that double stars are quite fixed, while for asteroids you need to have both the correct region of sky and the right timing to catch an object in the field by chance, as data mining projects tries to do. In addition, for double stars, the same field imaged multiple times at considerable time difference can generate multiple measurements, and also the historical data measurements can be extremely useful in some cases.

The Telescope and the Camera

I decided to use for this first project images taken with OmegaCAM from ESO VLT Survey Telescope [5]. I had already worked in the past with images from this telescope to recover some asteroids, so I had everything I needed. The instrument is really outstanding: a modified Ritchey-Chretien with a 2.61 meter primary mirror with active optics located at Cerro Paranal site at 2635m altitude, and a 256 Megapixel camera containing a 32 CCD mosaic covering one square degree of sky. The camera has also 4 supplemental CCDs used exclusively for autoguiding and field rotation corrections. The image is optically corrected and does not require any additional software corrections in order to provide very good astrometry, even near the edge of the field. With a resolution of 0.21 arcsec / pixel, the images are taken mostly in excellent sky conditions. Moreover, the telescope also provides data from the southern sky, which contains more unanalysed targets in double stars field than the northern hemisphere.

The Method

The idea of this project is to identify images, already produced in the past by a telescope, which might contain double stars and measure these found objects. Of course I addressed only images that are publicly available for research projects, but a lot of telescopes offer their images archives for free for such purposes. In most cases, there are some limitations only for new images, in general newer than six months to one year, depending by each observatory policy. At this time there are available probably millions of such images from hundreds of telescopes around the world.

It is clear than a lot of unmeasured double stars can be found on this huge amount of data, so I decided to try to focus on objects that lack measurements; and the primary search was targeted mainly on neglected double stars. On the other hand, even if I targeted first the images containing neglected stars, I decided to measure all doubles down to an established separation available on a selected image, because measuring more stars on an already downloaded image add only a little amount of supplemental effort and provides some extra measurements, even if not only on neglected objects. I might have occasionally skipped some doubles that already have a huge amount of measurements or some very close doubles. Even so, the amount of data is huge, so I decided to begin by analyzing images from a single instrument. I chose to start with the VLT Survey Telescope, which I already was familiar with. I also limited the first search to neglected objects with separation equal to or bigger than 3 arcseconds. I set this limit for the first set of analyzed neglected objects , but I'm quite sure that the limit can be easily lowered at least on OmegaCAM images which provide excellent quality.

For this purpose I needed first to search somehow automatically the neglected doubles on each OmegaCAM image archive. To do this I built a small java application which checks a list of WDS objects (in my case only 3 arcsec or higher separated neglected doubles) versus the list of freely available images from the targeted telescope archive. Here I used an already prepared image list from EURONEAR. At EURONEAR MegaArchieve[3] project, we have some crawlers which extract from different telescopes web-pages lists of available images containing basically the center of the field, names of images, and some other useful data. EURONEAR has an impressive collection of such references in the same unified format (text file with some position rules). I took the OmegaCAM reference file from this EURONEAR collection, wrote a small code to load the file data and, using the java app I've mentioned before, I produced a list OmegaCAM images which contains neglected doubles. Then for a part of the found images, I visited the ESO archive[4], downloaded the appropriate image, and started the measurement process. In addition, using another tool developed by me some years ago , named WDSFilter[8], I checked what other double stars different than the targeted one are contained in each downloaded image field, listing all doubles half a degree around the center of each image.

Having the images and the list of expected objects for each, I proceeded in the following way: I reduced the images with Astrometrica software[6] and measured the precise position of each targeted object component. These coordinates I inserted in a Google spreadsheet I built for a previous double star project described in a past JDSO article[9]. This spreadsheet parses the Astrometrica report output and computes the separation and position angle from the determined precise coordinates. In Astrometrica I've used the UCAC4 catalog[10] for field matching and sometimes the NOMAD catalog[11] when UCAC4 was not detailed enough (mostly on the fields close to south pole)

The OmegaCAM images came as FITS.FZ files containing 32 images each, one for each CCD of the instrument. To be able to work with them in Astrometrica, I used the Aladin software[7] to export FITS containing just one image each from the initial file (Astrometrica software is not able to work with FITS.FZ format).

I measured only a part of the candidates found by my java app stopping when I reached the limit of one hundred objects, but I intend to continue and present the next measurements in future articles. I intend to also reduce images from other instruments after the candidates from this instrument are finished. As I've mentioned before, there are hundreds of image sets available which might produce double stars measurements with this approach.

Even thought, I did not present in detail some of the tools which I built and used for this process, I am open to shareing them freely if anybody is interested in some similar research.

The Precision

Even though it seems quite obvious that the quality of images and resolution produced by the VLT Survey Telescope should provide excellent astrometry on close doubles, I wanted to also have a quantitative evaluation for the quality of my measurements. So I started the project with a set of test measurements and analyzed the results versus the already existing measurements. My first approach was to look for objects with a computed orbit of separation around 3 arcseconds range (±1 arcsecond), but unfortunately I was unable to find any OmegaCAM image containing such an object, at least in the archive analyzed in January 2016. So the next option was to try to measure some objects from images taken in the same year with other already published measurements. In addition, I tried to choose objects with as low movement as possible (deduced from the existing measurements). It is clear that this method is not as good as the first one because it is based on more presumptions like the precision of the comparing measurements, because that the comparing data is not produced by an orbital computation which is most pre-

Data Mining for Double Stars on VLT Survey Telescope Image Archive

Table 1: Comparison Between my Measurements and WDS Values

Measured PA	Measured Sep	WDS PA	WDS Sep	PA O-C	Sep O-C
35.28538348	3.038154645	35.3	2.99	0.01	0.05
83.9355074	11.35849075	84.2	11.38	0.26	0.02
52.70710493	23.1725325	52.8	23.40	0.09	0.23
43.58756383	27.54301679	43.8	27.85	0.21	0.31
291.2291559	2.844526324	291.5	2.83	0.27	0.01
291.1967401	2.959303839	292.0	2.96	0.80	0.00
89.27862978	2.382852467	90.0	2.39	0.72	0.01

cise, and so on. But I considered that analyzing multiple objects in this manner could prove that the measurements produced by this method and from that source of images are in the accepted error range. I present the list of the measurements in Table 1.

For a better overview of the results, I also built two graphs presenting the PA differences (Figure 1) and separation differences (Figure 2)

As it can be seen in the presented data and graphs, the differences between my measurements and other measurements made in the same year for seven objects stays under one degree on PA and under 2% from the separation of measured star. I wasn't able to find a fully agreed criteria for maximum acceptable error in the double stars literature I've checked (the values varying from case to case), but in all criteria I saw the limit for PA is not smaller than one degree and the percent of accepted error on separation for close doubles can vary between a few to even ten percent. So I've concluded that the obtained values are good proof that the measurements have a good quality.

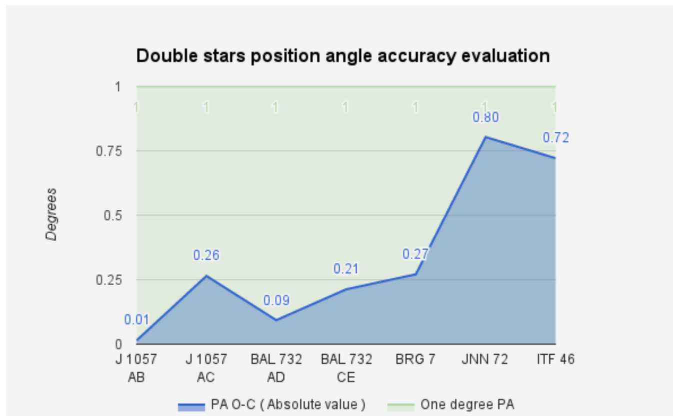

Figure 1: Position Angle differences for seven selected comparation objects

The Measurements

In the next tables I present the obtained measurements. All the magnitudes presented are taken from the WDS and not measured on images.

Even if I was targeting neglected doubles down to 3 arcsec separation, there were a few cases where I also found in the analyzed images not-targeted neglected doubles with a little smaller separation. Due to the good accuracy test results, I decided to also measure these objects down to 1.5 - 2 arcsec separation, even if not covered by the precision evaluation I presented earlier. I need to mention than the objects under 3 arcseconds separation were very clearly resolved by Astrometrica (Figure 3)

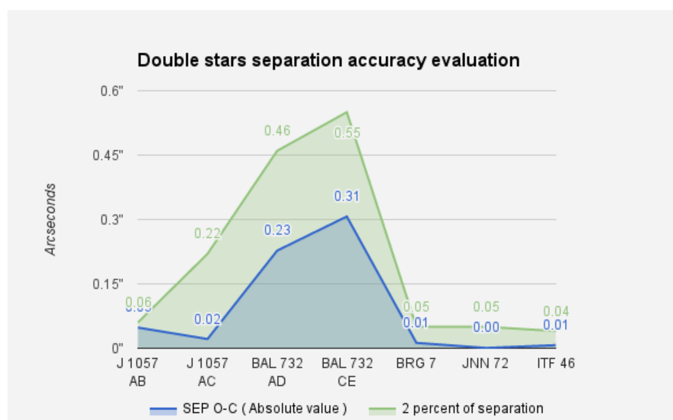

Figure 2: Separation differences for seven selected comparation objects

Neglected Measurements:

In Table 2 you will find a list of neglected double

(Text continues on page 211)

Data Mining for Double Stars on VLT Survey Telescope Image Archive

Table 2: Neglected Double Stars Measured on Analysed OmegaCAM Images

NAME	RA+DEC	MAGS	PA	SEP	DATE	N	NOTES
JSP 423	10430-5951	9.9,10.7	270.5	2.24	2015.084	1	
VOU 88	10434-6005	9.3,12.5	84.1	4.22	2015.084	1	
JSP 430	10458-6005	9.8,11.6	146.9	3.40	2015.084	1	
JSP 429	10453-6001	11.2,10.8	89.6	1.63	2015.084	1	
DAW 6AB	10440-6007	9.2,10.8	118.5	3.10	2012.124	1	
JSP 427	10442-6009	9.8,12.3	356.3	2.29	2012.124	1	1
DAW 8AC	10444-6000	8.1,13.5	92.5	8.40	2012.124	1	
HJ 4356BD	10440-5933	9.0,9.1	188.8	3.97	2013.301	1	
RUZ 2	12066-3137	16.8,19.4	6.4	5.52	2015.068	1	2
COO 70AB	08169-3452	10.8,11.0	137.8	2.25	2015.048	1	
RST5290	08171-3430	8.8,13.9	56.4	3.94	2015.048	1	
TDS6434	09161-4555	11.7,16.7	148.2	4.61	2015.026	1	3
RST5533	14204-3002	10.0,14.4	344.5	4.38	2015.024	1	4
B 268	14118-2954	11.6,13.0	84.9	2.35	2015.024	1	
BRT2673	07312-1215	10.4,12.3	111.5	55.51	2015.001	1	5
SLW 195	07305-1247	19.4,19.6	269.3	178.00	2015.001	1	
TDS4861	07296-1222	11.9,14.3	11.7	117.17	2015.001	1	6
RST3518	07284-1257	9.6,15.3	90.0	2.35	2015.001	1	
J 1049	06058+1652	12.3,12.4	118.3	3.02	2014.960	1	
TDS7204	10208-5408	12.5,14.6	80.9	6.73	2014.951	1	7
HJ1096	01550+1537	10.9,13.2	161.3	33.33	2014.799	1	8
TDS5111	07430-2337	12.2,14.0	256.5	1.67	2014.786	1	
TDS5158	07448-2250	12.3,16.1	190.6	5.34	2014.786	1	9
B144	07457-2331	10.5,14.2	179.3	3.54	2014.786	1	
RST4132	23460-1508	10.0,13.9	93.7	3.57	2014.752	1	

NOTES

1. Precise coordinates not available in WDS. From this measurement precise coordinates of the primary star are: 10 44 15.863 -60 09 04.33
2. There seems to be a small position difference of about 5 arcseconds.
3. Secondary magnitude is much fainter than WDS by about four magnitudes.
4. Very big movement in PA, but precise position fits, separation and magnitudes match very well. On the other hand, there are more than 60 years from last and only measurement. It might be also some quadrant identification mistake in the initial measurement.
5. There is a matching secondary by magnitude, but it is at 55 arcseconds distance. I presume there is a typo at the decimal separator of the separation. The PA is not exact, but is in a plausible range for more than one century of movement.
6. Primary star at precise coordinates, but secondary not found at expected position or neighborhood. Still a pretty good match could be a star which is not at two arcseconds, but at two arcminutes, having an appropriate PA and magnitude. Maybe the existing old measurement was incorrectly entered with arcseconds instead of arcminutes.
7. Quite big difference on PA and separation, but not impossible for 25 years period. Main star fits the catalog precise position. No other component in the close neighborhood, so the identification is probably correct. Maybe the initial measurement has low precision because the values are strangely rounded.
8. The objects do not have precise coordinates, but having a large imaged field around the star. I've studied the neighborhood as well and looked around with Aladin. The only nearly matching candidate is this one. The PA is plausible, but the difference in separation is quite big. The magnitudes are close. So In my opinion this could be the object in discussion, but the separation difference have to be explained or the object should be considered lost
9. Primary star at precise position. Most close match for secondary is the measured one but there are some big differences in PA and separation . Also the magnitude difference is big. Still no other candidate found in the field.

Table 3: Two Potential Variants for the Secondary Component of SIN 56 AC

NAME	RA+DEC	MAGS	PA	SEP	DATE	N
SIN 56AC	10440-6005	8.6, 16.1	308.9	19.76	2012.124	1
SIN 56AC	10440-6005	8.6, 11.6	292.3	23.63	2012.124	1

(Continued from page 209)

stars measured with the presented methods.

Neglected with More Secondary Candidates

The object presented in Table 3 has two candidates for the secondary component and I was not able to determine which is the correct one, so I preferred to mention both objects. Maybe someone will be able to clarify this issue.

In both cases the stars are close enough to the expected position to explain the movement in 29 years. Unfortunately there is only one other observation in the past so the movement speed and direction are unknown.

Other Double Stars Measurements

In Table 4 you will find a list of double stars measured with the presented methods. This stars were not mainly targeted but they was on the same FITS with one of the targeted objects, so it could be measured with a minimal supplemental effort. A big part of them was also not measured for a considerable timeframe (more than 15 years), so the measurement is pretty useful even they do not exceeded the 20-years neglected condition.

Statistics

Coming back to neglected searchs in the OmegaCAM data, I want to also specify some numbers which might be interesting. The January 2016 OmegaCAM available images list from EURONEAR had 119,219 images. After the search, I found that there are 8,113 images that contain at least one neglected double with separation bigger than 3 arcseconds. Of course there are a lot of duplicates in that attempt because there are pictures taken at a different time which cover at least partially areas of sky already imaged in another observing session. After removing duplicates, I found that 423 different neglected doubles can be found in OmegaCAM images. For this article I've measured doubles only from 25 images obtaining measurements or information for 33 neglected (7 of them missing ones) and 67 other doubles.

More details: from the 67 other doubles found, I found that 52 had their last measurement within the 15 to 20 year range, so they are potential neglected candidates. I found none in 10 to 15 years range and 15 in the 0 to 10 years range. For the precision analysis, I used 4 other different images from which I've collected the 7 comparison objects. I have to mention that I also

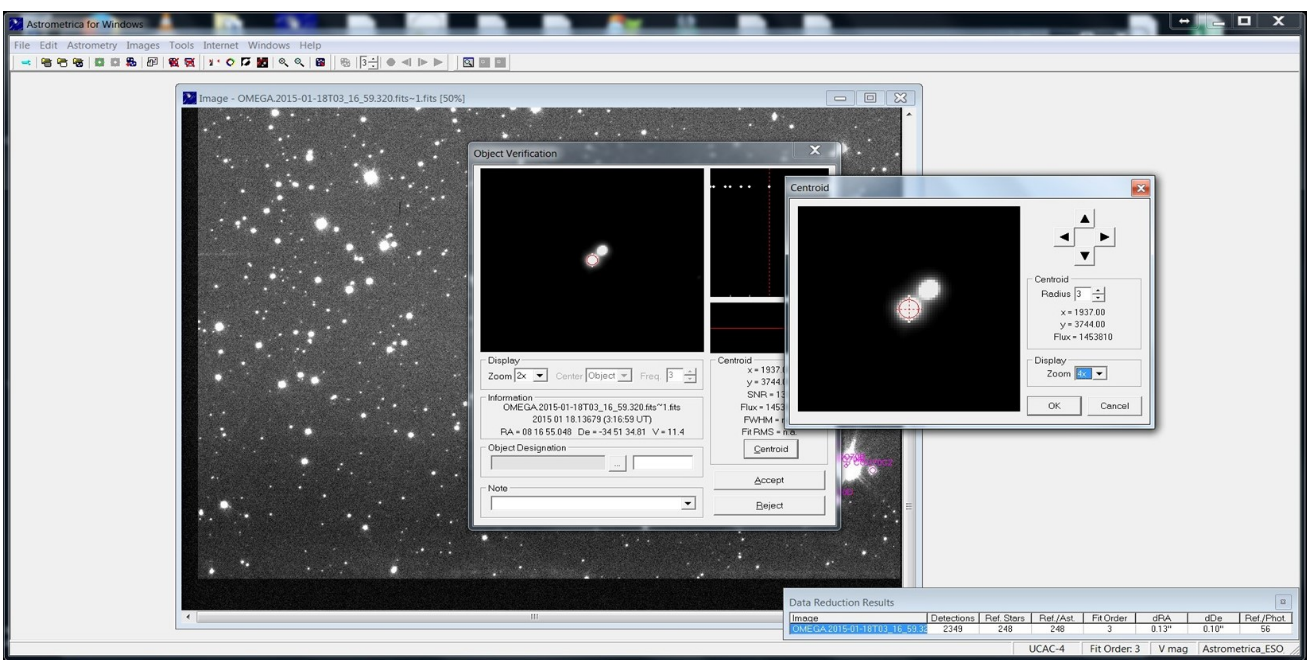

Figure 3: Measuring a close double star (COO 70 AB) on an OmegaCam image using Astrometrica. COO 70 AB is a 2.25 separated double with almost equal 9 magnitude components.

Table 4: Other Double Stars Found in Analysed OmegaCAM Images

Name	RA+DEC	Mags	PA	Sep	Date	N	Notes
BRT1993	12123-6444	11.3,10.1	151.9	2.61	2014.270	1	
HJ 4350	10432-5944	9.1,10.4	149.8	10.94	2015.084	1	
HJ 4354	10438-6005	9.6,10.4	214.9	10.09	2015.084	1	
HJ 4355	10438-5957	10.0,10.1	78.6	14.99	2015.084	1	
HJ 4353	10437-5935	11.0,10.5	181.1	4.96	2015.084	1	1
COO 112AB	10439-5933	9.8,10.1	240.4	6.46	2015.084	1	
SEE 123	10440-5932	10.4,11.1	307.0	3.90	2015.084	1	
HJ 4348AB	10421-5958	9.7,11.1	347.9	3.48	2015.084	1	
SEE 122AC	10421-5958	9.7,10.7	255.7	12.75	2015.084	1	
JSP 422AB	10428-6012	9.9,10.2	193.1	5.24	2015.084	1	
JSP 422AC	10428-6012	9.9,10.5	98.9	5.61	2015.084	1	
JSP 422AD	10428-6012	9.9,10.6	128.0	9.42	2015.084	1	
COO 113	10453-5945	10.0,9.9	195.1	14.63	2015.084	1	
DAW 7	10442-6008	10.4,10.6	359.4	3.83	2015.084	1	
HJ 4358AB	10440-6005	8.6,9.6	235.7	6.36	2012.124	1	
SIN 56AD	10440-6005	8.6,9.1	227.4	27.20	2012.124	1	
HJ 4359AC	10440-6007	9.2,9.7	195.5	7.98	2012.124	1	
DAW 8AB	10444-6000	8.1,10.6	276.8	7.03	2012.124	1	
HJ 4356AB	10440-5933	8.3,9.0	149.6	2.94	2013.301	1	
HJ 4356AC	10440-5933	8.3,10.7	268.8	4.86	2013.301	1	
SNA 12AF	10440-5933	8.3,12.5	8.1	3.67	2013.301	1	
SNA 12AG	10440-5933	8.3,12.3	337.3	5.05	2013.301	1	
J 2818	07267-1118	12.1,14.0	226.3	7.34	2015.078	1	
HJ 759AC	07273-1130	9.3,11.2	331.5	10.11	2015.078	1	
J 2476AB	07275-1145	11.4,11.8	304.2	5.36	2015.078	1	
J 2476AC	07275-1145	11.4,13.0	196.2	20.70	2015.078	1	
STF1097AC	07279-1133	7.6,9.6	312.8	19.91	2015.078	1	
BU 332AD	07279-1133	7.6,11.7	157.0	23.03	2015.078	1	
BU 332AE	07279-1133	7.6,13.2	43.3	32.32	2015.078	1	
BRT2672	07293-1128	13.1,12.8	39.8	4.59	2015.078	1	
BRT3198	07297-1125	11.4,12.0	5.9	3.55	2015.078	1	
LDS 407	12226-3103	13.0,12.1	38.9	9.86	2015.068	1	
SEE 152	12254-3108	9.8,12.0	84.8	2.54	2015.068	1	
RSS 281	12046-3111	8.5,13.5	160.3	8.57	2015.068	1	
HJ 4472	11464-2909	10.2,11.0	30.6	19.33	2015.067	1	

Table 4 concludes on next page.

Table 4 (conclusion): Other Double Stars Found in Analysed OmegaCAM Images

Name	RA+DEC	Mags	PA	Sep	Date	N	Notes
HJ 4472	11464-2909	10.2,11.0	30.6	19.33	2015.067	1	
BRT1620	08198-3456	11.1,11.3	298.4	3.62	2015.048	1	
WFC 65	08171-3447	10.6,12.3	175.5	11.77	2015.048	1	
DAM 21AB_C	08169-3452	10.8,14.2	76.9	16.25	2015.048	1	
I 9009AB_D	08169-3452	10.8,13.4	343.9	24.59	2015.048	1	
DAM 21AB_F	08169-3452	10.8,13.3	225.1	28.32	2015.048	1	
DAM 21AB_E	08169-3452	10.8,15.8	238.9	17.84	2015.048	1	
DAM 21FG	08169-3452	13.3,15.6	0.0	3.45	2015.048	1	
HDS1184	08200-3425	9.2,10.7	79.4	25.04	2015.048	1	
SEE 202AB-C	14129-3000	9.9,13.4	136.2	30.57	2015.024	1	
XMI 63	07317-1300	10.3,10.5	340.6	18.39	2015.001	1	
J 2479	07310-1226	12.7,13.4	274.2	5.93	2015.001	1	
J 2480AC	07311-1227	10.9,13.1	315.8	5.78	2015.001	1	
J 2480AB	07311-1227	10.9,12.7	238.0	7.70	2015.001	1	
LDS 185	07288-1303	13.8,14.3	293.0	12.06	2015.001	1	
LDS 183	07285-1235	12.3,14.0	237.7	24.50	2015.001	1	
J 1260	06082+1653	12.0,14.0	286.4	4.58	2014.966	1	
GWP 756	06093+1636	15.0,16.3	290.3	52.02	2014.966	1	
GWP 742	06057+1657	11.9,17.6	333.8	59.22	2014.966	1	
FIN 406	10198-5430	11.4,10.7	136.5	3.53	2014.951	1	
HDS1490	10213-5404	9.2,10.0	96.8	20.62	2014.951	1	
CVR 403	01559+1559	17.1,17.3	287.6	8.38	2014.799	1	
CBL 11	01579+1614	16.1,15.8	90.6	12.16	2014.799	1	
DAM 996	01583+1550	11.0,15.1	44.9	7.32	2014.799	1	
DAM 998	01588+1551	12.7,15.2	244.3	3.44	2014.799	1	
B 143	07446-2328	10.1,13.6	139.2	5.84	2014.786	1	
ARA2070	07448-2332	12.7,12.5	145.6	12.94	2014.786	1	
DON1067	07451-2312	9.1,12.0	23.4	8.93	2014.786	1	
B 2151	07458-2336	10.0,13.4	33.1	5.85	2014.786	1	
ARA2072	07460-2338	10.4,12.9	79.0	10.56	2014.786	1	
ARA1708	07461-2255	12.7,13.2	25.0	8.67	2014.786	1	
FOX 277	23433-1505	11.4,11.5	228.9	5.28	2014.752	1	
LDS6059	23456-1412	18.0,17.3	148.3	113.12	2014.752	1	

Notes:

1. The secondary component is a little elliptic. It looks very alike with a close binary with a PA around 20 and probably a separation under one arcsecond. Unfortunatelly the components can not be distinguished more to perform an appropriate measurement.

used a few other images for different initial tests, and also there were images on which the targeted objects were too close to margin or into CCD gaps, but were recovered from other images which contained the searched object. This increased the number of images used from the archives from 25 to 37.

I've only analyzed a small fraction (5.83%) of the images. Considering that this analyzed part could be statistically relevant, I estimate that from the whole list of 423 selected OmegaCAM images I could extract about 1700 measurements of double stars with separation over the 2 - 3 arcsecond limit, from which around 567 are neglected doubles Of course the number will probably grow considerably if we lower the separation limit. Also, knowing that there are many image collections such as OmegaCAM only in EURONEAR MegaArchive[3], and probably hundreds of collections in the whole world, the idea of data mining becomes very attractive and offers a huge amount of data which waits to be processed.

Conclusions

Measuring double stars on archive images from big telescopes can be a very efficient way of getting good precision measurements for a lot of doubles. As shown, the precision seems to be very good on 3 arcseconds separated stars. Besides the quantitative evaluation, the appearance of the 2 - 3 arcsec doubles in the images (Figure 3), show that in most cases close doubles are clearly separated and the position can be precisely determined with Astrometrica, suggesting that good precision can be obtained on much closer doubles as well. This encourages me to continue this project in the future in more directions. Firstly I intend to measure the already identified neglected from OmegaCAM images. In this paper I've only analyzed the first 100 objects found on 25 images, but a total of 423 images that contains at least one neglected star, and probably other doubles, was identified, and this leaves a lot of work to do. A second approach is to repeat in the future the search under the 3 arcsec limit used here. Of course this needs also a new precision analysis to be done for closer separations. For sure, the next step is to extend the search to other image collections.

Acknowledgements:

This project certainly could not have existed without the knowledge and experience which I've gained from the EURONEAR projects and also without the permission received from the EURONEAR project manager to use some data and scripts from their projects in my work. So, I want to express my gratitude especially to Mr. Ovidiu Vaduvescu who is the leader of EURONEAR project and also to the entire team of professional and amateur astronomers from EURONEAR.

The project is based on data obtained from the ESO Science Archive Facility[4] under the following request numbers: cluci203823 , cluci203826 , cluci203827 , cluci203828, cluci203829, cluci203833, cluci203853, cluci203864, cluci204341, cluci204342, cluci205539, cluci220408, cluci220551, cluci221469, cluci221649, cluci226454, cluci226834, cluci226875, cluci238943, cluci239928, cluci239940, cluci239942, cluci240027, cluci240028, cluci240030, cluci240031, cluci240032, cluci240034, cluci240461, cluci240462, cluci240463, cluci240788, cluci240787, cluci240897, cluci240898, cluci240899, cluci240900.

This research has made use of the Washington Double Star catalog maintained at the U.S. Naval Observatory [2].

Data reduction was carried out using the Astrometrica software developed and maintained by Herbert Raab[6].

This research has also made use of "Aladin Sky Atlas" developed at CDS, Strasbourg Observatory, France (http://cdsads.u-strasbg.fr/cgi-bin/nph-bib_query?2000A%26AS..143...33B&db_key=AST&nosetcookie=1 and http://cdsads.u-strasbg.fr/cgi-bin/nph-bib_query?2014ASPC..485..277B&db_key=AST&nosetcookie=1) [7]

References

[1] EURONEAR Projects, http://euronear.imcce.fr/

[2] Mason, D.B., Wycoff G.L., Hartkopf, W.I. Washington Double Stars Catalog, USNO, 2015.http://www.usno.navy.mil/USNO/astrometry/optical-IR-prod/wds/WDS

[3] Vaduvescu, O.; Popescu, M.; Comsa, I.; Paraschiv, A.; Lacatus, D.; Sonka, A.; Tudorica, A.; Birlan, M.; Suciu, O.; Char, F.; Constantinescu, M.; Badescu, T.; Badea, M.; Vidican, D.; Opriseanu, C. : Mining the ESO WFI and INT WFC archives for known Near Earth Asteroids. Mega-Precovery software , http://adsabs.harvard.edu/abs/2013AN....334..718V

[4] ESO Science Archive Facility : http://archive.eso.org/eso/eso_archive_main.html

[5] VLT Survey Telescope: http://www.eso.org/public/teles-instr/surveytelescopes/vst/

[6] Herbert Raab, Astrometrica software, http://www.astrometrica.at/

[7] Aladin Sky Atlas software : http://aladin.u-strasbg.fr/

[8] WDS Filter webtool http://brasov.astroclubul.org/wdsfilter/

[9] Lucian Curelaru,Ovidiu Tercu,Alexandru Dumitriu, Valentin Gavrila,Felician Ursache,Catalin Vladu : Neglected Double Star Measurements at the Astronomical Observatory of the Natural Science Museum Galati, Journal of Double Star Observations, Vol. 8 ,No.3 , Pages 201-209, 2012.

[10] UCAC Catalog: http://www.usno.navy.mil/USNO/astrometry/optical-IR-prod/ucac

[11] NOMAD Catalog: http://www.usno.navy.mil/USNO/astrometry/optical-IR-prod/nomad

Astrometric Measurements of WDS 15482+0134 EIS 1AB

Cassandra Kraver[1], Charles Van Steenwyk[1], Charles Ryan[2], Nancy Forrest[2], Jenae Irving[2], Aaron Krueger[2], Russell Genet[1,2], Jo Johnson[3], and Matthew Clifford[4]

1. California Polytechnic State University, San Luis Obispo, CA
2. Cuesta College, San Luis Obispo, CA
3. Newport High School, Bellevue, WA
4. Quakertown High School, Quakertown, PA

Abstract: Ten separations and position angles were obtained of WDS 15482+0134 AB with the CDK-700 telescope in the iTelescope array. The mean values of these measurements were compared to historical observations. Although there was a discrepancy between our separations and the historical data, the position angle matched quite well.

Introduction

Cuesta College, a community college in San Luis Obispo, California, offers ASTR 299, Astronomy Research Seminar. Once our team was formed we selected a double star system to observe. Our team decided to focus on double stars in the southern hemisphere and to obtain CCD images through the iTelescope array. The primary reason for choosing the southern hemisphere was to analyze systems that receive less telescope time, due to the large majority of earth-dwellers living in the northern hemisphere. The team was specifically interested in ordering observations from telescope T27, which resides in Siding Springs, because this Corrected Dall-Kirkham (CDK) telescope, manufactured by PlaneWave Instruments, was first prototyped by California Polytechnic students (Genet et al., 2010; Rowe, et al., 2010). By basing the selection in this defined location, the team narrowed the double stars based on a right ascension from 10 to 15 hours and a declination from 0 to -60 degrees for best viewing during spring.

Our student team selected WDS 15482+0134 / EIS 1AB, also known as the double star V382 Serpens, to obtain an updated separation and position angle. Discovered by astronomer T. Eisenbeiss in 1960, this system has only four recorded observations, with the latest observation made in 2006. What follows is the fifth separation/position observation of the 15482+0134 / EIS 1AB system reported to date.

This research project's goals were to contribute to the observations of this infrequently observed binary system. By doing this, the team hoped to learn the scientific process of research and publishing, as well as how to gather and analyze data as astronomers.

Figure 1: From left to right: Jenae Irving, Charles Ryan, Cassandra Kraver, Charles Van Steenwyk, and Nancy Forrest visiting the SOFIA airborne observatory at Armstrong Flight Research Center.

Observations and Reduction

Our observations utilize T27, a PlaneWave Instruments 27-inch (0.7m) CDK700 reflector (shown in Figure 2) with a focal length of 4638mm. This alt-az telescope was designed to be a multi-use telescope with the ability to accommodate for a variety of instruments. This telescope features a Finger Lake Instruments Pro-

Astrometric Measurements of WDS 15482+0134 EIS 1AB

Figure 2. Telescope 27 at the Siding Spring, Australia Observatory

Line PL09000 CCD Camera and acquired the T27 telescope's images, providing a resolution of 0.53 arc seconds per pixel for a field of view of 27.1' by 27.1' as suggested by iTelescope.

Observations were obtained on May 3, 2016 with exposure lengths of 60 and 90 seconds for a Luminance filter and 120 and 150 seconds for a Hydrogen-alpha filter. Additional observations were made with a Luminance exposure of 60 seconds and H-alpha exposures of 120, 150, and 180 seconds on May 19, 2016. With two sets of images from different nights, errors caused by fluctuations in weather and atmospheric turbulence were mitigated, allowing for more precise measurements of separations and position angles. Despite this mitigation, telescope, and location, inclement weather during the observation windows may have caused some loss of precision.

MaxIm DL determined the World Coordinate System (WCS) positions for all of the images. MaxIm DL's PinPoint Astrometry function performed this process by matching the stars in the CCD images to the Fourth U.S. Naval Observatory CCD Astrograph Catalogue (UCAC4). The images taken with the H-alpha filter and 150 second exposures were not able to resolve the approximate location of the image in both observation sets, so they were not used.

Table 1 shows the astrometric calibration data for the ten successful images. The column heading #UCAC4 Stars explains how many stars matched up with the fourth U.S. Naval Observatory CCD Astrograph catalog out of all the stars in the plate. The camera angle refers to the angle formed from the horizon to the plate center, with the large difference in values indicating the different time of night between each observation set. Focal length shows the magnification and viewing field, which can vary depending on atmospheric effects, while plate scale indicates the "resolving power" of each plate capture.

With ten out of the fourteen images resolved, separation and position angle of the double star system was determined using Mirametrics Mira Pro x64. The Distance and Angle Function determined the separation between and the position angle from the first star's centroid to the second star's centroid. The function's Sample Radius was set to 15 pixels to allow for a large

Table 1: MaxIm DL astrometric calibration data.

Date	Filter	#UCAC4 Stars	Image Center's RA/DEC	Camera Angle	Focal Length	Pixel Scale
5/3/2016	Luminance	193 of 1017	RA 15h 48m 09.3s, Dec +01° 34' 16.4"	+169° 29.9' (R)	4531.0 mm	0.54628"/Pixel
5/3/2016	Luminance	157 of 931	RA 15h 48m 09.3s, Dec +01° 34' 14.8"	+169° 30.0' (R)	4531.2 mm	0.54625"/Pixel
5/3/2016	Luminance	152 of 1074	RA 15h 48m 09.4s, Dec +01° 34' 13.5"	+169° 29.8' (R)	4531.0 mm	0.54628"/Pixel
5/3/2016	Luminance	159 of 1088	RA 15h 48m 09.4s, Dec +01° 34' 11.7"	+169° 30.1' (R)	4530.8 mm	0.54630"/Pixel
5/3/2016	H-alpha	68 of 209	RA 15h 48m 09.5s, Dec +01° 34' 09.1"	+169° 30.2' (R)	4532.6 mm	0.54608"/Pixel
5/3/2016	H-alpha	76 of 225	RA 15h 48m 09.4s, Dec +01° 34' 07.4"	+169° 29.2' (R)	4530.7 mm	0.54631"/Pixel
5/19/2016	Luminance	235 of 688	RA 15h 48m 09.4s, Dec +01° 34' 17.2"	+180° 07.4' (R)	4531.4 mm	0.54623”/Pixel
5/19/2016	H-alpha	48 of 193	RA 15h 48m 09.4s, Dec +01° 34' 15.4"	+180° 05.2' (R)	4530.3 mm	0.54636"/Pixel
5/19/2016	H-alpha	66 of 268	RA 15h 48m 09.4s, Dec +01° 34' 13.3"	+180° 05.2' (R)	4530.5 mm	0.54634"/Pixel
5/19/2016	H-alpha	50 of 284	RA 15h 48m 09.5s, Dec +01° 34' 13.5"	+180° 07.5' (R)	4538.4 mm	0.54539"/Pixel

Astrometric Measurements of WDS 15482+0134 EIS 1AB

Table 2: New observations performed by team, with overall means, standard deviations, and standard errors.

Date of Observation	Position Angle (°)	Separation (")
2016.336	352.17	17.493
2016.336	352.41	17.580
2016.336	352.29	17.447
2016.336	352.31	17.477
2016.336	352.43	17.672
2016.336	352.46	17.638
2016.380	352.27	17.250
2016.380	352.38	17.572
2016.380	352.32	17.499
2016.380	352.51	17.361
Mean	352.36	17.50
Standard Deviation	0.11	0.16
Standard Error	0.0335	0.0497

enough circumference of the tool annulus to properly locate each star's centroid. Excel was then used to compile the data retrieved from Mira Pro x64 and to derive the standard deviations and standard errors of mean of the separation and position angle.

Results

Table 2 shows the observational results from one set of six images, taken on May 3rd, 2016, and the second set of four images, taken on May 19th. In addition, Table 2 shows the overall means (also shown in Table 3), the standard deviations, and standard errors for position angle and separation. Table 3 lists the relevant historical data from the WDS catalog, as well as the latest set of new mean observations taken by the team, showing comparisons between the two sets of data.

Discussion

The deviation of our measurements could have been produced by the possible overexposure induced by the long exposure time, listed in Table 3. This was mitigated by limiting the centroid sample values in Mira Pro. However, many of the plates were overexposed, which may have led to systemic saturation, perhaps skewing the results.

As can be seen from Table 2, our position angle agrees well with the historical observations at 2000.327, and 2000.430, holding to a difference of 0.08° to 0.24° (less than 2 standard deviations), and agrees moderately with 1950.542 at 1.24° difference, but disagrees with the observation on 2006.301, the most recent, by 4.26° (close to 40 standard deviations), suggesting that this most recent observation may be an outlier.

The mean separation agrees somewhat less well with historical observations, whose values stay between a minimum of 17.83" (2000.327) and maximum of 17.90" (2000.430). Our listed separation differs from the historical range by 2.3 standard deviations, with a mean value of 17.50", around 2 standard deviations from all historical observations. The possible errors in finding the centroid due to overexposure may be responsible for this difference. Of note, however, is that the longer exposure times (potentially more saturated) tended to agree better with historical observations than did the normal exposures.

Conclusion

The Cuesta/Cal Poly team met all of our observational goals in this report by ordering observations from iTelescope and running analysis on the results. The team learned how to use Maxim DL and Mira Pro to analyze position angles and separations, how to resolve the plate scale, and how to go about preparing the data acquired for analysis and publication, all essential parts of the observation process. Doing all this allowed the team to add another data point on the observations of WDS 15482+0134 EIS 1AB, completing our primary goal of contributing to the WDS astronomical catalog.

Table 3: Historical data on double star system, courtesy WDS star catalog

Date of Observation	Position Angle (°)	Difference (°)	Separation (")	Difference (")	Observation Source
2016.380	352.36	-	17.50	-	***New***
1950.542	353.60	+1.24	17.85	+.35	Eisenbeiss et al. 2007
2000.327	352.42	+.06	17.83	+.33	Eisenbeiss et al. 2007
2000.430	352.60	+.24	17.90	+.40	Hartkopf et al. 2013
2006.301	356.62	+4.26	17.85	+.35	Eisenbeiss et al. 2007

Acknowledgements

This research has made use of the Washington Double Star Catalog maintained by the U.S. Naval Observatory. The students thank Pat and Grady Boyce and the Boyce Research Initiatives Educational Foundation for funding the observations as well as providing valuable resources and instruction to help our research. Lastly, the team thanks iTelescope for developing a network of easily accessed telescopes for projects like this one.

References

Eisenbeiss, T., Seifahrt, A., Mugrauer, M., Schmidt, T.O.B., Neuhauser, R.,and Roell, T., 2007, *AN*, **328**, 521.

Hartkopf, W.I., Mason, B.D., Finch, C.T., Zacharias, N., Wycoff, G.L., and Hsu, D., 2013, *AJ*, **146**, 76.

Genet, R., 2010, "An 18 inch Direct Drive Alt-Az Telescope", *The Alt-Az Initiative*, Russ Genet et al. editors, Santa Margarita. CA: Collins Foundation Press.

Rowe, D., 2010, "Corrected Dall Kirkham 700 mm Nasmyth-focus Telescope", *The Alt-Az Initiative*, Russ Genet et al. editors, Santa Margarita. CA: Collins Foundation Press.

Mason, B. and Hartkopf, W. The Washington Double Star Catalog, March 2015. Astrometry Department, U.S. Naval Observatory. http://ad.usno.navy.mil/wds/wds.html.

The Southern Double Stars of Carl Rümker I: History, Identification, Accuracy

Roderick R. Letchford,[1] Graeme L. White,[2] Allan D. Ernest[3]

1. Vianney College Seminary, Wagga Wagga NSW, Australia, rodvianney@yahoo.com.au
2. Astrophysics Group, Computational Engineering and Science Research Centre, University of Southern Queensland, Toowoomba, Australia QLD 4350, graemewhiteau@gmail.com
3. Charles Sturt University, Wagga Wagga NSW, Australia, aernest@csu.edu.au

Abstract: The second catalog of southern double stars was published by Carl Rümker 1832. We describe this catalog, obtain modern nomenclature and data and estimate the accuracy of his positions for the primary components. We have shown the equinox and epoch to be B1827.0. Of the 28 pairs, 27 could be identified. RMK 23 is RMK 22 and RMK 24 could not be identified. Five pairs observed by Rümker are credited to co-worker Dunlop (DUN) in the WDS. There are two typographical errors. We tentatively identify RMK 28 with COO 261. We have shown the positional data in the 1832 catalog to be accurate and we present a modern/revised version of Rümker's catalog.

Introduction

The finding, cataloging, and astrometric study of double stars dominated the astronomy of the 19th century. In the southern sky, the pioneering double stars work of Sir John Herschel (JH) in the 1830-40s is recognized for its accuracy and completeness.

However, some two decades prior to the work of JH, a small but well equipped privately owned observatory was established in the fledgling British Colony of New South Wales by Sir Thomas Makdougall Brisbane, the 6th Governor of the Colony. For about a decade, the Parramatta Observatory reigned supreme in the southern hemisphere, systematically exploring for the first time the deep southern skies.

The Parramatta Observatory was constructed by Sir Thomas Brisbane, and staffed by two astronomers, Carl Rümker (Figure 1) and James Dunlop. From Parramatta came dedicated catalogs of stars (Richardson, 1835), double stars (Dunlop, 1829) and non-stellar objects (Dunlop, 1828). This paper follows the work of one of the first of the double star catalogs, that of Rümker (Rümker, 1832).

Figure 1: Carl Rümker, from Wikipedia (artist and date unknown)

Biography

Carl Rümker (Figure 1) was born 1788 May 18 in Burg Stargard, Germany, and graduated as a Master-Builder in 1807. In 1808 he was teaching mathematics in Hamburg and from 1809 to 1811 he was a midshipman for the British East India Company, entering the

Merchant Navy in 1811. After being discharged in 1813 he was walking in London when he was suddenly pressganged into the Royal Navy. This unfortunate event turned out to have profound positive repercussions.

The captain of the vessel to which Rümker was assigned, discovered that Rümker was well-educated and a teacher of mathematics and so put him in charge of teaching navigation with an officer's rank. While serving with the Royal Navy, Rümker became firm friends with Baron Franz Xavier von Zach, a Hungarian astronomer and, at the time, editor of the important journal *Correspondance astronomique*. Zach recognized Rümker's astronomical talent and encouraged him to pursue the science.

Discharged from the Royal Navy in 1819 at the end of the Napoleonic Wars, Rümker returned to Hamburg where he became a teacher at the School of Navigation. However, in 1821, through a series of contacts, Rümker applied for the position of astronomer to Thomas Brisbane (Figure 2), hoping to make a name for himself by publishing data from the almost totally unknown far southern sky. Thomas Brisbane, a well-respected and keen amateur astronomer, had just been appointed Governor of the penal colony of New South Wales and was looking to personally fund a professional astronomer to take charge of an observatory he intended to build at the Governor's house at Parramatta, then a very small settlement about 20 miles west of Sydney, and now part of greater Sydney. Sir Thomas also employed James Dunlop (Figure 3), a young mechanically-minded Scot, 5 years Rümker's junior, to maintain the observatory's equipment. James Dunlop was later to learn the art of astrometry from Brisbane and in fact published the first catalogue of southern double stars in 1829, beating Rümker's publication by 3 years.

After arriving in Parramatta and overseeing the construction of the observatory which stood behind Government House, Rümker began work on 1822 May 2, not long before his 34th birthday. The Parramatta Observatory (Figure 4) was Brisbane's own personal observatory entirely funded by him. His main goal was to publish a catalogue of stars in the southern hemisphere that were south of declination -30°; a region beyond the reach of the main European observatories, especially Greenwich.

This work was to follow Lacaille's *Coelum australe stelliferum* which had been published in 1763 but contained many known errors and was incomplete. A complete reduction of Lacaille's stars was only published in 1847 (Lacaille, Henderson, Baily, & Herschel, 1847). The so-called "Brisbane Catalogue" was published in 1835 (Richardson, 1835).

Figure 2: Thomas Brisbane, from Wikipedia (artist and date unknown)

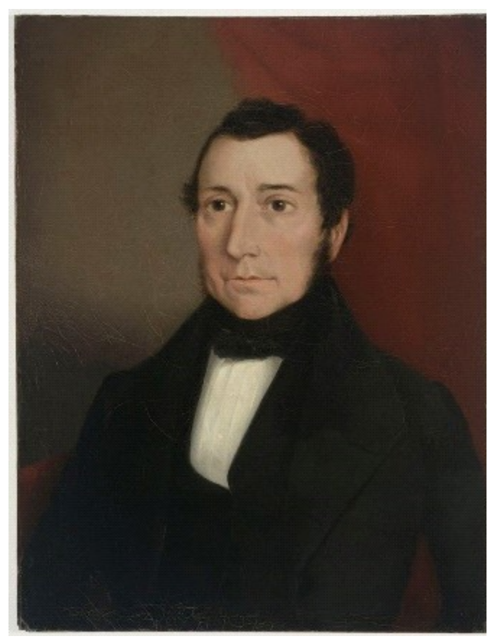

Figure 3: James Dunlop, from Wikipedia (by Joseph Blackler, c. 1843). Held by the Mitchell Library, State Library of New South Wales.

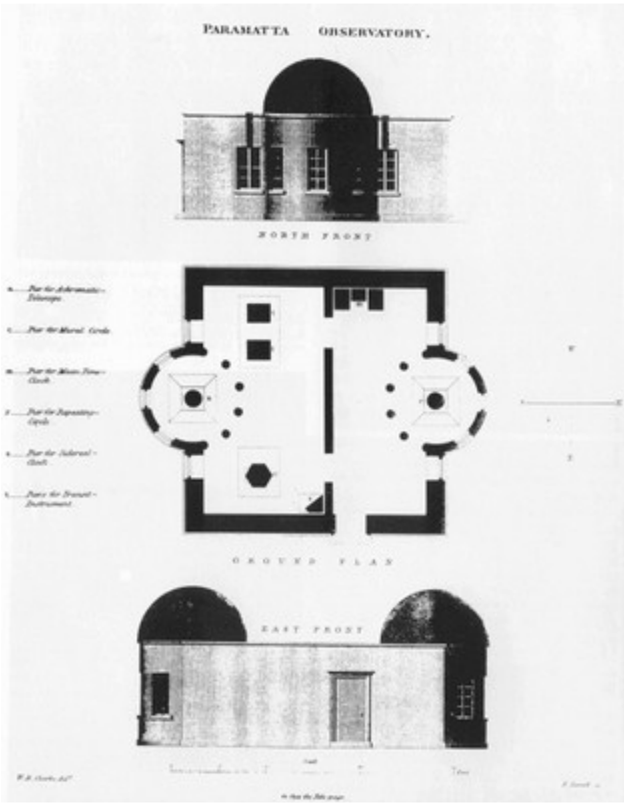

Figure 4: A drawing of the Parramatta Observatory by W. B. Clarke (1825). Published in Richardson (1835).

On the evening of 1822 June 2, Dunlop was the first in the world to sight the return of Encke's comet. Rümker had calculated its return position. Brisbane was justly proud of Rümker and as Governor granted him 1000 acres of land at Picton, south-west of Sydney.

However, for reasons which are not entirely clear, Rümker fell out with Brisbane and left Brisbane's employment a year later on 1823 June 16 and went to his farm. He continued some astronomical work there but was largely caught up in the demands of making a living.

Brisbane was re-called by the British Government and vacated his Governorship on 1825 Dec 1, to be replaced by Ralph Darling. Dunlop returned to England a few months later. The Parramatta Observatory moved into Government hands and Rümker returned to work at the observatory and on 1827 Dec 21 was appointed Government Astronomer.

Rümker was immensely proud and happy in this position and intended to stay. To that end he acquired another 3000 acres, tripling the size of his farm. He certainly had plenty of astronomy to do as well. At the time, there was no other southern observatory. In 1820 the English Board of Longitude had successfully petitioned for a permanent observatory in South Africa, but this did not begin observations until 1829 (Moore & Collins, 1977).

In 1828 Rümker made a requisition for more instruments and thought it best to go to England to supervise their procurement. While in England, he quarrelled with Sir James South, President of the Royal Astronomical Society, Fellow of the Royal Society and the King's own Astronomer; the upshot of which was his dismissal from the British Service on 1830 June 18.

His reputation was not entirely in tatters. At the beginning of 1831 he was appointed Director of the School of Navigation in Hamburg. On 1833 Oct 31 Rümker was appointed Director of Hamburg Observatory. He was awarded the Gold Medal for Arts and Science by the King of Hanover in 1850 and the Gold Medal of the (British) Royal Astronomical Society in 1854.

Rümker eventually married the Englishwoman Miss Mary Ann Crockford on 1848 Nov 24. He was 60 and she was 39 and the discoverer of Comet VI of 1847. Suffering from asthma and a disabling leg which he injured in a fall, he and his wife retired to Lisbon, Portugal. He died there on 1862 Dec 21 at the age of 74. His body is buried in the churchyard of the Anglican Church at Estrella, near Lisbon.

The Catalogue of Scientific Papers listed 231 papers published by Rümker (White, McLeod, & Morley, 1872; White & Morley, 1871). The standard biography on Rümker is still that of Bergman (1960) from which most of the above was adapted.

An Examination of Rümker's 1832 Catalogue of Double Stars

Accuracy of determination of stellar positions has steadily improved over the last few centuries and, in particular, since the advent of satellite-based astrometry (Høg, 2008, 2009, 2011).

Recent studies have retrospectively looked in detail at the accuracy of old star catalogs using HIPPARCOS astrometry (Ahn, 2012; Lequeux, 2014; Verbunt, 2004; Verbunt & van Gent, 2010a, 2010b, 2011, 2012). We acknowledge the work of Schlimmer's (2007) *Christian Mayer's Double Star Catalog of 1779* in looking at an old double star catalogue. Our intention here is to similarly look at the 1832 southern double star catalog of Carl Rümker.

Rümker's Southern Double Star Catalogue

The work we refer to here is the Catalogue of double stars found by Rümker at Parramatta as presented in the introduction to the 1832 *Preliminary Catalogue of Fixed Stars (Preliminary Catalogue of Fixed Stars:*

Intended for a Prospectus of a Catalogue of the Stars of the Southern Hemisphere Included Within the Tropic of Capricorn: Now Reducing from the Observations Made in the Observatory at Parramatta). This *Preliminary Catalogue of Fixed* Stars is one of Rümker's major works but curiously, it is not listed in *The Catalogue of Scientific Papers*.

Nor were double stars high on his list of priorities. The double star catalogue and its introduction covered just two (15 and 16) out of the 47 pages of the *Preliminary Catalogue of Fixed Stars*. As he stated: "I join here a list of double Star's (sic) extracted from my observations, which probably contain more of them." He did not attempt a systematic search for southern double stars, but merely noted them with the occasional measure whenever he came across one.

Rümker's double star catalogue is reproduced in Table 1, except for the first column (RMK) which has

Table 1: Rümker's 1832 Double Star Catalogue

RMK	Stellae Nomen	AR.	DEC	Diff AR. in arc.	Comes.	Diff. Declinat.	Comes ad
1		11° 27′	70° 27′				
2	ζ Phoenicis	15 16	56 10		praecedit		Austrum
3		63 56	63 41				
4		65 13	57 28	5.25″			
5		106 43	55 19				
6		109 03	52 00				
7	ε Piscis volant.	121 50	68 07		sequitur		Boream
8		123 09	62 13		sequitur		Boream
9	799 C. A.	130 15	58 06	13.5	sequitur		
10		138 56	69 04		sequitur		Boream
11	α Argus	145 42	64 16	12.0	sequitur		Austrum
12		147 53	68 24				
13	τ Argus	153 37	55 10		sequitur		Austrum
14	D Centauri	181 15	44 46		praeccedit		Austrum
15	α Crucis	184 16	62 08	12.3	sequitur	4.45″	Austrum
16	Θ Muscae	194 17	64 24				Austrum
17		200 08	62 10				
18		205 15	51 57	25.5	praecedit	5.0	Boream
19	Y Centauri	212 35	57 40	8.8	sequitur	10.0	Austrum
20		233 05	64 54		sequitur		Austrum
21	η Lupi	237 10	37 53	7.87	sequitur		Austrum
22		265 41	55 20				
23		265 44	60 20		sequitur		
24		285 16	57 29	0.0	praecedit		
25		300 15	57 30	10.5	praecedit	5.0	Boream
26		309 17	63 04	15.0	sequitur		
27	Θ Phoenicis	352 34	47 36				
28		354 32	61 30				

Explanation of Table 1: Rümker's 1832 Double Star Catalogue

Column 2: **Stellae Nomen**, name of star.

Column 3: **AR.**, right ascension in degrees (°) and min arc (').

Column 4: **DEC**, declination in degrees and min arc from the equator.

Column 5: **Diff AR**., difference in right ascension between the primary and secondary, in sec arc (").

Column 6: **Comes**., whether the secondary precedes (praecedit, praeccedit [sic]) or follows (sequitur) the primary.

Column 7: **Diff. Declinat**., difference in declination between the primary and secondary, in sec arc.

Column 8: **Comes ad**, whether the secondary is north (Boream) or south (Austrum) of the primary.

The Southern Double Stars of Carl Rümker I: History, Identification, Accuracy

been added to aid discussion and comparison.

In a modern context, this catalogue is deficient and/ or different in many ways. These include the fact the RA positions are given in degrees (rather than hours, minutes and seconds of time) and both the RA and the Declination positions are rounded off to a precision of min arc only. In addition, there is no stated Equinox or Epoch of the observations, and no computed separation (ρ) and Position angle (PA). There are no estimates of magnitude (on any color scale) given for any star.

Modern Assessment of the Rümker Catalogue

Of the 28 pairs listed in Rümker's double star catalogue, numbers 2 - 14, 16, 18, 20, 22, 25, and 26 have RMK as the discoverer code in the WDS.

The method of identification of the stars in modern catalogs is as follows.

1. Rümker's Equinox was first assumed to be B1825.0. This is assumed because Rümker worked at the Parramatta Observatory between 1822 and 1829, and because the Brisbane Catalogue is clearly identified as Equinox B1825.0.
2. The B1825.0 coordinates were processed to J2000.0 using an EXCEL custom function written for the purpose adopting the IAU 1976 equations (Lieske, Lederle, Fricke, & Morando, 1977), but without taking into account the, as yet, unknown proper motions. The IAU 1976 equations give smaller than 1" uncertainty over the time period.
3. Using ALADIN (Bonnarel et al., 2000), each J2000.0 position was examined using the DSS (Digitized Sky Survey from CDS) image.
4. The DSS image was overlaid with WDS, ASCC 2.5, UCAC4 and Gaia data. We preferred the use of the homogenized All-sky Compiled Catalogue of 2.5 million stars (Kharchenko, 2001). Four of Rümker's secondaries do not have UCAC4 numbers and there are still numerous lacunae in the current GaiaSource data and uncertain identifications (Collaboration, 2016). Cross-referencing of the ASCC 2.5, UCAC4 and Gaia data is given in Table 2.
5. The nearest double star was taken to be the A component intended by Rümker (except for RMK 23 and 24, see below).

The modern identification of Rümker's doubles are presented in Table 2.

In the WDS the discovery of RMK 1, 15, 17, 19, and 27 are attributed to co-worker James Dunlop, however as Dunlop also did not record the epoch of observation (nor Equinox) it is uncertain as to who made the initial discovery.

RMK 23 could not be identified by the above method. However, the *Southern Double Star Catalogue* (Innes, Dawson, & van den Bos, 1927) for RMK 22 (17^h 48.9^m at B1900.0) has the remark that RMK 23 is the same as RMK 22 "with error 5°" in declination. That is, Rümker's original declination should have been 55° 20'' and not 60° 20''. The small difference in RA of 3 min arc in the Rümker list can be accounted for by the real possibility that Rümker recorded the double stars on different days. Other typographical errors in Rümker's original catalogue were found during preparation of this paper (see below).

RMK 24 could not be identified at all. The J2000 position (precessed from B1825) is 19^h 15^m 50.6^s -57° 11' 47.4". The nearest WDS entry is 19116-5642 (HRG 130) at a distance of 46 min arc which we considered too far to be equated.

Rümker's original coordinates for RMK 28 precessed from, for example, B1827 forward to J2000 (without proper motion) yields a position of 23^h 47^m 30.96^s -60° 32' 21.3". At 75 sec arc the nearest WDS double is COO 361. If we precess COO 361 from J2000 back to B1827 using proper motion the coordinates are 23° 38^m 10.18^s -61° 28' 48.3" (from Table 3) or a separation of 1.2 min arc. From Figure 7 (the Histogram) we note that this is at the high end of separations, but less than some others (RMK 16 and 17) whose identity are accepted (see Table 3).

Estimation of the Equinox of Observations

Rümker did not record the Equinox for the Catalogue nor the epoch of each observation. However, we recovered the most likely Equinox via the following method.

With J2000.0 coordinates, and modern proper motion data, of the primaries as listed in ASCC 2.5 positions were found for a range of Equinoxes from B1821.0 to B1830.0.

The separation (in sec arc) at each Equinox between the Rümker coordinate and the processed coordinate was calculated.

By taking the average of each set of separations per Equinox, Figure 5 was obtained.

It is clear from Figure 5 that the Equinox with the lowest total separation is B1827.0. We therefore accept this to be the Equinox of the Rümker catalogue. This determination is supported - if not confirmed - by the fact that his Star Catalogue, also published in the *Preliminary Catalogue*, has a stated Equinox of "pro initio Anni 1827".

While undertaking the calculations for estimating the Equinox, we detected what we have taken to be two typographical errors in declination. The original

(Text continues on page 227)

The Southern Double Stars of Carl Rümker I: History, Identification, Accuracy

Table 2: Modern Identifications of Rümker's Southern Doubles

RMK	WDS	Disc. Code	ASCC 2.5	UCAC4	Gaia
1	00524-6930	DUN 2	2373287	103-000763	4691995687749952384
			2373289	103-000765	4691995996987597568
2	01084-5515	RMK 2 AB,C	2198437	174-001101	
			2198436	174-001098	4913847584861259392
3	04177-6315	RMK 3	2296521	134-003905	4676067715633387776
			2296522	134-003906	4676067715634544512
4	04242-5704	RMK 4	2202770	165-004328	4775347911905128064
			2202769	165-004326	4775347911905128192
5	07104-5536	RMK 5	2208862	173-010758	5490328643768957952
			2208857	173-010752	5490328643768958080
6	07204-5219	RMK 6	2114933	189-011558	5492026736399938560
			2114936	189-011559	5492026736399861888
7	08079-6837	RMK 7	2383172	107-017738	
			2383174	107-017740	5270986003994879744
8	08153-6255	RMK 8	2304832	136-013964	5277370356913491840
			2304833	136-013965	5277370352621451648
9	08451-5843	RMK 9 AB	2214637	157-017868	
			2214633	157-017864	
10	09179-6948	RMK 10	2386328	101-025487	5222647212228907136
			2386329	101-025489	5222650167166406656
11	09471-6504	RMK 11	2387890	125-024040	5249119019819706624
			2387893	125-024041	5249119019819706752
12	09551-6911	RMK 12	2388374	105-028729	5243135168304173440
			2388372	105-028727	5243135168305893504
13	10209-5603	RMK 13 AB	2227934	170-044959	
			2227939	170-044967	5354994808388487680
14	12140-4543	RMK 14	2048721	222-062225	6143569839228193536
			2048720		
15	12266-6306	DUN 252 AB	2333718	135-077813	
			2333721	135-077814	
16	13081-6518	RMK 16 AB	2401908	124-083590	
			2401910	124-083587	5858915762084797312
17	13321-6303	DUN 137	2340319	135-096113	5865249808055799936
			2340318	135-096111	5865249808055799168
18	13521-5249	RMK 18	2155481	186-097617	
			2155477	186-097609	6065984175603789440
19	14226-5828	DUN 159 AB	2260099	158-132657	
			2260102	158-132658	5891112108248454784
20	15479-6527	RMK 20 AB	2412907	123-149637	5825553383847202176
			2412908		5825553388138641024
21	16001-3824	RMK 21 AB	1873533	259-087966	
			1873535	259-087970	5998066826966118656
22 & 23	17572-5523	RMK 22	2279415	174-191989	
			2279416		
25	20149-5659	RMK 25	2285617	166-210020	6468703708258513152
			2285618	166-210021	6468703708258513024
26	20516-6226	RMK 26	2368303	138-190599	
			2368304		
27	23395-4638	DUN 251	2100751	217-192156	6525488226793694720
			2100750	217-192155	6525488226794240256
28	23476-6031	COO 261	2372217	148-236277	6488336862761979392
			2372219	148-236276	6488336862762255232

The Southern Double Stars of Carl Rümker I: History, Identification, Accuracy

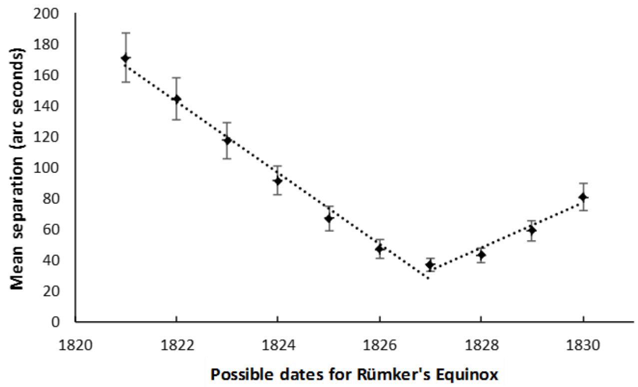

Figure 5: Finding Rümker's Equinox.

Table 3: Accuracy of Primary Star Location. All coordinates are Equinox and Epoch B1827.0.

RMK	RMK RA (h:m:s)	RMK DE (d:m)	ASCC 2.5 RA (h:m:s)	ASCC 2.5 DE (d:m:s)	ΔRA RMK-ASCC (min arc)	ΔDE RMK-ASCC (min arc)	Offset (min arc)
1	00 45 48	-70 27	00 45 47.56	-70 26 30.7	0.0	-0.5	0.5
2	01 01 04	-56 10	01 01 05.45	-56 10 20.8	0.2	0.3	0.4
3	04 15 44	-63 41	04 15 45.33	-63 40 36.0	0.1	-0.4	0.4
4	04 20 52	-57 28	04 20 50.42	-57 27 55.2	-0.2	-0.1	0.2
5	07 06 52	-55 19	07 06 53.63	-55 18 10.6	0.2	-0.8	0.9
6	07 16 12	-52 00	07 16 11.01	-51 59 43.3	-0.2	-0.3	0.3
7	08 07 20	-68 07	08 07 19.90	-68 06 33.0	0.0	-0.4	0.5
8	08 12 36	-62 23	08 12 37.75	-62 23 00.5	0.2	0.0	0.2
9	08 41 00	-58 06	08 40 58.78	-58 05 43.0	-0.2	-0.3	0.3
10	09 15 44	-69 04	09 15 46.35	-69 04 31.6	0.2	0.5	0.6
11	09 42 48	-64 16	09 42 46.28	-64 16 16.5	-0.2	0.3	0.3
12	09 51 32	-68 23	09 51 28.82	-68 22 13.5	-0.3	-0.8	0.8
13	10 14 28	-55 10	10 14 29.32	-55 10 27.1	0.2	0.5	0.5
14	12 05 00	-44 46	12 05 01.86	-44 45 41.5	0.3	-0.3	0.5
15	12 17 04	-62 08	12 17 02.65	-62 08 21.6	-0.2	0.4	0.4
16	12 57 08	-64 24	12 57 02.80	-64 22 42.1	-0.6	-1.3	1.4
17	13 20 32	-62 10	13 20 28.37	-62 08 44.8	-0.4	-1.3	1.3
18	13 41 00	-51 57	13 40 59.40	-51 56 56.2	-0.1	-0.1	0.1
19	14 10 20	-57 40	14 10 18.34	-57 39 46.5	-0.2	-0.2	0.3
20	15 32 20	-64 54	15 32 12.75	-64 53 17.8	-0.8	-0.7	1.0
21	15 48 40	-37 53	15 48 40.87	-37 53 36.5	0.2	0.6	0.6
22 & 23	17 42 44	-55 20	17 42 47.31	-55 20 16.5	0.5	0.3	0.5
25	20 00 60	-57 30	20 00 59.03	-57 28 57.2	-0.1	-1.0	1.1
26	20 37 08	-63 04	20 37 06.45	-63 03 36.9	-0.2	-0.4	0.4
27	23 30 16	-47 36	23 30 08.50	-47 35 50.5	-1.3	-0.2	1.3
28	23 38 08	-61 30	23 38 10.18	-61 28 48.3	0.3	-1.2	1.2

1. https://ma.as/258792.
2. https://ma.as/258735.

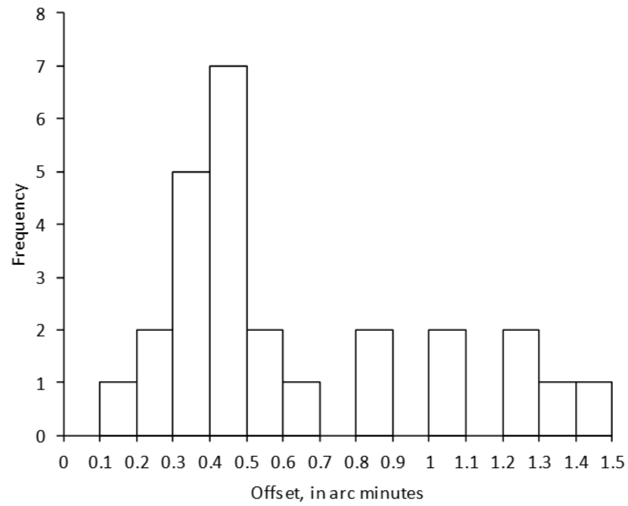

Figure 6: Histogram of Offset (column 6 of Table 3)

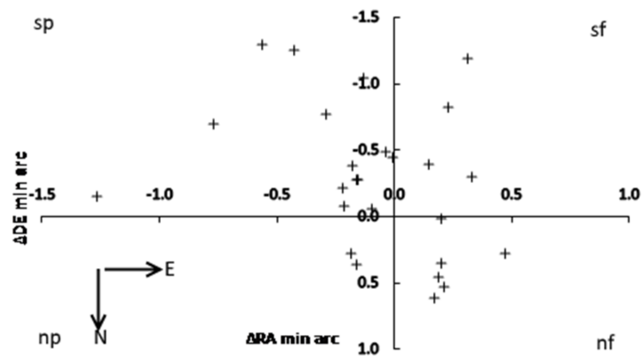

Figure 7: Target Diagram (Columns 6 & 7 of Table 3). ASCC 2.5 positions are at (0,0), and the relative respective Rümker positions are indicated by a '+'.

Rümker declinations for RMK 8 and 12 were 62° 13' and 68° 24' respectively. These yielded a ΔDE of +10.0 and -1.8 min arc respectively. Since these represent a significant departure from other ΔDE, we suggest that RMK 8 was 10' too far north and RMK 12 was 1' too far south in the original publication.

The Revised Rümker Double Star Catalogue

Armed with the assumption that Rümker's epochs were also B1827.0, we present here a revised Rümker Double Star Catalogue, based on modern astrometric data, with offset estimations for each double (Table 3).

Accuracy of Rümker's Original observations

We now look with retrospective vision at the accuracy of the Rümker catalogue of double stars using the results in Table 3; our intention being to ascertain the observational precision of this work.

Unfortunately, Rümker did not record the instrument he used. However, the instruments listed as being available at Parramatta were a 3.75-inch transit refractor made by Edward Troughton of London[1], and a 46-inch focal length, 3.25-inch aperture equatorial mounted refractor telescope made by Banks of London, fitted with a wire micrometer[2].

Within reason, it is possible to assume that the discovery of the pairs was by Rümker whilst he was using the transit instrument for the compilation of the star catalogue (the *Preliminary Catalogue of Fixed Stars)* where he noted the pairs for later observation, perhaps with the equatorial.

We note that both telescopes are very small with respect even to modern day amateur telescopes, and the quality of the results must be considered in that context.

Figures 6 and 7 are the distribution of the measured positions (by Rümker) relative to modern positions as precessed to B1827 and given in Table 3. There is a clear concentration of data points within ~0.5 min arc, with 3 outliers in the south preceding quadrant. The rounded-off precision of Rümker's positions to the nearest min arc accounts for most, if not all, of the spread in the positional accuracy.

We apply two measures to this data. In RA, we compute the standard deviation of the spread of these positional differences as 0.37 min arc, and the bias in the two data sets as -0.09 ± 0.07 min arc (being the SEM of the data set) and the sense being Rümker minus precessed modern data. Similarly, in declination, we have found that the standard deviation of the differences is 0.56 min arc, and the bias to be -0.28 ± 0.11 min arc. Rümker being to the north. These measures are well within the accuracy inferred in the Dunlop catalogue, as what we would expect from an observation set of this period using the instruments they had.

A Modern and Revised Rümker Catalog

Table 4 presents Rümker's southern double stars with associated modern data, which has been adopted from the Simbad data set utilizing the Aladin web interface. All positions are from the ASCC 2.5 catalog. Columns 6 and 7 were calculated from ASCC 2.5 data. The format is that of the WDS. Notes on individual pairs are

Text continues on page 230

1. https://ma.as/258792
2. https://ma.as/258735

Table 4: Rümker's Southern Double Stars with Modern Data. All at Equinox J2000.0 and Epoch J2000.0

RMK	RA	DE	WDS	Disc	PA	Sep	Vmag1	Vmag2	SpType1	SpType2	pmRA1	pmDE1	pmRA2	pmDE2
	h:m:s	d:m:s			(deg)	(as)					mas/yr	mas/yr	mas/yr	mas/yr
1	00 52 24.520	-69 30 13.56	00524-6930	DUN 2	81.4	20.44	6.646	7.317	F7IV/V	G1V	3.78	-69.94	1.97	-74.58
2	01 08 23.083	-55 14 44.75	01084-5515	RMK 2AB,C	241.4	6.61	3.977	8.668	B6V + B0V	F3:V	22.46	28.56	21.09	29.71
3	04 17 40.272	-63 15 19.49	04177-6315	RMK 3	3.2	4.26	6.012	7.651	B9 III/IV	B 9 V	5.46	31.62	8.02	46.2
4	04 24 12.208	-57 04 16.81	04242-5704	RMK 4	246.5	5.49	6.638	7.171	G4V+...	G6 V	-104.04	-73.19	-96.38	-60.77
5	07 10 24.466	-55 35 15.77	07104-5536	RMK 5	225.8	6.95	7.59	7.725	G8/K0III+G/K		-1.83	-9.14	-0.4	-9.48
6	07 20 21.416	-52 18 41.59	07204-5219	RMK 6	26.1	9.22	5.965	6.534	F0-2 IV-V	F9Ve+K3V+	-43.88	135.71	-29.69	135.69
7	08 07 55.795	-68 37 01.42	08079-6837	RMK 7	24.2	6.04	4.39	7.296	B6IV		-28.6	30.52	-29.78	30.51
8	08 15 15.920	-62 54 56.31	08153-6255	RMK 8	68.6	4.02	5.222	7.563	A2 V		-26.75	-10.64	-26.86	-10.93
9	08 45 05.545	-58 43 27.55	08451-5843	RMK 9AB	292.2	4.15	6.722	6.94	B7III		-4.73	0.67	-5.23	0.66
10	09 17 54.988	-69 48 16.82	09179-6948	RMK 10	18.5	10.40	8.142	8.515	A0V:	A0	-8.8	6.78	-11.85	7.55
11	09 47 06.122	-65 04 19.22	09471-6504	RMK 11	127.9	5.03	2.993	5.98	A8 Ib	F0	-11.31	5.05	-11.51	4.96
12	09 55 05.606	-69 11 20.31	09551-6911	RMK 12	213.0	9.21	6.844	8.819	B9V		-67.12	30.51	-67.51	31.28
13	10 20 54.796	-56 02 35.59	10209-5603	RMK 13AB	101.8	7.19	4.506	7.21	B3III		-18.65	1.42	-18.12	1.47
14	12 14 02.698	-45 43 26.11	12140-4543	RMK 14	243.1	2.85	5.565	6.782	K3III		-34.2	4.82	-42.08	3.97
15	12 26 35.896	-63 05 56.72	12266-6306	DUN 252AB	112.8	4.02	1.039	1.57	B0.5IV	B1 V	-35.56	-13.9	-42.52	-7.67
16	13 08 07.153	-65 18 21.64	13081-6518	RMK 16AB	187.0	5.38	5.649	7.552	WC6 + O9.5I	O9.5 II	-4.42	2.53	-5.34	-2.25
17	13 32 03.910	-63 02 30.82	13321-6303	DUN 137	357.7	15.98	7.478	8.484	B0.5III:		-3.8	-1.87	-3.16	-4.11
18	13 52 04.862	-52 48 41.52	13521-5249	RMK 18	288.7	18.17	5.25	7.469	B9Vn	B8V	-39.13	-28.37	-46	-26.69
19	14 22 37.070	-58 27 32.70	14226-5828	DUN 159AB	157.8	9.42	4.914	7.151	G8/K1 + F/G		-46.45	31.37	-32.04	-3.66
20	15 47 53.058	-65 26 32.15	15479-6527	RMK 20AB	146.9	1.84	5.861	6.395	A5 III-IV	F1IV	-26.65	-30.53	-26.42	-31.37
21	16 00 07.328	-38 23 48.14	16001-3824	RMK 21AB	19.3	14.84	3.414	7.467	B2.5IV	A3 Vn	-16.44	-26.18	-26.2	-29.52
22, 23	17 57 13.209	-55 22 52.52	17572-5523	RMK 22	94.4	2.46	6.755	7.894	K0III+...		-8.38	-27.75	-6.69	-25.86
25	20 14 56.171	-56 58 35.28	20149-5659	RMK 25	28.7	7.16	7.894	7.971	F6/8 + F		37.31	-90.2	35.41	-97.76
26	20 51 38.507	-62 25 45.61	20516-6226	RMK 26	82.3	2.45	6.173	6.518	A2 Vn	A2 Vn	82.51	-49.27	82.55	-44.88
27	23 39 27.947	-46 38 16.08	23395-4638	DUN 251	276.3	3.92	6.291	7.236	A8V+...		25.45	39.95	23.76	37.63
28	23 47 34.208	-60 31 09.89	23476-6031	COO 261	279.9	5.88	9.142	8.812	K0	K1/2 III	30.98	-1.17	16.2	3.79

The Southern Double Stars of Carl Rümker I: History, Identification, Accuracy

Table 4 Notes:

RMK 1	λ^1 Tuc.	λ^1 Tuc is the double (Vmag (m_v) ~ 6.7 + 7.3). λ Tuc a brighter single star separated from λ^1 by ~13.6'. Norton & Ridpath note for λ^1: "Optical; little change".
RMK 2	ζ Phe.	Components A and B are a detached Algol-type eclipsing binary. WDS gives PA = 120° and ρ = 0.6". Rümker pair is AB-C. Component C is a high proper-motion star.
RMK 3	θ Ret.	
RMK 4	HD 28255.	X-ray source ~20" from component A.
RMK 5	HD 55598.	X-ray source ~11" from component A.
RMK 6	HD 57852.	Component A. Spectroscopic binary.
RMK 7	ε Vol.	Component A is spectroscopic binary. Norton & Ridpath note "Fixed".
RMK 8	HD 69863.	X-ray source 18" from component A.
RMK 9	HD 75086.	Two 10th magnitude companion stars at ~1' make pretty field. WDS give stars A–D.
RMK 10	HD 80807.	X-ray source 16" from component A.
RMK 11	υ Car.	Excellent infrared source position coincident. Norton & Ridpath note as "Fixed".
RMK 12	HD 86388.	
RMK 13	J Vel.	Be star. Norton & Ridpath note "Little change".
RMK 14	D Cen.	Norton & Ridpath note "Fixed".
RMK 15	α Cru.	Norton & Ridpath note "little change. Very easy".
RMK 16	θ Mus.	Component A is a Wolf-Rayet star. Spectroscopic binary. Norton & Ridpath note as "Fixed".
RMK 17	HD 117460.	
RMK 18	HD 120642.	Component B is HD 120641.
RMK 19	HR 5371.	X-ray source ~15" from component A. Infrared source close to component A.
RMK 20	HD 140483.	Component B is HD 140484.
RMK 21	η Lup.	Norton & Ridpath note as "Fixed".
RMK 22 & 23	HD 163028.	Also RMK 23 (see text).
RMK 25	HD 191869.	Component A is a spectroscopic binary. X-ray source at 5.2" from component Aa.
RMK 26	HD 198160.	Component B is HD 198161. High proper-motion pair.
RMK 27	θ Phe.	Norton & Ridpath note as "Slow binary, little change"
RMK 28	HD 223186.	Listed in the WDS as C00 261.

The Southern Double Stars of Carl Rümker I: History, Identification, Accuracy

(Continued from page 227)

given below.

Because the Rümker catalogue was only the second list of southern hemisphere doubles, it includes many of the brighter and more interesting southern doubles. The combined visual magnitudes range from (Vmag) 0.5 to 8.2, and the faintest *Comes* is about 9.1 (RMK 28). The separations range from ~1.8 sec arc to ~20.4 sec arc (assuming little movement since discovery). These values are impressive considering the instruments available to Rümker at Parramatta.

Of the 285 "Interesting Objects - Double stars" in total in *Norton's Star Atlas and Reference Handbook* (Norton & Ridpath, 1998), 10 of Rümker's 27 are to be found. Six out of 28 (21%) are noted for the southern polar map (Maps 15 and 16) alone.

Notes on Individual Pairs in Table 4

There are 26 binary pairs in Table 4. Of these, 6 are associated with X-ray sources and 2 are associated with infrared sources. There are 3 spectroscopic binaries, one Algol-type eclipsing variable and another non-specific variable. θ Muscae (RMK 16) is a complicated system containing a spectroscopic binary, one component of which is a most spectacular Wolf-Rayet star, and J Velorum (RMK 13) is a Be type star. The high X-ray content (23%) is in keeping with the recognized association between visual binaries and X-ray sources (see, for example, Makarov & Eggleton, 2009; Makarov, 2002, 2003).

Conclusion

Of the 28 pairs in Rümker's original catalogue of double stars of 1832, 27 could be identified. RMK 23 is the same as RMK 22 and only RMK 24 could not be identified. We identify 5 pairs observed by Rümker that have the discoverer code DUN (for James Dunlop) in the WDS, and two with typographical errors in the minutes' column of Rümker's declination. We tentatively identify RMK 28 with COO 261.

Rümker did not specify an equinox or epoch of observation, however, we have shown that B1827.0 is appropriate.

We have shown the positional data in the original catalogue to be accurate to within the precision allowed in the original observations, and we present tables of modern identifications of pairs and a modern/revised version of Rümker's Double star catalogue.

Acknowledgements

This research has made use of Aladin sky atlas developed at CDS, Strasbourg Observatory, France, and the Washington Double Star Catalog maintained at the U. S. Naval Observatory

References

Ahn, S.-H. (2012). Identification of stars in a J1744.0 star catalogue Yixiangkaocheng. *Monthly Notices of the Royal Astronomical Society*, *422*(2), 913–925. Retrieved from http://adsabs.harvard.edu/abs/2012MNRAS.422..913A

Bergman, G. F. J. (1960). "Christian Carl Ludwig Rümker (1788-1862), Australia's First Government Astronomer." *Journal of the Royal Australian Historical Society*, *46*(5), 247–289. Journal Article. Retrieved from http://www.rahs.org.au/publications/rahs-journal/

Bonnarel, F., Fernique, P., Bienaymé, O., Egret, D., Genova, F., Louys, M., … Bartlett, J. G. (2000). The ALADIN interactive sky atlas. *Astronomy and Astrophysics Supplement Series*, *143*(1), 33–40. Retrieved from http://adsabs.harvard.edu/abs/2000A%26AS..143...33B

Collaboration, G. (2016). VizieR Online Data Catalog: Gaia DR1 (Gaia Collaboration, 2016). *VizieR On-Line Data Catalog: I/337. Originally Published in: Astron. Astrophys., in Prep (2016)*, *1337*. Retrieved from http://cdsads.u-strasbg.fr/cgi-bin/nph-bib_query?2016yCat.1337....0G

Dunlop, J. (1828). A Catalogue of Nebulae and Clusters of Stars in the Southern Hemisphere, Observed at Paramatta in New South Wales. *Royal Society of London Philosophical Transactions (Series I)*, *118* (1), 113–151. Journal Article. Retrieved from http://adsabs.harvard.edu/abs/1828RSPT..118..113D

Dunlop, J. (1829). Approximate Places of Double Stars in the Southern Hemisphere, observed at Paramatta in New South Wales. *Memoirs of the Royal Astronomical Society*, *3*(1), 257–275. Journal Article. Retrieved from http://adsabs.harvard.edu/abs/1827MmRAS...3..267D

Høg, E. (2008). Astrometric accuracy during the past 2000 years. *Contribution to the History of Astrometry*, *7*, 1–20. Journal Article. Retrieved from http://astro.ku.dk/~erik/Accuracy.pdf

Høg, E. (2009). 400 years of astrometry: from Tycho Brahe to Hipparcos. *Experimental Astronomy*, *25*(1–3, August), 225–240. Journal Article. Retrieved from http://adsabs.harvard.edu/abs/2009ExA....25..225H

Høg, E. (2011). Astrometry history: Roemer and Gaia. *ArXiv E-Prints*. Electronic Article. Retrieved from http://adsabs.harvard.edu/abs/2011arXiv1105.0879H

Innes, R. T. A., Dawson, B. H., & van den Bos, W. H. (1927). *Southern double star catalogue -19 deg to -90 deg*. Book, Johannesburg, S.A.: Union Observatory. Retrieved from http://adsabs.harvard.edu/abs/1927sdsc.book.....I

Kharchenko, N. V. (2001). All-sky compiled catalogue of 2.5 million stars. *Kinematika I Fizika Nebesnykh Tel*, *17*, 409–423. Retrieved from http://cdsads.u-strasbg.fr/abs/2001KFNT...17..409K

Lacaille, N. L., Henderson, T., Baily, F., & Herschel, J. F. W. (1847). *A catalogue of 9766 stars in the southern hemisphere, for the beginning of the year 1750, from the observations of the Abbe de Lacaille made at the Cape of Good Hope in the years 1751 and 1752*. (N. L. de Lacaille, Ed.), *London, R. and J. E. Taylor, 1847.* (Vol. 1...). Book. Retrieved from https://books.google.cat/books?id=hbEvAQAAMAAJ

Lequeux, J. (2014). From Flamsteed to Piazzi and Lalande: new standards in 18th century astrometry. *Astronomy & Astrophysics*, *567*, A26. Retrieved from http://adsabs.harvard.edu/abs/2014A%26A...567A..26L

Lieske, J. H., Lederle, T., Fricke, W., & Morando, B. (1977). Expressions for the precession quantities based upon the IAU /1976/ system of astronomical constants. *Astronomy and Astrophysics*, *58*, 1–16. Journal Article. Retrieved from http://adsabs.harvard.edu/abs/1977A&A....58....1L

Makarov, V. V. (2002). The Rate of Visual Binaries among the Brightest X-Ray Stars. *The Astrophysical Journal*, *576*(1), L61–L64. http://doi.org/10.1086/343088

Makarov, V. V. (2003). The 100 Brightest X-Ray Stars within 50 Parsecs of the Sun. *The Astronomical Journal*, *126*(4), 1996–2008. http://doi.org/10.1086/378164

Makarov, V. V., & Eggleton, P. P. (2009). The Origin of Bright X-Ray Sources in Multiple Stars. *The Astrophysical Journal*, *703*(2), 1760–1765. http://doi.org/10.1088/0004-637X/703/2/1760

Moore, P., & Collins, P. (1977). *The astronomy of Southern Africa*. Book, London: Robert Hale & Co. Retrieved from https://books.google.cat/books?id=H3LvAAAAMAAJ

Norton, A. P., & Ridpath, I. (1998). *Norton's star atlas and reference handbook (epoch 2000.0)*. *Norton's star atlas and reference handbook (epoch 2000.0)* (19th ed.). London: Longman. Retrieved from http://adsabs.harvard.edu/abs/1998nass.book.....N

Richardson, W. (1835). *A Catalogue of 7385 Stars : Chiefly in the Southern Hemisphere, Prepared from Observations Made in the Years 1822, 1823, 1824, 1825, and 1826, at the Observatory at Paramatta, New South Wales, Founded by Lieutenant General Sir Thomas Makdougall Brisbane*. Book, London: William Clowes and Sons. Retrieved from http://adsabs.harvard.edu/abs/1835acos.book.....R

Rümker, C. (1832). *Preliminary Catalogue of Fixed Stars: Intended for a Prospectus of a Catalogue of the Stars of the Southern Hemisphere Included Within the Tropic of Capricorn : Now Reducing from the Observations Made in the Observatory at Paramatta*. Book, Hamburg: Perthes and Besser. Retrieved from http://adsabs.harvard.edu/abs/1833AN.....10..377R

Schlimmer, J. S. (2007). Christian Mayer's Double Star Catalog of 1779. *Journal of Double Star Observations*, *3*(4, Fall), 151–158. Journal Article. Retrieved from http://adsabs.harvard.edu/abs/2007JDSO....3..151S

Verbunt, F. (2004). Interferometry and the study of binaries. *ArXiv Astrophysics E-Prints*. Electronic Article. Retrieved from http://adsabs.harvard.edu/abs/2004astro.ph.12522V

Verbunt, F., & van Gent, R. H. (2010a). The star catalogue of Hevelius. Machine-readable version and comparison with the modern Hipparcos Catalogue. *Astronomy and Astrophysics*, *516*(A29), 1–22. Journal Article. Retrieved from http://adsabs.harvard.edu/abs/2010A&A...516A..29V

Verbunt, F., & van Gent, R. H. (2010b). Three editions of the star catalogue of Tycho Brahe. Machine-readable versions and comparison with the modern Hipparcos Catalogue. *Astronomy and Astrophysics*, *516*(A28), 1–24. Journal Article. Retrieved from http://adsabs.harvard.edu/abs/2010A&A...516A..28V

Verbunt, F., & van Gent, R. H. (2011). Early Star Catalogues of the southern sky: De Houtman, Kepler (second and third classes), and Halley. *Astronomy and Astrophysics*, *530*(A93), 1–26.

Journal Article. Retrieved from http://adsabs.harvard.edu/abs/2011A%26A...530A..93V

Verbunt, F., & van Gent, R. H. (2012). The star catalogues of Ptolemaios and Ulugh Beg. Machine-readable versions and comparison with the modern Hipparcos Catalogue. *Astronomy and Astrophysics*, *544*(A31), 1–34. Journal Article. Retrieved from http://adsabs.harvard.edu/abs/2012A&A...544A..31V

White, H., McLeod, H., & Morley, H. F. (1872). *Catalogue of Scientific Papers (1800-1900): 1st ser., 1800-1863: Volume VI*. BOOK, London: Royal Society of London. Retrieved from https://books.google.cat/books?id=JBUfAQAAMAAJ

White, H., & Morley, H. F. (1871). *Catalogue of Scientific Papers (1800-1900): 1st ser., 1800-1863: Volume V*. book, Royal Society of London. Retrieved from https://books.google.cat/books?id=7BQfAQAAMAAJ

Displaying New Measurements on WDS Orbit Plots

Robert K. Buchheim

Altimira Observatory, Coto de Caza, CA USA
Bob@RKBuchheim.org

Abstract: Students who observe and measure a visual double star often want to see how their measurement compares with the historical record and with the orbit (if one has been determined). This paper describes how PowerPoint's graphical tools can display a newly-measured data point on the orbit plot from USNO's 6th Orbit Catalog, and how a simple spreadsheet can transform measurements expressed as (ρ,θ) into a Cartesian plot of the sky positions (E, N). This information is presented as a resource for future students.

Introduction

Observing and measuring visual double stars is a fruitful project for student research (Genet, et al 2012). It provides the students with a genuine research experience, it requires only a few hours of telescope time, and it provides the double-star community with a new source of measurements (separation and position angle) of neglected pairs.

Students frequently want to see how their measurement "fits in" with the historical record, and they are particularly interested in comparing their measurements to the published orbit of the pair they have measured.

This paper describes two tools that have been used by students under my guidance, that seem to meet their needs: (1) a graphical method of displaying their new measurements on the orbit plot from the 6th Orbit Catalog, and (2) a spreadsheet method to display the new measurement alongside the historical measurements for a pair whose orbit has not yet been determined.

Displaying a New Measurement on the Orbit Plot

If the pair under study has an orbit in the 6th Orbit Catalog, students would like to display their new measurement on the orbit plot, at a level of accuracy that is appropriate for an illustration in their report, such as Figure 1.

The concept is straightforward: draw a line whose length represents the measured separation (ρ), at the scale of the orbit diagram, and rotate the line to align it with the measured position angle (θ). The presentation

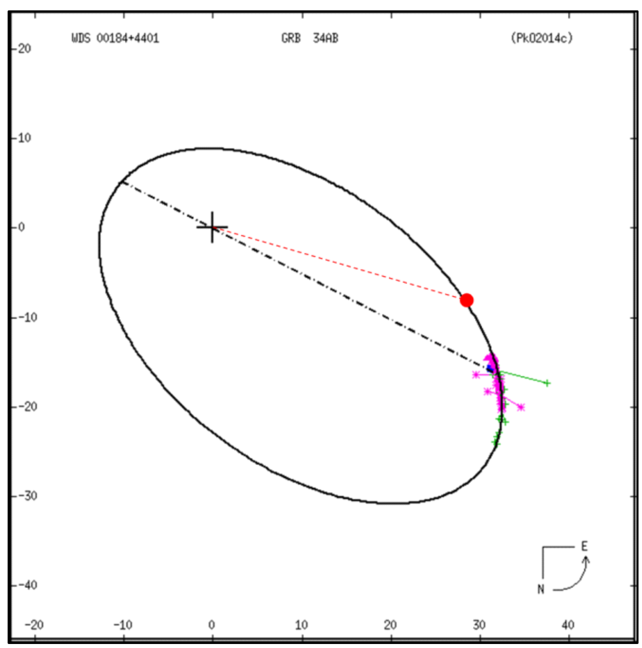

Figure 1. Example of an illustration that shows how a newly-measured position "fits in" to the orbit of a visual double star. The red dot is the student-measured position (ρ, θ).

Displaying New Measurements on WDS Orbit Plots

software MS PowerPoint contains graphics capability that can do this. The procedure – and the relevant commands – for doing this in PowerPoint 2010 are described in the following.

- Step 1: From the WDS 6th orbit catalog, display the orbit plot (in your browser). COPY and PASTE it into PowerPoint.

Scale it larger/smaller to make it nearly fill the PowerPoint frame. Use the setting FORMAT – SIZE - "lock aspect ratio" to maintain the same scale in x- and y-axes. The exact size of the image is not important.

- Step 2: Use the command INSERT-SHAPES to draw a horizontal line that spans an appropriate distance along the x-axis. (In the example below, the line was drawn to span 20 arc-sec, according to the scale on the orbit plot)

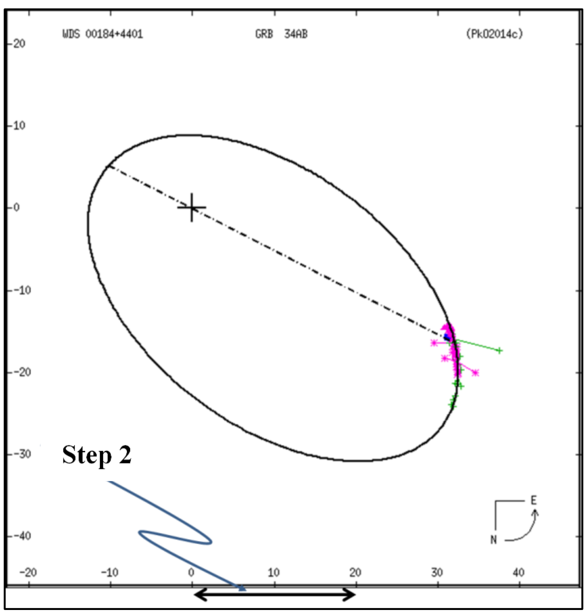

Use the FORMAT command to set the height of the line to zero (i.e. a perfectly horizontal line). The FORMAT block will then display the length of the line, to ±0.01 inch.

Read the length of the line (in inches) and calculate the scale factor of the image.

In the example shown, the reference line as drawn was 1.77 inches long. So, in this example, the scale factor is 1.77 inches per 20 arc-sec.

- Step 3: Use the command INSERT-SHAPES to draw a vertical line (hence aligned with North).

Use the FORMAT command to set the width of the line to zero (i.e. a perfectly vertical line). Set its length ("height") to match your separation measurement:

For example: suppose your measured separation was ρ= 29.75 arc sec,

Convert this to inches at the drawing's scale:

29.75 arc-sec *1.77/20 (inches/arc-sec) = 2.63 inches.

Note, at this point, it isn't necessary that the line be sitting on the location of the primary star ... just get it vertical and make it the correct length. An example is shown below.

Optionally, you can use the FORMAT – SHAPE OUTLINE command to set the color of the line, and FORMAT – SHAPE OUTLINE – ARROWS to put a symbol at the south end (e.g. the large "dot" shown in the example). You can also use FORMAT – SHAPE OUTLINE – DASHES to select the type of dashed line, and FORMAT – SHAPE OUTLINE – WEIGHT to set the desired thickness of the line.

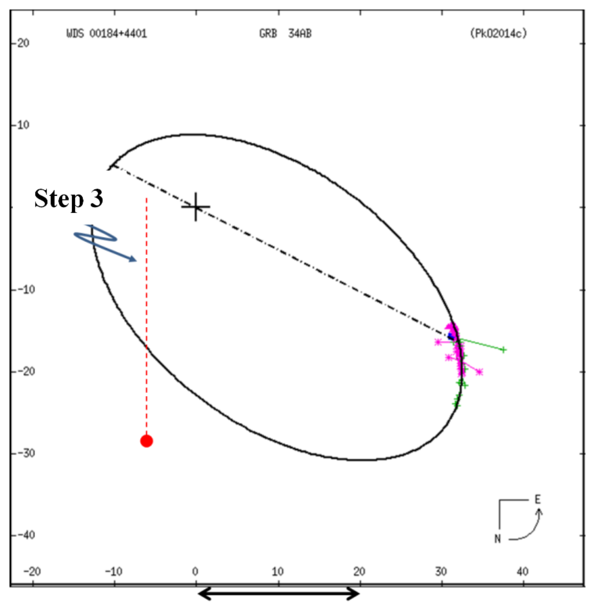

- Step 4: Rotate the line by selecting it (click on it), and using the Drawing tool FORMAT – ROTATE – MORE ROTATION OPTIONS. This will open a window that allows you to enter a rotation angle.

Beware of the sign convention for rotation. On the USNO orbit plots, position angle increases in the counter-clockwise direction ("North toward East"). In PowerPoint, counter-clockwise rotation is *negative*.

For example: If your measured position angle was θ = 74 degrees, then in PowerPoint you select the line and set the rotation angle to -74 degrees (i.e. a *negative* angle).

The result for this example is illustrated below.

Displaying New Measurements on WDS Orbit Plots

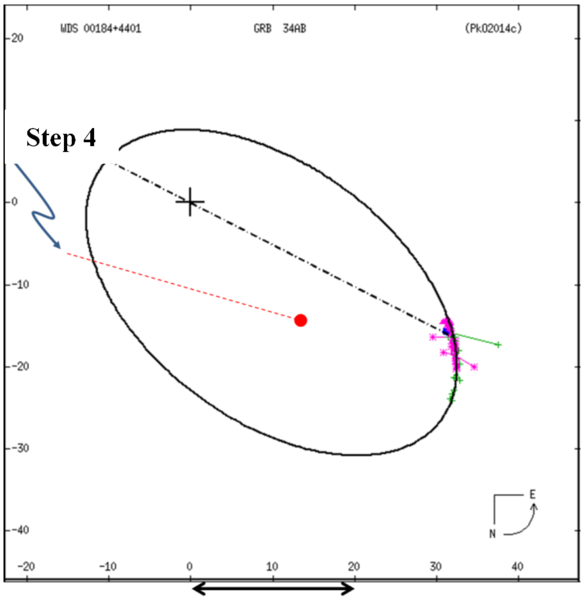

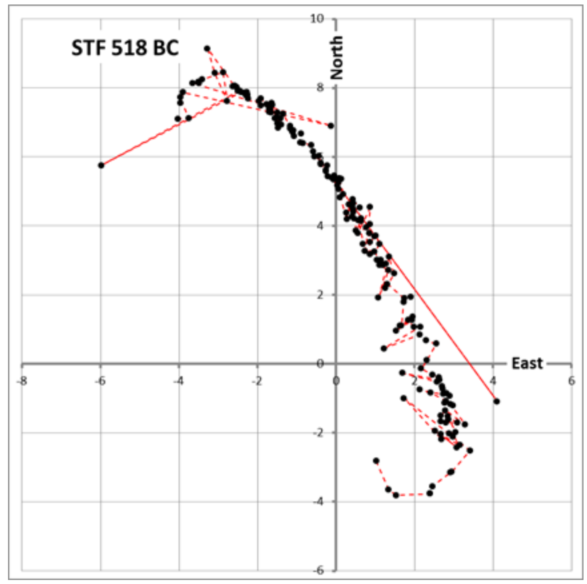

Figure 2: Example of a plot of historical measurements (ρ,θ) converted into a Cartesian-coordinate display of the trajectory of the secondary star as it would be seen relative to the primary, in the plane of the sky.

When PowerPoint rotates the line, it uses the midpoint of the line as the center of rotation. As a result, both ends of the line move and it may appear as if the line has translated. This is not a problem: the next step is to translate the line into the correct position.

- Step 5: Translate the line so that one end sits on the position of the primary star (the "+" on the orbit diagram). In PowerPoint, click-hold on the line and drag it up/down and left/right so that one end sits on the location of the primary star. The other end will then mark the position that represents your new measurement of ρ, θ, as was illustrated in Figure 1.

You can then put this diagram into your report. In PowerPoint, use SELECT ALL, then right-click to COPY; and in your Word processor right-click and use PASTE OPTIONS to paste the diagram as a PICTURE.

Plotting Historical Data

An e-mail request to USNO will return all of the historical measurements of a double-star of interest (including all components, if there are more than two). The data is provided as a plain text file that contains (among other parameters) the date, measured position angle, and measured separation for each historical measurement of the pair. It is instructive for students to visualize the apparent motion of the pair as it would be seen in the plane of the sky, and to insert their own measurement to see how it "fits" with the historical data. This is a simple exercise with a spreadsheet, and it is a practical application of the lessons they had in their math classes, about Cartesian coordinates and trigonometry functions. Figure 2 shows an example of the goal of this exercise.

The concept should be familiar to high school students who have taken trigonometry, except that the angle θ is defined differently than the angle used in standard cylindrical coordinates.

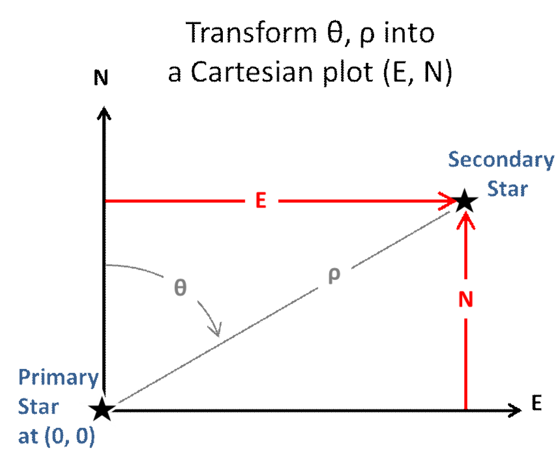

The description of the position of the secondary star is transformed from ρ, θ (cylindrical coordinates) into E, N (Cartesian coordinates) using equations that should be familiar to high school students:

$$\cos(\theta) = \frac{N}{\rho}$$

and

$$\sin(\theta) = \frac{E}{\rho}$$

so that the transformation is

$$E = \rho \sin\theta \qquad \text{in arc-seconds} \tag{1}$$

and

$$N = \rho \cos\theta \qquad \text{in arc-seconds} \tag{2}$$

Doing the transformation and plotting the trajectory of the secondary star is a simple spreadsheet exercise:

- Step 1: Prepare a spreadsheet workbook with three columns, for Date, Position angle, and Separation. Enter all historical observations, one observation per row, into this spreadsheet. Dates should follow the WDS format (decimal year). Position angle (θ) will be in degrees (measured from North toward the East) and Separation (ρ) will be in arc-seconds.
- Step 2: At the bottom of the table of observations (date, θ, ρ), insert the students' new measurement (date, theta, θ, ρ).
- Step 3: In two columns to the right, program the equations Eq. 1 and Eq. 2, to calculate the Cartesian coordinates E ("east") and N ("north). Copy these equations downward, so that each observation is transformed to E, N coordinates.

Beware that most spreadsheets (such as MS Excel) expect the angle in trig formulas to be expressed in radians (not degrees). Thus, the spreadsheet formulas will be sin($\theta\pi$ / 180) and cos($\theta\pi$ / 180), when the angle θ is expressed in degrees.

- Step 4: Create a graph that shows the measurements in Cartesian coordinates, to illustrate the trajectory of the secondary star relative to the primary, as it would appear in the sky. Select the two columns containing the calculated "E" and "N" coordinates, including all of the rows for all historical (and new) measurements. With the data array selected, use the command INSERT – SCATTER to create a scatter chart from this data.

This will yield a plot similar to Figure 2

This sort of display can highlight several features of the data. First, the graph is an intuitive visual display of the trajectory of the secondary star. In the example of Figure 2, a little imagination will suggest the shape of a probable elliptical orbit.

Second, the plot nicely displays the more-or-less random "scatter" in the observations, with individual points being arrayed near the probable orbit, but not lying cleanly on it. The inevitability of some random uncertainty in any scientific measurement is an important lesson for the students, and it can be seen in their own double star measurements.

Third, most plots will show some discordant data points – measurements that fall significantly "off" of their expected locations, given the overall trend of the majority of data points. In situations where there are only a few historical measurements, the student can be challenged to think about whether a discordant measure is "wrong", or if it is just a manifestation of normal measurement uncertainty; and of the difficulty of reaching a conclusion about an individual data point. This can lead to a discussion of when – if ever – it might be appropriate to "toss out" a data point.

Finally, it may be useful to format the data point that represents the students' measurement so that it is highlighted relative to the historical measurements. This gives the student a clear picture of how their measurement "fits in" to the historical record.

Limitations

The display methods presented here (Figure 1 and Figure 2) are intended only as tools for visualization of double-star motion. They are not appropriate for determining orbits, nor for quantitative assessment of the residuals between an orbit versus a new measurement. If a quantitative comparison of a new measurement to an orbit is needed, then the student must refer to the orbit ephemeris (USNO 6th Orbit Catalog) and use a rigorous calculation of the residual, such as that described in Smith et al 2016.

Acknowledgement

This research has made use of the Washington Double Star Catalog and Sixth Catalog of Orbits of Visual Binary Stars, both of which are maintained at the U.S. Naval Observatory.

References

Smith et al 2016: Nick Smith, Chris Foster, Blake Myers, Barbel Sepulveda, and Russell Genet, "Orbital Plotting of WDS 04545-0314 and WDS 04478+5318", JDSO Vol 12 No 1 (January 2016)

Genet et al 2012: Russell M. Genet, "Observing Double Stars", Proceedings of 31st SAS Symposium (May 2012)

How Likely are Wide Pairs to be Physically Connected?

T. V. Bryant III

Little Tycho Observatory
703 McNeill Road, Silver Spring, Md 20910
rkk_529@hotmail.com

Abstract: There are numerous binary pairs that are not in the Washington Double Star Catalog (WDS)[1] that appear to be physical binaries. We show in this study that such pairs are often optical using Monte Carlo simulations of the sky.

A casual glance at the photos in the DSS[2] with Aladin[3] or WikiSky[4] will reveal pairs of stars that seem to be isolated from other stars in the field. These wide (> 4") pairs, whose components are within a visual magnitude of each other, are sometimes not in the WDS. If they also have similar blue magnitudes, this would imply that their spectral types are also similar, which further suggests they are at similar distances, and probably orbiting one another.

To test the idea that two stars within 60 arc seconds of one another are physically connected, all stars brighter than 15mv and within 20 degrees of the north galactic pole (NGP) were selected from the UCAC4[5] CCD astrograph catalog. The NGP was selected as the stellar density there is less than in other regions of the sky, thereby increasing the probability that pairs in that region are physically connected.

To be included in the study, the stars had to be:

- Within 20 degrees of the NGP.
- Brighter than 15.0mv.
- Each star's proper motion had to be greater than twice its proper motion error.

There were 129,762 stars found within 20 degrees of the NGP that met these criteria for the study.

A program was used to create an artificial sky, randomly assigning the stars to different positions within 20 degrees of the NGP. The magnitudes and proper motions of the stars themselves were unchanged.

A program to locate binaries was created to search the data, both real and simulated, for binary pairs using the following rules:

- Components of a pair of stars needed to be closer than 60" of one another.
- The magnitudes of the stars needed to be within 2mv of each other.
- Once a star was identified as a member of a pair, it was removed from the list, preventing it from being chosen as a member of another pair.
- The proper motions of the stars had to be greater than 2 milliarcseconds per year, and the directions of their motion needed to be within 2 radians (~115 degrees) of one another, and finally not differ in magnitude by more than +/- 50% of each other's proper motion.
- The proper motion of each star in the pair needed to exceed the error in it's proper motion by a factor of two or more.

The pairs that were found were divided into 5 zones, based on their separations (ρ).

The results from the stars of the UCAC4 yielded 1271 possible pairs, with the following distribution of separations:

- 32 pairs less than 4".
- 57 pairs between 4 and 8".
- 123 pairs between 8 and 15".
- 275 pairs between 15 and 30".
- 784 pairs between 30 and 60".

The artificial sky was simulated 100 times, and the results shown are the averages of these runs. There were 893 possible pairs found with the following distribution of separations:

- 2 pairs less than 4".
- 10 pairs between 4 and 8".

How Likely are Wide Pairs to be Physically Connected?

- 35 pairs between 8 and 15".
- 158 pairs between 15 and 30".
- 688 pairs between 30 and 60".

These results are graphed in Figure 1. The X axis value of each datum reflects the minimum value of a zone, e.g. 0 = zone 0" - 4". This can be shown more clearly if the number of simulated pairs for a given bin is shown as a percentage of UCAC4 for that bin, Figure 2. The UCAC4 data are set to 100, in a line across the top of Figure 2.

Note that for the simulated pairs, the wider the pair zone, the closer its numbers get to those found in the UCAC4 survey. This indicates that many wide pairs, which at first glance appear to be mutually orbiting one another, are actually optical pairs or that their orbit is so large as to be easily disrupted when the pair interacts with the other stars, clusters, and spiral arms of the rest of the galaxy.

For details on the computing required to conduct this study, please see the appendix below.

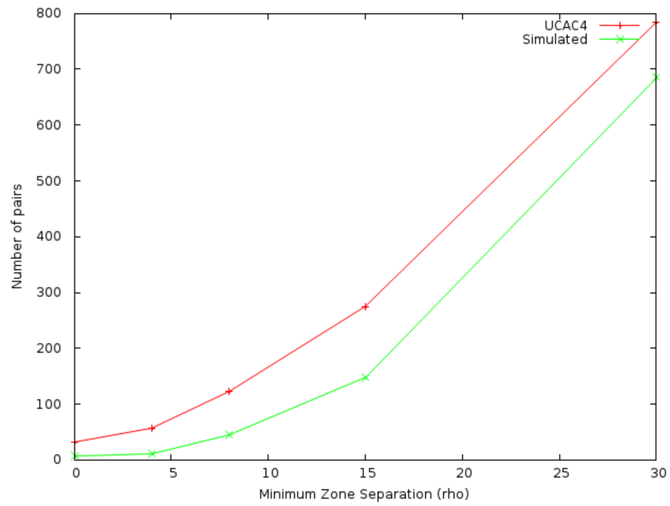

Figure 1. Distribution of separation of double stars for the artificial sky (green line) and from UCAC4 (red line).

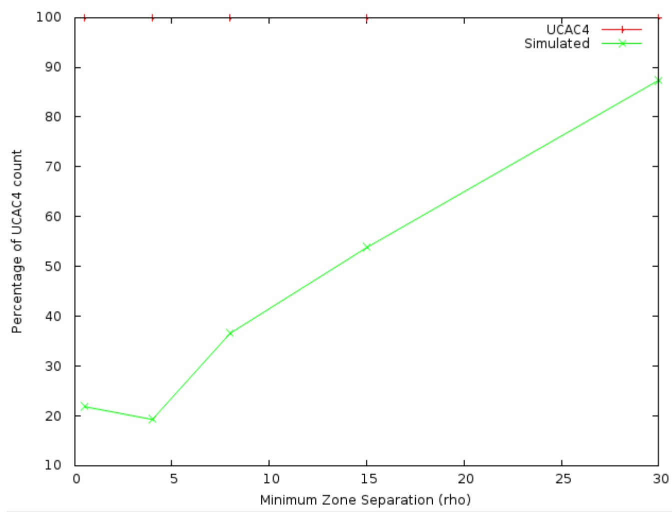

Figure 2. Number of simulated pairs as a percentage of UCAC4 pairs.

Acknowledgements

The author is deeply grateful to Tom Corbin and Bill Hartkopf for their many technical comments and error catches that significantly added to the accuracy of this paper. He also recoginzes the grammatical edits that Kathie Bryant made, which enhanced its readability.

References

1) The Washington Double Star Catalog. Brian D. Mason, Gary L. Wycoff, William I. Hartkopf, Geoffrey G. Douglass, and Charles E. Worley, 2001, http://ad.usno.navy.mil.wds.

2) The Sloan Digital Sky Survey web site, http://www.sdss.org.

3) Aladin web site, http://aladin.u-strasbg.fr.

4) The WikiSky web site, http://www.wikisky.org.

5) The Fourth US Naval Observatory CCD Astrographic Catalog (UCAC4). Zacharias, et al, 2012, http://www.usno.navy.mil/USNO/astrometry/optical-IR-prod/ucac.

Appendix

The programs used to generate this study are available on SourceForge:
https://sourceforge.net/projects/are-wide-binaries-optical/files/AreWideBinaries/OpticalSource.

You'll also need the gcc compiler and perl on your machine, as well as about 100GB of disk space for the data to reproduce this study. Windows users can run them under cygwin.

The UCAC4 catalog is available on line (see its on line site in the above references) in binary format.

The catalog data are placed in a data directory. On the author's system, for example, it is /work/astro/data/.

The UCAC4 data are first parsed with readUcac4.c, and then ucac4TextToNA_Format.pl and splitUCAC4intoDecZoneFiles.pl create the data read by getDataFromCatalogs.c.

The format of the transformed UCAC4 data are then rendered into a "standard" format:

```
ra|dec|R|G|B|Visual Magnitude|Catalog|Name|pmRa|pmDec|ePmRa|ePmDec
1   2  3 4 5        6            7      8     9   10    11    12
```

Definition of each field is as follows:

1. ra: Right ascension in radians.
2. dec: Declination in radians.
3. Red color estimate for the star. Not used in this study.
4. Green color estimate for the star. Not used in this study.
5. Blue color estimate for the star. Not used in this study.
6. Visual magnitude. Usually the Johnson V band magnitude.
7. Catalog: A single character identifier for the catalog the data was from.
8. Name: The star's identifier in the catalog.
9. pmRa: Proper motion in right ascension. In milliarcseconds / year.
10. pmDec: Proper motion in declination. In milliarcseconds / year.
11. ePmRa: Error in proper motion in right ascension. In milliarcseconds / year.
12. ePmDec: Error in proper motion in declination. In milliarcseconds / year.

The data itself is split into 180 different files, one for each degree of declination, and placed in directories named naFormatData which are placed in a sub directory, e.g. /work/astro/data/UCAC4/naFormatData.

From these files, the stars within 20° of the NGP are found and placed in their own file.

We are now ready to create a simulation of the NGP stars. SimulateNGP.c does this by assigning a randomly chosen position for each of the stars in NGPstars. The magnitude and proper motion data for the stars are left intact.

Binaries are then found by findBinaries.c

Note that the following command will compile the C programs, where programName.c is the C source code and executableName is the executable the compiler creates:

gcc -std=gnu99 -O2 -o executableName -Wunused programName.c -lm

The graphs were made using gnuplot.

Astrometric CCD Observations of Three Double Stars Measurements

Angela Nand
University of Hawaii
Leeward Community College, HI

Abstract: CCD astrometric observations of three double star groups from the Orion constellation were made. Position angles and separations of corresponding pairs were obtained from the data acquired and compared to previous observations listed in the Washington Double Star Catalog. Present data agrees with previous observational data.

Introduction

As a child I have always wondered about the stars and planets glowing above me. When I grew into my teenage years I found a love for astronomy. I used to watch any type of documentaries that would come on television as well as read up and look at all the pictures in text books. Two years ago, enrolling in an astronomy class at Leeward Community College rekindled my curiosity and passion for stars that has been a fantasy luxuriated by watching plenty of colorful astronomy programs on TV during my school years.

After completing the course I was able to enroll into an independent study class for hands on experience on operating telescopes and observing the night sky, eventually leading to an opportunity to conduct research in astronomy as well. Using the Eagle Creek Observatory web site, I chose three binary stars from the Orion constellation for their appearance near zenith and visibility, thus making them ideal double stars to take good images.

Instrumentation and Data Acquisition Methods

Observations were made on a 0.5 meter f/8.1 Ritchey-Chretien Optical Guidance Systems telescope at the Leeward Community College Observatory. Images of interested objects were captured using an Apogee Alta U6 CCD camera with 24 micron pixels cooled to -10^0 C. No filters were used for these observations. After cooling the camera to the desired temperature, with the help of Sky6 software from Software Bisque, the telescope was slewed and centered on the first target, and a sample star field was captured using suitable exposure time (special care was taken to not saturate the star field). The exposure time was 10 seconds. The camera software was CCDSoft, also from Software Bisque. Using the same exposure time, ten dark background exposures were captured and the average of these ten frames was obtained for image processing. A sample image plate after background processing for star system SAO 113315 is shown in Figure 2.

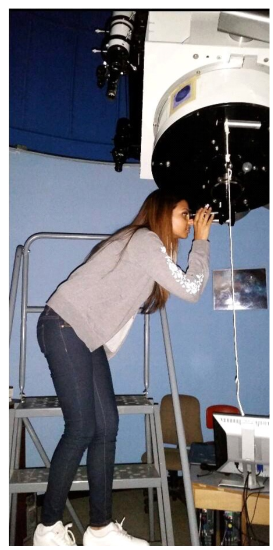

Figure 1. The author at the telescope.

The software used for determining the astrometric solutions also provided the plate scale and orientation of the camera. For the observational set up, the plate scale was computed to be 1.21″/pixel and the camera angle to be 357.32 degrees respectively.

Astrometric CCD Observations of Three Double Stars Measurements

Figure 2: Background corrected Plate for SAO 113315 in Orion.

Results

Astrometric solutions for the acquired pairs of double stars were obtained by analyzing the collected data using the CCDSoft software in conjunction with the Sky6 software. Separation between the primary and secondary stars and their Position Angles were determined for each ten sets of observations, their average was computed, and the results are presented in the Table 1. The last column, current data, is compared to the last observed data provided in the Washington Double Star Catalog.

Conclusion

Three sets of double star astrometric measurements using a CCD camera were successfully made and their separation and position angles were determined. The observational data agrees with previous reported data (WDS). This unique opportunity has helped me understand and appreciate astronomy more than before.

Acknowledgments

My thanks to the US Naval Observatory for use of the *Washington Double Star Catalog*. I also thank the Eagle Creek Observatory on Double Stars. Finally, I am grateful to the Leeward Community College Math and Science Department for allowing me to conduct this research program.

References

Eagle Creek Observatory, 2016; http://www.eaglecreekobservatory.org/eco/doubles

Mason,B., Wycoff, G., and Hartkopf, W. The Washington Double Star Catalog, http://ad.usno.navy.mil/proj/WDS

Table 1: Present Observational Data compared to their last reported values in WDS Catalog.

Double Star ID	Separation (arc sec)			Position Angle (degrees)		
SAO Number	Last	Present	Difference	Last	Present	Difference
SAO 95002 05561+1356s 503BC	24.1	24.27	.17	166	167.18	1.18
SAO 113315 05584+0150ARN	36.5	37.15	0.65	206	205.55	0.45
SAO 113435 06051+0053STF	40.5	40.24	0.25	329	328.82	0.18

Speckle Interferometry of Four Close Binaries

First Results of the Tierra Astronomical Institute Telescope

Rick Wasson[3], Jesse Goldbaum[1], Pat Boyce[4], Robert Harwell[1], Jerry Hillburn[5], Dave Rowe[6], Sina Sadjadi[1], Donald Westergren[2], and Russell Genet[7]

1. Tierra Astronomical Institute (TAI), San Diego, CA
2. TAI and Morris Ranch Observatory, San Diego, CA
3. Orange County Astronomers, Murrieta, CA
4. Boyce Astronomical Research Institute, San Diego, CA
5. San Diego Astronomical Association, San Diego, CA
6. PlaneWave Instruments, Rancho Dominguez, CA
7. California Polytechnic State University, San Luis Obispo, CA

Abstract: This paper documents first use for speckle interferometry of the Tierra Astronomical Institute's 24-inch telescope, located at Terra Del Sol, some 60-miles east of San Diego, CA. Measurements are reported for four close binary systems - STF2173AB, D15, STF2205, and HSD2685 - observed over the weekend of July 1-3, 2016. The objectives of this engineering checkout run were to evaluate the integration of the telescope and ZWO ASI 290MM high speed CMOS camera, and to establish observational procedures for future speckle observations, including those made with advanced high school and college student researchers. Difficulties encountered in the checkout are described, along with suggestions for overcoming them in the next run.

Introduction

Small Telescope Student Research in the San Diego Area

Members of the San Diego astronomical community are developing a collaborative initiative to introduce high school and college students to science through small telescope astronomical research. As part of this initiative, three community colleges and four high schools are adopting the Astronomical Research Seminar supported by the Institute for Student Astronomical Research (InStAR), see http://www.in4star.org.

As part of the seminar, student teams, with assistance from the astronomy community, focus on double star research that results in published papers. Expansion of this research to time-series photometry of exoplanet transits, binary star eclipses, brightness variations of intrinsically variable stars, and tumbling asteroids is planned. In addition to time and advice, assistance from the astronomy community extends to providing the facilities (telescopes, etc.) to support student research. One such facility is Tierra Astronomical Institute's (TAI) 24-inch F/8 Ritchey-Chretien telescope located at the San Diego Astronomical Association (SDAA) in the high desert sixty miles east of San Diego (see www.tierra-astro.org). While primarily available for student and instructor projects, this telescope also supports other student activities such as class field trips and teacher training (Figure 1).

InStAR seminars support various types of double star research which are tailored for students with different skill sets. One of the more advanced types of research project includes speckle interferometry measurements of binary systems. These measurements require 'small' telescopes with a large enough aperture to obtain useable SNR values for a target system. Of course the larger the aperture, the better the theoretical resolving power. The telescope must also be capable of high precision pointing because of the high magnification required to obtain speckle images. Fortunately, the 24-inch telescope was recently upgraded with Renishaw encoders on each axis to provide high resolution position feedback.

Project Goals

First use of the TAI facilities for speckle interferometry of close binary systems took place over the

Speckle Interferometry of Four Close Binaries ...

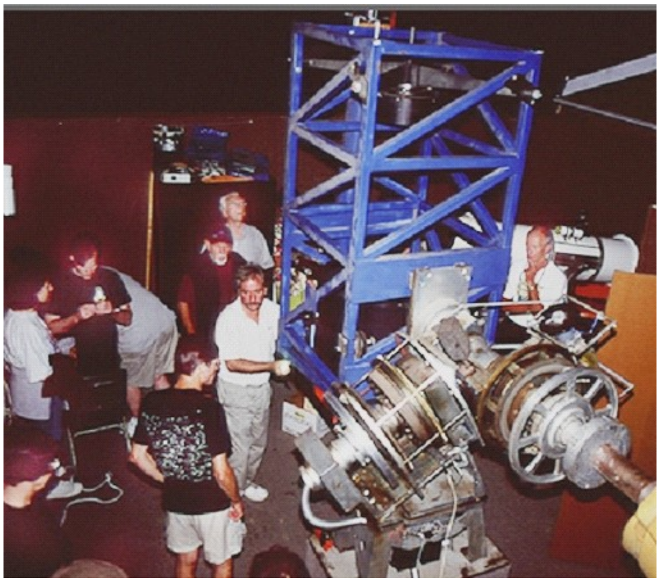

Figure 1. Tierra Astronomical Institute's 24-inch F/8 R-C telescope.

weekend of July 1-3, 2016. The project had three primary goals. The first goal was to perform an engineering checkout to see if all the assembled components (hardware, software, and procedures) work together properly. The second goal was to validate the suitability of the 24-inch telescope facility for speckle interferometry of binary star systems, and define required or desired improvements to hardware, software, or procedures. The final goal was to make precise speckle interferometry observations of several binary star systems.

Binary Stars

Repeated measurements of the position angles (θ) and separation (ρ) of the two components of a gravitationally bound binary star can lead to the determination of its orbit (Heintz 1978). From Kepler's first law, we know that the observations must form an ellipse. However, the apparent ellipse we see from Earth could actually be oriented in almost any way in three-dimensional space. To determine this orientation, we use Kepler's second law of equal areas being swept out in equal intervals of time to determine the three-dimensional orientation that best fits the observational data.

With an orbit in hand, we know, besides the spatial orientation and the orbital period, the semi-major axes of the orbit as an observed angle in arc seconds (″). If we also know the distance to the binary, often the case from observations made by Tycho (and being greatly refined by Gaia), then we can convert this angular value into an actual physical length of the semi-major axis. We can then apply Kepler's third law which relates the period, semi-major axis, and combined mass of the two stars:

$$p^2 = \frac{a^3}{M_1 + M_2}$$

where p is the period in years, a is the semi-major axis in astronomical units, and M_1 and M_2 are the masses of the two stars in solar masses

The dynamical (combined) mass of the two stars can be parsed into individual stellar masses using one of several methods. The most accurate method uses radial velocity curves. Accurate, assumption-free knowledge of individual stellar masses is the foundation of stellar evolutionary theory, hence the scientific importance of binary star astrometric measurements.

Obtaining accurate orbital parameters via binary astrometry requires a nearly complete orbit of high quality observations. Binaries with orbital periods less than a century, and ideally less than a decade or so, allow accurate observations to build up within practical time frames. The problem is that binaries with short periods also have small apparent angular separations, even if they are fairly close to the Earth. These separations are often so small that they are below the seeing limit, and thus the binary appears as a single star (perhaps with a slight elongation).

Speckle Interferometry

Anton Labeyrie (1970) realized that very short exposures would freeze out atmospheric fluctuations that were blurring images. Many very short exposures could then be analyzed to determine the position angles and separations of close binary stars, with separations only limited by the resolution of the telescope (about 0.3″ for a 24-inch telescope), not atmospheric seeing. The analysis consisted of taking the Fourier transforms of all of the short-exposure images (typically hundreds or thousands), averaging these, and then taking the inverse transform to produce an autocorrelogram from which the position angle and separation could be obtained (although there is a 180° ambiguity in the position angle).

Recent Hardware and Software Developments

Unfortunately, the read noise of CCD cameras operated at high speed is too high for practical speckle interferometry, so images either had to be optically intensified, or (more recently) they had to be obtained with an electron-multiplying CCD camera (emCCD) with a gain register just prior to the camera's analog-to-digital converter. However, emCCD cameras cost between \$10,000 and \$40,000, are somewhat large and heavy, and have to be used carefully so as not to degrade the gain register with overexposures (Genet 2013).

Speckle Interferometry of Four Close Binaries ...

Sony, very recently, developed very low read noise (some less than 1 electron), low cost CMOS chips that have been incorporated into astronomical cameras by firms such as ZWO (Genet et al. 2016 and Ashcraft 2016) and QHY. In addition, Sony just this year released a new line of back-illuminated CMOS detectors with improved near-IR sensitivity. Driven by the mass market for cameras in hand-held electronic devices and many other applications, these low cost CMOS chips offer excellent potential for low-cost speckle imaging.

Equipment

A schematic diagram of the TAI speckle interferometry imaging effort is shown in Figure 2. The yellow arrows represent the optical paths. The blue arrows represent the software applications controlling their associated hardware components. The red arrows represent manual operation, viz. of the flip mirror, centering eyepiece, and ZWO filter wheel.

Optical Paths and Mount

The 24-inch f/8 Ritchey-Chretien supports two optical paths, ‘open’ and ‘flipped,’ which are selected and indicated by use of a manual flip mirror. The speckle imaging setup was installed on the ‘flipped’ optical path which provides a standard 2-inch interface, as seen in Figure 3.

The optical tube assembly sits on a German Equatorial mount that uses a Sidereal Technology (SiTech) controller (Grey 2016) for computer controlled pointing and tracking. The SiTech controller was part of a recent upgrade that started in the spring of 2015 that included a complete 12-month maintenance overhaul of the telescope system. Along with the new controller, the RA/

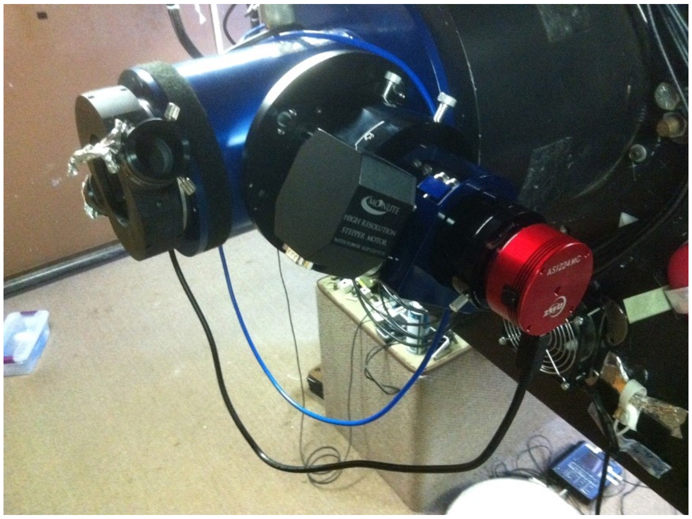

Figure 3. Close-up of the TAI 24-inch optical paths for Speckle Interferometry. A 30mm illuminated reticle eyepiece (not shown) was installed in the “open” path at left. For the engineering run, a ZWO ASI290MM speckle camera was used in place of the ZWO ASI224MC seen here.

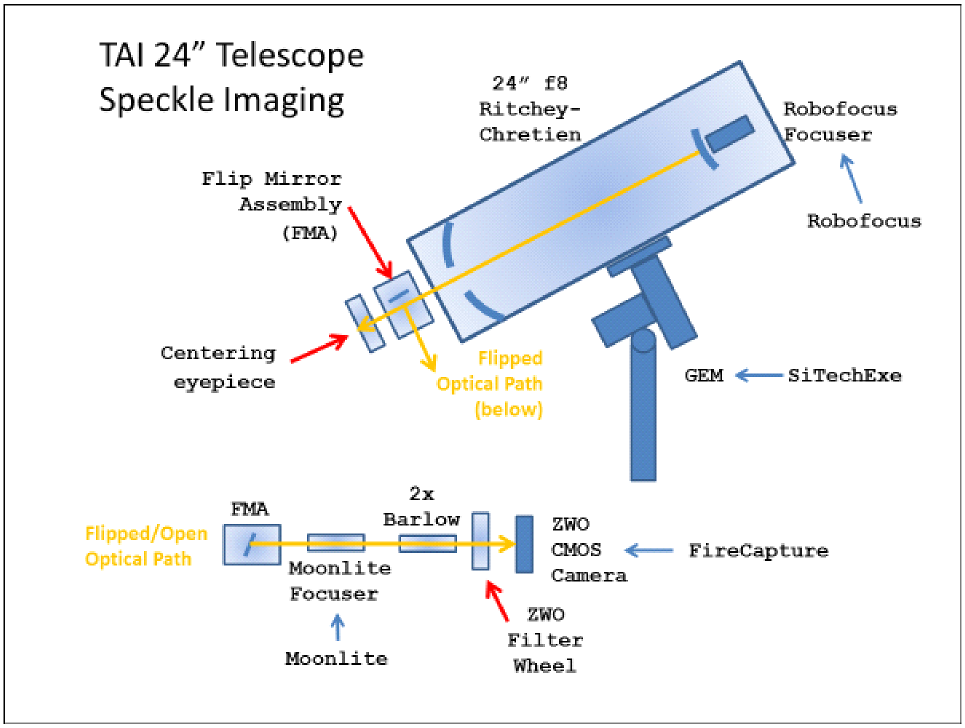

Figure 2. Diagram of the TAI Speckle Interferometry Components.

Speckle Interferometry of Four Close Binaries ...

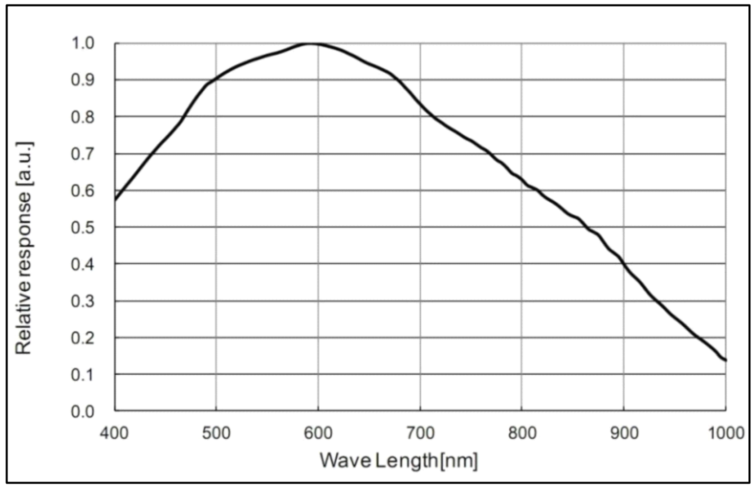

Figure 4. Left: The ZWO ASI290MM back-illuminated, low noise, high speed CMOS camera (fisheye lens installed). Right: Quantum efficiency relative to peak value, which is likely to be about 80%.

DEC stepper motors were replaced with brushless DC servo motors and absolute encoder feedback was added to each axis. The brushless servos have shaft encoders on the armature shaft which provide closed loop control of the servos. The Renishaw mount encoders provide additional feedback accuracy (over 67 million ticks/ revolution) and very linear motion of the telescope axes—virtually eliminating any periodic error using the controller's Cascade Mode. The SiTech control software used for this session was SiTechExe version 0.91T.

In the open optical path, a 30mm illuminated reticle eyepiece was used for centering target stars in the field of view. The RoboFocus secondary focuser was used for focusing. After the target star was focused and centered, the flip mirror was manually flipped and the star would appeared in the speckle camera field-of-view.

High magnification is required in speckle interferometry so that details of the speckle pattern can be seen. Simulation studies have shown that Airy disk sampling should optimally be 6 to 8 pixels (Rowe, 2016). Filters are typically used in speckle work to minimize color dispersion by the atmosphere, which tends to spear out the speckles. Four standard 1¼ inch photometric filters, mounted in a ZWO 5-position manual filter wheel, were used for this checkout run: Johnson B and V, and Cousins R and I, filters were located in positions 1 through 4, respectively. Even with filtering, stars beyond about 35-degree zenith angle were not observed because no atmospheric dispersion corrector was yet available.

For this first TAI speckle run, it was estimated that a magnification of about 1.75 was needed to magnify the native f/8 focal ratio to about f/14, yielding a little less than 8 pixels across the Airy Disk. A 2x Barlow was available, providing approximately f/16, for 9 pixels across the Airy disk, or a plate scale estimated to be 0.06 arc-sec/pixel (but subsequently measured with high precision).

A Moonlite focuser was used for focusing the magnified image onto the ZWO high-speed imaging camera (see below). The camera was under the control of FireCapture software (Edelmann, 2016). The Moonlite focuser was periodically adjusted to account for changing environmental conditions during the observing session.

Speckle Camera System

The camera used was a ZWO ASI290MM high-speed monochrome camera, shown in Figure 4 (https:// www.*zwoptical.com*). It has a Sony IMX291 Back-Illuminated CMOS detector with 2.9µ square pixels in a 1936 x 1096 array, and rolling shutter. This camera was chosen because of its advertised low read noise (~1e$^-$ rms), high Quantum Efficiency (likely ~80% peak), good near-IR sensitivity, high speed USB3.0 interface (170 fps full frame), and moderate price ($449). The detector size (6.46mm diagonal) is small by CCD camera standards, but the very small pixels require less magnification than other cameras for speckle work, still providing a reasonable field of view for acquiring stars at high magnification and for evaluation of the sidereal drift method to calibrate images for orientation and plate scale (discussed in detail below).

Camera Issues

This was the first use of the new ZWO ASI290MM CMOS camera by everyone on the team. The camera had two issues that affected our results. Number one was a significant “read” (line pattern) noise component that created horizontal bands in each image. This noise was small in most lines, but very much larger in other lines. Apparently, the advertised low noise level (~1e-rms) is the result of most lines being low, but some still large—significant for faint stars. This noise is created by the CMOS camera electronics; each row of pixels has its own amplifier and A/D converter, so it is often called “line pattern noise.” This noise is non-repeatable, so it cannot be calibrated by taking bias and dark frames, as is commonly done with CCD cameras. Because it is in one direction only, the line noise can be nearly eliminated in Fourier transform processing, simply by selecting the “interference” filter feature of the Speckle Tool Box (STB) data reduction software (Rowe 2016).

The second issue was the camera gain setting. The maximum gain is 600. Unfortunately, the digital gain process reduces dynamic range. Since our gain was set to 550, which apparently increases the read noise, this affected all the data we gathered. In the future, the gain must be evaluated carefully, to find the best gain versus noise and dynamic range for detection of faint stars.

Observing Procedures

Target List

A master Target List of double stars, in Excel workbook format, had been prepared in advance of the run. Stars suitable for the TAI and similar size telescopes were chosen from the WDS Catalog, based on separation (0.3″ to 2.5″), brightness (V<10 and Δ V<2.5), and Declination (between +70 and -30). The nifty WDS on-line search tool of Bryant (2015) was used to quickly find all candidates with the desired characteristics. Stars were then further selected by interest; for example, those already having an orbit solution, those with common proper motion, or recent Hipparcos discoveries.

Each sheet consisted of all the selected doubles within a two-hour RA window. Within each sheet, the stars were arranged generally by declination to minimize telescope slewing movements. Reference stars were chosen using the planetarium program Megastar5 (Mitchell 2003). For groups of doubles that happened to be near each other (typically 2 to 5 stars less than a few degrees apart), an appropriate Reference star was chosen to serve all doubles in the group. The workbook spanned RA from 06 to 22 hours, with each sheet generally containing 50 to 80 double stars, most of which were appropriate targets for the TAI 24-inch telescope.

Several stars were chosen from the master Target List, within the boundaries of appropriate RA and Dec, to aid the goals of this engineering checkout run. A bright pair with moderate separation and a well-defined (Grade 1) orbit, 17304-0104 STF2173AB, was selected as a check on the accuracy of our observations. Several pairs of varying brightness and separation, having poorly defined orbits, were also selected with the hope that our observations would lead to a more refined orbit. Finally, a few challenging pairs were selected with a faint or close secondary. All the stars were observed with the Johnson-Cousins B, V, Rc, and Ic photometric filters.

Observing Organization and Work Flow Overview

- The observing team was organized into several functional tasks:
- Telescope control: target RA/Dec, slewing, focus, centering star on camera (JG)
- Manual operation: flip mirror, filter setting, centering in eyepiece reticle (BH & BW)
- Camera control: set file directory, FITS format, star type, filter, exposure, ROI, number of frames, etc. (JG)
- Run logging: record target star, sequence number, filter, time (PB)
- Quick-look data reduction: calibration, FITS cubes, speckle reduction (DR & RW)

For the engineering checkout run, it was convenient for both the telescope and camera to be operated by the same person (JG). To help avoid mistakes and later confusion during data reduction, the work flow sequence followed a repeating pattern for each target star:

- Double Star: one sequence of 1000 frames for each filter: B, V, R, I in that order.
- Reference Star: one sequence of 1000 frames for each filter: B, V, R, I in that order.
- Drift Calibration: two drifts of Reference Star, any filter easily visible.

Telescope Configuration and Control

Telescope pointing and tracking were accomplished using SiTechExe v0.91T. This program offers a variety of features including the capability of defining custom ‘databases’ of targets that can be manually selected via the SiTechExe user interface for the next GoTo or Sync operation. The program has the ability to read text file coordinates and then GoTo those coordinates. For the speckle imaging run, one of us (DW) translated the Excel double star Target List into the format required for SiTechExe.

Figure 5 shows an example of a Messier database object loaded into SiTechExe. An example of the double star database format is also shown in Figure 5. The database targets included all the double stars and their

Speckle Interferometry of Four Close Binaries ...

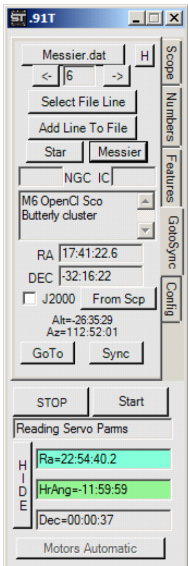

11 3 43.84	61 45 4	N= 1	BU 1077
11 29 4.7	61 46 40	N= 2	RefStar
11 32 20.76	61 4 57.9	N= 3	STT 235
11 5 34.65	54 48 28.7	N= 4	A 1591
11 3 27.91	54 31 33	N= 5	A 1590
10 59 0.4	55 0 42	N= 6	RefStar
11 51 57.86	48 5 19.5	N= 7	HU 731
11 55 5.74	46 28 36.6	N= 8	A 1777
11 38 44.6	45 6 27	N= 9	RefStar
11 30 49.91	41 17 12.7	N= 10	STT 234
10 28 43.86	45 57 51.1	N= 11	A 1993

Figure 5. Left: Example of the SiTechExe user interface, showing M6 from the Messier database accessible through the SiTechExe control system. Right: Example of a SiTechExe Double Star Database input text file, consisting of RA, Dec, Target List line number, and star ID.

reference stars that were used as the basis for telescope pointing. The purpose in creating the SiTech text files was to eliminate errors of manually typing in the coordinates during an observing run. Unfortunately, conversion of the coordinates from the Excel spreadsheet to SiTech data file required a lot of manual intervention (on every input) to get the correct format.

The process for target acquisition was simply to select the target from the SiTechExe database and instruct the telescope to slew to the target. The star of interest always appeared in the FOV of the illuminated reticle eyepiece. Using manual controls, the star was positioned at the appropriate spot to align it with the Barlow-amplified optical path. The manual operator (SS) did the centering and knew where the star needed to be placed to be centered on the Barlow path for the camera. The Barlow path was then selected by the manual flip mirror, and the camera operator confirmed that the target was in the speckle camera FoV. The star was then positioned as needed by the Telescope/Camera operator. During the run, the telescope was periodically and manually synced on known targets when centered in the camera FoV to maintain reliable pointing.

In the near future, a Finger Lakes Instruments CCD camera will be used for plate solving and object centering. The manual flip mirror will still be used in the near term, but eventually it will be motorized. This will enable the Telescope/Camera operator to have complete control over the target acquisition process.

Camera Control

The data acquisition software used was FireCapture (FC) (Edelmann, 2016). This program, designed primarily for planetary imaging, was selected because it can handle many types of cameras and can output frames as FITS files, which is a convenient format for speckle data reduction. The highly-magnified, turbulent image of a moderately bright star did not fill the complete camera FOV; after the target was located, a smaller Region of Interest (RoI) was manually selected in FC to facilitate download speeds and subsequent processing, and minimize hard disk storage. The ROI was typically 512x512 pixels or less for this imaging setup. After the RoI was selected, the camera's exposure time, gain, and gamma were manually set to optimize signal-to-noise-ratio (SNR) for the target. Focus was also manually verified and adjusted when necessary using the MoonLite focuser control software, such that speckles became clearly visible on the screen.

The next step included manual verification that the correct filter on the ZWO 5-position manual filter wheel was selected. FireCapture was then configured for the appropriate target type (double, reference, or drift) and filter, then commanded to record a sequence of 1000 frames. A Log entry for each FC sequence was added to the Log spreadsheet. The display was monitored as the star boiled and danced for about 20 to 30 seconds, to be sure it didn't drift too near an edge of the ROI field. Only bright and well-separated double stars (more than about 1 arc-sec) were obviously seen as double; a tight and/or faint companion was invisible in the seeing mess, but it was still there!

The targets alternated between double and reference, where the reference is a nearby single star used for "deconvolution" analysis in data reduction. All the same optical imperfections that affect the double star are captured in the reference star images as well, including even focus and some atmospheric effects. By Fourier Transform deconvolution, these small effects are cancelled from the double star data, greatly improving and sharpening the Autocorrelation end product.

Run Log

The Run Log was a simplified version of the Target List, containing only the observed stars. Data for the Double and Reference stars were first copied from the Target List. As the session progressed, the Log was edited in real time by the dedicated Log Master (PB) while the images were being recorded. For each sequence of 1000 frames, the star type, FC sequence number, filter, date, and time were added to the Log. After the Reference star observations were completed, two Calibration Drifts, also using the Reference star, were performed and entered into the Log.

Data Reduction

Workflow

Data Reduction utilized two programs which are freely available on-line to amateur astronomers and students, by request to the authors: REDUC (Losse 2015) and Speckle Tool Box (STB) (Rowe 2016). Excel spreadsheet software was also used. The workflow followed this general outline:

- Drift Calibration
    - ◊ Inspect images and delete images with no sidereal motion star (REDUC)
    - ◊ STB drift calibration analysis (STB)
    - ◊ Summarize and plot results in spreadsheet (Excel)
- Creation of FITS cubes for STB processing (STB)
- Processing FITS cubes (STB)
    - ◊ STB Fast Fourier analysis of each frame
    - ◊ Average all transforms
    - ◊ Write average Power Spectral Density (PSD) file
- Speckle Reduction (STB)
    - ◊ Select input double star and single star reference cubes
    - ◊ Select appropriate dimensional and wavelength filters
    - ◊ Enter camera angle and pixel scale calibration values
    - ◊ Select Output File directory and name
    - ◊ Measure autocorrelogram
    - ◊ Save results

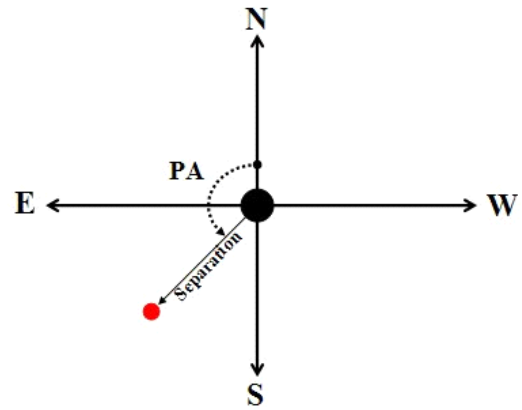

Figure 6. The parameters of a double star measurement are Separation of the two components (arc-sec), and Position Angle (degrees) of the secondary from North (toward East first).

Calibration

The end products of any double star measurement are simply two quantities: Separation (arc-seconds) and Position Angle (degrees), as shown in Figure 6. In order to maximize accuracy of the measurement, two calibration factors must be determined: Pixel Scale or "Plate Scale" (arc second/pixel) and orientation of the camera on the sky. One way to calibrate the setup is by making multiple Calibration Drifts throughout the night. This method applies only to equatorially-mounted telescopes (no field rotation), and no adjustments can be made which could change the magnification or rotate the camera.

We used a special RoI for drift calibration, having full frame width (east-west) but fewer pixels in height (north-south), in order to speed up the frame rate, get more samples within the camera field, and reduce image storage space. To make a calibration drift sequence, a moderately bright star (we used a reference star) is moved slightly outside the east edge of the frame. The recording sequence is started and the telescope is commanded to *stop* tracking. After the star has drifted at sidereal rate across the chip, the telescope is commanded to begin tracking again, the star is re-centered in the field, and the SiTech control system is re-synced on that star to re-establish accurate telescope pointing.

For this optical and camera combination, a drift typically lasted about 8 seconds near the equator, and longer at higher declination. The sidereal drift path of the star defines the true east-west direction, distorted

Speckle Interferometry of Four Close Binaries ...

slightly by the star bouncing around in the seeing disk. The short exposures, typically the same as the speckle exposures, stop the sidereal motion in each frame, as well as the seeing motion. The least squares slope of the star positions (assumed to be a straight line over the small FOV) calibrates the rotation angle of the camera relative to the true east-west direction. Each frame has a time tag, written by FC into the FITS header; thus the drift sequence records several hundred star positions (star image centroid in pixels) at known times. The sidereal drift rate across the camera field is a function only of the star's declination; spacing of the star pixel positions versus time is used to calculate the pixel scale calibration constant (arc-seconds / pixel).

The drift calibration data reduction process has been implemented in the STB freeware speckle data reduction program, making data reduction fast and easy. The only preparation needed is to edit the calibration sequence to include only valid frames. Although STB can eliminate out-lying points, a number of non-valid frames, where the star has not yet entered, or has already left, or is not moving at the sidereal rate, would add needlessly spurious data points that should not be included in the calibration. The REDUC program was used to inspect each drift sequence; unwanted frames which didn't show the star clearly within the frame and moving at the sidereal rate were edited out simply by deleting them. REDUC can calculate the drift angle, and this was used for comparison with STB results.

For calculation of pixel scale, STB reads the time of each frame from the standard FITS header format, written there by FireCapture to the nearest millisecond. The computer clock time does not have to be accurate, but it is assumed to be self-consistent during the short duration of the drift, so that the frames are properly located in time relative to each other.

The STB calibration procedure is very simple for the user: just enter the declination of the star (hh_mm_ss) and select the folder having the (edited) calibration sequence of FITS frames; they do not have to be in FITS cube format. When the first file is selected, STB immediately begins its analysis, centroiding the brightest (usually only) star in each frame and plotting its pixel coordinates as a new point on a rapidly-growing X-Y plot.

As each drift sequence was analyzed in STB, the drift angle and pixel scale results were entered into a spreadsheet, and the results of all the drifts were plotted and averaged. In this way, any suspicious shift in angle or scale could immediately be noticed. The good calibration data from our second night is seen in Figure 7. The scatter is caused primarily by seeing, which bounces the data points around randomly; the least squares curve fit could be slightly rotated (affecting drift angle) or stretched or compressed in length (affecting pixel scale) if there were a net shift in any one direction. Corresponding drift angles from the REDUC program are also shown, with a similar average value.

The calibration shows that we ended up with a pixel scale of 0.0498 arc-sec per pixel. This corresponds to an effective focal ratio of about f/20, and sampling of about 11 pixels across the Airy disk – a bit more than estimated or desired, but our stars were still bright enough to record adequately.

Validation of Camera Orientation

A robust technique for establishing the proper sign of the camera rotation angle is to observe the same double star with two different camera angles. Only one combination of signs will then yield consistent Position Angle measurements.

The double star 16439+4329 D15 was observed on

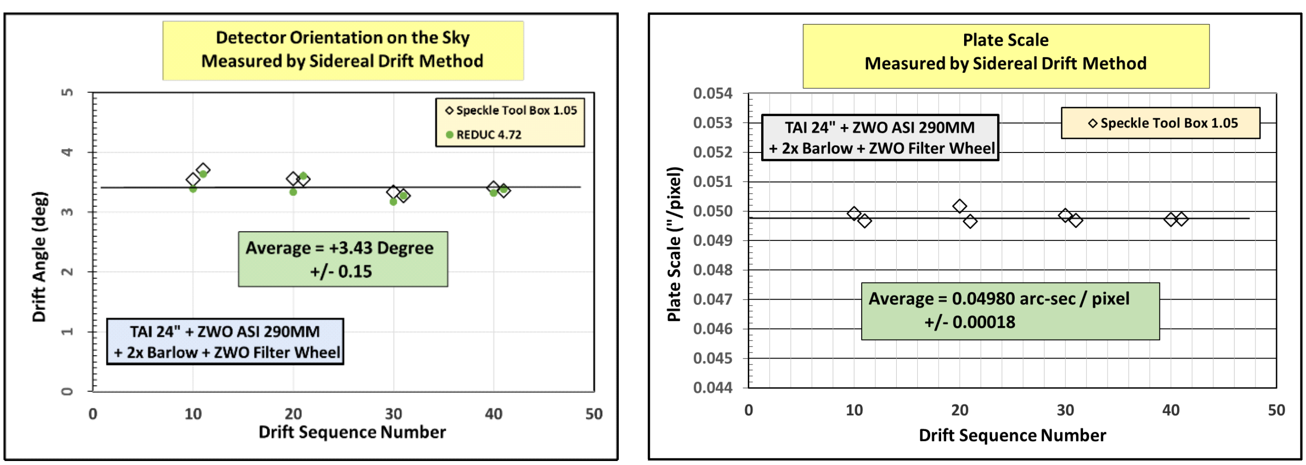

Figure 7. Results of 8 Drift Calibration sequences during the Speckle run of night 2, July 2-3, 2016, using the methods of Speckle Tool Box (Rowe 2016) and REDUC (Losse 2015).

Table 1. Validation of Calibration Results for Star D15. Different camera rotation angles (positive clockwise) on two nights produced good agreement for Position Angle

Calibration and Measurement Summary for 16439+4329 D15					
Night	Camera Angle	Plate Scale	Filter	Observed	
				PA	Sep.
Friday	9.42	0.0441	V	24.6	0.579
			R	25.2	0.587
			I	25.3	0.578
Saturday	3.43	0.0498	V	25.5	0.578
			R	24.7	0.583
			I	24.4	0.577

both nights of our run, with different camera rotation angles and somewhat different Barlow magnification. The STB calibration data are shown in Table 1. The camera was rotated clockwise on each night, but by much different angles. Only the positive sense used in speckle data reduction gave consistent results for the star PA. The separation results also agree well, even though only three calibration drifts were done on the first night.

Later, during Speckle Data Reduction, it was realized that the Position Angles in Table 1 were actually mirror-reversed about the north-south axis, because the camera was mounted on the mirror leg of the Flip Mirror, giving three reflections instead of two. This effect was accounted for in the final measurements presented in Table 2.

The image files were stored automatically by FC in folders labeled by star type: Double, Reference, or Drift. All images were saved as 16-bit FITS files, with computer clock time (to the millisecond) included in the FITS Header. Since the camera produces only 12-bit data, FC automatically padded the four least significant bits with zeros. Within each folder, the file names included the FC Sequence number (automatically incremented after each group of requested files was captured by FC), the filter (B, V, Rc, or Ic), date, start time, and an order-identifying integer for each of the 1000 files in the sequence.

The first task in data reduction was to re-organize the data by creating new folders for each Double star / Reference star / filter combination observed, and move the sequences to the proper folders. The Sequence Number and Run Log (see below) are critical to keeping the thousands of files and dozens of folders straight! Easily-recognized folder and file names (e.g., Double star designation, Sequence, Filter, Reference) go a long way toward avoiding confusion and mistakes later on.

FITS Cubes

STB requires all data (except Drift Calibration files) to be in the form of FITS Cubes, and has a handy tool to create cubes from any number of separate FITS files. This process is simply reading and re-writing the data in the consolidated "cube" format, but considerable computer time is needed because of the large number of files.

Power Spectral Density

This is the simplest step for the STB user, but the most complex number-crunching task for the computer. STB takes the Fast Fourier Transform of every image in the FITS cube, then averages all the transforms to create the average power spectrum (Power Spectral Density (PSD) file). This step condenses the multi-image cube (up to a GB in size) to roughly the size of one image (MB), which retains the essential spacing and orientation characteristics of the double star, with most of the atmospheric distortion and noise averaged out.

Speckle Reduction

Several inputs are required in the "Speckle Reduction" tool of STB. Here the user has many choices, all well-explained in the User's Guide (Rowe and Genet 2015). Although the guide was written for a previous version of the software, PS3, the essential parameters have not changed. Some practice and "playing around" to see what happens will help the new user climb the learning curve. An excellent tutorial on PS3 speckle data reduction has been produced by Richard Harshaw (2015), and it is still applicable to STB.

In the Speckle Reduction window, the Double star and Reference star FITS cubes are first selected. STB1.05, the version used for the TAI data reduction, has inputs for filter center wavelength, photon noise filtering, and interference (line pattern) noise filtering, which are simple and intuitive. Likewise, the calibration inputs are obvious. Inputs for High-Pass and Low-Pass dimensional filters must be calculated, and are explained in detail in the User's Guide (Rowe and Genet 2015). As soon as the inputs are selected, the Autocorrelogram appears, and a box allows toggling between the power spectrum and autocorrelogram displays. Other buttons display control size and brightness.

To make double star measurements of position angle and separation, the Astrometry button is selected, and a new window opens with three more inputs, including the calibration angle and pixel scale again. The third input controls the size of the measuring circle which has appeared on the autocorrelogram display, with an "x" inside that marks the centroid. When the circle is placed over one of the secondary peaks, the measured position angle and separation values appear in the "Observed" boxes. The circle should be sized to contain all of the secondary peak, but none of the primary (central) peak or diffraction rings. When the circle can be moved slightly without the x moving at all, the circle is sized correctly, the centroid is well defined, and the measurement is "solid." A right-click opens another window, where the "Set Target Location" (bottom option) is selected to freeze the measurement.

Results Output

A browse button makes it easy to designate the output file directory and name. A comment may be added, and "Save Results" writes the measurement data to the output file, which is a spreadsheet in .csv format. For each new double star, a new line is added to the output file. When all the doubles have been measured, it may be convenient to open the .csv file and save it also as an Excel workbook sheet, which gives more formatting flexibility, such as column width or sorting.

Results

Results of the first TAI speckle run are presented in Table 2. All four binaries were observed in all four standard photometric filters. The quality of the Speckle Tool Box autocorrelation solutions varied, as described in the notes. Some distortion of the autocorrelation peaks into elongated shapes was noted, particularly for

Double Star Speckle Interferometry Observations					
TAI 0.60-m R-C Telescope		ZWO ASI 290MM Camera		Date: 2016.504	
WDS	**Discovery**	**Filter**	**Theta**	**Rho**	**Notes**
16439+4329	D 15	B	336.35	0.564	5
16439+4329	D 15	V	334.86	0.584	1
16439+4329	D 15	Rc	335.33	0.583	1
16439+4329	D 15	Ic	335.71	0.591	2
17304-0104	STF2173AB	B	142.03	0.669	2
17304-0104	STF2173AB	V	141.87	0.624	2
17304-0104	STF2173AB	Rc	142.04	0.683	1
17304-0104	STF2173AB	Ic	142.89	0.678	1
17457+1743	STF2205	B	11.67	0.972	3
17457+1743	STF2205	V	10.75	0.946	1
17457+1743	STF2205	Rc	10.78	0.941	1
17457+1743	STF2205	Ic	10.51	0.936	1
18571+3451	HDS2685	B	214.72	0.586	4
18571+3451	HDS2685	V	221.33	0.665	4
18571+3451	HDS2685	Rc	218.46	0.616	4
18571+3451	HDS2685	Ic	223.92	0.618	5

Table 2 Notes

1. Bright, clear Autocorrelogram. Solid measurement.
2. Bright but smeared peaks. Fairly good measurement.
3. Companion faint, but measurement solid.
4. Companion faint. Measurement uncertain.
5. Companion too faint. Measurement NOT valid.

Speckle Interferometry of Four Close Binaries ...

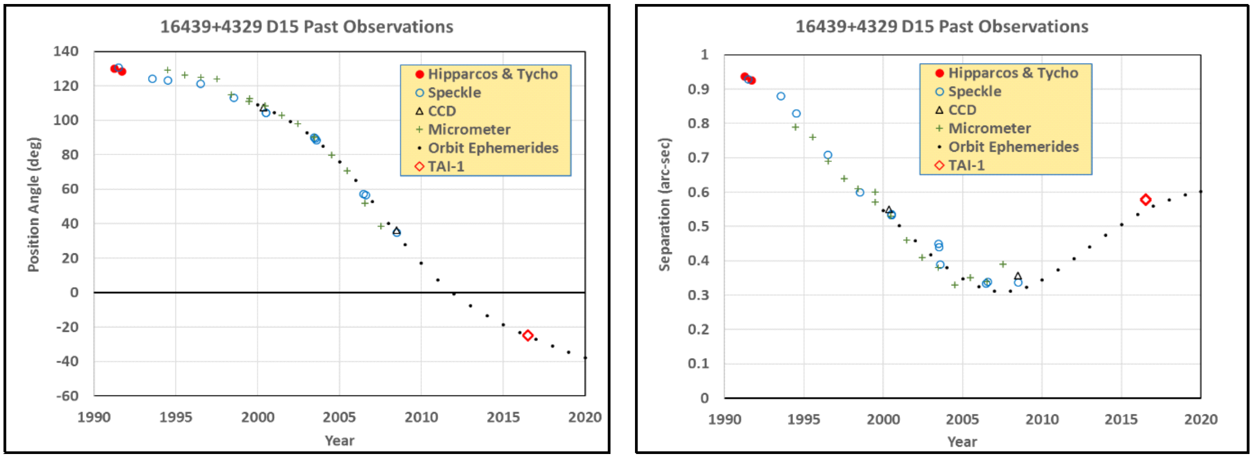

Figure 8. All observations of Double Star D15 since Hipparcos, including all Speckle data.

STF 2173AB in the B and V bands, presumably caused by atmospheric dispersion due to its southerly declination (-1 degree).

D 15

The WDS gives magnitudes 9.04 and 9.27, spectral type K5 for D 15. The latest orbit solution (Alzner 2007) has a period of 120 years and distance of about 88 light years. The orbit is classed as Grade 2 (good) because of complete coverage by micrometer observations.

Position angle and separation data for all observations since the Hipparcos era are shown in Figure 8. (Note that for PA, all data after 2012 are actually in the 360- to 320-degree range, but 360 was subtracted to show continuity). This star has been neglected since 2008, but our new PA data agree well with the projected orbit. However, speckle separation data since about 2000 seem to be slightly higher than the orbit, and our new points continue that trend. If future observations verify the trend, this star will be a candidate for an updated orbit solution. In Figure 8 and following, the orbit points at the beginning of each year from 2000 to 2020, were taken from the Stelle Doppie WDS search site (Moltisanti 2016).

The WDS orbit plot and an example autocorrelogram (Rc band) are shown in Figure 9. The new TAI points have been superimposed on the orbit, showing all observations and the continued speckle trend toward a slightly wider orbit.

The STB autocorrelogram was 256x256 pixels, and shows the STB solution "ship's wheel" marking the selected secondary peak. The STB assumption is that

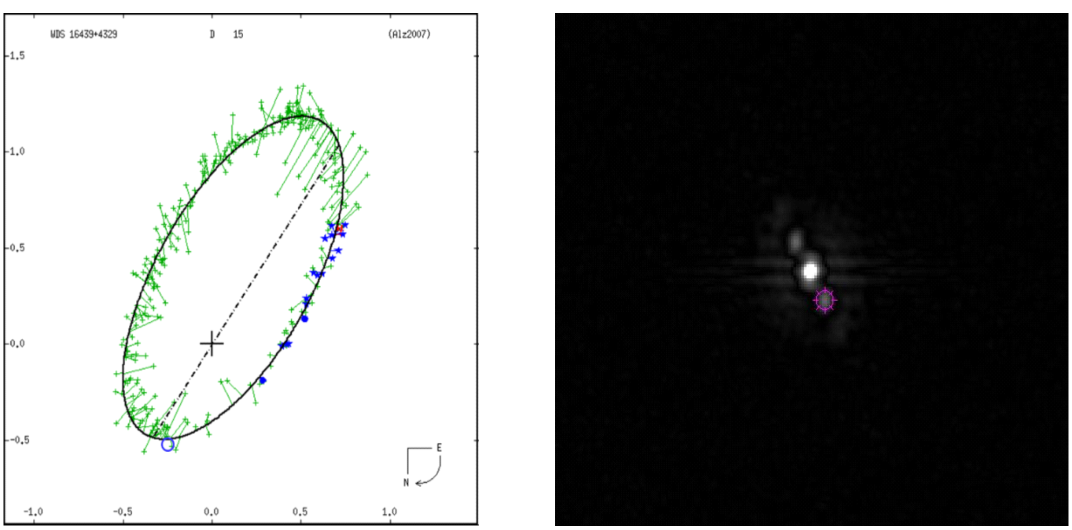

Figure 9. Left: WDS orbit plot of D15 with new TAI Rc speckle point added (blue open circle). Right: STB Autocorrelogram in the Rc band. (Orientation is North up, East right.)

Speckle Interferometry of Four Close Binaries ...

the ob-

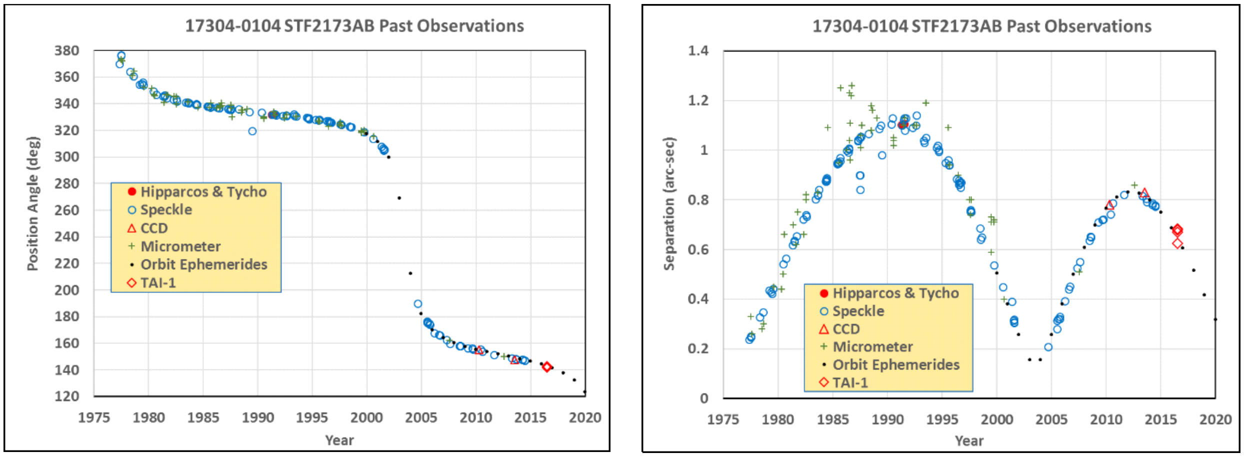

Figure 10. All observations of Double Star STF2173AB in the era of Speckle Interferometry.

served orientation is the same as in the WDS orbit plots. When that is not true, care must be taken to select the peak which gives the proper PA quadrant, or as in our case, the mirror image quadrant.

The WDS gives magnitudes 6.06 and 6.17, spectral type G5V for STF2173AB. The latest orbit solution (Heintz 1994) has a period of 46.4 years, and Hipparcos gives a distance of 53 light years. The orbit is classed as Grade 1 (definitive) because of complete coverage by micrometer observations over several orbits, and nearly complete coverage by speckle and other more accurate techniques. This binary has been well observed since 1829, but only measurements since the first speckle observations in 1977, by Harold McAlister with the Kitt Peak 2.1-meter and 4-meter telescopes (McAlister 1979 & 1982) are shown in Figure 10. (The earliest handful of speckle observations, before 1979, had PA values in the 0- to 20-degree range, but are plotted here with 360 degrees added, for continuity).

STF2173AB was observed in the engineering checkout run to help evaluate the accuracy of the TAI speckle system, and Figure 10 shows that the measurements were indeed close to the predicted orbit ephemerides. On our observation date, the predicted PA was 142.85 degrees; our measurements were within 1 degree in all four bands. The predicted separation was 0.648″; our B, Rc and Ic measures were as much a 0.036″ higher, while the V band measure was 0.024″ lower. These comparisons give a first rough assessment of the overall system accuracy.

The WDS orbit plot is shown in Figure 11. Our largest and smallest measured separation points (V and Rc bands of Table 2) have been superimposed on the orbit plot, while the nearby smaller circle is a measure

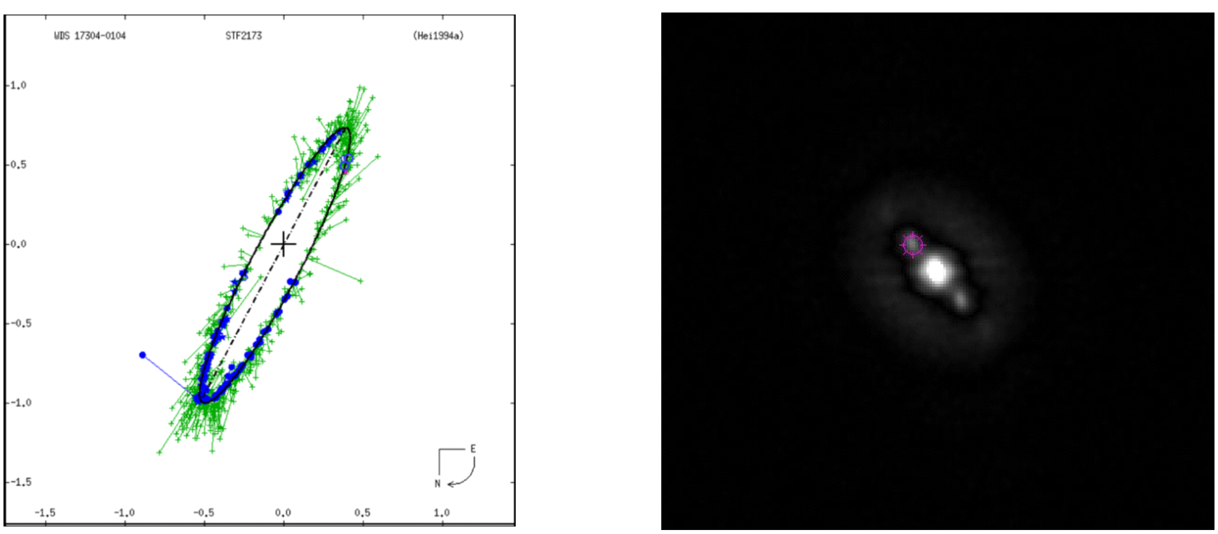

Figure 11. Left: WDS orbit plot of STF2173AB with the two farthest apart new TAI points (blue circles). Right: STB Autocorrelogram in the V band. (Orientation is North up, East right.)

Speckle Interferometry of Four Close Binaries ...

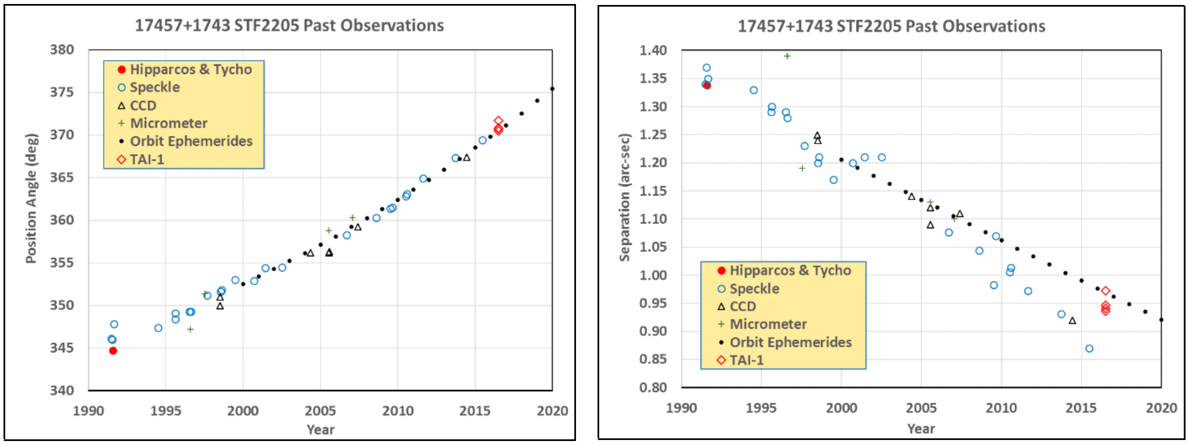

Figure 12. All observations since 1990 of Double Star STF2205, including all Speckle data.

made in 1970 by a visual interferometry technique on the previous orbit (Laques et al. 1971). Both new points fall very near the orbit. The STB autocorrelogram, also seen in Figure 11, was 256 x 256 pixels, and shows the STB solution "ship's wheel" marking the selected secondary peak. The slight smearing of the peaks into an oval shape, as noted in Table 2, was likely caused by atmospheric dispersion; it was greatest in the B and V bands, but not noticeable in Rc and Ic. Although the star was observed not far from the meridian, its declination is about -1 degree, so it was at least 34 degrees from the zenith at our latitude, and atmospheric dispersion is strongest at shorter wavelengths.

STF 2205

The WDS gives magnitudes 9.37 and 9.59, spectral type K0 for STF2205. The orbit solution (Cvetkovic et al. 2008) has a period of 1,971 years, but there is no estimate of distance. The orbit has been observed by micrometer since 1830, but the first speckle measurements were not made until 1991, about the same time as Hipparcos. Position angle and separation data for all observations since the Hipparcos era are shown in Figure 12.

Our new PA data are in reasonable agreement with the orbit ephemerides. Since this star is fairly faint and has spectral type K0, the data quality was poor in the B band, but much better in V, Rc, and Ic. In B, the companion was very faint, giving weak autocorrelogram peaks hardly distinguishable from the noise; therefore, it is not considered reliable. Likewise, the separation measurement in B is poor and displaced from those of

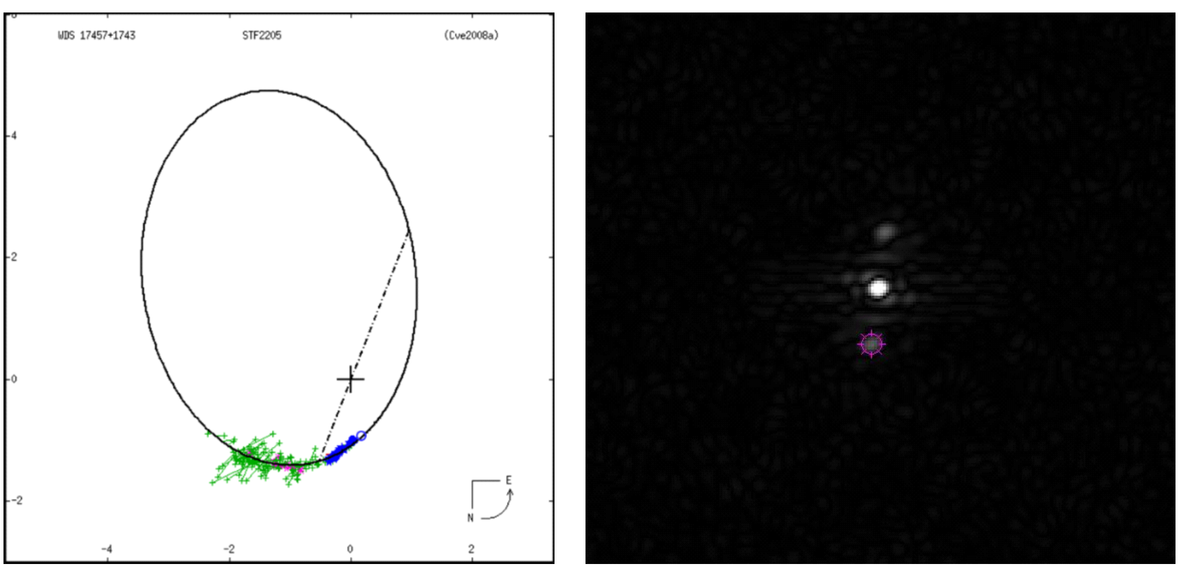

Figure 13. Left: WDS orbit plot of STF2205, with our new Rc band point added (blue circle). Right: STB Autocorrelogram in the Ic band. (Orientation is North up, East right.)

Speckle Interferometry of Four Close Binaries ...

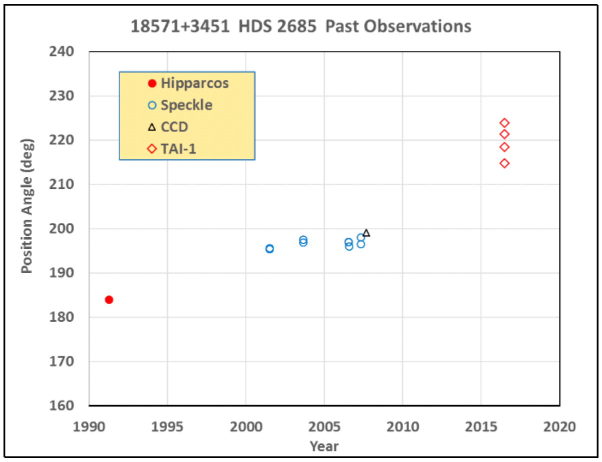

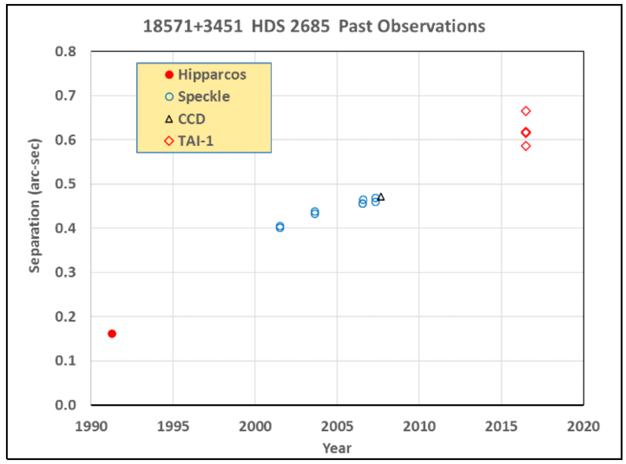

Figure 14. All observations Double Star HDS2685.

the V, Rc, and Ic bands.

Note that there is considerable scatter in all the historic speckle interferometry separation data; in addition, there are large systematic deviations from the orbital solution, and our new data seem out of line with other recent data. However, close inspection suggests the *possibility of a cyclic pattern*, indicating that one of the components may itself be a close binary, perhaps with a period on the order of 15 years.

The WDS orbit plot and an example autocorrelogram (Ic band) are shown in Figure 13. The new TAI Rc point has been superimposed on the orbit plot, showing close agreement with the ephemerides, but as in Figure 12, shifted from the earlier speckle trend. Since the period is so long, nearly 200 years of observations have covered very little of the orbit so far. It will probably be classified as Grade 4 (preliminary) for a long time to come, but good measurements now will be appreciated by future astronomers! Frequent observations will still be useful in the near-term as the companion moves faster through periastron, and to explore the possibility of third body motion. The STB autocorrelogram was 256x256 pixels, and shows the STB solution “ship’s wheel” marking the selected secondary peak.

The WDS gives magnitudes 7.8 and 9.78, and spectral type F8 for HDS2685. There is no orbit solution, since this star has only been observed 11 times since its discovery by the Hipparcos satellite in 1991. Hipparcos measured its distance as 247 light years. All position angle and separation observations are shown in Figure 14.

This star was chosen as a challenge for our engineering checkout run, to evaluate performance on a faint, close target. All the HDS2685 measurements in Table 2 are considered uncertain at best, because the companion peaks in the autocorrelograms, although well separated from the primary peak, were so faint as to not be unique or clearly distinguishable from numerous other small “noise” patches. This was true even in the Ic band, which should have had the best chance of reaching the faint, presumably red companion. Therefore, it is clear that this star was “in the noise,” exceeding the capabilities of the current TAI speckle interferometry system.

It is noteworthy that the only successful speckle measurements prior to our attempt were made by professional astronomers with large telescopes: the 3.5-meter WIYN telescope at Kitt Peak (Horch 2008 and 2010) and the Mt. Wilson 100-inch telescope (Hartkopf and Mason 2009).

Conclusions

The TAI 24-inch speckle imaging system, as it was configured for the July run, was still essentially an engineering exercise. As such, we were still able to successfully observe position angle and separation for the binary systems STF2173AB, D15, and STF2205, but obtained poor results for HDS2685.

There are currently too many manual steps involved in the data acquisition process for it to be of practical use for student research. Fortunately, many of these steps can be removed by hardware upgrades and increasing automation. TAI already has a 4K x 4K Finger Lake Instruments CCD camera that will be used for plate solving, which will eliminate manual centering of each target. In fact, the camera has already been installed. Automated target pointing and centering should also easily be accomplished by writing scripts to communicate with the mount using standard instrument software interfaces.

The speckle imaging camera was new and not fully understood. Because the camera had a digital gain setting that was likely not optimum, much of the camera's dynamic range was lost. Additionally, the operators had little experience with the FC camera control software that added extra time to the data acquisition process. Obtaining more experience with the complete system will be necessary to develop efficient procedures for student researchers to follow.

Acknowledgments

We thank TAI for use of the 24-inch telescope, the SDAA for use of its Tierra del Sol facilities, and Jerry Hillburn for hosting the engineering checkout barbecue. David Rowe's Speckle Tool Box enabled the data reduction and measurements, and REDUC aided in calibration. Bob Buchheim kindly provided his method for superimposing new points on WDS orbit plots. We thank Vera Wallen for paper edits. Additionally, we thank the Boyce Research Initiatives and Education Foundation (BRIEF) for their support. This research made extensive use of the Washington Double Star Catalog maintained by the U.S. Naval Observatory, and Brian Mason kindly answered questions and supplied all previous observations.

References

Alzner, A. 2007. *IAUDS Information Circulars,* **163**, 1A.

Ashcraft, C. 2016. Speckle Interferometry with a Low Read-Noise CMOS Video Camera. *Journal of Double Star Observations*, 12, 280.

Bryant, Tom, 2015. http://mainsequence.org/html/wds/getListOfDoubles/listWithOrbits.html

Cvetkovic, Z., Novakovic, B., & Todorovic, N. 2008. *New Astronomy* **13**, 125.

Edelmann, Torsten, 2016. www.firecapture.de/

Genet, R.M. 2013. Portable Speckle Interferometry Camera System. *Journal of Astronomical Instrumentation,* 2, 1340008.

Genet, R., Rowe, D. Ashcraft, C., Wen, S., Jones, G., Schillings, B, Harshaw, R., Ray, J, & Hass, J. 2016. Speckle Interferometry of Close Visual Binaries with the ZW Optical ASI 224MC CMOS Camera. *Journal of Double Star Observations,* **12**, 270.

Grey, Dan, 2016. Sidereal Technology web site, http://www.siderealtechnology.com

Hartkopf, W.I. & Mason, B.D., 2009. *AJ*, **138**, 813.

Heintz, W.D. 1978. Double Stars. Dordrecht, Holland: D. Reidel.

Heintz, W.D. 1994. *AJ*, **108**, 2338.

Horch, E.P., van Altena, W.F., Cyr, W.M., Jr., Kinsman-Smith, L., Srivastava, A., & Zhou, J., 2008, *AJ,* **136**, 312.

Horch, E.P., Falta, D., Anderson, L.M., DeSousa, M.D., Miniter, C.M., Ahmed, T., & van Altena, W.F., 2010. *AJ*, **139**, 205.

Laques, P., Bucher, A., & Despiau, R., 1971. *A&A*, **15**, 179.

Losse, Florent, 2015. http://www.astrosurf.com/hfosaf/uk/speckle10.htm

McAlister, H. A., 1979. *ApJ,* **230**, 497.

McAlister, H.A. & Hendry, E.M., 1982. *ApJS*, **48**, 273.

Moltisanti, Enrico, 2016. Stelle Doppie WDS search web site http://stelledoppie.goaction.it/index2.php

Mitchell, Larry, 2003. Megastar5, www.wilbell.com

Rowe, David, 2016. STB1.05, private communication.

Rowe, David and Genet, Russell, 2015. User's Guide to PS3 Speckle Interferometry Reduction Program, *JDSO*, **11**, 266-276, September 2015.

Jonckheere Double Star Photometry – Part IV: Cetus

Wilfried R.A. Knapp
Vienna, Austria
wilfried.knapp@gmail.com

Abstract: If any double star discoverer is in urgent need of photometry then it is Jonckheere. There are over 3000 Jonckheere objects listed in the WDS catalog and a good part of them have magnitudes which are obviously far too bright. This report covers the Jonckheere objects in the constellation Cet. Only one image per object was taken as despite the risk of random effects even a single measurement is better than the currently usually given estimation although the J-objects in this southern constellation are better covered with observations as usual for Jonckheere doubles.

Preamble

This report in no way intends to belittle the work of Jonckheere – on the contrary: He was obviously a very dedicated and able double star observer fighting with a lot of obstacles up to equipment destroyed in war. It seems that the basic double star parameters, RA/Dec coordinates and separation as well as position angle, were his main concern and the estimation of magnitudes was rather a side aspect to him. The often crass over estimation of magnitudes may also be a side effect of his obviously extraordinary eyesight.

Introduction

The degree of contamination of the WDS catalog with wrong magnitude data is rather high – this might very well be a side effect of magnitudes considered being not as important as the basic double star parameters separation and position angle. Measurements of magnitudes without these basic parameters are not even counted as observations in the WDS catalog. As follow up to the report on J-objects so far I selected this time all J-objects in Cet to be imaged for measurements with iT27 located in Australia due to the low altitude. The number of objects is with ~20 rather small so I decided to have also a look at other catalogs like SDSS, URAT1 and GAIA DR1 with recent position data if available for the objects in question for counter-checking. This should compensate also for the questionable quality of some of the taken images.

Results of Photometry and Catalog Checking

For each of the selected J-objects one single image was taken with iTelescope iT27 with V-filter and 3s exposure time, plate solved with Astrometrica using the UCAC4 (or if available URAT1) catalog with reference stars in the Vmag range of 10.5 to 14.5 giving not only RA/Dec coordinates but also photometry results for all reference stars used including an average dVmag error. The J-objects were then located in the center of the image and photometry was then done by the rather comfortable Astrometrica procedure with point and click at the components delivering Vmag measurements based on all reference stars used for plate solving.

The results are given in Table 1 with the following structure:

- The header line gives the WDS catalog data for each object per 08/2016 with RA/Dec in the HH:MM:SS/DD:MM:SS format and Date giving the date of the last observation
- The following rows give the data for the object in existing catalogs as far as available with
  - ◊ RA/Dec in decimal degrees with the catalog reference given in the Source/Notes column
  - ◊ Estimated visual M1 and M2 for 2MASS objects calculated from J- and K-band magnitudes if available
  - ◊ Visual M1 and M2 for URAT1 objects if available

Jonckheere Double Star Photometry – Part IV: Cet

- ◊ Used Aperture and observation method code is given in the Ap and Me columns. As GAIA uses a rectangular aperture the value given in the Ap column is the calculated diameter for a corresponding circular surface
- ◊ Date gives the Bessel observation epoch
- ◊ If 2MASS and URAT1 or GAIA DR1 positions are available then also proper motion data is calculated (using the formulas provided by Buchheim – 2008 to determine proper motion vector direction and proper motion vector length) and checked for potential common proper motion with the CPM rating procedure according to Knapp and Nanson 2016. With the new GAIA DR1 data several objects qualify now for common proper motion pairs – in all cases with a relationship of Sep/PM of far less than 1000 years, in most cases even less than 100 years indicating a high probability of being real

- The last row gives then the measurements based on the iT27 images
    - ◊ RA/Dec in decimal degrees from plate solving
    - ◊ Sep and PA are calculated from the RA/Dec coordinates in degrees using the formulas provided by Buchheim - 2008
    - ◊ Visual magnitudes M1 and M2 based on the plate solving results
    - ◊ Error estimations calculated on base of the average plate solving errors are given in the Notes column

Summary

Table 1 shows with few exceptions significant differences for the magnitudes compared with the WDS data even if the J-objects in Cet seem rather well researched in comparison with northern constellations. A surprisingly high percentage of the objects qualify as CPM pairs based on calculations with the now available GAIA DR1 data.

Acknowledgements:

The following tools and resources have been used for this research:

- 2MASS catalog
- 2MASS images
- AAVSO APASS (via the UCAC4 catalog)
- AAVSO VPhot
- Aladin Sky Atlas v9.0
- Astrometrica v4.10.0.427
- AstroPlanner v2.2
- iTelescope iT27: 700mm CDK with 4531mm focal length. CCD: FLI PL09000. Resolution 0.53 arcsec/pixel. V-filter. Siding Spring, Australia. Elevation 1122m
- GAIA DR1 catalog
- MaxIm DL6 v6.08
- POSS images
- SDSS DR9 and DR7 catalogs
- SDSS images
- SIMBAD
- UCAC4 catalog
- URAT1 catalog
- VizieR
- Washington Double Star Catalog

References

Buchheim, Robert, 2008, "CCD Double-Star Measurements at Altimira Observatory in 2007", *Journal of Double Star Observations*, **4**, 27-31.

Knapp, Wilfried; Nanson, John, 2017, "A New Concept for Counter-Checking of Assumed CPM Pairs", *Journal of Double Star Observations*, **13**, 31-51.

Jonckheere Double Star Photometry – Part IV: Cet

Table 1. J Objects in Cetus

J#	RA	Dec	Sep"	PA°	M1	M2	pmRA1	pmDec1	e_pm1	pmRA2	pmDec2	e_pm2	Spc1	Spc2	Ap	Me	Date	CPM Rat	Source/Notes
302	00:50:23.480	-01:05:55.9	4.4	71.0	10.91	11.90	12	-14		26	-11		F2				2000		WDS00508-0052 values per 08/2016
	12.59784200	-1.0988670	4.38	70.2											2.5	Es	2003.809		SDSS DR9
	12.59790417	-1.0989194	3.89	67.2	10.47	12.19									0.7	C	2016.023		iT27 1x3s/UCAC4. Touching star disks, image quality not very good. Err_Sep 0.297", Err_PA 4.364°, Err_Mag 0.105/0.109
																			Despite the clear elongation in the 2MASS images indicating touching star disks there is no 2MASS catalog object for B, the same goes for URAT1 and GAIA DR1
303	03:04:50.230	+08:06:49.0	3.0	38.0	10.29	11.83	2	3					F8				2010		WDS03048+0807 values per 08/2016
	46.20931621	8.1136483	3.01	39.9											0.96	Hg	2015		GAIA DR1
	46.20929583	8.1137528	2.46	39.4	10.41	11.08									0.7	C	2016.024		iT27 1x3s/URAT1. Touching/ Overlapping star disks. Err_Sep 0.234", Err_PA 5.445°, Err_Mag 0.082/0.088
304	03:21:34.880	+08:04:35.0	4.3	85.0	10.84	11.50	2	-23		-12	-11		G5				2014		WDS03214+0803 values per 08/2016
	50.39532800	8.0764200	4.55	84.0	10.78	12.02									1.3	E2	2000.019		2MASS. M1/M2 estimated from J- and K-band
	50.39546440	8.0763144	4.41	84.0	10.33		35.84	-28.02	12.55	25.63	-28.28	12.42	G3		0.2	Eu	2013.658	CCC	URAT1. PM data calculated from position comparison with 2MASS - not obviously CPM pair. Spc according to B-V color index
	50.39546010	8.0763076	4.54	83.7			31.43	-27.00	11.37	30.76	-25.38	11.37			0.96	Hg	2015	AAC	GAIA DR1. PM data calculated from position comparison with 2MASS suggests CPM despite the rather large 2MASS position error
	50.39547500	8.0763194	4.41	86.2	10.54	12.12									0.7	C	2016.024		iT27 1x3s/URAT1. Err_Sep 0.120", Err_PA 1.566°, Err_Mag 0.090/0.091
648	02:28:55.340	+00:43:17.2	2.5	157.0	10.70	11.00											2001		WDS02289+0044 values per 08/2016
	37.23044900	0.7216480	2.83	155.1											2.5	Es	1998.878		SDSS DR9. A and B same observa- tion date
	37.23043800	0.7216520	2.82	155.9											2.5	Es	2000.904		SDSS DR9. A and B same observa- tion date
	37.23041900	0.7216470	2.77	151.6											2.5	Es	2001.723		SDSS DR9. A and B same observa- tion date
	37.23041700	0.7216150	2.44	158.4											2.5	Es	2001.890		SDSS DR7
	37.23042900	0.7216070	2.53	154.9											2.5	Es	2004.841		SDSS DR9. A and B same observa- tion date
	37.23044000	0.7216330	2.66	157.5											2.5	Es	2004.861		SDSS DR9. A and B same observa- tion date
	37.23036853	0.7215815	2.74	155.5			-17.97	-14.84	5.99	-21.19	-10.20	5.99			0.96	Hg	2015	CAC	GAIA DR1. PM data calculated from position comparison with SDSS DR9 1998.878 suggests not CPM
	37.23036250	0.7216250	2.34	154.1	10.53	10.96									0.7	C	2016.023		iT27 1x3s/URAT1. Err_Sep 0.219", Err_PA 5.367°, Err_Mag 0.092/0.095
																			The spread within the SDSS meas- urements is amazing

Table 1 continues on next page.

Table 1. J Objects in Cetus

J#	RA	Dec	Sep"	PA°	M1	M2	pmRA1	pmDec1	e_pm1	pmRA2	pmDec2	e_pm2	Spc1	Spc2	Ap	Me	Date	CPM Rat	Source/Notes
1252	03:02:08.210	+07:09:42.0	4.6	269.0	11.98	12.17	21	-2		-23	3						2014		WDS03021+0710 values per 08/2016
	45.53424900	7.1616660	4.59	269.2	11.84	11.91									1.3	E2	1999.932		2MASS. M1/M2 estimated from J- and K-band
	45.53424330	7.1616564	4.60	269.1			-1.46	-2.47	10.31	-2.00	-3.29	10.22			0.2	Eu	2013.980	ACC	URAT1. PM data calculated from position comparison with 2MASS, values too small to be significant
	45.53424981	7.1616565	4.62	268.9			0.19	-2.28	9.57	-1.70	-4.03	9.57			0.96	Hg	2015	CCC	GAIA DR1. PM data calculated from position comparison with 2MASS suggests not CPM
	45.53428750	7.1617139	5.17	264.5	12.04	12.11									0.7	C	2016.023		iT27 1x3s/URAT1. Average position error after plate solving rather large. Err_Sep 0.391", Err_PA 4.324°, Err_Mag 0.112/0.112
1432	00:11:01.280	-06:26:24.2	7.2	274.0	11.10	12.70	-8	-13		-40	-4						1999		WDS00110-0627 values per 08/2016
	2.75534000	-6.4400870	7.25	274.4	10.84	12.48									1.3	E2	1998.790		2MASS. M1/M2 estimated from J- and K-band
	2.75533100	-6.4400910	7.34	273.8			-4.06	-1.82	26.36	-16.26	-11.82	26.36			2.5	Es	2006.711	CCC	SDSS DR9. PM data calculated from position comparison with 2MASS, values do not suggest CPM
	2.75528054	-6.4401229	7.17	274.0			-21.78	-13.86	13.73	-0.91	-11.55	13.73			0.96	Hg	2015	CCC	GAIA DR1. PM data calculated from position comparison with SDSS9 - not CPM
	2.75525000	-6.4400583	7.16	274.6	10.85	12.65									0.7	C	2016.029		iT27 1x3s/UCAC4. Err_Sep 0.184", Err_PA 1.470°, Err_Mag 0.071/0.072
1436 AB	00:33:37.360	-16:55:42.7	6.1	113.0	10.70	11.70	-77	-47		10	-84						2008		WDS00336-1656 values per 08/2016
	8.40566600	-16.9285220	6.10	113.3	11.22	11.82									1.3	E2	1999.604		2MASS. M1/M2 estimated from J- and K-band
	8.40556800	-16.9286470	5.99	112.5			-47.27	-63.02	14.01	-55.95	-46.39	14.01			2.5	Es	2006.744	CBC	SDSS DR9. PM data calculated from position comparison with 2MASS, values do rather not suggest CPM
	8.40543534	-16.9287133	6.05	113.2			-51.60	-44.73	6.50	-54.10	-42.94	6.50			0.96	Hg	2015	AAB	GAIA DR1. PM data calculated from position comparison with 2MASS suggests solid CPM
	8.40530833	-16.9288139	6.20	111.1	11.10	11.82									0.7	C	2016.023		iT27 1x3s/UCAC4. Err_Sep 0.262", Err_PA 2.425°, Err_Mag 0.091/0.093
1436 AC	00:33:37.360	-16:55:42.7	23.9	72.0	10.70	11.18	-77	-47		78	-88						2008		WDS00336-1656 values per 08/2016
	8.40566600	-16.9285220	23.03	70.7	11.22	11.27									1.3	E2	1999.604		2MASS. M1/M2 estimated from J- and K-band
	8.40556800	-16.9286470	23.77	72.2			-47.27	-63.02	14.01	78.62	-111.93	14.01			2.5	Es	2006.744	CCC	SDSS DR9. PM data calculated from position comparison with 2MASS, values suggest optical pair. Different PM direction causes Sep and PA change over time
	8.40543534	-16.9287133	24.68	74.0			-51.60	-44.73	6.50	77.01	-96.65	6.50			0.96	Hg	2015	CCB	GAIA DR1. PM data calculated from position comparison with 2MASS suggests not CPM
	8.40530833	-16.9288139	24.91	73.8	11.10	11.21									0.7	C	2016.023		iT27 1x3s/UCAC4. Err_Sep 0.262", Err_PA 0.604°, Err_Mag 0.091/0.091
1438	00:46:12.600	-05:14:17.1	5.8	348.0	12.10	12.30	57	10		59	14						1999		WDS00462-0514 values per 08/2016
	11.55250300	-5.2380810	5.77	347.2	11.73	11.90									1.3	E2	1998.746		2MASS. M1/M2 estimated from J- and K-band
	11.55268900	-5.2380620	5.82	347.4			65.05	6.67	8.28	65.75	11.59	8.28			2.5	Es	2008.997	BAC	SDSS DR9. PM data calculated from position comparison with 2MASS, values suggest to some degree CPM
	11.55277602	-5.2380473	5.81	347.5			60.22	7.46	5.22	61.56	10.08	5.22			0.96	Hg	2015	AAB	GAIA DR1. PM data calculated from position comparison with 2MASS suggests solid CPM
	11.55275000	-5.2381750	5.56	348.5	11.88	12.09									0.7	C	2016.023		iT27 1x3s/UCAC4. Huge average position error after plate solving suggests fast PM of several reference stars or very bad image. Err_Sep 0.262", Err_PA 0.604°, Err_Mag 0.091/0.091
1441	00:53:24.610	-05:45:20.6	7.5	334.0	10.40	12.40	-19	-37		-18	-37		G0				2014		WDS00534-0545 values per 08/2016
	13.35259700	-5.7557320	7.54	335.0	10.18	11.78									1.3	E2	1998.823		2MASS. M1/M2 estimated from J- and K-band
	13.35251500	-5.7557930	7.41	334.5			-28.87	-21.58	10.63	-28.52	-36.44	10.63			2.5	Es	2008.997	CCC	SDSS DR9. PM data calculated from position comparison with 2MASS, values suggest not CPM
	13.35249912	-5.7558880	7.50	334.5			-21.67	-34.72	6.69	-24.35	-38.84	7.05			0.96	Hg	2015	ACC	GAIA DR1. PM data calculated from position comparison with 2MASS. Potential CPM - difference in PM vector length might suggest an orbit
	13.35239167	-5.7557889	7.75	335.2	10.03	11.66									0.7	C	2016.023		iT27 1x3s/UCAC4. Huge average position error after plate solving suggests fast PM of several reference stars or very bad image. Err_Sep 0.587", Err_PA 0.433°, Err_Mag 0.101/0.103

Table 1 continues on next page.

Jonckheere Double Star Photometry – Part IV: Cet

Table 1. J Objects in Cetus

J#	RA	Dec	Sep"	PA°	M1	M2	pmRA1	pmDec1	e_pm1	pmRA2	pmDec2	e_pm2	Spc1	Spc2	Ap	Me	Date	CPM Rat	Source/Notes
1444 AB	01:19:10.760	-04:39:24.9	6.9	190.0	10.13	14.80	26	0		-36	-29						1999		WDS01192-0439 values per 08/2016
	19.79483300	-4.6569920	6.50	184.9	9.97	14.00									1.3	E2	1998.714		2MASS. M1/M2 estimated from J- and K-band
	19.79493600	-4.6569180	6.94	182.6			35.94	25.91	8.25	59.67	-18.55	8.25			2.5	Es	2008.997	CCC	SDSS DR9. PM data calculated from position comparison with 2MASS, values suggest not CPM
	19.79496845	-4.6569249	6.92	182.3			30.04	14.93	6.69	47.44	-12.42	6.69			0.96	Hg	2015	CCC	GAIA DR1. PM data calculated from position comparison with 2MASS suggests not CPM
	19.79483333	-4.6569639	6.29	184.9	9.94	14.54									0.7	C	2016.023		iT27 1x3s/UCAC4. Image quality questionable. Err_Sep 0.342", Err_PA 3.111°, Err_Mag 0.080/0.139
1444 AC	01:19:10.760	-04:39:24.9	51.0	168.0	10.13	11.80	26	0		2	4						2013		WDS01192-0439 values per 08/2016
	19.79483300	-4.6569920	51.06	167.0	9.97	12.43									1.3	E2	1998.714		2MASS. M1/M2 estimated from J- and K-band
	19.79493600	-4.6569180	51.06	167.3			35.94	25.91	8.25	9.42	18.90	8.25			2.5	Es	2008.997	CCC	SDSS DR9. PM data calculated from position comparison with 2MASS, values suggest not CPM
	19.79496845	-4.6569249	50.99	167.5			29.84	14.83	5.21	4.42	13.11	5.21			0.96	Hg	2015	CCC	GAIA DR1. PM data calculated from position comparison with 2MASS suggests not CPM
	19.79483333	-4.6569639	50.91	167.6	9.94	12.38									0.7	C	2016.023		iT27 1x3s/UCAC4. Image quality questionable. Err_Sep 0.342", Err_PA 0.385°, Err_Mag 0.080/0.083
1444 CD	01:19:11.530	-04:40:14.8	8.6	89.0	11.80	11.90	2	4		11	9						2013		WDS01192-0439 values per 08/2016
	19.79803600	-4.6708100	8.50	88.4	12.43	12.80									1.3	E2	1998.714		2MASS. M1/M2 estimated from J- and K-band
	19.79806300	-4.6707560	8.59	88.6			9.42	18.90	8.25	18.84	15.40	8.25			2.5	Es	2008.997	CCC	SDSS DR9. PM data calculated from position comparison with 2MASS, values too small to suggest CPM
	19.79805607	-4.6707507	8.64	88.7			4.42	13.11	5.21	13.10	10.26	5.21			0.96	Hg	2015	CCC	GAIA DR1. PM data calculated from position comparison with 2MASS - values too small to suggest CPM
	19.79789167	-4.6707722	8.70	89.4	12.38	12.87									0.7	C	2016.023		iT27 1x3s/UCAC4. Image quality questionable. Err_Sep 0.587", Err_PA 2.251°, Err_Mag 0.083/0.088
1446	01:27:24.290	-02:04:01.8	10.6	143.0	10.05	13.20	-32	-24		-24	-42						1999		WDS01274-0204 values per 08/2016
	21.85124800	-2.0671810	10.63	143.2	10.06	12.43									1.3	E2	1998.719		2MASS. M1/M2 estimated from J- and K-band
	21.85112100	-2.0672180	10.61	142.7			-45.19	-13.17	15.64	-39.50	-5.70	15.64			2.5	Es	2008.830	CCC	SDSS DR9. PM data calculated from position comparison with 2MASS, values suggest not CPM
	21.85111826	-2.0672753	10.57	143.0			-28.67	-20.85	9.71	-29.09	-16.48	9.71			0.96	Hg	2015	CBC	GAIA DR1. PM data calculated from position comparison with 2MASS - values too small to suggest CPM. Yet comparison POSS I and II images show very well a quite similar if small proper motion
	21.85103333	-2.0672694	10.55	141.9	9.79	12.37									0.7	C	2016.023		iT27 1x3s/UCAC4. Image quality questionable. Err_Sep 0.331", Err_PA 1.799°, Err_Mag 0.090/0.093
1447	01:39:31.580	-06:11:53.8	3.3	207.0	11.50	11.60	29	64		-14	-16		K4				2004		WDS01395-0612 values per 08/2016
	24.88156500	-6.1982820	2.60	204.5	9.97	10.33									1.3	E2	1998.815		2MASS. M1/M2 estimated from J- and K-band
	24.88159500	-6.1981860	3.40	205.9			10.50	33.79	13.90	-29.39	-33.44	18.68			2.5	Es	2009.044	CCC	SDSS DR9. PM data calculated from position comparison with 2MASS, values suggest not CPM
	24.88158178	-6.1981973	3.23	206.0			3.71	18.83	9.77	-17.19	-14.05	9.77			0.96	Hg	2015	CCC	GAIA DR1. PM data calculated from position comparison with 2MASS - values suggest not CPM
	24.88158750	-6.1983389	2.95	207.4	10.95	11.02									0.7	C	2016.023		iT27 1x3s/URAT1. Touching/Overlapping star disks. Err_Sep 0.201", Err_PA 3.902°, Err_Mag 0.093/0.093
1448 AB	01:45:32.210	-02:24:13.1	8.0	150.0	11.60	13.20	62	14		11	-17		G8				1999		WDS01456-0224 values per 08/2016
	26.38419700	-2.4036300	8.09	150.9	11.32	12.71									1.3	E2	1998.728		2MASS. M1/M2 estimated from J- and K-band
	26.38420600	-2.4038660	7.53	146.9			3.20	-84.09	9.13	20.65	-8.20	9.13			2.5	Es	2008.831		SDSS DR9. PM data calculated from position comparison with 2MASS, values suggest not CPM
	26.38418810	-2.4039453	7.34	145.7			-2.16	-76.55	6.22	11.50	-8.37	6.29			0.2	Eu	2013.474	CCC	URAT1. PM data calculated from position comparison with 2MASS, values suggest not CPM
	26.38418597	-2.4039822	7.25	145.1			-2.44	-77.91	5.67	10.24	-9.06	5.67			0.96	Hg	2015	CCC	GAIA DR1. PM data calculated from position comparison with 2MASS - values suggest not CPM
	26.38414583	-2.4040167	7.34	143.4	11.20	12.65									0.7	C	2016.023		iT27 1x3s/URAT1. Err_Sep 0.113", Err_PA 0.883°, Err_Mag 0.110/0.112

Table 1 continues on next page.

Jonckheere Double Star Photometry – Part IV: Cet

Table 1. J Objects in Cetus

J#	RA	Dec	Sep"	PA°	M1	M2	pmRA1	pmDec1	e_pm1	pmRA2	pmDec2	e_pm2	Spc1	Spc2	Ap	Me	Date	CPM Rat	Source/Notes
1448 BC	01:45:32.470	-02:24:20.1	14.4	257.0	13.20	12.80	11	-17		-10	-11						1999		WDS01456-0224 values per 08/2016
	26.38529200	-2.4055940	14.37	257.6	12.71	11.77									1.3	E2	1998.728		2MASS. M1/M2 estimated from J- and K-band
	26.38535000	-2.4056170	14.70	254.9			20.65	-8.20	9.13	4.98	-81.24	9.13			2.5	Es	2008.831		SDSS DR9. PM data calculated from position comparison with 2MASS, values suggest not CPM
	26.38533890	-2.4056281	14.79	254.0			11.50	-8.37	6.29	-0.44	-75.06	6.22			0.2	Eu	2013.468	CCC	URAT1. PM data calculated from position comparison with 2MASS, values suggest not CPM
	26.38533833	-2.4056350	14.82	253.6			10.24	-9.06	5.67	-1.05	-75.94	5.67			0.96	Hg	2015	CCC	GAIA DR1. PM data calculated from position comparison with 2MASS - values suggest not CPM
	26.38536250	-2.4056528	14.83	254.3	12.65	11.64									0.7	C	2016.023		iT27 1x3s/URAT1. Err_Sep 0.113", Err_PA 0.437°, Err_Mag 0.112/0.111
1449 AB	01:58:55.780	-09:48:41.6	8.6	328.0	11.70	13.20	-21	-32		16	4						2010		WDS01588-0949 values per 08/2016
	29.73243700	-9.8116200	8.39	323.1	11.46	12.14									1.3	E2	1998.810		2MASS. M1/M2 estimated from J- and K-band
	29.73242700	-9.8116260	8.38	323.0			-18.40	-11.20	55.14	-20.24	-18.67	55.14			2.5	Es	2000.738		SDSS DR9. Time frame far too short to get reliable pm data from comparison with 2MASS
	29.73235460	-9.8117511	8.44	328.1	11.18		-19.37	-31.27	7.04	19.41	-0.81	7.03			0.2	Eu	2013.912	CCC	URAT1. PM data calculated from position comparison with 2MASS, values suggest not CPM
	29.73235792	-9.8117474	8.45	328.6			-17.33	-28.32	6.57	22.00	2.48	6.57			0.96	Hg	2015	CCC	GAIA DR1. PM data calculated from position comparison with 2MASS, values suggest not CPM
	29.73232917	-9.8117500	8.43	328.5	11.41	12.19									0.7	C	2016.023		iT27 1x3s/URAT1. Err_Sep 0.114", Err_PA 0.775°, Err_Mag 0.071/0.071
1450 AB	02:05:24.77	-09:47:31.1	5.9	1.0	10.18	10.48	147	-37		147	-38		K2				2009		WDS02054-0947 values per 08/2016
	31.35321300	-9.7920010	6.06	2.5	10.18	10.28									1.3	E2	2000.803		2MASS. M1/M2 estimated from J- and K-band
	31.35322600	-9.7919970	5.94	2.5											2.5	Es	2000.738		SDSS DR9. Time frame far too short to get reliable pm data from comparison with 2MASS
	31.35376310	-9.7921044	6.19	2.2			148.48	-28.32	17.38	146.26	-18.79	17.43			0.2	Eu	2013.928	BAC	URAT1. PM data calculated from position comparison with 2MASS, values suggest CPM despite some difference in the pm vector direction and a rather large 2MASS position error range
	31.35382135	-9.7921045	6.14	2.1			152.01	-26.23	16.09	149.04	-20.68	16.09			0.96	Hg	2015	AAC	GAIA DR1. PM data calculated from position comparison with 2MASS, values suggest CPM
	31.35384583	-9.7920694	6.05	1.0	10.17	10.52									0.7	C	2016.023		iT27 1x3s/URAT1. Err_Sep 0.214", Err_PA 2.026°, Err_Mag 0.080/0.080
1451 AB	02:29:14.930	-07:13:24.6	5.4	172.0	11.00	12.40	-23	3		-7	-10						2004		WDS02292-0712 values per 08/2016
	37.31226000	-7.2235650	5.44	171.1	10.83	12.04									1.3	E2	1998.761		2MASS. M1/M2 estimated from J- and K-band
	37.31223100	-7.2235710	5.33	172.2											2.5	Es	2000.882		SDSS DR9. Time frame far too short to get reliable pm data from comparison with 2MASS
	37.31211080	-7.2235436	5.36	171.4	10.48		-35.09	5.07	9.15	-37.46	9.46	9.11			0.2	Eu	2013.979	CBC	URAT1. PM data calculated from position comparison with 2MASS, values suggest rather not CPM
	37.31212070	-7.2235341	5.44	171.9			-30.64	6.86	8.55	-35.27	6.09	8.55			0.96	Hg	2015	ACC	GAIA DR1. PM data calculated from position comparison with 2MASS, values suggest despite very similar pm vector direction rather not CPM as pm vector length is too short to be significant
	37.31212917	-7.2235611	5.22	172.3	10.71	12.03									0.7	C	2016.023		iT27 1x3s/URAT1. Err_Sep 0.175", Err_PA 1.917°, Err_Mag 0.100/0.101
1900 AB	01:18:47.720	-03:17:43.5	4.0	191.0	9.50	10.40	15	96		-12	-38						2013		WDS01188-0318 values per 08/2016
	19.69886800	-3.2954280	3.97	191.6	11.25	11.87									1.3	E2	1998.714		2MASS. M1/M2 estimated from J- and K-band
	19.69882700	-3.2953740	4.03	192.6			-14.57	19.22	13.44	-22.03	15.30	13.44			2.5	Es	2008.830	CCC	SDSS DR9. PM data calculated from position comparison with 2MASS, values suggest not CPM
	19.69882384	-3.2953495	3.98	191.0			-9.75	17.36	8.35	-6.98	16.68	8.35			0.96	Hg	2015	CBC	GAIA DR1. PM data calculated from position comparison with 2MASS, values suggest not CPM
	19.69864167	-3.2951306	4.10	188.4	10.89	11.71									0.7	C	2016.023		iT27 1x3s/URAT1. Err_Sep 0.294", Err_PA 4.099°, Err_Mag 0.121/0.124

Table 1 continues on next page.

Jonckheere Double Star Photometry – Part IV: Cet

Table 1 Explanations Notes column:

- "iT27 1x3s/URAT1 or UCAC4" indicates the use of telescope iT27 images with 3s exposure time and use of URAT1 or UCAC4 for plate solving
- „Err_Sep ", Err_PA °, Err_Mag M1/M2" gives the error estimations calculated as Err_Sep = SQRT (dRA^2+dDec^2) with dRA and dDec as average RA and Dec plate solving errors, Err_PA = arctan (Err_Sep/Sep) assuming the worst case that Err_Sep points perpendicular to the separation vector and Err_Mag = SQRT(dVmag^2+(2.5*LOG10(1+1/SNR))^2) with dVmag as average Vmag plate solving error and SNR as signal to noise ratio for the given object
- "Touching star disks" indicates that the rims of the star disks are touching and that the measurement results might be a bit less precise than with clearly separated star disks
- "Touching/Overlapping star disks" indicates that the star disks overlap to the degree of an elongation and that the measurement results is probably less precise than with clearly separated star disks
- "SNR <20" indicates that the measurement result might be a bit less precise than desired due to a low SNR value but this is already included in the calculation of the magnitude error range estimation
- "SNR <10" indicates that the measurement result is probably a bit less precise than desired due to a very low SNR value but this is already included in the calculation of the magnitude error range estimation
- "Image quality questionable" or similar indicates rather large average errors for the reference stars used for plate solving for different reasons. But this is already included in the calculation of the error range estimation

Gamma Cassiopeiae and HR 266: A Massive Septuplet Illuminating the IC 59 and IC 63 Nebulae at d = 168 pc

Eric Mamajek

Jet Propulsion Laboratory, California Institute of Technology, Pasadena, CA
University of Rochester, Rochester, NY

Abstract: The unusual prototype Be shell star γ Cas is part of a triple system (WDS J00567+6043) that illuminates two arc-shaped nebulae: IC 59 and IC 63. The HR 266 system (WDS J00568+6022) is a massive quadruple lying 1274" away from γ Cas (projected separation 1.0 pc), opposite of the reflection nebulae, which appears to be physically associated with this system based on common proper motion, radial velocity, and parallax. The entire γ Cas system appears to constitute a massive septuplet (at least), with approximately 15 $\mathcal{M}_{Sun}$ in mass associated with the γ Cas triplet, and about 13.5 $\mathcal{M}_{Sun}$ in mass associated with the HR 266 quadruplet. The γ Cas system appears to be one of the highest multiplicity systems known (N=7).

Introduction:

γ Cas (HR 264, HIP 4427, ADS 782, 2MASS J00564251+6043002) is a famous eruptive Be shell star, which has shown irregular brightness variations since its discovery as the first Be star by Secchi (1867; see historical discussion by Harmanec, *et al.* 2000 and also Jim Kaler's summary at http://stars.astro.illinois.edu/sow/cas.html).

It is listed with magnitude V = 2.15 in the Hipparcos catalog (ESA 1997), but V = 2.47 in the Bright Star Catalog (Hoffleit & Warren 1991). γ Cas has varied between approximately V ~ 1.6 to 3.0 over much of the past century, and at times it outshines both α Cas (Schedar; V ~ 2.2) and β Cas (Caph; V ~ 2.2), making it the brightest star in the "W" of Cassiopeia. The XHIP catalog (Anderson & Francis 2012) places γ Cas as the 28th most luminous star known within 200 pc of the Sun. γ Cas illuminates two bright rim nebulae in its immediate vicinity (IC 59 and IC 63) as well as a small, irregular H II region nearly 3 deg in diameter (Karr, *et al.* 2005). γ Cas and the nebulae IC 59 and IC 63 are shown in Digitized Sky Survey imagery shown in Figure 1.

γ Cas A is a spectroscopic binary with P = 203 day (Harmanec, *et al.* 2000; Nemravova, *et al.* 2012). The primary Aa is a B0.5IVe with mass ~13 $\mathcal{M}_{Sun}$[1], and the secondary Ab has a mass of approximately 1.0 $\mathcal{M}_{Sun}$ (Nemravova, *et al.* 2012). The primary Aa itself has a 1.1 day photometric periodicity which has been attributed to a close-in white dwarf companion (Apparao 2002), however the existence of such a companion has not yet been confirmed, and more recent work favors this periodicity as being due to the primary's rotation (e.g. Shrader, *et al.* 2015). The circumstellar disk of the Be star has been resolved interferometrically, and the disk appears to have inclination 42° (Stee, *et al.* 2012). With this inclination, γ Cas A is likely rotating near its critical velocity (Stee, *et al.* 2012). The γ Cas A pair companion further out at 2.2" separation (WDS J00567+6043 B = BU 1028) appears to be a V=10.9 F6V star sharing common proper motion. The WDS lists another companion at wider separation (WDS J00567+6043 C) at separation 54.3" with V=12.9, however the UCAC4 proper motion of this star (UCAC4 754-011021 = 2MASS J00564070+6043518; μ_α, μ_δ = -5.3 ± 2.7, +9.3 ± 3.8 mas/yr) is a poor match for γ Cas A (μ_α, μ_δ = +25.17 ± 0.08, -3.92 ± 0.08 mas/yr; van Leeuwen 2007), so it is unlikely to be a physical companion. At present, the γ Cas system appears to be at least a triple with a total mass of ~15 $\mathcal{M}_{Sun}$. Adopting

1. "$\mathcal{M}_{Sun}$" throughout should be understood to be nominal solar mass units, equivalent to the IAU 2015 nominal solar mass parameter ($\mathcal{GM}_\odot$) divided by the CODATA 2014 estimate of the Newtonian gravitational constant $\mathcal{G}$ (Prsa, *et al.* 2016).

Gamma Cassiopeiae and HR 266: A Massive Septuplet Illuminating the IC 59 and IC 63 Nebulae ...

Table 1. Positions, Proper Motions, and Trignometric Parallaxes for g Cas and HR 266 from revised Hipparcos Catalog

NAME	RA(deg)	Dec(deg)	pmRA(mas/yr)	pmDec(mas/yr)	plx(mas)
γ Cas	014.17708782	60.71674955	25.17±0.08	-3.92±0.08	5.94±0.12
HR266	014.19558681	60.36284788	26.13±0.30	-3.79±0.33	6.06±0.41

its trigonometric parallax from van Leeuwen (2007) of 5.94 ± 0.12 mas, and its radial velocity from Harmanec, *et al*. (2000) of -7.38 ± 0.64 km/s, I estimate the velocity of the γ Cas system in Galactic coordinates to be U, V, W = -12.7, -17.4, -2.4 (± 0.5, 0.5, 0.4) km/s (total heliocentric velocity 21.6 ± 0.5 km/s).

HR 266 (ADS 784, WDS J00568+6022, 2MASS J00564697+6021463) is a quadruple system consisting of stars of type B7IV (A), B9IV HgMn (Ba), and A1V (Bb) star, plus an astrometrically detected component Bc which may be a single B/A-type star or a pair of lower-mass stars (Fekel 1979, Cole, et al. 1992, Docobo & Andrade 2006). The system lies ~0.35 degree south of γ Cas, diametrically opposite of the IC 59 nebula (Fig. 1). Component B splits into Ba and Bb with a short orbital period of 4.2 days, and that duo orbits the unseen star Bc with period 4.8 yr, detected via speckle astrometry as a perturbation on the motion of Ba+Bb around A (see e.g. Fig. 7 of Cole, et al. 1992). The B trio and component A have a well-characterized visual orbit with period 83 yr. The component C listed in the WDS at separation 41.3" (BU 1353; PA = 157 deg) has near-IR colors consistent with a K3 dwarf. However the star is approximately a magnitude too faint to be a dwarf co-distant with HR 266, and so it is a likely interloper.

The HR 266 system has at least 4 components, and possibly 5 if Bc is a tight pair as speculated by Cole, et al. (1992). The total mass of the HR 266 system is approximately 13.5 $\mathcal{M}_{Sun}$ (Cole, et al. 1992). Adopting the revised Hipparcos parallax for the system (6.06 ± 0.41 mas; van Leeuwen 2007) and the radial velocity from Cole, et al. (1992) of -8.7 ± 0.2 km/s, I estimate the velocity of the HR 266 system in Galactic coordinates to be U, V, W = -12.2, -18.7, -2.2 (±1.2, 0.7, 0.4) km/s (total velocity 22.4 ± 0.9 km/s).

The positions, proper motions, and trigonometric parallaxes for γ Cas and HR 266 in the revised Hipparcos catalog (van Leeuwen 2007; epoch 1991.25, ICRS) are given in Table 1.

Using the revised Hipparcos astrometry, HR 266 lies at separation 1274.4669 ± 0.0004 arcseconds from γ Cas at position angle 178.52 deg. The uncertainty in the separation is dominated by the uncertainty in the position of HR 266 (± 0.3, 0.4 mas in RA, Dec), as the uncertainty in the position of γ Cas is 0.07 mas in both RA and Dec. The revised Hipparcos trigonometric parallaxes for γ Cas (5.94 ± 0.12 mas) and HR 266 (6.06 ± 0.41 mas) from van Leeuwen (2007) are statistically consistent (differing only at the 0.3σ level), and correspond to distances of 168.4 ± 3.4 pc and 165.0 ± 11.2 pc, respectively. Their weighted mean trigonometric parallax (5.95 ± 0.12 mas) is consistent with a distance of 168.1 ± 3.3 pc. At this distance, the projected separation is 214,000 AU or 1.04 pc. The tidal radii t_d for the individual subsystems γ Cas and HR 266 can be estimated using the expression in Mamajek, *et al*. (2013): $r_t = 1.35$ pc $(M_{tot}/\mathcal{M}_{Sun})^{1/3}$. Using the previously mentioned subsystem mass estimates, I estimate the tidal radii of the γ Cas and HR 266 subsystems to be $t_d \sim 3.3$ and 3.2 pc, respectively. The stars are clearly projected within ~1 pc of each other, and their trigonometric parallax distances are statistically consistent to within ~3 ± 12 pc. Their proper motions differ negligibly – Δ(pmRA) = 0.96 ± 0.31 mas/yr and Δ(pmDec) = 0.13 ± 0.34 mas/yr. At d = 168 pc, these differences in proper motion translate to a miniscule difference in tangential velocity of 0.77 ± 0.37 km/s. The radial velocities for γ Cas and HR 266 (from Harmanec, *et al*. 2000, Cole, *et al*. 1992, respectively) differ only at the 1.3 ± 0.7 km/s. Indeed, when comparing the 3D velocity vectors previously calculated, we see that they only differ at the Δ(U,V,W) = -0.5, 1.3, -0.3 (± 1.3, 0.8, 0.5) km/s level. Hence, γ Cas and HR 266 are not only very close in position and distance, but they are demonstrably comoving to within 1.4 ± 1.6 km/s. This case is fairly similar to the examples of the very wide Mizar-Alcor sextuplet (Mamajek, *et al*. 2010) and the case of Fomalhaut B and C (Mamajek, *et al*. 2013). I conclude that the γ Cas+HR 266 system is likely to be physical, designate it MAM 20, and list HR 266 as component "D" to WDS 00567+6043 (B. Mason, priv. comm.). Table 2 gives PA, separation and magnitudes of the proposed MAM 20 multiple system.

Discussion

Eggelton & Tokovinin (2008) examined the multiplicity of the 4559 brightest stars (V < 6) and identified only 2 septuplets (ν Sco and AR Cas), and none of higher multiplicity. Both of these systems appear to be quite young (< tens Myr) and within OB associations (Sco-Cen and Cas-Tau, respectively). A search for ad-

Table 2. Measurements of MAM 20

NAME	RA+DEC	MAGS	PA	SEP	DATE	N	NOTE
MAM 20	00567+6043	2.15, 5.56	178.5	1274.5	1991.25	1	1

1. Revised Hipparcos astrometry (van Leeuwen 2007), magnitudes from original Hipparcos catalog (ESA 1997).

ditional co-moving stars in the close vicinity (<1°) of γ Cas system has yielded no interesting candidates, however the system could be a cluster remnant of a subgroup within the greater Cas-Tau OB association (see Fig. 19 of de Zeeuw, *et al*. 1999). The Cas-Tau OB association is an extremely diffuse stellar group, and despite its proximity (d ~ 170 pc) it has been barely studied since it was first proposed by Blaauw (1956). Age estimates range from 20 to 50 Myr (e.g. Blaauw 1956, Blaauw 1983, de Zeeuw & Brand 1985), however it has been proposed to be associated with the Alpha Persei cluster, whose age is more like ~90 Myr (Stauffer, *et al.* 1999). De Zeeuw, *et al*. (1999) did *not* select either γ Cas (HIP 4427) or HR 266 (HIP 4440) as members of the Cas-Tau group. Only two purported members of Cas-Tau from de Zeeuw, *et al*. (1999) lie within 5 deg (HD 5409 and HR 342), however they appear to be background (~340 pc) and foreground (~124 pc) stars, respectively. Neither HD 5409 nor HR 342 appears to share the motion of the γ Cas system, nor lie within its estimated tidal radius. De Zeeuw, *et al*. (1999) estimates the space velocity of Cas-Tau to be (U,V,W) = (-13.2, -19.7, -6.4 km/s). Given the rarity of early B-type stars in the field, and their short lifetimes, plus the similarities in position, distance, and velocity between the γ Cas and Cas-Tau association (only ~4 km/s mismatch), it seems likely that the γ Cas system is somehow related to the Cas-Tau association.

Cas-Tau has relatively few early B-type stars, with the hottest members among the de Zeeuw et al. (1999) Hipparcos membership being of spectral type B1.5 (1 Per and Phi Per). It is possible that the B0.5IVe star γ Cas is a blue straggler, having been disrupted to its near-critical rotational speed by interaction(s) with member(s) from its evaporating cluster. With ~6 or ~7 members with mass >1 $\mathcal{M}_{Sun}$, and assuming a typical initial mass function (Kroupa, *et al*. 2001), the γ Cas proto-cluster likely had at least ~70 stellar members. If the γ Cas and HR 266 subsystems have close passes, the perturbations among the components could account for the high eccentricity of the tight subsystem HR 266 Ba+Bb (e = 0.415, P = 4.24 day). Among 677 spectroscopic binaries in the SB9 catalog (Pourbaix, *et al*. 2004) with orbital periods within ±50% of 4.24 day, one finds only 17 (2.5%) with eccentricities exceeding 0.4, making HR 266 Ba+Bb a ~2σ outlier in terms of eccentricity compared to comparably tight binaries.

The γ Cas+HR 266 septuplet may constitute one of the highest-N multiple systems known. The evolution of disintegrating young clusters into high-order multiples like this system may provide some context for the dynamical conditions which spawn the classic Be star phenomena.

Acknowledgements

Figure 1 was generated using SkyView. I acknowledge the use of NASA's *SkyView* facility (http://skyview.gsfc.nasa.gov) located at NASA Goddard Space Flight Center. DSS1 blue imagery was taken by CalTech with compression and distribution by Space Telescope Science Institute. DSS2 blue and red data were taken by ROE, AAO, and CalTech, with compression and distribution by Space Telescope Science Institute. This research has made use of the SIMBAD database and Vizier catalogue access tool operated at CDS, Strasbourg, France. Thanks are extended to Brian Mason and Bill Hartkopf for comments.

The research was carried out at the Jet Propulsion

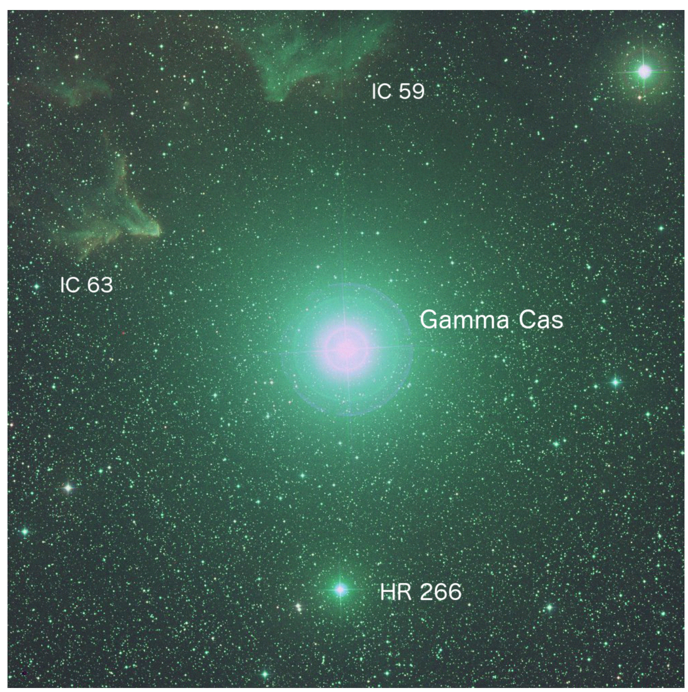

Figure 1. One degree field of view image of γ Cas and vicinity generated using Skyview. The image is RGB using DSS2 red (red), DSS1 blue (green), and DSS2 blue (blue). At d = 168 pc, 1 degree equals about 2.9 pc.

Gamma Cassiopeiae and HR 266: A Massive Septuplet Illuminating the IC 59 and IC 63 Nebulae ...

Laboratory, California Institute of Technology, under a contract with the National Aeronautics and Space Administration.

This article has been approved for Unlimited Release (URS264428).

References

Anderson, E. & Francis, F. 2012, *Astron. Letters*, 38, 331.

Apparao, K.M.V. 2002, *A&A*, 382, 554.

Blaauw, A. 1956, *ApJ*, 123, 408.

Blaauw, A. 1983, *Irish Astronomical Journal*, 16, 141.

Dias, W.S., Alessi, B.S., Moitinho, A. & Lepine, J.R.D, 2002, *A&A*, 389, 871.

Docobo, J.A. & Andrade, M., 2006, IAU Commission 26 (Double Stars) Information Circular, 159, 1 (June 2006).

Eggleton, P.P., & Tokovinin, A.A. 2008, *MNRAS*, 389, 869.

Harmanec, P., Habuda, P., Stefl, S. , *et al*. 2000, *A&A*, 364, L85.

Hoffleit, D. & Warren Jr., W.H. 1991, *The Bright Star Catalogue, 5th Revised Edition (Preliminary Version)*.

Mamajek, E.E., Bartlett, J.L., Seifahrt, A. , *et al*. 2013, *AJ*, 146, 154.

Mamajek, E.E., Kenworthy, M.A., Hinz, P.M., & Meyer, M.R. 2010, *AJ*, 139, 919.

Nemravova, J., Harmanec, P., Koubsky, P. , *et al*. 2012, *A&A*, 537, A59.

Pecaut, M.J., Mamajek, E.E., & Bubar, E.J. 2012, *ApJ*, 746, 154.

Pourbaix, D., Tokovinin, A.A., Batten, A.H. , *et al*. 2004, *A&A*, 424, 727.

Secchi, A. 1867, *Astron. Nachr.*, 68, 63.

Shrader, C.R., Hamaguchi, K., Sturner, S.J. , *et al*. 2015, *ApJ*, 799, 84.

Stauffer, J.R., Barrado y Navascues, D., Bouvier, J. , *et al*. 1999, *ApJ*, 527, 219.

Stee, P., Delaa, O., Monnier, J.D. , *et al*. 2012, *A&A*, 545, 59.

Van Leeuwen, F. 2007, *A&A*, 474, 653.

De Zeeuw, P.T. & Brand, J. 1985, Birth and Evolution of Massive Stars and Stellar Groups, 120, 95.

Measurements of Close Visual Binaries with a 280 mm Reflector and the ASI 290MM Camera

J. Sérot
jocelyn.serot@free.fr

Abstract: This paper presents the measurements of 305 visual binary stars obtained between Feb and Oct 2016 with an 11" reflector telescope and a ASI 290MM CMOS-based camera. Binaries with a secondary component up to mag 12 or as close as 0.5 arcsec could be routinely measured. Exceptionally, pairs with very faint secondary components (up to mag 13) or with separation at the theoretical diffraction limit (0.4 arcsec) have also been measured. We also point out several binaries with known orbits for which our measurement, together with the latest ones, suggest a recalculation of the orbit. Finally, we report the discovery of a yet unobserved component for the star A 303 (WDS 21555+2724).

1. Introduction

This paper is a continuation of the work published in previous issues of JDSO [1,2]. It presents the measurements of 305 visual binary stars obtained between Feb and Oct 2016 with an 11" reflector telescope. Compared with the previously published work, the two most significant changes are i) the replacement of the EM-CCD camera by an ASI 290MM camera; ii) the modification of the calibration procedure, which is now based upon analysis of timed star drifts instead of calibrating pairs; and iii) a systematic estimation of observational errors by means of repeated acquisitions and measurements.

2. Instrumental setup

As described in [1] and [2] the telescope is a 280 mm Schmidt-Cassegrain reflector (Celestron C11). The EM-CCD used in the previous papers has here been replaced by an ASI 290MM camera [3]. This camera is equipped with a 1/3" (1936 x 1096) Sony IMX290 CMOS back-illuminated sensor, providing unprecedented sensibility and very low read-out noise. Figure 1 shows the so-called Variance Photon Transfer Curve (as defined in [4] for example) actually obtained for this camera for a system gain setting of 300 (full range is 0-600). The inverse sensor gain and read-out noise derived from this curve are K = 1.78 e^-/ADU and RON=1.3 e^-. Compared to previous CMOS sensors, the IMX290 sensor also has an improved sensibility in the red and near infrared parts of the spectrum (QE > 0.9 up to 660 nm and QE > 0.7 up to 800 nm), which could be useful when imaging double stars with K or M spectral types. Finally, the IMX290 sensor has relatively small pixels (2.9 x 2.9 µm), making it easier to reach the very small plate scales required for close double star imaging. In our case, a simple 2x Barlow lens gives a resulting focal length of 6225 mm and a plate scale of

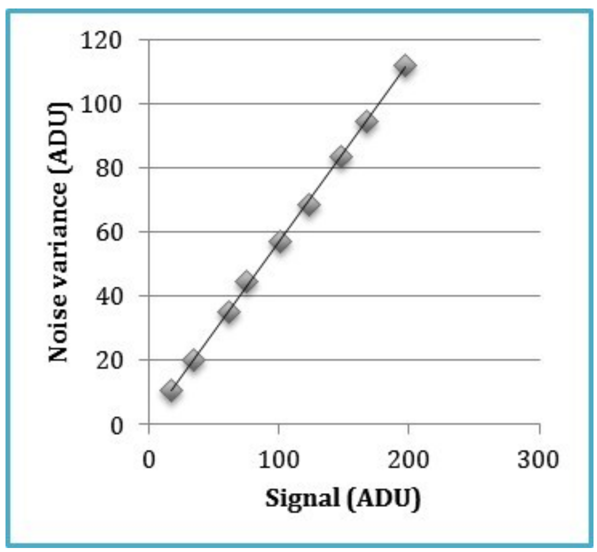

Figure 1. Variance Photon Transfer Curve for the Sony IMX290 sensor of an ASI 290MM camera as measured by the author

96 mas / pixel. Figure 2 shows the used optical train, with, from left to right: the focusing mechanism, the flip-mirror (with 12 mm eyepiece), the filter wheel, the Barlow lens, the atmospheric dispersion corrector (ADC) and the ASI 290MM camera. It can be noticed that the ADC is placed after the Barlow lens, minimizing potential astigmatism problems (ADCs generally work better at high F-ratios). The filter wheel offers the possibility to easily switch from the large L-band filter (400 - 700 nm) generally used for acquisitions to a narrower band filter such as the G-band (500-580 nm) we used for very close binaries.

Figure 2. Used optical setup behind the Celestron C11

3. Image acquisition and reduction

As in [1] and [2], acquisition is carried out with the Genika Astro software [5]. The gain of the camera is set at 550 (range is 0 - 600). Experiments with higher settings did not show significant improvements in detectability. Exposure time for individual images range from 10 to 60 ms typically.

For each target star, we now acquire four sequences of 1000 images. This gives us the possibility to improve the reliability of our measures and estimate their internal precision by computing the mean and standard deviation of the values obtained for the separation and position angle from each sequence. The standard deviations, when they can be computed, are reported in Table 1 along with the position angle and separation values (PA and SEP resp.) between brackets. The average value of these standard deviations for the whole set of measurements are respectively 0.89° for PA and 13 mas for SEP, giving a mean estimated precision of 0.45° and 7 mas respectively.

For precise on-sky scale and orientation calibration, we also have replaced our previous method based upon calibrating pairs by a method based upon the analysis of timed star drifts. Each observing night, we record five distinct drifts of a single, relatively bright star at declination between approximately 10 and 30°. The duration of each drift is typically 6 - 8 sec and it contains 180-250 images. Precise data extraction of each frame is performed by the Genika software. After conversion of the corresponding .SER files to FITS images, each drift is analyzed using the DriftAnalysis module integrated to the latest version of the Speckle Toolbox software developed by D. Rowe [6]. In order to assess the precision of the calibration values obtained with this method, we recorded, for 15 observing nights, the corresponding data. Results are given in Table 4. For each line, the table gives, in columns 1 - 8 : the date, the name of the star, its J2000 declination, the number of drifts used, the mean and standard deviation values obtained for the camera orientation (in degrees) and plate scale. In columns 9-11, we also give, when available, the calibration values obtained by using a single calibrating pair. The name of the calibrating pair, obtained from the list given in [7] is given in column 9. Note that these latest values were <u>not</u> used to produce the measures reported in this paper; they are only given to assess the precision of the method based upon such calibrating pairs. The variation in mean values observed in Table 4 should be ignored because they only reflect the fact that the optical setup is not installed on a permanent basis on the telescope (which is also used for planetary imaging with a slightly different configuration). Columns 6 and 8 respectively give the standard deviation of the camera orientation and plate scale, computed from the five distinct drifts. The maximum value is 0.43° (1.2 mas/pixel). The mean value is 0.28° (0.5 mas/pixel). Comparison of the mean values obtained with two distinct drifts during the same night (28/09/2106, ρ Psc and 16 Peg) also shows a very good consistency, with a difference of 0.12° and 1.8 mas/pixel. Comparison of the values obtained by the drift analysis method on the one hand and the calibrating pair method on the other hand is also instructive. In the eleven cases reported here, the difference in calibration obtained calibration values that never exceeded 0.76° and 1.3 mas/pixel respectively. This justifies *a posteriori* the use of the latter in our previous papers. We have nevertheless chosen to rely on the former from now on for two reasons. First, it provides, along with the calibration values themselves, estimations of the associated precision (by computing standard deviations). Second, it does not require finding calibration pairs in the observed area of the sky (which, in certain situations, can be difficult).

Selection of the binaries to measure is carried out using the latest, online version of the WDS catalog [8] with the help of the WdsPick software described in [9]. We now almost systematically restrict ourselves to

Measurements of Close Visual Binaries with a 280 mm Reflector and the ASI 290MM Camera

pairs with a primary component having a magnitude <12, separation in the range 0.4 - 1 arcsec and for which the latest reported measure is more than 10 years old. This maximizes the chance, in our opinion, to observe significant displacement since the last reported measure. In this campaign, we also included a dozen pairs having separations in the range 1 - 5 arcsec but showing a relatively large difference in magnitude (up to 3) in order to assess the ability of the IMX290 sensor to detect faint companions relatively close -but not too close- to the primary. These pairs are listed with Note 10 in Table 1.

Image reduction is still carried out with the Reduc software [10] using the pixel autocorrelation technique described in [1] and [2]. The only difference is that the measurement of the peak positions is now performed on the autocorrelogram obtained from each of the 1000 frames acquisition sequence, giving four values both for the position angle and separation. Reduc then computes the mean and standard deviation of these values (as reported in Table 1).

4. Results

The reported measurements were obtained on 28 nights, between 2016-04-18 and 2016-10-31. The total number is 305 measures, concerning 304 binaries. Of these, 49 have a published orbit.

Figures 3, 4 and 5 show the distribution of all measurements according to the magnitude and separation of components.

The measures themselves are listed in Table 1. As indicated in Section 3, the values for the position angle (PA) and separation (SEP) are given with their corresponding standard deviation when the latter can be computed. The standard deviation was derived, as described in Section 3, from *n* distinct measures, where *n* is given in column 8 (in most of cases, n=4). A selection of reduced images from which the measures were obtained is given in Plate 1. The details of all measurements are available online [12].

We also report in Table 2 on 25 stars which were either viewed as simple or perceived as binaries but cannot be reliably measured because their separation was too close (<0.4 arcsec typically).

For several pairs, our measurement shows a significant deviation with respect to the latest one reported in the WDS catalog. Our observations for these pairs are shown in Plate 2. For COU2525 the quadrant inversion may have been induced by the small difference in magnitude. For COU1468, the observed magnitudes do not match those reported in the WDS (10.16/10.14 whereas our observation shows a significantly fainter secondary component). The same discrepancy in magnitudes is

(Text continues on page 273)

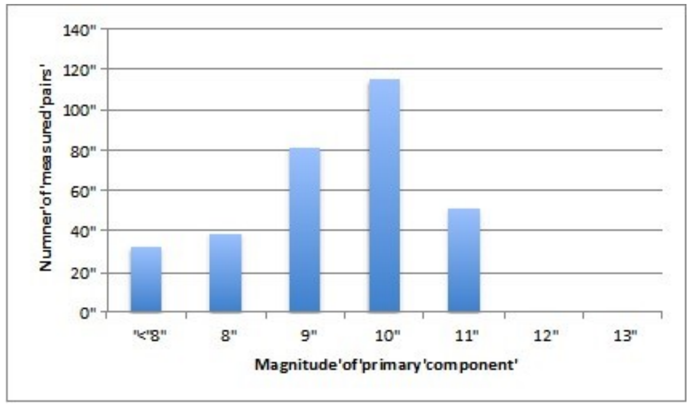

Figure 3. Distribution of measurements according to the magnitude of the primary component

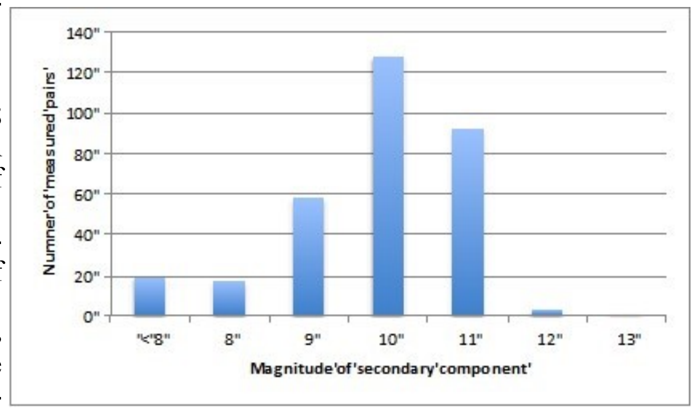

Figure 4: Distribution of measurements according to the magnitude of the secondary component

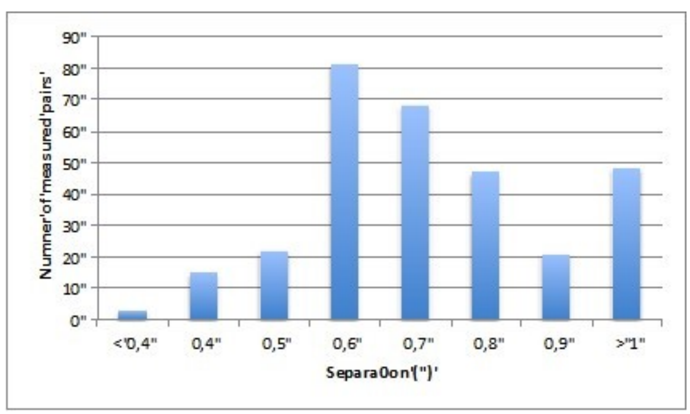

Figure 5: Distribution of measurements according to the separation of components

Measurements of Close Visual Binaries with a 280 mm Reflector and the ASI 290MM Camera

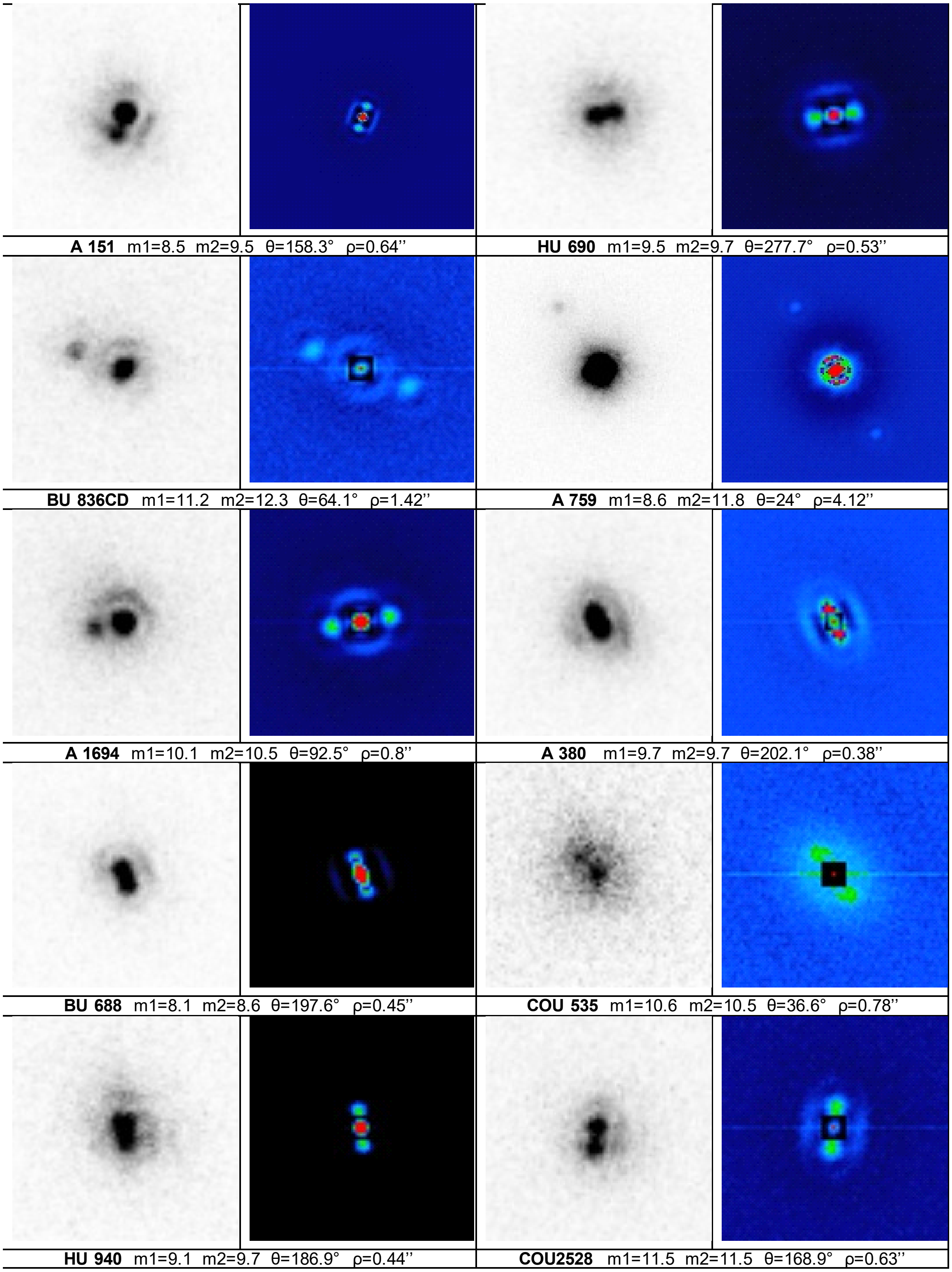

Plate 1 – Examples of images after reduction. (left: co-addition of 10-20 best frames, right: auto-correlogram computed on 1000 frames. N up, E left)

Measurements of Close Visual Binaries with a 280 mm Reflector and the ASI 290MM Camera

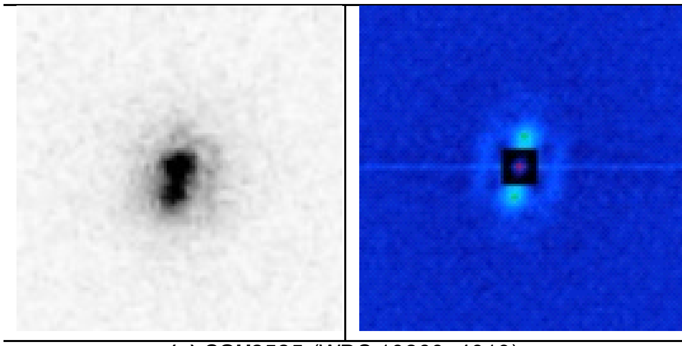

(a) COU2525 (WDS 19263+4319)
m1=10,9, m2=10,99
Observed (2016.682) : PA=164, Sep=0.61
Latest measure reported in WDS (2008) : PA=345, Sep=0.5

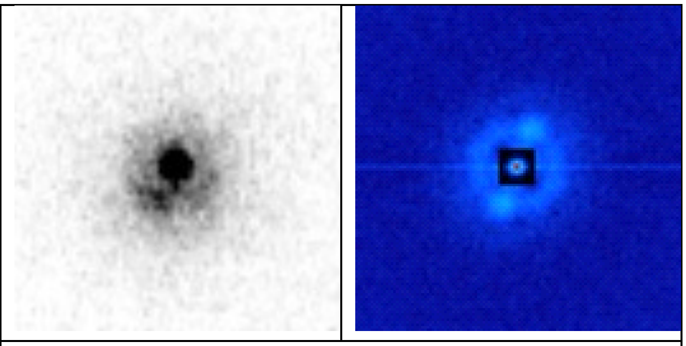

(b) COU1468 (WDS 19503+3127)
Observed (2016,674)
Magnitudes reported in WDS (2016,8) : m1=10,16 m2=10,14

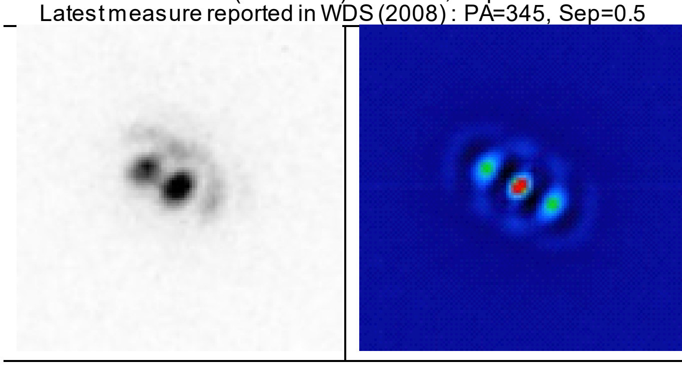

(c) A 1286BC (WDS 03238+5436)
Observed (2016,833)
Magnitudes reported in WDS (2016,8) : m1=11,2 m2=11,2

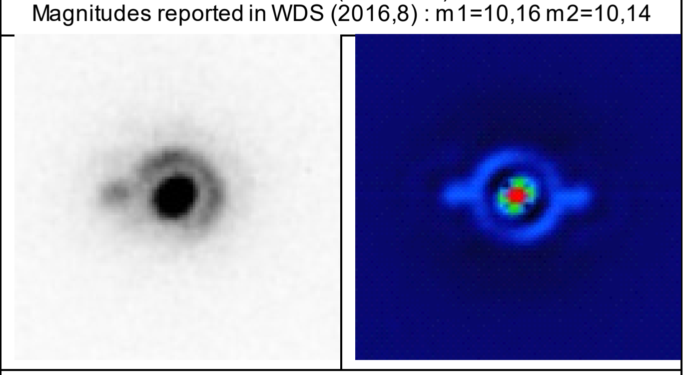

(d) COU1504AC (WDS 00586+4153)
m1=10,9, m2=10,99
Observed (2016.742) : PA=84.5, Sep=1.06
Latest measure reported in WDS (1992) : m1=10,6 m2=12,
PA=359, Sep=0.9

Plate 2 – Images of pairs for which observations do not match the data recorded in the WDS catalog (as of Oct 2016). (left: co-addition of 15 best frames, right: auto-correlogram computed on 1000 frames. North up, East left)

Measurements of Close Visual Binaries with a 280 mm Reflector and the ASI 290MM Camera

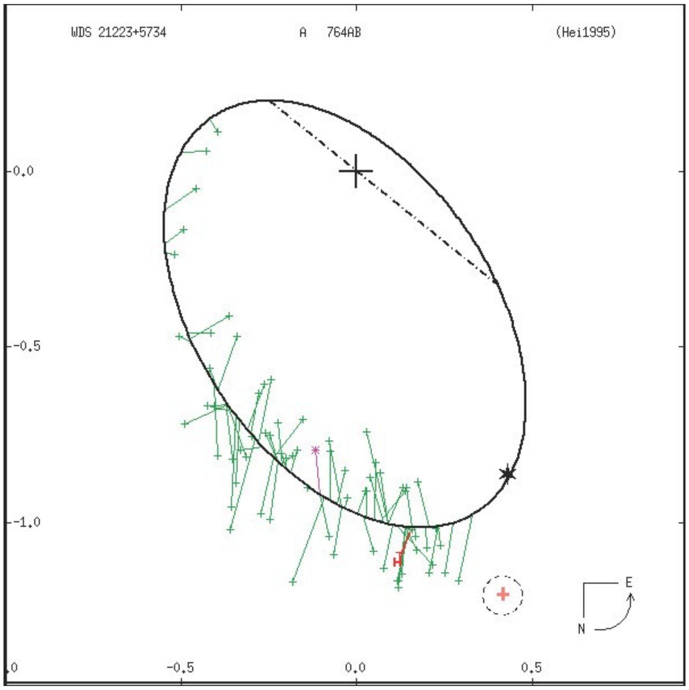

Figure 6. Orbit of A 764AB with predicted (✶) and observed (✚) positions of component B

(Continued from page 270)

observed, to a lesser extent, for A1286BC. For COU1504AC, the observed theta value is not in agreement with the latest measure reported in WDS (theta=359°, 1992). There could be a confusion with the AB pair (TDS1697AB), reported at theta=86°, rho=0,4" in 1991) but the magnitudes do not match (10.58/10.59) whereas the observed magnitudes seem to match those reported for COU1504AC (10.56/11.91), as shown in the corresponding image of Plate 2.

For pairs having a known orbit, Table 3 gives the O-C residuals, computed from the ephemerides published in the 6th Catalog of Orbits [11] (such as published at Oct 1, 2016). Only three pairs show significant O-C values: A 764AB, COU 812 and HU 991. For A 764AB and COU 812, these values are coherent with the latest measures published in the WDS Catalog, as shown in Figure 6 and 7, and suggest a revision of the orbital parameters. For HU 991, we have no explanation for the large deviation between our measure and the latest ones.

For pairs having a orbit with grade 1 or 2, the residuals are plotted using a polar to rectangular conversion in Figure 9 in order to assess the precision of the measurements.

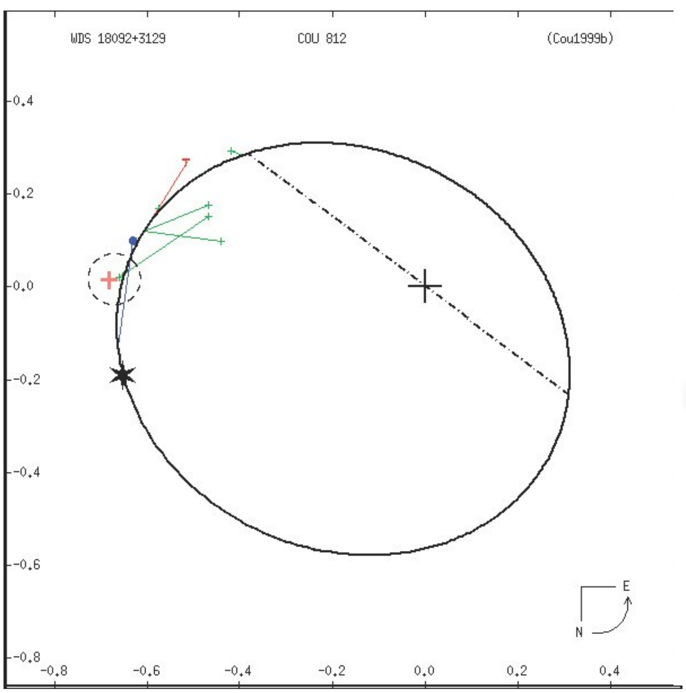

Figure 7 – Orbit of COU 812 with predicted (✶) and observed (✚) positions of component B

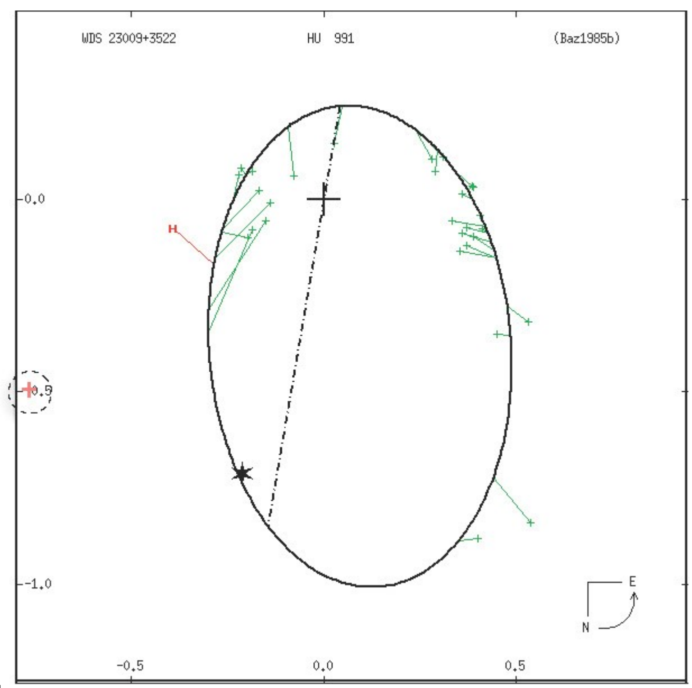

Figure 8. Orbit of HU 991 with predicted (✶) and observed (✚) positions of component B

Measurements of Close Visual Binaries with a 280 mm Reflector and the ASI 290MM Camera

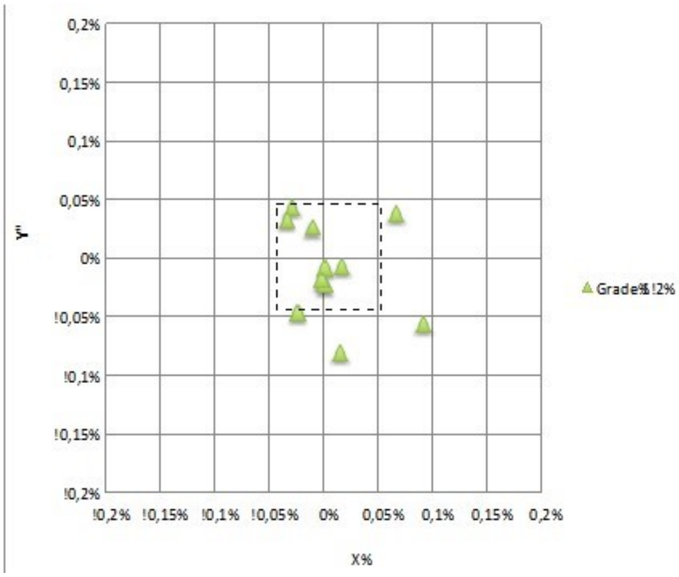

Figure 9. O-C residuals plotted in rectangular coordinates for pairs having an orbit graded 1-2. The dash-lined square represents a pixel in the used instrumental setup.

5. A new component for WDS 21555+2724

A 303 (WDS 21555+2724) was observed for the first time in the night of Sep 1, 2016 because of the relatively large difference in magnitude of its two components (9.2 and 11.6 respectively). When reducing the data, a very faint companion was noticed on an image obtained by co-adding the 100 best frames of the sequence. The presence of this companion was confirmed on the four auto-correlograms computed on 1000-frames sequences (see Figure 10). The pair was re-observed on two subsequent nights (27 and 28 Sep 2016), with similar results, thus excluding any possibility of an artifact due to seeing or induced by the reduction methods. We did not find mention of this component in the literature and it has no entry in the WDS catalog. The measured position angle and separation are (mean and standard deviation computed on N=4 samples): PA = 337.4° (0.57) and SEP = 3.41" (0.015)

A rough estimation of the magnitude of this new component, based upon that of the B component and the exposure times needed to record it (50 ms at minimum) gives 13 - 13.5.

6. Conclusion

The results reported here show that cameras equiped with the most recent back-illuminated CMOS sensors, such as the ASI 290MM, can provide results on the par with those obtained with low-end EM-CCDs. We think this opens unprecedented opportunities for the community of double star observers, by dramatically extending the range of pairs which can be reliably measured with « small » telescopes, both in terms of magnitudes and separation.

Acknowledgments

This research has made use of the Washington Double Star and 6th Orbit catalogs maintained at the U.S. Naval Observatory. Data reduction was carried out using the Reduc software (v 5.0) developed and maintained by F. Losse and the Speckle Toolbox software developed and maintained by D. Rowe. We would also like to thank S. Wen (ZWO Optical), R. Genet and R. Harshaw for allowing us to test one of the first prototype of the ASI 290MM camera.

(Text continues on page 284)

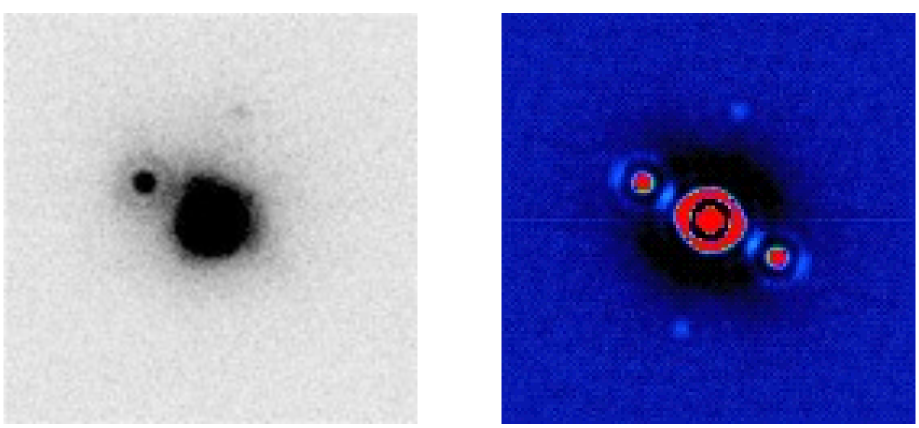

Figure 10. Images of A 303 (WDS 21555+2724) showing the new companion in Q4 (left: co-addition of 100 best frames, right: auto-correlogram computed on 1000 frames. North up, East left)

Measurements of Close Visual Binaries with a 280 mm Reflector and the ASI 290MM Camera

Table 1. Measurements

NAME	RA+DEC	MAG 1	MAG 2	PA (°)	SEP (arcsec)	DATE	N	NOTES
HLD 60	00014+3937	9	9.7	166.4 (0.2)	1.36 (0.006)	2016.745	4	
WOR 30	00037+5329	9.6	10.3	183 (1.2)	0.81 (0.008)	2016.742	4	
STF3056AB	00047+3416	7.7	8	142.6 (0.4)	0.75 (0.005)	2016.745	4	
BU 862	00048+3810	10	10.1	28.1 (1)	0.85 (0.007)	2016.745	4	
STF3062	00063+5826	6.4	7.3	359.3 (0.1)	1.58 (0.006)	2016.745	4	
A 1252	00065+5213	10.5	10.5	185.3 (1.3)	0.63 (0.013)	2016.742	4	
ROE 82AB	00088+4955	10.8	11.1	281.7 (0.5)	0.86 (0.006)	2016.742	4	
COU1851	00103+4920	10.4	10.9	171 (1.4)	0.72 (0.007)	2016.742	4	
A 903	00149+5315	9.4	10	135.5 (0.9)	0.91 (0.02)	2016.742	4	
COU 848	00156+3751	11.5	11.8	296 (0.7)	0.75 (0.017)	2016.742	4	
A 905	00185+5945	9.7	10.5	284.1 (0.6)	0.87 (0.01)	2016.825	4	
POP 35	00195+3544	11.2	11	295.8 (0.7)	0.71 (0.009)	2016.742	4	
HU 1005	00195+5030	10.1	10.3	191.4 (2.2)	0.71 (0.013)	2016.742	4	
POP 36	00197+3501	10.9	11.8	102.3 (1.8)	0.69 (0.007)	2016.742	4	
BU 1093	00209+1059	6.7	8.5	119.3 (0.7)	0.81 (0.006)	2016.745	4	
AC 1	00209+3259	7.2	8.2	288.9 (0.1)	1.91 (0.012)	2016.745	4	
A 907	00226+5417	9.2	9.6	211 (0.7)	0.81 (0.008)	2016.742	4	
HO 491	00244+3629	10.9	11.6	26.4 (0.2)	1.22 (0.01)	2016.742	4	
A 1504AB	00287+3718	8.8	8.9	46.2 (0.3)	0.64 (0.005)	2016.745	4	
BU 394AB	00308+4732	8.4	8.7	278.5 (0.3)	0.81 (0.003)	2016.745	4	
COU2152	00329+5004	11.8	11.8	74.2 (1.6)	0.63 (0.012)	2016.742	4	
HU 411	00376+2240	9.6	9.4	287.1 (0.6)	0.7 (0.005)	2016.825	4	
COU1652	00395+4426	12	12	104.6 (1.2)	0.69 (0.021)	2016.825	4	
COU 853	00408+3844	11.2	11.2	89.3 (0.7)	0.87 (0.003)	2016.742	4	
A 651	00434+4726	9.6	10.2	140.9 (0.6)	0.87 (0.026)	2016.745	4	
MLR 625	00441+5655	10.7	10.9	319.4 (0.7)	0.79 (0.004)	2016.825	4	
HEI 19	00465+1558	11	11	244.3 (0.7)	0.69 (0.006)	2016.742	4	
COU1205	00467+3945	11.2	11.8	92.7 (0.7)	0.86 (0.009)	2016.742	4	
COU2003	00484+4701	11.1	11.4	206.6 (0.8)	0.74 (0.011)	2016.742	4	
BU 232AB	00504+5038	8.4	8.7	255.2 (0.5)	0.89 (0.004)	2016.745	4	
STT 20AB	00546+1911	6.1	7.1	176.8 (0.1)	0.71 (0.007)	2016.745	4	
STF 73AB	00550+2338	6.1	6.5	331.4 (0.2)	1.15 (0.001)	2016.745	4	
HEI 304	00571+1239	11.8	11.8	86.5 (0.7)	0.79 (0.009)	2016.742	4	
COU1504AC	00586+4153	10.5	12	84.5 (0.3)	1.06 (0.022)	2016.742	4	1
STT 515AB	01095+4715	4.5	5.6	114.9 (1.2)	0.58 (0.023)	2016.825	4	
HU 531AB	01409+4952	9.5	10	351.5 (0.9)	0.45 (0.008)	2016.825	4	
BU 453AB	01450+5707	10	10.4	110.7 (0.4)	0.78 (0.005)	2016.825	4	
STF 228	02140+4729	6.5	7.2	303.5 (0.1)	0.68 (0.001)	2016.825	4	
COU2563	02172+5048	10.7	10.8	273.2 (0.6)	0.85 (0.007)	2016.833	4	
STF 248	02211+4246	9.5	9.8	206 (0.4)	0.75 (0.001)	2016.825	4	
COU2160	02215+4714	11.3	11.6	286.6 (0.1)	0.71 (0.001)	2016.833	4	
MLR 656	02239+5751	8.7	10.7	38.8 (1.2)	0.72 (0.003)	2016.833	4	
FOX 55	02248+5719	10.4	10.9	262.9 (0.4)	0.82 (0.01)	2016.833	4	
HU 203	02348+5246	10.2	10.2	91.5 (1.2)	0.63 (0.01)	2016.833	4	

Table 1 continues on next page.

Measurements of Close Visual Binaries with a 280 mm Reflector and the ASI 290MM Camera

Table 1 (continued). Measurements

NAME	RA+DEC	MAG 1	MAG 2	PA (°)	SEP (arcsec)	DATE	N	NOTES
STT 43	02407+2637	7.9	9	335.5 (0.5)	0.67 (0.009)	2016.825	4	
COU 863	02420+3255	10.3	10.4	174.4 (0.3)	0.66 (0.009)	2016.833	4	
COU1376	02505+4044	11.7	12	25.7 (0.9)	0.79 (0.007)	2016.833	4	
HEI 99	02513+1515	10.8	10.8	159.2 (0.1)	0.85 (0)	2016.833	4	
A 1281AB	02517+4559	8.9	10.7	146.2 (0.5)	0.68 (0.021)	2016.825	4	
MET 17AB	02524+3729	9	13.4	74	5.06	2016.833	1	2
COU1222	02549+3857	11.2	11.1	142.8 (0.5)	0.7 (0.014)	2016.833	4	
COU1513	03176+4322	9.5	11.1	117.7 (0)	1.4 (0.001)	2016.833	4	
A 1286BC	03238+5436	11.2	11.2	55.9 (1.1)	0.71 (0.003)	2016.833	4	3
COU1684	03266+4415	10.6	11	43 (1.6)	0.64 (0.002)	2016.833	4	
COU2022	03291+4632	10.7	11.1	227.8 (0.1)	0.98 (0.005)	2016.833	4	
A 1832	04101+3639	9.7	11	168.5 (0.4)	0.79 (0.006)	2016.833	4	
HU 212AC	04142+5149	10.3	12.3	191.2	4.31	2016.833	1	2
HU 212AB	04142+5149	10.3	10.2	24.4 (1.4)	0.57 (0.005)	2016.833	4	
COU2027	04187+4426	11.1	11.1	91.6 (0.6)	0.72 (0.006)	2016.833	4	
COU 37	04392+1724	10	10.5	261.5 (1.4)	0.57 (0.018)	2016.833	4	
A 1302	04559+4432	11.2	12	2.5 (0.3)	0.62 (0.003)	2016.833	4	
A 1550	04565+4311	10	10.3	149.4 (1.9)	0.65 (0.022)	2016.833	4	
A 2163	12022+2108	10.2	10.3	168.9 (0.2)	0.68 (0.017)	2016.296	4	4
STF1613	12126+3546	9.2	9.3	6.1 (0.2)	1.15 (0)	2016.296	4	
HU 570	12137+2118	9.2	11.8	115.4	2.63	2016.296	1	
HU 569	12138+2143	10.1	11.2	161.6 (0.2)	1.19 (0.024)	2016.296	4	
COU1425	12430+4008	10.9	11.1	354.7 (1.6)	0.77 (0.01)	2016.296	4	
HU 1141	13004+3545	10	10.6	343.2 (0.2)	0.61 (0.018)	2016.326	4	5
POP 119	13232+4029	10.6	10.6	7.5 (1.6)	0.74 (0.007)	2016.296	4	
HU 1260	13254+3548	10.6	11.1	184.9 (0.5)	0.69 (0.006)	2016.296	4	
A 1609AB.C	13258+4430	8.3	13	220.2	2.58	2016.326	1	2.5
A 1857	13305+3430	8.1	9.4	344.1 (0.1)	0.63 (0.026)	2016.326	4	
A 685	13512+2948	9.9	10.3	18.1 (0)	0.78 (0)	2016.326	3	
A 569	14012+2522	10.1	10.3	150 (0.2)	0.61 (0.042)	2016.326	4	
STT 276AB	14082+3645	8.9	9.4	207 (3.2)	0.42 (0.007)	2016.326	4	5
COU1916	14241+4331	10.6	10.8	268.9 (0.4)	0.73 (0.001)	2016.296	4	
COU 99	14432+2246	11	11.5	205.6 (2.4)	0.67 (0.011)	2016.296	4	
COU 972	15092+3508	10.7	12	144.3 (0)	1.44 (0)	2016.296	3	
A 1630	15192+4329	10	10.5	245.1 (0.2)	0.78 (0.006)	2016.296	4	
COU 103	15200+2338	10.1	10.1	281.2 (0.6)	0.61 (0.004)	2016.326	2	
HU 147	15204+5309	10.2	10.3	286.6 (2.2)	0.59 (0.033)	2016.296	4	
HU 146	15210+2104	9.5	9.7	122.7 (1.9)	0.72 (0.012)	2016.326	4	5
STF1937AB	15232+3017	5.6	5.9	217.2 (0.3)	0.63 (0.001)	2016.326	4	5
A 1367AB	15233+3619	10.9	11	155.5 (0.4)	0.62 (0.028)	2016.296	4	
COU1443	15272+4133	8.6	10.3	169.8 (0)	0.59 (0)	2016.296	2	
COU 610	15329+3122	4.2	6.2	199.1 (0.2)	0.79 (0.021)	2016.326	4	
A 1640	16013+4529	10.6	10.6	344.9 (1.2)	0.65 (0.004)	2016.326	4	
COU1290	17007+3951	10.4	10.5	27.4 (2)	0.74 (0.009)	2016.51	6	
COU1593	17043+4445	10.5	10.4	191.4 (0.2)	0.62 (0.007)	2016.51	4	

Table 1 continues on next page.

Measurements of Close Visual Binaries with a 280 mm Reflector and the ASI 290MM Camera

Table 1 (continued). Measurements

NAME	RA+DEC	MAG 1	MAG 2	PA (°)	SEP (arcsec)	DATE	N	NOTES
COU1454	17250+4306	10.5	10.6	147.7 (0.7)	0.94 (0.011)	2016.51	7	
STF2267	18017+4011	8.4	8.8	276.3 (0.2)	0.54 (0.024)	2016.573	4	
BU 1127AB	18025+4414	7.3	9.2	42.3	0.77	2016.507	1	6
COU1147	18036+3731	11	11.3	174.6 (0.4)	0.74 (0.008)	2016.512	4	
COU2513	18054+5155	10.9	11.3	57.2 (2.8)	0.88 (0.014)	2016.512	4	
STT 341AB	18058+2127	7.3	8.8	105.8 (0.2)	0.37 (0.005)	2016.573	4	
COU 812	18092+3129	10.7	10.8	264.2 (0.5)	0.69 (0.01)	2016.512	4	
HU 318	18146+2335	10.6	10.7	154.5 (1.1)	0.71 (0.004)	2016.512	4	
A 241	18172+2640	10.5	10.7	287.7 (0.5)	0.67 (0.053)	2016.573	4	
A 244	18242+2818	10.4	10.4	267.6 (0.7)	0.64 (0.014)	2016.512	4	
HU 583	18304+1348	10.2	10.4	305.4 (0.2)	0.77 (0.002)	2016.6	4	
COU1928	18306+4429	10	11.1	262.6 (1.7)	0.47 (0.03)	2016.575	4	
COU1150Aa.Ab	18309+3417	9.8	10.1	283.3 (1.2)	0.41 (0.028)	2016.575	4	
A 248	18312+2516	11	10.9	31.4 (4.3)	0.55 (0.017)	2016.575	4	
COU 639	18349+2717	10.9	11.1	267.8 (1.6)	0.73 (0.021)	2016.575	4	
HU 247	18370+1016	9.9	10	358.5 (0.5)	0.44 (0.004)	2016.6	4	
COU 641	18406+2636	10.2	10.3	56.3 (0.9)	0.61 (0.011)	2016.512	4	
A 1381	18423+3616	10.4	10.3	92.9 (4.6)	0.38 (0.091)	2016.573	4	
COU1309	18459+3657	11.3	11.3	175 (0.1)	0.53 (0.001)	2016.6	4	
COU1930	18505+4335	10.3	10.1	325.9 (2)	0.42 (0.021)	2016.512	4	
COU1611	18572+3845	11	11.2	110.8 (1.4)	0.67 (0.04)	2016.6	4	
COU1156	19006+3300	11.1	11.2	111 (1.8)	0.74 (0.035)	2016.586	4	
A 2991	19034+2511	10.4	10.8	81.7 (1.1)	0.72 (0.022)	2016.586	4	
HU 940	19055+3352	9.1	9.7	186.9 (2.5)	0.44 (0.024)	2016.575	4	
COU1614	19061+3549	9.9	9.9	116.9 (1.1)	0.5 (0.038)	2016.575	4	
ES 1658	19088+4004	11.4	11.9	106.5 (0.6)	1.36 (0.016)	2016.682	4	
A 151	19114+2116	8.5	9.5	158.3 (0.9)	0.64 (0.009)	2016.6	4	
A 1177	19177+1147	10.3	10.6	14.1 (1.4)	0.65 (0.072)	2016.586	4	
COU 422	19208+1717	10.6	11.3	218.9 (0.8)	0.95 (0.013)	2016.6	2	
HEI 269	19232+1320	9.8	10.3	10.6 (0.5)	0.75 (0.007)	2016.6	4	
A 2196BC	19238+3119	10.8	11.2	234.1 (1.5)	0.69 (0.016)	2016.575	4	
COU2399	19243+4038	10.4	11	332.5 (0.3)	0.96 (0.003)	2016.682	4	
COU2122	19253+3749	10.8	10.9	20.5 (0.7)	0.79 (0.013)	2016.682	4	
COU2525	19263+4319	10.9	10.9	164 (0.1)	0.61 (0)	2016.682	4	7
A 1648	19270+1606	9.6	9.8	180.7 (0.5)	0.82 (0.001)	2016.682	4	
A 593	19272+4307	9.9	10.4	355 (0.9)	0.69 (0.004)	2016.682	4	
COU2401	19303+4204	11.1	11.5	193.6 (1.3)	0.93 (0.04)	2016.682	4	
A 269	19305+2714	9.3	9.8	208 (0.6)	0.69 (0.01)	2016.6	4	
HU 949	19335+3305	9.7	9.6	87 (0.3)	0.46 (0)	2016.586	4	
A 271	19345+2620	10.5	10.4	124.7 (0.9)	0.65 (0.006)	2016.575	4	
STT 375	19346+1808	7.7	8.8	187.5 (0.9)	0.7 (0.012)	2016.6	4	
BU 1132	19432+2701	9.3	9.9	211.9 (1)	0.62 (0.007)	2016.586	4	
BU 657	19438+2238	9.7	10.4	132.5 (2.1)	0.85 (0.015)	2016.674	4	
COU2284	19460+3717	8.9	10.1	330.6 (1.1)	0.62 (0.01)	2016.6	4	
HU 758	19471+3321	9.4	9.4	145.5 (0.2)	0.88 (0.002)	2016.575	4	

Table 1 continues on next page.

Measurements of Close Visual Binaries with a 280 mm Reflector and the ASI 290MM Camera

Table 1 (continued). Measurements

NAME	RA+DEC	MAG 1	MAG 2	PA (°)	SEP (arcsec)	DATE	N	NOTES
BU 1473AB	19480+3513	11.4	11.3	16.3 (0.8)	0.98 (0.013)	2016.682	4	
STT 387	19487+3519	7.1	7.9	106.4 (0.8)	0.49 (0.017)	2016.575	4	
HU 346	19496+1707	9.2	9.9	190 (2.6)	0.65 (0.007)	2016.674	4	
COU1468	19503+3127	10.1	10.1	150.6 (0.8)	0.74 (0.027)	2016.674	4	8
COU2528	19508+3906	11.5	11.5	168.9 (0.2)	0.63 (0.013)	2016.682	4	
HO 580	19525+2227	8.5	8.9	270.9 (0.2)	0.77 (0.005)	2016.586	4	
A 603	19528+4045	8.9	10.2	98.4 (1.5)	0.73 (0.005)	2016.6	4	
BU 831	19556+4723	9.6	10.3	127 (0.1)	0.94 (0.001)	2016.682	4	
COU 519	19593+2237	10.5	10.6	72 (1.5)	0.65 (0.037)	2016.586	4	
HU 1308	20001+3423	9.5	9.8	207.6 (1.2)	0.52 (0.008)	2016.685	4	
A 1664	20005+1317	10.2	10.5	68.4 (1.7)	0.7 (0.019)	2016.584	4	
BU1289AB	20010+3742	8.1	9.2	55.3 (0.8)	0.71 (0.006)	2016.685	4	
STT 395	20020+2456	5.8	6.1	127 (0.4)	0.78 (0.003)	2016.742	4	
COU1473	20027+2939	9.4	9.7	345.9 (0.5)	0.63 (0.006)	2016.685	4	
A 1412	20034+3815	9	9.9	227.8 (2.6)	0.78 (0.015)	2016.685	4	
A 380	20036+3220	9.7	9.7	202.1 (0.7)	0.38 (0.008)	2016.685	4	
A 382	20080+4223	7.2	9.4	96.3 (0.1)	1.68 (0.005)	2016.666	2	10
COU2413	20098+3629	10.2	10.4	91.1 (1)	0.8 (0.03)	2016.674	4	
STT 400	20102+4357	7.6	9.8	329 (0.2)	0.7 (0.019)	2016.742	4	
COU1323	20110+2834	10.3	10.4	334.1 (0.3)	0.78 (0.019)	2016.674	4	
A 1202	20133+1047	9.9	10	124 (0.6)	0.79 (0.001)	2016.584	4	
A 1420	20143+3657	9.9	9.7	70.2 (2.4)	0.64 (0.018)	2016.685	4	
STF2659AB.C	20157+4339	8.6	10.8	313.2	2.97	2016.666	1	
A 1669	20179+1508	8.8	11.4	247 (0.3)	3.12 (0.022)	2016.668	4	10
A 1205	20182+2912	9.1	10	96.2 (0.4)	1.21 (0.012)	2016.742	4	
A 725	20210+4437	9.4	10.2	25.9 (0.8)	0.81 (0.009)	2016.742	4	
A 1209AB	20244+1213	9.2	10.6	324 (0.3)	1.9 (0.001)	2016.668	4	10
WOR 33Aa.Ab	20244+1213	8.6	9.3	131.8 (1.3)	0.65 (0.008)	2016.668	4	
HU 1198	20244+1301	8.5	10	32.7 (1.4)	0.62 (0.02)	2016.584	4	
A 291AB	20253+4355	9.8	10.4	148.2 (1.2)	0.78 (0.022)	2016.597	4	
A 392	20256+2504	9.5	10.4	293.2 (0.4)	0.9 (0.003)	2016.674	4	
COU2643	20256+4132	10.8	11.3	107.6 (4.8)	0.53 (0.009)	2016.74	4	
A 1429	20257+5508	8.5	9.3	186.8 (0.6)	0.68 (0.003)	2016.685	4	
A 292	20264+4125	9.2	11.7	134.3 (0.1)	2.1 (0.009)	2016.666	2	10
A 393	20268+2804	9.2	9.9	216.5 (0.7)	0.53 (0.002)	2016.685	4	
A 732	20274+4727	9.6	9.8	78.4 (1)	0.71 (0.004)	2016.685	4	
HU 587	20280+4829	9.9	10.2	338.4 (2.2)	0.62 (0.021)	2016.732	4	
A 394	20290+2658	9.7	10.1	286.3 (2.6)	0.7 (0.011)	2016.732	4	
COU1960	20300+3222	10.1	10.6	217.3 (1)	0.89 (0.039)	2016.732	4	
WOR 9AB	20302+2651	10.5	10.6	230.1 (0.6)	0.62 (0.008)	2016.742	4	
BU 1136	20318+4933	7.7	9.1	215 (0.9)	0.66 (0.008)	2016.685	4	
A 1677	20321+1511	8.1	10.9	183.9 (0.4)	1.32 (0.021)	2016.668	4	10
BU 670AB	20329+1357	9.4	9.8	5.3 (0.3)	0.84 (0.006)	2016.584	4	
L 35CD	20329+1357	10.6	10.9	142.5 (1.4)	0.6 (0.012)	2016.742	4	
COU2644	20329+1906	10.2	11.5	286.3 (2.6)	0.81 (0.01)	2016.584	4	

Table 1 continues on next page.

Measurements of Close Visual Binaries with a 280 mm Reflector and the ASI 290MM Camera

Table 1 (continued). Measurements

NAME	RA+DEC	MAG 1	MAG 2	PA (°)	SEP (arcsec)	DATE	N	NOTES
A 740	20338+4540	9.6	9.9	312.5 (0.1)	0.83 (0.01)	2016.685	4	
COU1632	20355+3241	11.4	11.8	253.9 (1.9)	0.63 (0.018)	2016.74	4	
COU2289	20357+3908	11.2	11	154.9 (1.3)	0.67 (0.03)	2016.74	4	
A 2793	20365+2342	9.9	10.2	209.7 (0.3)	0.85 (0.004)	2016.597	4	
A 744	20381+2953	9.6	9.8	272.3 (0.3)	0.74 (0.005)	2016.685	4	
A 746	20389+4741	7.8	11.6	150.2 (0.2)	2.01 (0.015)	2016.666	4	10
COU2219	20390+3702	11.3	11.6	42.7 (2)	0.88 (0.014)	2016.74	4	
STT 410AB	20396+4035	6.7	6.8	3.6 (0.2)	0.87 (0.007)	2016.671	4	
COU2419	20413+4051	10.5	11.3	68.6 (0.7)	0.81 (0.014)	2016.597	4	
A 749	20437+4733	9.5	9.8	305.8 (0.7)	0.49 (0.03)	2016.674	4	
A 171	20444+2119	8.3	10.9	325.2 (0.1)	5.42 (0.01)	2016.668	4	10
HU 690	20445+3409	9.5	9.7	277.7 (0.5)	0.53 (0.028)	2016.685	4	
BU 64AB	20450+1244	9.1	8.5	354.1 (0.5)	0.68 (0.021)	2016.671	4	
COU2293	20453+4010	10.7	11.5	200.6 (1.1)	1.06 (0.024)	2016.74	4	
A 173	20458+2416	9.1	10.2	126.3 (0.6)	0.96 (0.006)	2016.674	4	
STT 413AB	20474+3629	4.7	6.2	3.1 (1.3)	0.89 (0.007)	2016.671	4	
COU 827Aa.Ab	20482+2622	11.2	11.6	331.9 (2)	0.58 (0.047)	2016.74	4	
J 194AB	20494+1124	10.3	9.9	309.3 (0.1)	0.67 (0.024)	2016.671	4	
COU2426	20495+4035	11.1	11.4	327.7 (0.2)	1.24 (0.007)	2016.584	4	
A 1212	20521+1014	9	9.6	11.3 (0.8)	0.62 (0.01)	2016.674	4	
COU 830	20547+2516	11.5	12	169.4 (0.5)	1.01 (0.023)	2016.584	4	
STT 418	20548+3242	8.2	8.2	283.3 (0.7)	0.96 (0.013)	2016.742	4	
A 754	20559+5906	9.3	9.9	3.7 (0.5)	0.91 (0.003)	2016.674	4	
A 753AB	20562+4615	9.6	10	255.6 (0.3)	0.96 (0.002)	2016.674	4	
A 1436	20566+3858	10.3	10.4	52.4 (1.3)	0.61 (0.006)	2016.584	4	
A 1685AB	20577+1402	10.1	10.3	85.7 (0.7)	0.74 (0.013)	2016.674	4	
A 756AB	20577+5849	8.2	9.2	208.4 (0.3)	0.62 (0.01)	2016.674	4	
HU 363	20587+1823	10.3	10.6	101 (1.4)	0.8 (0.003)	2016.674	4	
A 1687	21021+1423	10.4	10.8	190.4 (0.3)	0.78 (0.008)	2016.597	4	
COU1181	21025+2958	11	12	213.7 (0.9)	0.74 (0.01)	2016.597	4	
COU2432	21032+4158	11.2	11.4	23.7 (1.5)	0.79 (0.004)	2016.682	4	
COU2434	21048+4144	10.8	11	189.4 (0.7)	0.87 (0.027)	2016.682	4	
COU2298	21050+4125	10.2	10.9	147.3 (0.6)	0.87 (0.021)	2016.682	4	
BU 679	21058+4341	11.5	11.9	75 (1.1)	0.7 (0.024)	2016.756	4	
BU 836AB	21065+4823	9.9	9.6	177.4 (0.3)	0.79 (0.014)	2016.756	4	
BU 836CD	21065+4823	11.2	12.3	64.1 (0.4)	1.42 (0.006)	2016.756	4	
A 881	21073+4440	7.4	11	217.6 (0.1)	4.25 (0.007)	2016.668	4	10
A 759	21077+4718	8.6	11.8	24 (0.2)	4.12 (0.003)	2016.668	4	10
J 1328	21081+2615	10.5	10.6	147.9 (0.5)	1 (0.012)	2016.756	4	
COU2693	21084+5118	11.2	11.1	132.2 (1.4)	0.59 (0.007)	2016.756	4	
COU2545	21097+4820	10.6	10.6	74.2 (1.7)	0.69 (0.007)	2016.682	4	
FOX 41BC	21125+3720	10.6	11	123.5 (1.6)	0.92 (0.03)	2016.756	4	
STF2783	21141+5818	7.7	8	351.8 (1.1)	0.72 (0.003)	2016.742	4	
AGC 13AB	21148+3803	3.8	6.5	198.3 (0.2)	0.87 (0.017)	2016.742	4	
A 1440	21153+4017	10	10.9	212.8 (0.3)	1.16 (0.01)	2016.668	4	

Table 1 continues on next page.

Measurements of Close Visual Binaries with a 280 mm Reflector and the ASI 290MM Camera

Table 1 (continued). Measurements

NAME	RA+DEC	MAG 1	MAG 2	PA (°)	SEP (arcsec)	DATE	N	NOTES
COU2229	21161+4101	10.1	10.3	272 (0.7)	0.78 (0.011)	2016.685	4	
COU2437	21170+4704	11	11.2	241.3 (3.7)	0.5 (0.056)	2016.682	4	
BU 163AB	21186+1134	7.3	8.8	256.2 (0.4)	0.87 (0.008)	2016.742	4	
HU 769	21186+3430	9.6	10.2	178.8 (0.9)	0.78 (0.006)	2016.597	4	
A 1694	21197+5455	10.1	10.5	92.5 (0.5)	0.8 (0.009)	2016.668	4	
COU2439	21199+4307	9.6	9.9	265.7 (0.7)	0.78 (0.012)	2016.685	4	
STT 437AB	21208+3227	7.1	7.4	19.3 (0.1)	2.48 (0.002)	2016.742	4	
A 764AB	21223+5734	8.2	10.6	19.2 (0.7)	1.27 (0.029)	2016.742	4	
COU 428	21235+1728	10.4	11.4	137.1 (1.3)	0.89 (0.024)	2016.756	4	
A 1892	21237+5518	8.1	9.3	350.9 (0.7)	0.76 (0.007)	2016.685	4	
A 765AB	21238+4710	9	7.3	21.6 (1)	0.55 (0.012)	2016.732	4	
A 618	21256+4138	9.8	10.2	275.8 (0.8)	0.62 (0.018)	2016.668	4	
COU2306	21257+4043	11.1	11.3	17.8 (0.4)	0.66 (0.035)	2016.682	4	
HEI 285	21277+1431	9.5	10.5	95 (0.2)	0.85 (0.008)	2016.597	4	
COU 535	21297+1719	10.6	10.5	36.6 (1.7)	0.78 (0.043)	2016.732	4	
A 768	21305+4620	10.3	10.5	335.4 (0.2)	0.68 (0.008)	2016.685	4	
A 1893AB	21346+5633	10.2	10.6	23.7 (1.6)	0.71 (0.017)	2016.668	4	
ROE 127	21354+1344	10.8	11.2	35.3 (1.1)	0.76 (0.015)	2016.756	4	
HO 463	21362+4253	8.9	9.3	179.9 (1.1)	0.55 (0.036)	2016.597	4	
COU2309	21370+4520	10.7	11	53.4 (2)	0.7 (0.02)	2016.74	4	
COU2310	21372+4527	10.4	10.4	9.9 (0.5)	0.5 (0.005)	2016.74	4	
COU2310	21372+4527	10.4	10.4	8.4 (2.4)	0.49 (0.071)	2016.732	4	
A 402	21380+4153	9.1	10.5	46.6 (0.1)	0.83 (0.003)	2016.685	4	
BU 1331	21392+4411	9.3	10.4	339.8 (1.6)	0.72 (0.042)	2016.732	4	
A 1444	21398+3749	10.5	10.7	82.4 (0.3)	1.11 (0.015)	2016.668	4	
BU 688AB	21426+4103	8.1	8.6	197.6 (2.3)	0.45 (0.05)	2016.742	6	
COU2548	21429+5053	11.1	11.2	166.9 (0.4)	1.04 (0.005)	2016.74	4	
A 1222	21431+3149	10.3	10.1	352.6 (0.6)	0.67 (0.018)	2016.597	4	
COU 536	21434+2147	11.4	11.8	226.8 (0.8)	0.95 (0.015)	2016.756	4	
A 773	21470+4759	8.2	11.1	201.1 (0.1)	3.33 (0.002)	2016.668	4	10
COU2316	21477+4759	11.4	11.8	184.9 (0.6)	0.71 (0.011)	2016.756	4	
A 774	21511+4711	8.9	10.8	14.4 (0.9)	0.62 (0.01)	2016.668	4	10
COU2321	21539+4839	11.1	10.9	255.3 (0.8)	0.66 (0.011)	2016.74	4	
HO 173	21553+1842	10.3	10.6	73.1 (0.7)	0.9 (0.013)	2016.597	4	
BU 75AB	21555+1053	8.4	8.5	25.5 (0.3)	1.04 (0.001)	2016.685	4	
A 303	21555+2724	9.2	11.6	52.3 (0)	2.3 (0.006)	2016.668	4	9
COU2656	21558+5052	10.8	11	64.6 (0.5)	1.13 (0.019)	2016.74	4	
A 780AB	22013+4515	9.4	9.9	148.5	1.51	2016.764	1	
A 780CD	22013+4515	10.5	11	110 (0.7)	0.98 (0.008)	2016.764	4	
COU 445	22029+3436	11.5	11.8	34.9 (2.6)	0.85 (0.014)	2016.764	4	
A 407AC	22061+4159	10	11	58.3	13.15	2016.764	1	
A 407AB	22061+4159	10	10.1	21.5 (0.6)	0.68 (0.006)	2016.764	4	
STF2872BC	22086+5917	7.9	8	297 (0.1)	0.81 (0.005)	2016.742	4	
COU1828	22099+4254	11	11	273.3 (0.7)	0.86 (0.009)	2016.764	4	
COU2660	22115+5110	10.3	11.6	249.4 (1.7)	0.66 (0.004)	2016.764	4	

Table 1 concludes on next page.

Measurements of Close Visual Binaries with a 280 mm Reflector and the ASI 290MM Camera

Table 1 (conclusion). Measurements

NAME	RA+DEC	MAG 1	MAG 2	PA (°)	SEP (arcsec)	DATE	N	NOTES
COU2659	22115+5232	10.5	11.3	161.4 (0.6)	1.24 (0.016)	2016.764	4	
HU 695	22129+5058	10.8	10.9	17.2 (0.1)	0.83 (0.005)	2016.764	4	
COU2327	22226+4738	10.2	12	332.8 (0.9)	0.86 (0.007)	2016.764	4	
COU2142	22229+4637	11.2	11.3	116.7 (1.6)	0.61 (0.056)	2016.764	4	
HO 183AB	22248+2233	9	11.5	221.3 (0.1)	2.48 (0.005)	2016.742	4	
COU1984	22257+4353	11.2	11.4	284.6 (0.3)	0.86 (0.011)	2016.764	4	
COU1832AB	22262+4228	11.5	11.6	157.3 (0.3)	1 (0.014)	2016.764	4	
KR 60AB	22280+5742	9.9	11.4	265.5 (0)	1.5 (0)	2016.742	4	
COU2242	22360+4515	10.7	10.7	274.2 (0.3)	0.81 (0.008)	2016.729	4	
COU2334	22373+4653	10.8	10.8	112.6 (0.8)	0.52 (0.021)	2016.764	4	
HO 296AB	22409+1433	6.1	7.2	49.7 (0.4)	0.57 (0.001)	2016.742	4	
COU2697	22430+5012	11	10.9	301.9 (3.8)	0.7 (0.02)	2016.729	4	
COU2663	22497+5007	10.4	10.5	109.9 (0.1)	0.66 (0.001)	2016.729	4	
COU1990	22532+4157	11.1	11.3	47.1 (3.2)	0.64 (0.015)	2016.729	4	
HEI 193AB	22545+1517	11	11.5	210.6 (0.6)	0.93 (0.014)	2016.764	4	
COU2666	22548+4908	11.4	11.6	138.3 (0.5)	1.02 (0.009)	2016.729	4	
COU2144	22564+4443	11	11.1	156.1 (0.5)	0.93 (0.012)	2016.729	4	
A 1477	22579+5439	9.1	9.5	354 (1.2)	0.59 (0.024)	2016.729	4	
HU 991	23009+3522	10.2	11.1	303.2 (0.4)	0.93 (0.014)	2016.745	4	
A 196	23055+4643	8.7	9.3	315.5 (1.2)	0.52 (0.026)	2016.729	4	
COU1492	23091+4153	10.9	11.6	256 (1)	0.86 (0.003)	2016.764	4	
BU 385AB	23103+3229	7.4	8.2	83 (0.5)	0.74 (0.01)	2016.745	4	
COU1645	23195+4225	10	11	77.3 (0.5)	0.77 (0.014)	2016.764	4	
COU2668	23207+4739	11.4	11.2	10.9 (3.3)	0.71 (0.034)	2016.729	4	
COU1495	23216+3901	11.1	11.9	254.7 (0.3)	0.84 (0.007)	2016.729	4	
ROE 135	23218+1151	11.1	11.6	141 (0.5)	1.19 (0.029)	2016.764	4	
COU1994	23237+4425	11	11.2	43.6 (0.6)	0.95 (0.011)	2016.729	4	
BU 720	23340+3120	5.6	6.1	102.1 (1)	0.65 (0.012)	2016.745	4	
COU2346	23352+4732	11.4	11.6	206.9 (4)	0.76 (0.034)	2016.729	4	
COU2249	23377+4457	10.3	10.5	27.4 (1.1)	0.57 (0.01)	2016.729	4	
COU2675	23392+5033	10.7	11	16 (2.4)	0.66 (0.018)	2016.764	4	
HU 1325	23401+1258	9.8	10	36.4 (1.2)	0.87 (0.022)	2016.745	4	
A 1242	23431+1150	9.3	9.6	340.2 (0.2)	1.04 (0.014)	2016.745	4	
A 794BC	23509+4730	11.4	11.8	10.2 (1.5)	0.78 (0.004)	2016.729	4	
STT 510AB	23516+4205	7.8	8.4	299.5 (0.5)	0.65 (0)	2016.745	4	
HEI 415	23588+4647	11.8	11.6	51.4 (0.5)	1.07 (0.015)	2016.729	4	

Notes for Table 1

1. Observed theta value is not coherent with the latest measure reported in WDS (theta=359°, 1992).
2. Direct measure with Reduc (no auto-correlation)
3. The observed magnitudes do not match those reported in WDS (11.2/11.2). Secondary component is fainter
4. Astronomik R filter
5. Astronomik G filter
6. Auto-correlation computed on a single sequence of 10000 frames
7. Quadrant inversion wrt. WDS data (see Plate 2, Fig. a)
8. The companion is much fainter than indicated in WDS (see Plate 2, Fig. b)
9. New C companion observed (see Sec. 5 and Fig. 10)
10. Large dM pair

Table 2 – Pairs Observed but for Which no Measure was Obtained

NAME	RA+DEC	MAG 1	MAG 2	DATE	NOTES
COU1854	00425+4808	12	12	2016.825	2
A 1819	02400+3910	10.2	11.4	2016833	1
MET 17Aa,Ab	02524+3729	9.3	10.7	2016833	2
COU 565	04255+1942	9.8	10.3	2016833	2
A 690	15092+2809	10	10.5	2016326	1
COU1787	18054+4306	11.1	11	2016573	1
COU1928	18306+4429	10	11.1	2016575	2
COU1150Aa,Ab	18309+3417	9.8	10.1	2016512	2
COU1150Aa,Ab	18309+3417	9.8	10.1	2016575	1
A 1381	18423+3616	10.4	10.3	2016573	1
COU2407	19401+3943	10	10.6	2016.6	2
COU2636	19592+4233	11.6	11.8	2016.6	2
A 720	20012+4821	10.4	10.4	2016685	1
STF2659AB	20157+4339	8.6	10.8	2016666	1
COU2220Aa,Ab	20463+3646	11.4	11.5	2016756	1
COU2426	20495+4035	11.1	11.4	2016584	1
COU 523	21010+1910	10.3	10.3	2016597	2
COU2442	21321+4828	8.9	10.3	2016756	2
LBU 2Aa,Ab	21420+1856	8	9.5	2016756	2
COU 837	21561+2846	11.1	11.6	2016597	2
COU2325	22166+5036	10.7	11.2	2016764	2
KUI 112Aa,Ab	22329+5348	10.8	10.8	2016742	1,4
A 632	22520+5743	8.5	9.3	2016742	1,3
A 192	22590+4617	9.9	10	2016729	2
CHE 504	23338+1159	10.5	10.7	2016764	2

Notes for Table 2:

1. Viewed elongated but too close to be measured
2. Viewed as simple
3. Has orbit, grade=3. Ephemerides give sep=0,37’’ for 2016
4. Has orbit, grade=3. Ephemerides give sep=0,40’’ for 2016

Measurements of Close Visual Binaries with a 280 mm Reflector and the ASI 290MM Camera

Table 3 – O-C Residuals for pairs having an known orbit

NAME	RA+DEC	DATE	O-C - PA (deg)	O-C - SEP (arcsec)	GRADE	REF	NOTE
HLD 60	00014+3937	2016.745	-0.5	0.05	3	Hrt2011a	
BU 862	00048+3810	2016.745	-0.5	0	4	Cou1986b	
STF3062	00063+5826	2016.745	0.1	0.02	2	Sod1999	
BU 1093	00209+1059	2016.745	-0.3	0.04	5	Lin2010c	
BU 394AB	00308+4732	2016.745	1.2	-0.01	4	Zul1997b	
A 651	00434+4726	2016.745	-1	-0.02	5	USN2002	
BU 232AB	00504+5038	2016.745	-0.3	0.03	3	Sca2008a	
STT 20AB	00546+1911	2016.745	0.5	0.12	3	Doc2014a	
STF 73AB	00550+2338	2016.745	0.3	0.01	2	Mut2010b	
STT 515AB	01095+4715	2016.825	-1	0.05	4	Mut2010b	
HU 531AB	01409+4952	2016.825	1.7	-0.01	4	Msn2014b	
BU 453AB	01450+5707	2016.825	-4.7	0.05	5	Sul1984	
STF 228	02140+4729	2016.825	1.3	0.01	2	Sca2015c	
STF 248	02211+4246	2016.825	1.8	0.06	4	Pbx2000b	
STT 43	02407+2637	2016.825	0.4	0.07	4	Sca2001d	
A 1281AB	02517+4559	2016.825	2	0.02	4	Hrt2014a	
STF1937AB	15232+3017	2016.326	-0.4	0.05	1	Mut2010b	
BU 1127AB	18025+4414	2016.507	-5.5	-0.03	4	Cve2006e	
STT 341AB	18058+2127	2016.573	5.9	0.07	2	Hei1982b	
COU 812	18092+3129	2016.512	-22.4	0.01	5	Cou1999b	2
HU 940	19055+3352	2016.575	-2.4	-0.02	3	Doc2009g	
STT 387	19487+3519	2016.575	-1.4	0.01	2	WSI2006b	
STT 395	20020+2456	2016.742	0.3	-0.07	4	Zir2013a	
STT 400	20102+4357	2016.742	0.4	0.05	2	Hei1997	
A 1205	20182+2912	2016.742	-0.5	-0.01	5	WSI2006b	
A 725	20210+4437	2016.742	0	0.03	4	Hrt2009	
WOR 9AB	20302+2651	2016.742	7.9	0.09	5	Zir2003	
L 35CD	20329+1357	2016.742	-0.6	0.12	3	Hrt2014b	
STT 410AB	20396+4035	2016.671	0	0	4	Hrt2011a	
BU 64AB	20450+1244	2016.671	-1.8	0.03	4	USN2007a	
STT 413AB	20474+3629	2016.671	4.3	-0.03	4	Rab1948b	
J 194AB	20494+1124	2016.671	1.9	0.09	3	Sod1999	
STT 418	20548+3242	2016.742	-0.2	0.01	4	Zir2013a	
AGC 13AB	21148+3803	2016.742	0.7	-0.08	1	Mut2010e	
BU 163AB	21186+1134	2016.742	178.5	-0.03	2	Fek1997	1
STT 437AB	21208+3227	2016.742	0.7	0.05	4	Hrt2011a	
A 764AB	21223+5734	2016.742	-6	0.29	5	Hei1995	3
BU 688AB	21426+4103	2016.742	-2.3	0.01	3	USN2006a	
BU 75AB	21555+1053	2016.685	0.1	-0.03	2	Hei1996a	
STF2872BC	22086+5917	2016.742	0.2	0.01	5	USN2002	
HO 183AB	22248+2233	2016.742	0.9	0.09	4	Zir2003	
KR 60AB	22280+5742	2016.742	-1.1	0.04	2	Hei1986b	
HO 296AB	22409+1433	2016.742	2.1	0.11	1	Mut2010b	
HU 991	23009+3522	2016.745	-41.8	0.15	5	Baz1985b	4
BU 385AB	23103+3229	2016.745	-1.1	0.06	4	Lin2010c	
BU 720	23340+3120	2016.745	-2.9	0.08	4	Mut2010e	
HU 1325	23401+1258	2016.745	4.5	0	5	Sca2003a	
A 1242	23431+1150	2016.745	0.7	0.06	5	Lin2004c	
STT 510AB	23516+4205	2016.745	-0.3	0.05	4	Nov2006e	

Notes for Table 3:

1. The ephemerides reported in The Sixth Orbit Catalog should probably be offset by 180°
2. The large O-C reported here is coherent with the latest measures published in the WDS Catalog. A revision of the orbit is likely to be necessary. See Fig. 6
3. The large O-C reported here is coherent with the latest measures published in the WDS catalog. A revision of the orbit is likely to be necessary. See Fig. 7

Measurements of Close Visual Binaries with a 280 mm Reflector and the ASI 290MM Camera

Table 4 – Drift calibration data for 15 nights

DATE	STAR	J2000 Dec	N	ORIENT (°)	SDEV	SCALE (arcsec)	SDEV	CAL.PAIR	ORIENT	SCALE
31/10/2016	44 Tau	26°28'51"	5	5.19	0.26	0.09604	0.000091	STF 534	5.18	0.09575
28/10/2016	HD9780	17°26'02"	5	5.68	0.31	0.09627	0.00062	STF 222	5.89	0.09568
06/10/2016	71 Peg	22°29'55"	5	4.25	0.27	0.09641	0.00047	STF 222	4.71	0.09614
03/10/2016	Omi Peg	29°18'27"	5	8.11	0.18	0.09698	0.00066	STF2922	7.55	0.09594
25/09/2016	HD5316	24°33'25"	5	5.23	0.19	0.0978	0.00102			
28/09/2016	Rho Psc	19°10'21"	5	2.78	0.25	0.09677	0.00035	STF2769	2.58	0.09575
28/09/2016	16 Peg	25°55'31"	5	2.66	0.21	0.09695	0.00035			
27/09/2016	Omi Peg	29°18'27"	5	2.98	0.41	0.09643	0.0012			
24/09/2016	31 Peg	12°12'19"	5	4.82	0.18	0.09697	0.00086			
23/09/2016	58 Psc	11°58'25"	5	13.16	0.34	0.09666	0.00016	STF2985	12.4	0.09613
07/09/2016	33 Vul	22°19'33"	5	0.71	0.23	0.09559	0.00052	STF2691	1.03	0.09629
06/09/2016	70 Cyg	33°07'00"	5	3.89	0.34	0.09753	0.00026	STF2691	3.97	0.09636
02/09/2016	Zet Del	14°40'28"	5	5.68	0.43	0.09699	0.00076	STF2691	5.34	0.09626
03/09/2016	9 Peg	17°21'00"	5	9.79	0.41	0.09753	0.00037	STF2691	9.94	0.09622
01/09/2016	HD209761	26°40'26"	5	8.47	0.24	0.09666	0.00042	STF2691	8.47	0.09609

(Continued from page 274)

References

[1] Sérot, J., "Measurements of Double Stars Using a 280 mm Reflector and an EM-CCD", *JDSO*, **11**, 361-389, 2015.

[2] Sérot, J., "Speckle Interferometry of Close Visual Binary Stars with a 280 mm Reflector and an EM-CCD", *JDSO*, **12**, 488 - 499, 2016.

[3] https://astronomy-imaging-camera.com/products/usb-3-0/asi290mm

[4] Janesick, J.R., "Photon Transfer DN to Lambda", SPIE Press, 2010.

[5] www.airyab.com/genika-astro

[6] Harshaw, R., Rowe, D., and Genet, R., "The Speckle Toolbox: A Powerful Data Reduction Tool for CCD Astrometry", *JDSO*, **13**, 52-67, 2017.

[7] Mauroy, F., Mauroy, P. et Morlet , G., "Liste de 32 couples étalons", *O&T*, 67-68, 2007. Available online at http://saf.etoilesdoubles.free.fr/documents/COUPLES%20ETALONS%20Guy%20-%20Pascal.pdf

[8] Mason, D.B., Wycoff, G.L., Hartkopf, W.I.,Washington Double Star Catalog, USNO, 2015, http://www.usno.navy.mil/USNO/astrometry/optical-IR-prod/wds/WDS

[9] Sérot, J. "Users Guide to the WdsPick Software", *JDSO*, **12**, 535-540, 2016.

[10] Losse, F., Reduc, v5.0, http://www.astrosurf.com/hfosaf

[11] Hartkopf, W.I., Mason, D.B., Sixth Catalog of Orbits of Visual Binary Stars, USNO, 2009. http://www.usno.navy.mil/USNO/astrometry/optical-IR-prod/wds/orb6

[12] http://www.astrosurf.com/legalet/MesuresDoubles/mesures.html

Journal of Double Star Observations

April 1, 2017
Volume 13, Number 2

The Journal of Double Star Observations (ISSN 2572-4436*) is an electronic journal published quarterly. Copies can be freely downloaded from http://www.jdso.org.*

Questions, comments, or submissions may be directed to rclark@southalabama.edu or to rmollise@bellsouth.net

The *Journal of Double Star Observations* (*JDSO*) publishes articles on any and all aspects of astronomy involving double and binary stars. The *JDSO* is especially interested in observations made by amateur astronomers. Submitted articles announcing measurements, discoveries, or conclusions about double or binary stars may undergo a peer review. This means that a paper submitted by an amateur astronomer will be reviewed by other amateur astronomers doing similar work.

Submitted manuscripts must be original, unpublished material and written in English. They should contain an abstract and a short description or biography (2 or 3 sentences) of the author(s). For more information about format of submitted articles, please see our web site at http://www.jdso.org

Submissions should be made electronically via e-mail to rclark@southalabama.edu or to rmolise@bellsouth.net. Articles should be attached to the email in Microsoft Word, Word Perfect, Open Office, or text format. All images should be in jpg or fits format.